PEPTIDE-CARBOHYDRATE MIMICRY: SYNTHESIS AND IMMUNOLOGICAL EVALUATION OF EXPERIMENTAL BACTERIAL VACCINES

by

Bibi Rehana Hossany
B.Sc. (Hons), University of Mauritius, Reduit, Mauritius, 1999

THESIS SUBMITTED IN PARTIAL FULFILLMENT OF
THE REQUIREMENTS FOR THE DEGREE OF

DOCTOR OF PHILOSOPHY

In the
Department of Chemistry

SIMON FRASER UNIVERSITY

Fall, 2009

APPROVAL

Name: **Bibi Rehana Hossany**

Degree: **Doctor of Philosophy**

Title of Thesis: **PEPTIDE-CARBOHYDRATE MIMICRY: SYNTHESIS AND IMMUNOLOGICAL EVALUATION OF EXPERIMENTAL BACTERIAL VACCINES**

Examining Committee:

Chair: **Dr. Erika Plettner**
Associate Professor, Department of Chemistry

_____

Dr. B. Mario Pinto
Senior Supervisor
Professor, Department of Chemistry

_____

Dr. Andrew J. Bennet
Committee Member
Professor, Department of Chemistry

_____

Dr. Peter D. Wilson
Committee Member
Associate Professor, Department of Chemistry

_____

Dr. Melanie A. O'Neill
Internal Examiner
Assistant Professor, Department of Chemistry

_____

Dr. Martin E. Tanner
External Examiner
Professor, University of British Columbia

Date Defended/Approved: November 18th 2009

Declaration of
Partial Copyright Licence

ABSTRACT

One of the most pressing global issues in human health today includes the need to develop new, safer, and more effective vaccines against the ever increasing range of emerging, re-emerging, and antibiotic-resistant infectious diseases. The discovery that peptides could mimic the structure of microbial polysaccharides in carbohydrate-specific immunological reactions, and hence have potential as surrogate vaccines, is emerging as a new paradigm in vaccine research and development to replace traditional carbohydrate vaccines against microbial infections. While the basis and origin of mimicry at the molecular level between these two chemically unrelated molecules (carbohydrate and peptide), but functionally equivalent molecular structures have been determined, the requirements for immunogenicity of these carbohydrate-mimetic peptides in raising a long-lasting, cross-reactive protective immune response against the original microbial polysaccharides are currently unknown. This knowledge is fundamental for the development of effective surrogate vaccines to target microbial surface carbohydrates.

This thesis deals with the examination of the immunogenicity in mice of two carbohydrate-mimetic peptides, DRPVPY and MDWNMHAA, both identified from phage-displayed libraries, as mimics of the cell-surface polysaccharides of two pathogenic bacteria *Streptococcus* Group A and *Shigella flexneri* Y. As a crucial part of the studies, an efficient strategy has been developed to synthesize experimental vaccines comprising these two mimetic peptides, as well as a polysaccharide (ten repeating units) of *Shigella flexneri* Y. The results obtained

from the immunogenicity studies provide insight into the requirements for immunologically cross-reactive mimics of carbohydrates, as well as demonstrate whether these two mimetic peptides could be used as surrogates in the development of vaccines against the two respective bacterial pathogens.

Rational drug design, which is emerging as a powerful technique to improve upon initial discoveries, has been used in this thesis work to design a second generation of ligands for anti-carbohydrate antibodies, hopefully with much higher affinity. Two glycopeptides comprising features of both the original polysaccharide and the mimetic peptide have been designed by molecular modeling using information based on X-ray crystal structures of the two bound original ligands. Synthetic strategies have successfully been developed in this thesis work to synthesize the designed chimeric glycopeptides.

Keywords: vaccines, immunological, carbohydrate-mimetic peptides, immunogenicity, *Streptococcus* Group A, *Shigella flexneri* Y, immune response, design, glycopeptide, synthesis, modeling

DEDICATION

To my mother, sister and three brothers, with love, and gratitude for all their support and guidance, and to all my teachers and mentors who have inspired me, and always been supportive and encouraging in everything I have undertaken.

ACKNOWLEDGEMENTS

This thesis would not have been possible without the help and support of many people. I would like to thank all these people who have helped and inspired me during my doctoral study. First and foremost, I owe my deepest gratitude to my supervisor, Dr. B. M. Pinto, who has given me this golden opportunity to work in his laboratory and for always supporting me throughout my thesis work with his guidance and patience whilst allowing me the room to work in my own way. I attribute the level of my doctoral degree to his constant encouragement and faith in me, and without him, this thesis would not have been completed or written. One simply could not wish for a better supervisor. Thank you very much for everything.

I would also like to extend my deepest appreciation to the members of my supervisory committee, Dr. Andrew J. Bennet, Dr. Peter D. Wilson, and Dr. Jason Clyburn for all their support, patience and helpful suggestions.

Many thanks go to Dr. Blair D. Johnston for his assistance in the synthesis of the α-glycopeptide; Dr. Adewale A. Eniade for the synthesis of one of the peptides; Dr. Silvia Borrelli for performing the immunological studies; Dr. Margaret A. Johnson for her contribution in the immunochemical characterization study; Dr. Xin Wen and Yue Yuan for performing the modeling study.

I offer my enduring gratitude to all my laboratory colleagues, both past and present, for making the work environment a convivial place to work. I would also

like to thank them for all their support, help, and encouragement, which were very much needed during my doctoral study. Thank you very much.

My deepest gratitude goes to my family for their unflagging love and support throughout my life. I am indebted to my father, Fareed Hossany, for all his care and love. Although he is no longer with us, he is forever remembered. I am sure he shares our joy and happiness in the heaven. I also owe my deepest gratitude to my mother for showing much interest in my doctoral study as well as for her constant encouragement during my studies here in Canada. Furthermore, I am also very grateful to my twin sister, Rooksana, for all her encouragement and love. She had been a role model for me to follow unconsciously when I was a teenager, and has always been one of my best counselors. I am also indebted to my three brothers for their belief in me as well as for their constant encouragement.

I would also like to thank Department of Chemistry for its contribution in the completion of this thesis work, as well as Simon Fraser University for financial support.

Last but not least, heartfelt thanks be to God for my life through all tests and challenges in the past eight years. You have made my life more bountiful. May your name always be exalted, honored, and glorified.

TABLE OF CONTENTS

LIST OF FIGURES

LIST OF TABLES

LIST OF SCHEMES

ABBREVIATIONS

ABTS	Antibiotics
BALB	Barringer Laboratory
COSY	Correlation Spectroscopy
DBU	1,8-Diazabicyclo[5.4.0]undec-7-ene
DIC	N,N'-Diisopropylcarbodiimide
DIPEA	N,N-Diisopropylethylamine
DNA	Deoxyribonucleic acid
DMF	Dimethylformamide
DTBMP	2,6-di-tert-butyl-4-methylpyridine
EtOH	Ethanol
FAB	Fast Atom Bombardment
HBTU	*O*-Benzotriazole-N,N,N',N'-tetramethyl-uronium-hexafluoro-phosphate
HMQC	Heteronuclear Multiple Quantum Coherence
HOBt	N-Hydroxybenzotriazole
HPLC	High Performance Liquid Chromatography
HRMS	High Resolution Mass Spectrometry
KDO	2-Keto-3-deoxyoctulosonic Acid
KCN	Potassium cyanide
LC/MS	Liquid chromatography/Mass spectrometry
LSIMS	Liquid Secondary Ion Mass Spectrometry
MALDI	Matrix Assisted Laser Desorption Ionization

MBHA	4-Methylbenzhydrylamine
MHC	Major Histocompatibility Complex
NBS	N-Bromosuccinimide
NCBI	National Center for Biotechnology Information
NMR	Nuclear Magnetic Resonance
NMWL	Nominal Molecular Weight Limit
NOE	Nuclear Overhauser effect
NOESY	Nuclear Overhauser Enhancement spectroscopy
NBS	Phosphate buffered saline
PMB-Br	*p*-Methoxybenzyl bromide
RP	Reference point
SDS	Sodium dodecyl sulphate
STD	Saturation Transfer Difference
TFA	Trifluoroacetic acid
THF	Tetrahydrofuran
TIPSiH	Triisopropylsilane
TLC	Thin Layer Chromatography
TMSOTf	Trimethylsilyl trifluoromethanesulfonate
TOCSY	Total Correlation Spectroscopy
TOF	Time of Flight
DE	Delayed Extraction

Shoot for the moon.
Even if you miss, you'll land among the stars.

-Lee Brown

CHAPTER 1: GENERAL INTRODUCTION

As we enter the 21st century, infectious diseases continue to be a major threat to humankind, regardless of age, gender, lifestyle, ethnic background, and socioeconomic status. Out of the 57 million of all deaths each year, 15 million are directly attributed to infectious diseases (Figure 1-1).[1] After cardiovascular disease, they account for more deaths than cancer in developed countries,[2] while they remain the number one killer in developing countries[3], where children are the most affected, a direct effect of poverty, malnutrition, poor sanitation and hygiene, as well as low access to needed preventive care.[1,3] Besides being one of the leading causes of death, infectious diseases, which are commonly qualified as contagious, due to their capability of transmission from one person to another, or one species to another, are also responsible for much of human suffering and disability, imposing enormous financial burdens on societies, as well as disrupting entire populations, economies, and governments worldwide.

Even though, infectious diseases have plagued us since the dawn of time, it was not until the early 19th century that it was recognized that infectious diseases, which are human illnesses that impair the ability of the body to function, are caused by microscopic organisms.[4-6] Today, it is recognized that these organisms include bacteria, viruses, fungi, protozoa, multicellular parasites, and aberrant proteins known as prions, each responsible for a particular disease that can range from mild to deadly.[4-6] These disease-causing microorganisms,

which are often referred to as microbes, or pathogens, owe their major success as human pathogens in many cases to their ability to utilize host's resources to colonize, and rapidly multiply and spread throughout the body, while evolving efficient strategies to evade, subvert, or circumvent the human's immune defenses.[7,8,9,10]

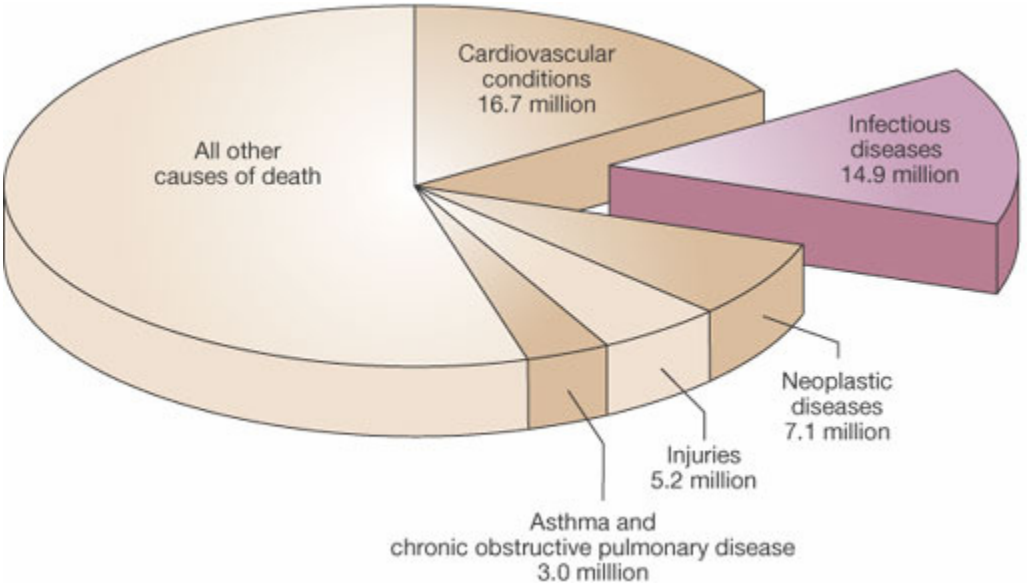

Figure 1-1: Leading causes of death worldwide. (Figures published by the World Health Organization, http://www.who.int/whr/en and ref. 1).

Despite the fact that more than 150 antibiotics have been developed in the 20th century that have saved millions of lives, and cured many of the deadliest infectious diseases that were long thought to be incurable, the mistake that was made with the use of antibiotics was to go blindly toward a "quick remedy" in order to control infectious diseases.[11-13] The use of these novel "wonder drugs"

that were based merely on empirical discovery worked for some time, but not as well, or for as long as they should have been. Misuse of these antimicrobial agents in clinics for treating common infectious diseases, together with the extensive use of antibiotics in agriculture in feed to livestock, have instead tilted the balance in favor of the microbes, which are constantly evolving to adapt to new challenges. The microbes' genetic flexibility in conjunction with the selective force of the overuse of antimicrobial drugs has resulted not only in a global-Darwinian evolution of antimicrobial-resistant microbes (natural selection and the survival of the fittest), but also in those with stronger virulence factors, and higher adaptability. New strains of old microbes responsible for causing diseases such as tuberculosis, measles, staphylococcal and streptococcal infections, once believed to be conquered by the use of antibiotics are now reappearing with stronger virulence factors to an unusual extent, causing more severe infections, particularly in immunocompromised patients, children, and older people.[11-14] The last three decades have not witnessed the discovery of new classes of effective antimicrobial agents, and as soon as new derivatives of current antibiotics are introduced, they soon encounter resistance.[11-14] Although there has been rapid development in detection techniques and accurate diagnosis methods for identifying novel pathogens, and application of control measures such as improvements in nutrition, housing, sanitation, hygiene, and the availability of safer food and water that can control microbial infections, there is still a desperate need for new anti-infective agents to eliminate current, and re-emerging diseases that were previously treated with conventional antibiotics, in

order to reduce the world death toll by infectious agents, and the burden they are imposing on societies.

According to a World Health Organization report released in 2007,[15] not only known and re-emerging infectious diseases continue to spread at a higher rate than at any time in history, but also newly emerging infectious diseases are being discovered at an alarming rate, more rapidly than ever before. Over 1000 new infectious diseases that have the potential to quickly become global epidemics were identified in just the past five years.[15] Recent outbreaks and epidemiologic studies predict that while the world's population continues to grow, together with the rapid changes in society, technology, and the environment, as well as, changes in microbial evolution and adaptation, so is the incidence of new emerging infectious diseases worldwide. While our environment is being highly exploited, in every corner of the globe to accommodate more people as well as to allow a higher quality of life, it is this very act of exploitation that is disrupting many ecosystems, and is having a negative impact on the human-microbe interaction, allowing humans to be highly exploited as new hosts by entirely new classes of microorganisms, previously inhabiting non-human vertebrates or plants, (natural pathogen reservoirs), but which have evolved capabilities to infect humans.[7,9,16,17]

Although, our increasing global interconnectedness has created economic opportunities and growth throughout the world, the globalization of food supply, the expansion of international travel and commerce, and the development of mega cities that concentrate people in huge cities, at the same time, are creating

such opportunities for the global spreading of infectious diseases.[18] Moreover, the faster the speed, and the further the distance people, products, and food travel, the more likely a small, newly localized outbreak can develop into a large worldwide epidemic in a matter of days due to the ease in which infectious agents, vectors, contagious contaminated hosts, and the increased overlap between human and pathogen habitats are spreading around the world.[19] Moreover, with the current increase in global temperature[20,21] due to global warming, the spatial distribution of certain disease-carrying vectors, for example, mosquitoes, from warmer to colder regions is extending, while extreme weather events associated with global warming, such as flooding, high intensity storms, and drought are contributing highly to the increased transmission of a variety of new emerging infectious diseases among populations.[20-24] Not only microbial organisms are emerging and re-emerging as new disease treats, but they are also found to be linked to chronic diseases including ulcers, coronary artery disease, diabetes, multiple sclerosis, chronic lung diseases that were long thought to be non-infectious.[25,26] In addition, the intentional use of highly virulence microbes to cause sudden, massive, and devastating epidemics of diseases, as a potential weapon of war among terrorists, individuals, and rogue nations is a growing fear among countries in the sudden spreading of deadly infectious diseases.[27]

Owing to the ability of microbes to mutate at such a faster rate as well as current lifestyles, an entirely new paradigm for fighting infectious diseases is needed, one which, unlike antibiotics, is not only fast, but specific and long-

lasting, in order to prevent the development of microbial resistance. With the advent of DNA sequencing technology, Polymerase Chain Reaction (PCR) techniques, more sophisticated electron microscopes, the exploitation of cell biology, and cellular immunology, the impact of crystallographic methods, and other molecular structure-function studies, we now have the opportunity to understand the fundamental factors that underlie the mechanisms of pathogenicity by microbes, their evolutionary pathways, as well as the genes that encode their virulence factors.[28] It is these understandings that will eventually allow us to devise better means to combat current, new emerging, and re-emerging pathogens.

Infections by microbes and host defenses are always in a dynamic equilibrium that is dependent on two major factors, the pathogenicity (virulence factors) of the pathogens, and the rapidly responding immune system of the host. If this balance could be shifted in favor of the human immune system, this may lead us to one-step ahead of these agents, no matter how fast and strong their virulence factors are evolving. Vaccines, unlike antibiotics, have the capability to boost the effector mechanism of the host immune system and potentially shift this equilibrium in favor of the host are now being exploited as powerful means, to eradicate deadly infectious diseases, to reduce the death toll as well as the burden infectious diseases impose on societies.[29]

1.1 The emergence of bacteria

As far as we are able to tell from the fossil record, bacteria, which are responsible for causing 90% of all infectious diseases, arose some 3.5 billions years ago, and successfully monopolized the planet for the next two billions years by proliferating and spreading in all elements of earth, air, water, and soil, as well as inhabiting every conceivable niche including the coldest, hottest, most acidic, and most highly pressurized environments.[30-33] What was crucial for their flexibility, adjustment and adaptation to the existing harsh and unliveable conditions, including constant environmental changes, was their ability to constantly mutate their genes, and most importantly, share these acquired genes among colonies to allow them to adapt and live in diverse environments. Consequently, they have evolved to display a substantial range of diversity in structure, nutrition, metabolism, and reproduction, accounting for their most abundant form of life on earth in terms of both biomass and total number of species of all time.[34] Not only were these single celled organisms the first living things on Earth, but were also crucial to the Earth's evolution. It was these microscopic organisms that for the billions years had slowly transformed the poisonous atmosphere of earth into one that contained enough oxygen to sustain complex and multicellular forms through the action of photosynthesis.[35,36] With their underlying ability to recycle the essential elements needed to build biological systems, such as phosphorus, calcium, iron, carbon, oxygen, hydrogen, magnesium, potassium, sulfur, and many more, they also created a

suitable environment including chemical conditions necessary for the survival of those larger life forms that arrived later on earth.[36,37]

Even though bacteria were the oldest organisms on Earth, it was not until 1674 that the Dutchman Antony Van Leeuwenhoek first proved their existence under a microscope as unicellular organisms with an average size of 0.5-1.0 µm in diameter and 2.0 to 5.0 µm in length.[38,39] Because of the absence of a membrane bound nucleus and other organelles such as mitochondria or chloroplast,[40] they were later further characterized as prokaryotes, and were found in Nature to exist mainly as spherical (cocci), rod-like (bacilli), or spiral (spirilla) shape (Figure 1-2).[41] A typical bacterial cell commonly consists of a fairly rigid layer of cell-wall[42] that surrounds a thinner cytoplasmic membrane in which the ribosomes, some inclusions, and nucleoid are moving freely into the cytoplasm.[43-46] Although they may be described as "primitive unicellular cells", they are capable of exhibiting all life processes such as growth and multiplication, including metabolism, allowing them to successfully grow and reproduce on their own, to take-in, and digest organic and inorganic matter, to get rid of toxic matter, and waste products, and more importantly to constantly mutate to adapt to new environments.[47-50] Even though bacteria do not develop or differentiate into multicellular forms, they often combine in regularly structured aggregates called colonies, usually for mutual benefit, such as stronger defenses or the ability to attack bigger prey.[51]

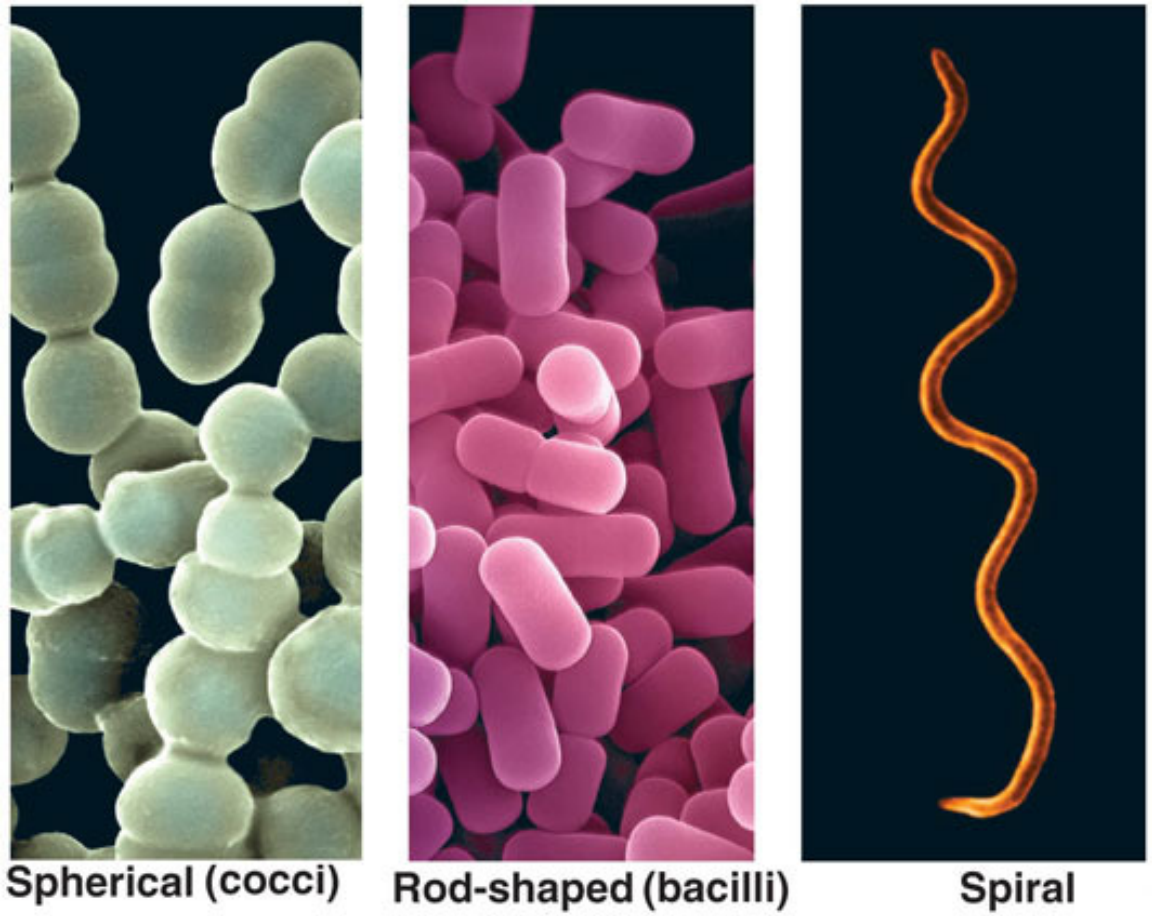

Figure 1-2: Different shapes of bacteria. (Figure published by University of Miami, http://www.bio.miami.edu/~cmallery/150/proceuc/proceuc.htm).

Like any other living organisms, each bacterium is recognized by a scientific name most often Latinized, which comprises two parts, its genus preceding its species.[52,53] The scientific name is often associated either with the characteristics of the organism such as on the basis of their metabolism, or describing the habitat of the species, or simply to honor a researcher.[52,53] On the other hand, among the practical methods to differentiate groups of species from

such a diverse mass of different bacteria, which are commonly based on cell-shape, nature of multicell aggregates, motility, and formation of spores, reaction to the Gram stain is the most commonly used method.[54,55] This stain distinguishes between two fundamentally different kinds of bacterial cell-wall and reflects a natural division among bacteria. Gram-positive bacteria are those that are stained violet by Gram staining because of the higher amount of peptidoglycan in their cell-wall that reacts to give the positive coloration, while Gram-negative bacteria are those that cannot retain this crystal violet stain mainly due to the presence of an extra outer layer on their cell surface that covers their peptidoglycan cell-wall.[54,55] Figure 1-3 and Table 1-1 summarize the differences between Gram-positive and Gram-negative bacteria.

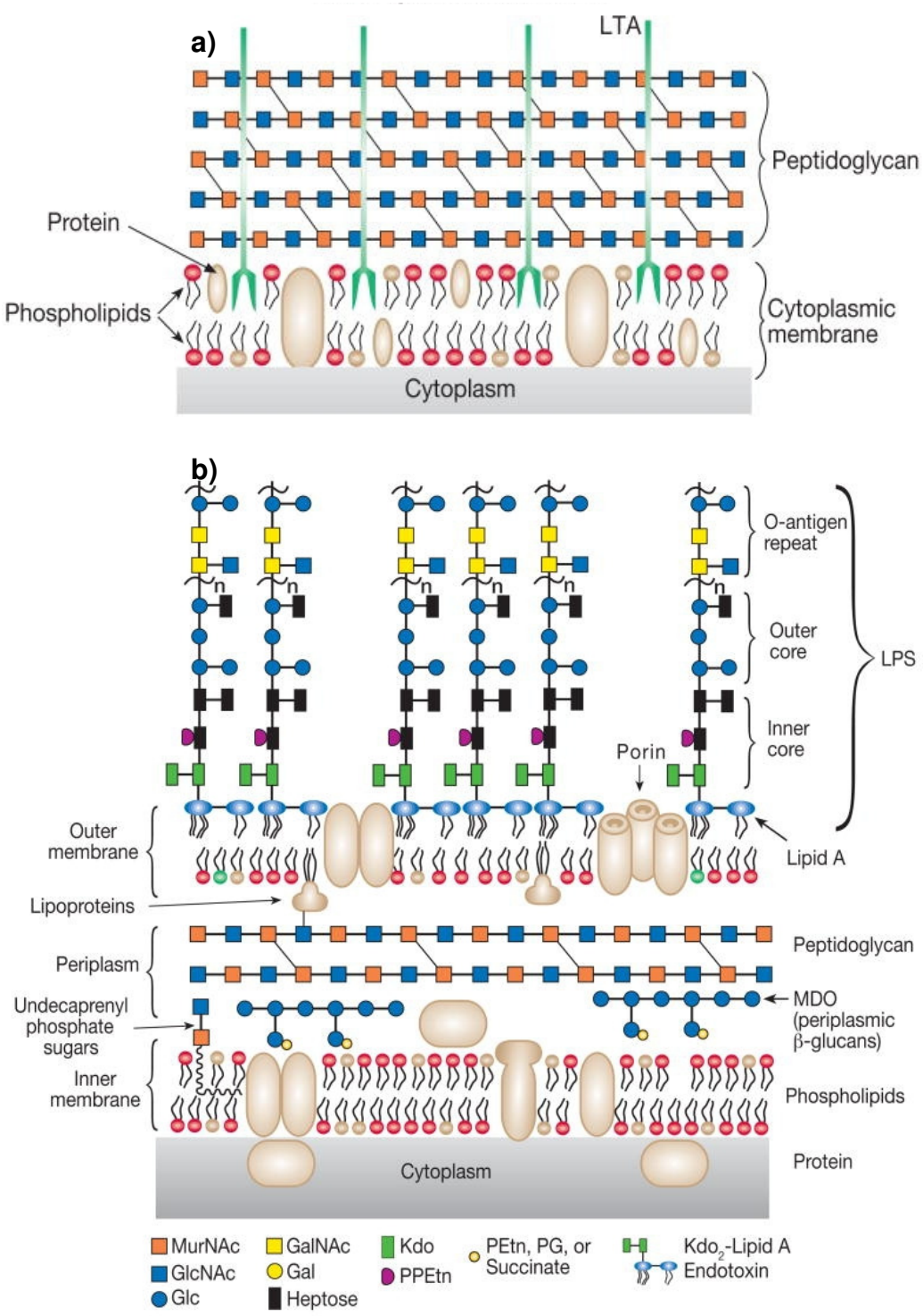

Figure 1-3: Schematic representation of the cell wall of (a) Gram-positive bacteria showing lipoteichoic acid (LTA), peptidoglycan, cytoplasmic membrane, and cytoplasm, (b) Gram-negative bacteria showing lipopolysaccharides (LPS) of

the outer membrane, peptidoglycan, phospholipids, and cytoplasm. (Figures published by Cold Spring Harbor Laboratory Press, http://www.ncbi.nlm.nih.gov/bookshelf/br.fcgi?book=glyco2&part=ch20).

Table 1-1: Major differences between Gram-positive and Gram negative bacteria

Gram-positive bacteria	Gram-negative bacteria
The cell-wall or peptidoglycan is relatively thick	Peptidoglycan constitutes a thin layer
No outer membrane. Presence of capsule (polysaccharide chains)	Outer membrane consists of LPS, surface proteins, and phopholipids. Absence of capsule.
No distinct periplasmic space	A distinct periplasmic space separating outer and inner membrane
Teichoic acids are covalently bonded to the peptidoglycan	No teichoic acids
No LPS	LPS content is high
Lipid and lipoprotein contents are low	Lipid and lipoprotein contents are high
Toxins produced are mainly exotoxin	Toxins produced are mainly endotoxin

Although bacteria have evolved to thrive in a variety of extreme environments, most flourish best in conditions that also support other living organisms such as the mild environment of the latter. With their tremendous diversity in structural and functional organization, bacteria have developed a very high affinity for eukaryotic cells of all organizational hierarchies including man that evolved much later, to perpetuate their survival. These relationships involve

a large variety of interactions including mutualistic, where both organisms benefit from the association, commensal, where one of them benefits, while the other is unaffected, and parasitic, where the bacteria live off a host while the host is often severely damaged.[56] Shortly after birth, the human body, especially the skin and parts of the digestive system, are quickly colonized by trillions of bacteria, upon which our many basic bodily processes depend on, such as fighting off other disease-causing microbes by occupying the spaces, digesting polysaccharides for which we have no enzymes, synthesizing vitamin K, and absorbing certain nutrients.[57,58] It is indeed very rare that this commensal relationship between man and these bacteria become harmful, partly because they lack specific genetic information that would allow them to cause harm, but most importantly due their inability to survive the powerful immune defenses that humans have developed to protect themselves from invasion. Nonetheless, those that have developed into human pathogens are those that have evolved elaborate strategies for overcoming the host immune defenses, and in addition, have the capability of sharing the acquired genes that express their new faculties both among colonies, as well as, across species, hence constantly turning harmless variants into virulent ones that can severely damage their host.[56] With the effect of overuse of antibiotics on the normal microbial flora, there is now a growing increase in disease-causing pathogenic bacteria that are derived from the harmless commensal bacteria that reside in the human body.[59]

1.2 Host immune defenses

Evolutionary studies showed that vertebrates, which are surrounded by a sea of microbes, have inherited an evolutionarily conserved, rapid defence mechanism, originating from their invertebrate ancestors.[60-62] It is the natural immunity one is born with and is ready from the moment we are born, to attempt to destroy within hours all invading microorganisms from any sites of the body before they could establish an infection. What make this innate defense system so successful and powerful is its ability to block entry of most potential pathogens, as well as, recognizing those that break in as non-self, and more importantly can react immediately with these non-self molecules, while producing its own chemicals and cells to eliminate the foreign invaders.[61-63]

Therefore, from the physical surface barriers to the production of millions of specialized effector cells, intracellular sensors, and signaling molecules that harmoniously function together in recognizing, attacking, and destroying foreign particles, this incredible dynamic regulatory-communications network of innate immunity results in a sensitive system of surveillances and balances that produce an immune response that is prompt, appropriate, effective, and self-limiting for all multicellular forms. This system has become the cornerstone of the ability of all living organisms, including plants, to fight against those microbes that have evolved to exploit the advantages of growth in other living organisms.[61-63]

1.2.1 Innate defenses against bacterial invasion

Before pathogenic bacteria are able to colonize the body and cause disease, they must overcome a series of non-specific defenses of the innate immune system. While most of them cannot penetrate the keratinized skin barrier of the innate system,[64] many others are constantly being trapped by the mucous membrane that line the main portals of entry when the skin is intact, such as the gastrointestinal, respiratory and urinogenital tracts.[62,63,65] Similarly, some body tissues such as oral cavity, eye, and genital organs are continually being flushed with saliva, tears, and urine, respectively, in order to prevent pathogenic bacteria from adhering to the corresponding body tissues.[33,62,63] The importance of the epithelia (skin and mucous membrane) in innate immunity is obvious when they are breached as in cuts, abrasions, injury, and burns, exposing the body tissues, where bacterial infection is a major cause of mortality and morbidity.[33,62,63] In the absence of wounding or disruption, many bacteria evolving as human pathogens often overcome these physical barriers either by secreting specialized enzymes that can digest the skin and the mucous layers, or inserting a hollow tube directly into the sub-epithelial tissue layer or blood vessel to deposit their toxic substances, or simply by directly being inoculated into the body by the help of a vector, such as a mosquito bite, or often via contaminated syringes.[33,62,63]

Once inside the body, the intruders are immediately recognized by the innate immune components, which are normally concentrated in blood, tissues, and at sub-epithelial surfaces. Those pathogens that are encountered in the

blood are usually susceptible to opsonization by the alternative pathway of complement activation by a group of plasma proteins.[33,62,63] However, some bacteria have devised specialized capsules, coats made up of long chains of sugar molecules (polysaccharides), or protective outer membranes to resist the action of the complement system. In order to overcome this problem, the innate immune system has developed large professional phagocytes called neutrophils (Figure 1-4a) that are capable of eliminating such bacterial pathogens mainly by the action of phagocytosis.[33,62,63] While the neutrophils actively protect the blood, macrophages (Figure 1-4b) are another class of long-lived phagocytic cells that are extremely efficient in constantly phagocyting bacterial pathogens both inside and outside the interstitial spaces of tissues. Basophils (Figure 1-4c), mast cells (Figure 1-4d) and eosinophils (Figure 1-4e), on the other hand, are other white blood cells that play crucial roles in eliminating pathogens especially on the epithelial surfaces that line the gastrointestinal, respiratory, and urinogenital tracts. These phagocytic cells (Figure 1-4), which are rich in lysosomes comprising a number of hydrolyzing enzymes, normally engulf these bacteria by means of their pseudopodes and transport them inside their vacuoles, which then fuse with the cell lysosomes forming phagolysosomes, within which the bacteria are hydrolyzed and successfully destroyed by the hydrolyzing enzymes.[33,62,63]

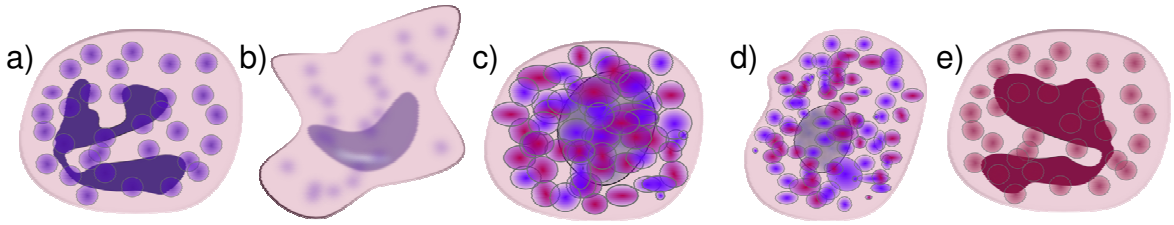

Figure 1-4: Structures of the (a) neutrophil, (b) macrophage, (c) basophil, d) mast cell, e) eosinophil. (Figures published by Royalty free & Public Domain, http://www.clker.com.).

Since, the external surface of microbial pathogens is the principal interconnection between host and pathogen, the exposed surface components are therefore the key signatures that are recognized by the immune system as non-self, and are hence, the principal targets of the immune system in microbial clearance. To be able to provide a rapid response to such a large subset of potential pathogens, innate immunity operates via evolutionary conserved pattern recognition receptors, recognizing conserved surface components of pathogens that are not shared by their host, but are shared among many related pathogens.[62,66] These conserved surface components that are being recognized are normally very essential to the integrity, function or replication of microbes, and are so crucial for their survival that they are relatively invariant and do not evolve rapidly by mutation. In fact, for each of these unique microbial conserved surface molecules, which are known as Pathogen-Associated Molecular Patterns (PAMPs), there exists a corresponding Pattern Recognition Receptor (PRR) found in one or more of the cells within the innate defense network, thus allowing

innate immunity to recognize and eliminate such a diverse range of microbes.[62,66] In the case of bacteria, the complement system normally recognizes conserved proteins on their surfaces, while the phagocytes comprise PRRs that usually recognize LPS that protrude from the outer membrane of Gram-negative bacteria (Figure 1-3b), and have high affinity for peptidoglycan and lipoteichoic acids of Gram-positive bacterial cell-wall (Figure 1-3a), as well as lipoproteins and sugar moieties found on their capsules. It is estimated that several hundred PRRs that form the bedrock of innate immunity, exist in the mammalian innate defense system and their role in the receptor-ligand interaction is so crucial that all their genes are preserved to ensure limited variability in their molecular structures.[62,66]

Not only are the immune components of innate immunity immediately available to combat a wide range of bacteria, but through their PRRs that recognize the signature surface molecules of microbes (PAMPs), are also activated to produce small specialized glycoprotein mediators called cytokines that amplify the immune response to microbial infection.[62,66] Their release, which results in an increase in the permeability of blood vessels, as well as, changing their adhesive properties, allows additional immune cells and other molecules of the immune system to move rapidly to sites of infection. The net result, which is referred to as acute inflammatory response, is an aggressive immune attack on the colony of the bacterial cells by an army of immune cells and molecules that function collectively to clear up the invaders. This inflammatory response is often characterized by symptoms such as heat, redness, swelling and pain, associated with an immune response against microbes in tissues.[62,63,66]

1.2.2 The adaptive immune system

As microbes continue to exert a permanent, and strong evolutionary selection pressure on multicellular organisms, the pre-existing innate defense systems, which are only limited to those pathogens that bear surface molecules that are common to many pathogens, cannot always protect against all infections.[62] While the recognition system of the innate immune system has remained unchanged in the course of evolution, the surface molecules of some pathogens, on the other hand, are evolving so rapidly that they are rarely recognized by the PRRs of phagocytes, and hence prevent induction of an immune response against them.[62] Other successful strategies by microorganisms involve blocking one or more of the steps in phagocytosis, thereby inhibiting the anti-microbial process. Table 1.2 describes some of the common ways pathogenic bacteria have developed to overcome innate immunity.[36]

Table 1-2: Bacterial interference with phagocytes

BACTERIUM	TYPE OF INTERFERENCE	MECHANISM
Streptococcus pyogenes	Kill phagocyte	Streptolysin induces lysosomal discharge into cell cytoplasm
	Inhibit neutrophil chemotaxis	Streptolysin is chemotactic repellent
	Resist engulfment (unless Ab is present)	M Protein on fimbriae
	Avoid detection by phagocytes	Hyaluronic acid capsule

Staphylococcus aureus	Kill phagocyte	Leukocidin lyses phagocytes and induces lysosomal discharge into cytoplasm
	Inhibit opsonized phagocytosis	Protein A blocks Fc portion of Ab; polysaccharide capsule in some strains
	Resist killing	Carotenoids, catalase, superoxide dismutase detoxify toxic oxygen radicals produced in phagocytes
	Inhibit engulfment	Cell-bound coagulase hides ligands for phagocytic contact
Bacillus anthracis	Kill phagocytes or undermine phagocytic activity	Anthrax toxin EF
	Resist engulfment and killing	Capsular poly-D-glutamate
Streptococcus pneumoniae	Resist engulfment (unless Ab is present)	Capsular polysaccharide
Klebsiella pneumoniae	Resist engulfment	Polysaccharide capsule
Haemophilus influenzae	Resist engulfment	Polysaccharide capsule
Pseudomonas aeruginosa	Kill phagocyte	Exotoxin A kills macrophages; Cell-bound leukocidin
	Resist engulfment	Alginate slime and biofilm polymers
Salmonella typhi	Resist engulfment and killing	Vi (K) antigen (microcapsule)
Salmonella enterica (typhimurium)	Survival inside phagocytes	Bacteria develop resistance to low pH, reactive forms of oxygen, and host "defensins" (cationic proteins)
Listeria monocytogenes	Escape from phagosome	Listeriolysin, phospholipase C lyse phagosome membrane
Clostridium perfringens	Inhibit phagocyte chemotaxis	ø toxin
	Inhibit engulfment	Capsule
Yersinia pestis	Resist engulfment and/or killing	Protein capsule on cell surface

Yersinia enterocolitica	Kill phagocytes	Yop proteins injected directly into neutrophils
Mycobacteria	Resist killing and digestion	Cell wall components prevent permeation of cells; soluble substances detoxify of toxic oxygen radicals and prevent acidification of phagolysosome
Mycobacterium tuberculosis	Inhibit lysosomal fusion	Mycobacterial sulfatides modify lysosomes
Legionella pneumophila	Inhibit phagosome-lysosomal fusion	Unknown
Neisseria gonorrhoeae	Inhibit phagolysosome formation; possibly reduce respiratory burst	Involves outer membrane protein (porin)
Rickettsia	Escape from phagosome	Phospholipase A
Chlamydia	Inhibit lysosomal fusion	Bacterial substance modifies phagosome
Brucella abortus	Resist killing	Cell wall substance (LPS)
Treponema pallidum	Resist engulfment	Polysaccharide capsule material
Escherichia coli	Resist engulfment	O antigen (smooth strains); K antigen (acid polysaccharide)
	Resist engulfment and possibly killing	K antigen

Consequently, higher vertebrates, including mammals have responded with the development of a more specific, more complex and organized multilevel defense system, known as induced or adaptive immunity (Figure 1-5), which has evolved to overcome these problems by reinforcing the mechanism of innate immunity with a more elaborate recognition system and a more efficient effector mechanism that are unique to the adaptive immune system.[62] Although most infectious agents are successfully cleared up by the early innate defenses, the

adaptive immune system, however, is required when the innate host defenses are overwhelmed, bypassed, or evaded by foreign organisms, or by their poisonous by-products. It normally takes over after the pathogens have succeeded in lodging themselves within the cells, or tissues, but eliminates the infection before disease normally occurs. The adaptive immune system consists of a sophisticated network of specialized cells, mediators, and organs (Figure 1-5), that work in synergy with the innate immune system to eliminate an endless amount of foreign invaders. It gets its name from the fact that once it is activated, it has the ability to modify itself, and potentially adapt to any weapon that the invading pathogen throws at it. The remarkable variety of pathogens that overcome the innate immunity has required the adaptive immunity to develop three very crucial universal features, which are: (1) specificity, (2) diversity, and (3) memory. It is said to be specific because instead of bearing receptors that can recognize several common conserved components, the recognition system of adaptive immunity allows each immune cell to specifically recognize and target a conserved surface molecule of a pathogen.[62] Moreover, it is characterized as diverse because, although each individual adaptive immune cell carries the receptor of one specificity in order to have room for matching all possible foreign molecules that may exist in the universe, the specificity of each cell is different, and hence, with trillions of such immune cells in the body, any conceivable foreign molecule together with all its possible mutated forms it may eventually encounter can be recognized. Each specific immune cell, upon encountering its matched molecule is then stimulated to proliferate into a full-scale colony of the

same specificity to target the invader. This clonal selection of the adaptive immune cells is the single most important principle that makes adaptive immunity largely effective over the innate one. In addition to the successful clearance of infectious agents that failed to be eliminated by innate immunity, adaptive immunity is said to have memory because it improves in efficiency on repeated exposures to a given infection by "remembering" the invader. Therefore, faster and stronger attacks are mounted each time the same pathogen is being encountered without restimulation, by mechanisms that are not fully understood, since for some infectious agents, this protection is essentially absolute, while for others, infection is reduced or attenuated upon re-exposure by the same infectious agents. In general, the host is rendered resistant to those particular microorganisms throughout its lifetime, making this immune system largely effective even in the face of concerted evolutionary selection for evasion by pathogens.[62]

The adaptive immune system is mediated mainly by two classes of leukocytes called B-lymphocytes (B-cells) and T-lymphocytes (T-cells), which are derived from precursors in the bone marrow, but only B-cells mature there while T-lymphocytes migrate to the thymus to complete their maturation (Figure 1-5).[62] Any foreign substances that are recognized as non-self by lymphocytes are termed antigens, and are referred to as immunogens if they are large enough on their own to stimulate an adaptive immune response. Most macromolecules including all proteins, most polysaccharides, nucleoproteins, lipoproteins, and various small molecules linked to proteins or polypeptides are capable of

stimulating an adaptive immune response, and are therefore excellent immunogens. Since the binding sites of lymphocytes are only 600 to 1700 Å, these receptors specifically recognize a portion of the complex antigens, which is known as an antigenic determinant or epitope.[67,68]

Unlike the phagocytic cells of innate immunity, the antigen receptors of lymphocytes, due to their higher affinity and immense diversity, do not distinguish components of microbial agents from harmless ones. It is therefore the innate immune system, which alerts the more developed adaptive immune system to the fact that pathogen invasion has begun, and more importantly determines which pathogen molecules the acquired immune system needs to respond to; the nature of these responses is also controlled in order to prevent autoimmune reactions to self-determinants. Since, it is very unlikely that the very few number of lymphocytes of each specificity among the trillion lymphocytes will encounter its matching antigen, adaptive immunity is equipped with a specialized architecture of tissues called the lymphoid tissues (Figure 1-5), which are highly organized to collect antigens from any site of infection throughout the body and ensure that each antigen is continually brought into contact with the lymphocytes in the lymphoid organs to initiate adaptive immune responses. The spleen, which is a fist-sized organ just behind the stomach, collects antigens from the blood, the lymph nodes, which are highly organized lymphoid structures, collect antigens from tissues, and the mucosal-associated lymphoid organs collect antigens from epithelial surfaces (Figure 1-5). Since pathogenesis of microorganisms occurs either outside or inside cells, adaptive immunity has

evolved two major arms, which are the humoral and cell-mediated immunity arms that specifically target extracellular and intracellular pathogens respectively (Figure 1-5).[62]

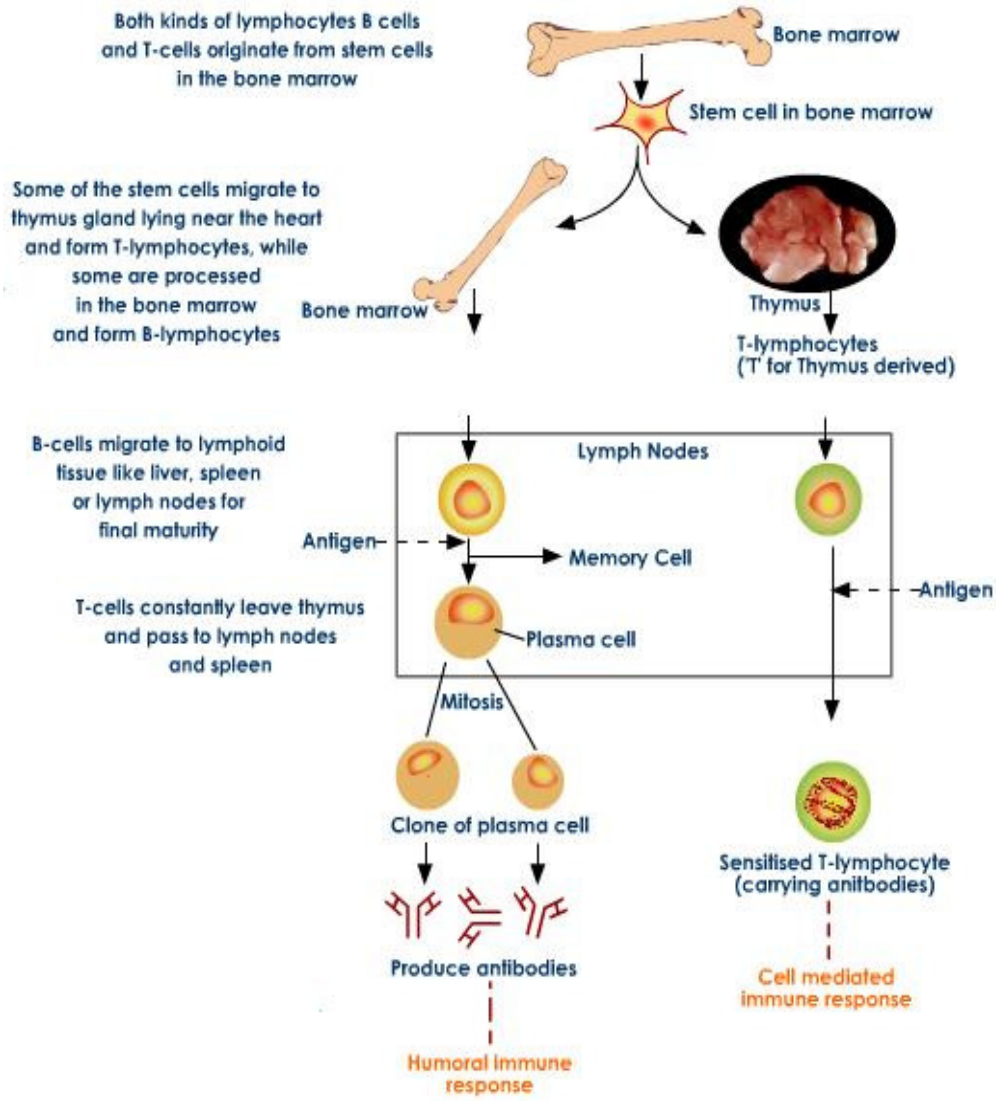

Figure 1-5: The adaptive immune system.

1.2.2.1 Humoral immune response against bacterial infection

Bacteria that are human pathogens are mainly obligate extracellular organisms and cause infection either in the blood or in the interstitial spaces of body tissues depending on their mode of entry. Their clearance, which is very crucial for the survival of the host, is normally achieved by antigen-specific soluble antibodies secreted by B-lymphocytes of the humoral immunity system on their first encounter, and memory cells that prevent subsequent re-infection with the same pathogenic bacteria.[62]

During an invasion by bacteria that persists in the extracellular spaces or in the blood, while the phagocytes are actively controlling and holding the infection, it is the dendritic cells, a specialized class of phagocytes that collect large amounts of microorganisms at the site of infection, mainly by non-specific means, internalize them, and break them into small peptide fragments, travel to the nearest lymphoid organs, and display these peptide antigens for recognition by corresponding T-lymphocytes, which have very high affinity for small peptide antigens; this process induces an adaptive immune response (Figure 1-6).[62] When a naïve T-lymphocyte recognizes its matching antigen on the surface of a professional antigen-presenting dentritic cell in the lymphoid organs, signaling through the T-cell receptor induces the association between the antigen-presenting cell and the antigen-specific T-cell, which can persist for several days during which the naïve T-cell proliferates, and its progeny differentiate into effector helper T-cells known as CD4-helper T-cells that respond quicker and more efficiently than the naïve T-cell. This activation of the naïve T-cell into

armed effector helper T-cells is the crucial first step in adaptive immunity against extracellular microbes (Figure 1-6).[62]

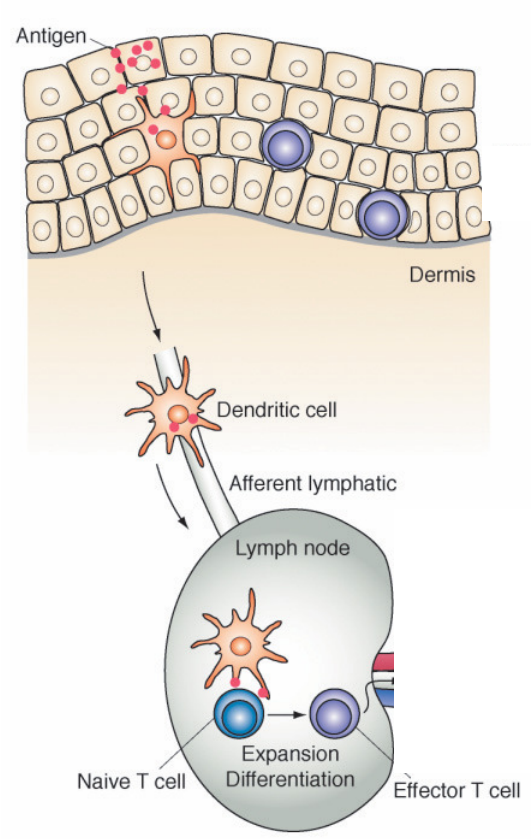

Figure 1-6: First step in the humoral immune response: activation of T-cell by the professional antigen-presenting cell, the dendritic cell. (Figure originated from that published by Osaka University, http://www.biken.osaka-u.ac.jp/COE/eng/project/pro14.html).

The effector phase of humoral immunity (Figure 1-7) is initialized when a B-cell exhibits on its surface an immunoglobulin receptor specific for an epitope

of the same protein antigen, from which the peptide fragment recognized by the original naïve T-cell is derived from. The surface immunoglobulin antigen receptor then internalizes the infectious agent to where it is degraded and from where it is returned to the surface of the B-cells as peptide epitopes bound to MHC class II molecules. The effector helper CD4 T-cells, on recognition of its corresponding peptide epitope, in turn, trigger the B-cell to proliferate into identical B-cell copies. The latter differentiate into antibody-secreting plasma cells, and memory cells. The plasma cells then secrete millions of antibodies that leave the lymphoid organ and are widely distributed throughout the body to carry out the ultimate goal of combating the infection, while the memory cells allow both a quantitatively and a qualitatively superior secondary response to be mounted after a subsequent encounter with the same antigen (Figure 1-7). It is vital that the peptide recognized by the T-cell be a part of the antigen recognized by the B-cell, even though the epitope recognized by the two lymphocytes need not be the same, so that upon internalization of antigen bound to the surface immunoglobulin of the B-cell, the specific peptide that activates the original naïve T-cell to differentiate into effector helper T-cells could be produced.[62]

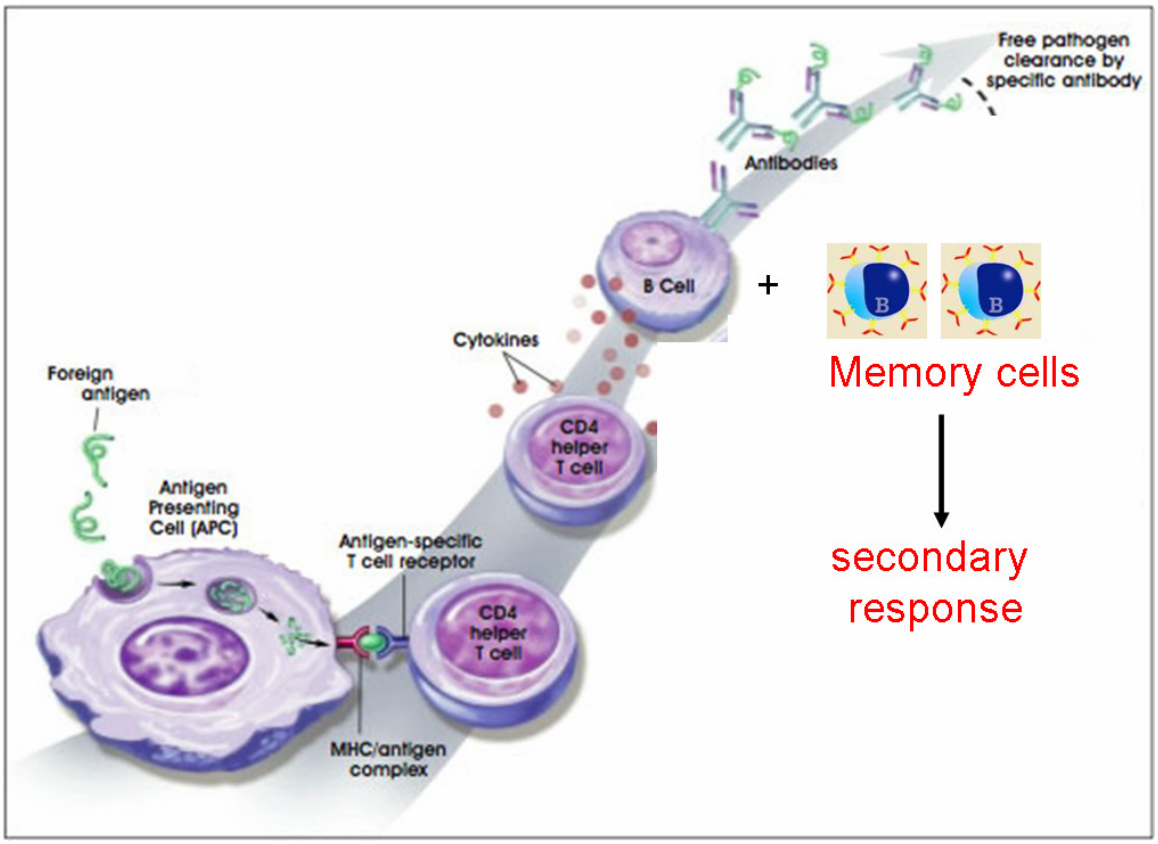

Figure 1-7: The effector phase of humoral immunity. (Figure originated from that published by Terese Winslow, http://stemcells.nih.gov/info/scireport/chapter6.asp).

Some microbial antigens such as polysaccharides are T-cell independent antigens (TI-2) that can activate B-cells directly to rapidly produce antibodies without activation by helper T-cells (Figure 1-8a).[62] This adaptive response plays a critical role in rapidly defending against many important bacterial pathogens, especially against those, which have the capability of replicating at a faster rate. However, the class of antibody (IgM) produced is of low affinity, less variable,

and less functionally versatile than those (IgG) induced when T-cells are involved (Figure 1-8b).[62]

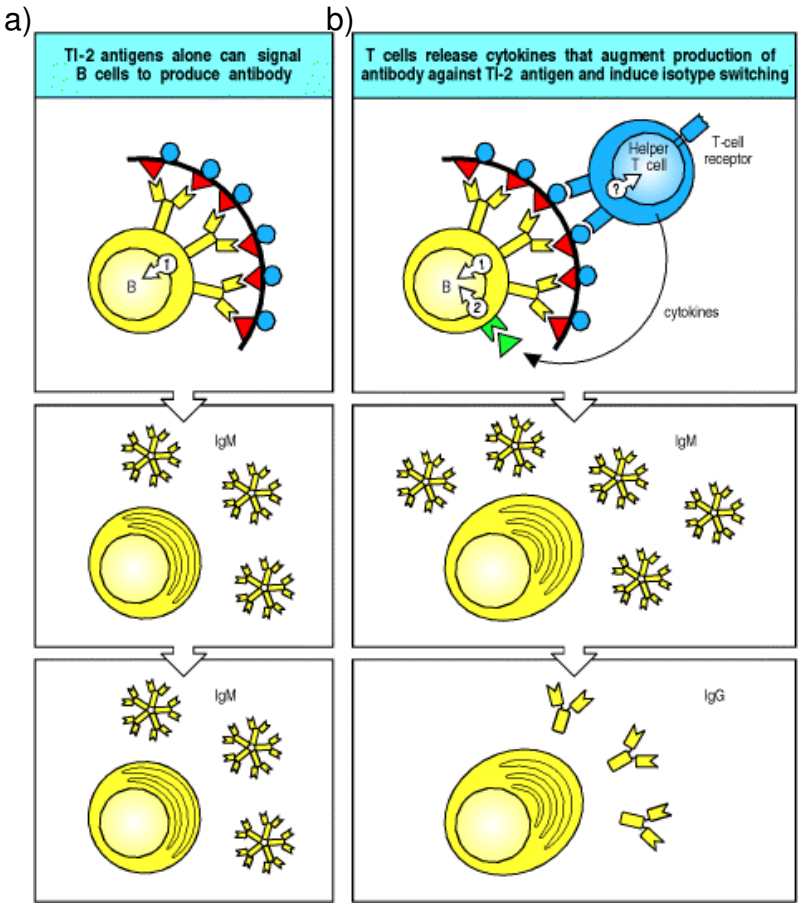

Figure 1-8: (a) T-cell independent (TI-2) immune response, (b) T-cell dependent immune response. (Figure published by Garland, http://www.ncbi.nlm.nih.gov/b-ooks/bv.fcgi?rid=imm.figgrp.1210).

1.2.2.1.1 Immunoglobulins

Antibodies, which are the secreted form of the membrane-bound antigen receptor of B-lymphocytes of the adaptive immune response to extracellular invading pathogens, play a major role both in the recognition of specific antigens, as well as in their versatility as effector molecules in humoral immune responses that ultimately lead to the destruction of the invading pathogens. These antibodies, which are also known as immunoglobulins (Ig),[69] are heavy globular plasma proteins (~150kDa) with sugar chains attached to some of their amino acid residues. While the proteins provide the backbone including the antigen-binding sites, as well as the effector action of the antibody, the carbohydrates, on the other hand are believed to play a role in recruiting other elements of the immune system that aid in the elimination of microbial infections.[62,70]

While billions of different specificities are produced by the B-lymphocytes, the general structure of antibodies falls into just five classes namely IgM, IgD, IgG, IgA, and IgE, where each isotype is adapted for a distinct effector function, appropriate for each antigenic challenge, and is often specifically required to effectively eliminate an antigen.[62,71] Before encountering antigen, naïve B-cells normally co-express IgM and IgD antibodies as antigen receptors on their cell surfaces. However, by the time B-cells proliferate and differentiate into plasma cells and memory cells, the latter have usually switched to the use of IgG, IgA, or IgE as their antigen receptors.[62]

During a T-cell activated humoral immune response, low-affinity antibodies (IgM) are rapidly produced by the antigen-bound B-cell followed by

extensive mutation of immunoglobulin genes and selection for higher affinity variant antibodies (mostly IgG) with much higher protective potency, which are then secreted in large amounts by the differentiated B-cell clone (plasma cells) to clear up the invader (Figure 1-9). A stronger immunological response with an exponential amount of antibodies (IgG) of the same specificity is then produced on subsequent exposures of the immune system to the same antigen or to a structurally related antigen by memory cells that were generated in the course of the primary immune response (Figure 1-9).[62] T-cell independent humoral immune responses, on the other hand, follow the same response pattern both in primary and subsequent exposures with the production of only IgM antibodies (Figure 1-10). Most immune responses are polyclonal, involving many different clones, since even relatively simple antigens bear several different epitopes where each has the capacity to bind to a unique clone.[62]

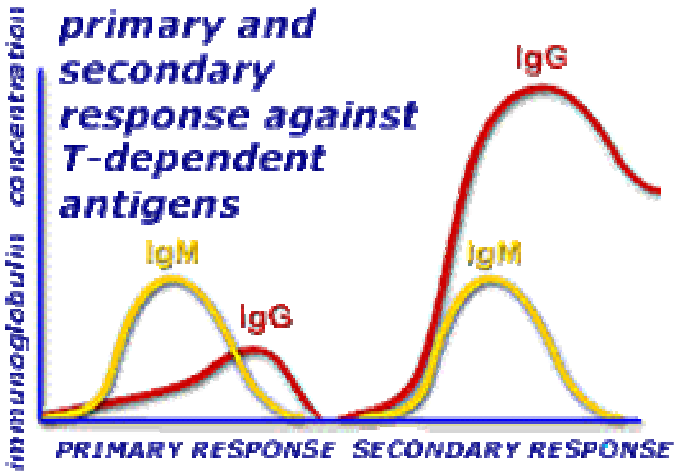

Figure 1-9: T-cell dependent humoral immune response on first and subsequent exposures to a pathogen. (Figure published by José Manuel Sánchez-Vizcaíno Rodríguez, http://www.sanidadanimal.info/cursos/inmun/tercero2.htm).

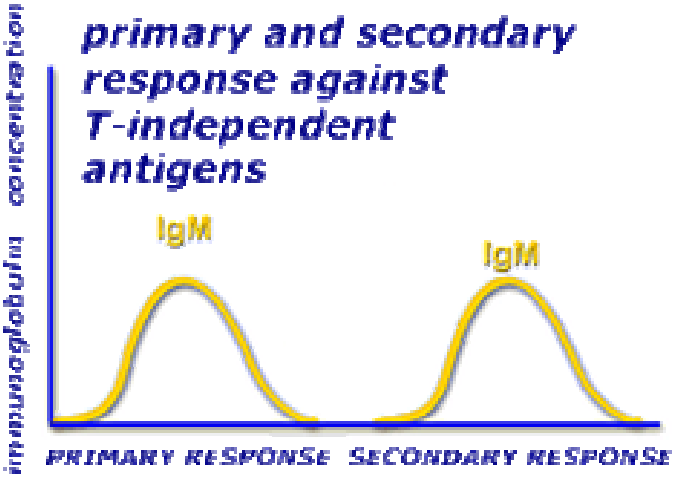

Figure 1-10: T-cell independent humoral immune response on first and subsequent exposures to a pathogen. (Figure published by José Manuel Sánchez-Vizcaíno Rodríguez, http://www.sanidadanimal.info/cursor/inmun/terce-o2.htm).

The major success of the humoral immune system in clearing extracellular pathogens that failed to be removed by the innate immunity, as well as preventing intracellular ones from infecting other cells is mainly due to the three major contributions of antibodies to immunity (Figure 1-11). The function of antibodies begins with the neutralization of the pathogenicity of pathogens simply by binding to them, whereby binding also marks the pathogens that have previously resisted direct recognition and phagocytosis as foreign. The antibodies then facilitate the removal of these pathogens, either by enabling phagocytic cells, which have very high affinity to bound antibodies, to successfully ingest and destroy the pathogens in a process known as opsonization, or by activating the complement system of the plasma proteins, to either directly lyse the pathogens, especially those infecting the blood, or like antibodies, enable phagocytes to engulf and destroy bacteria they would otherwise not recognize (Figure 1-11).[62]

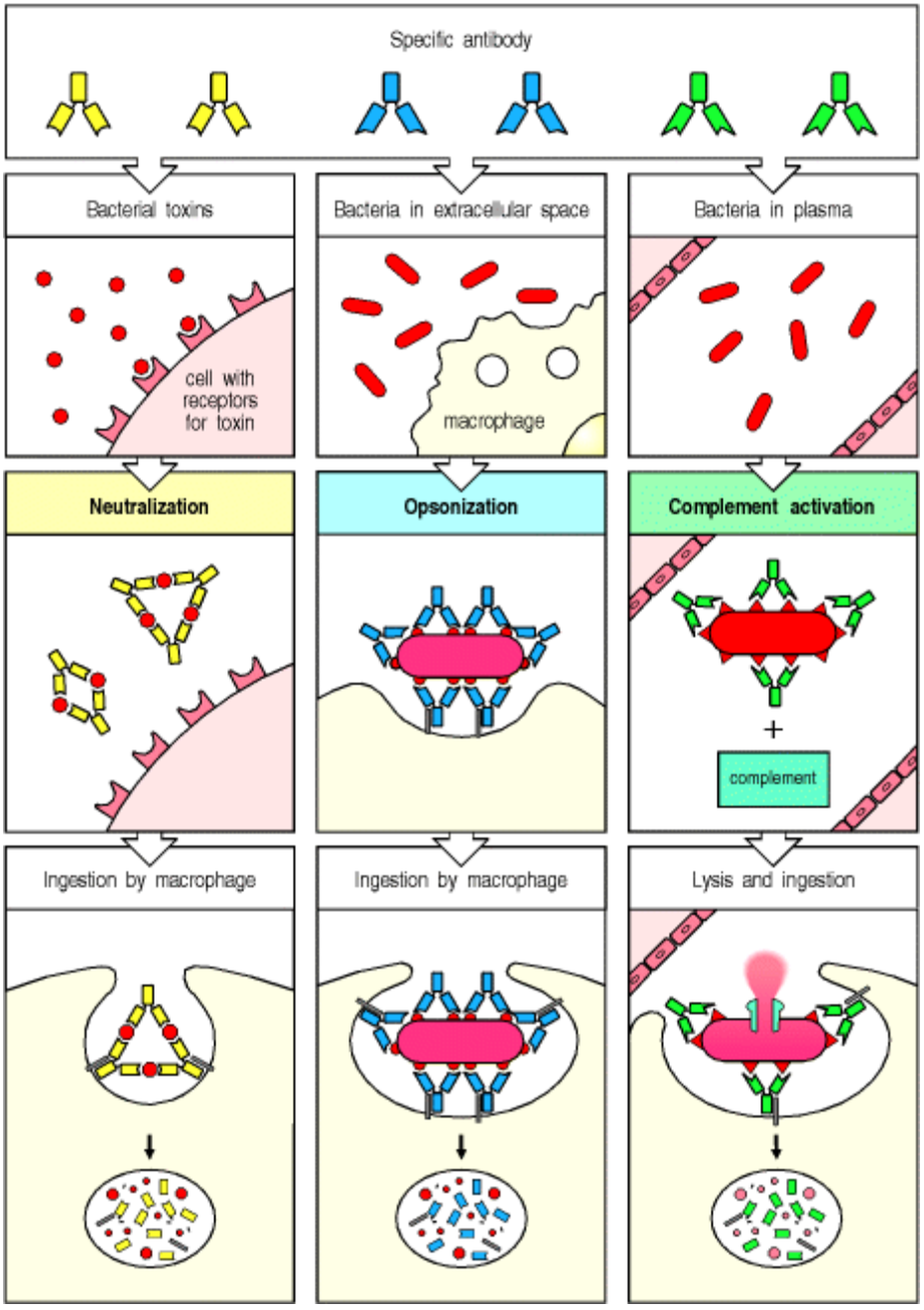

Figure 1-11: The three major functions of immunoglobulins in humoral immune responses. (Figure published by Garland, http://www.ncbi.nlm.nih.gov/books/bv.fcgi?highlight=opsonization&rid=imm.figgrp.78).

1.2.2.1.2 Structural variation and functional properties of immunoglobulins

An antibody (monomer) is typically made up of four polypeptide chains (two light and two heavy chains), forming roughly a 'Y' shape, where the polypeptide chains are joined together by disulfide bonds (Figure 1-12).[62] The antibody molecule comprises two distinct regions namely a constant region at the C-terminus, and a variable region at the N-terminus. While the constant region defines the class (isotype) of the antibody out of the five major forms, including the functional properties of the antibody, for example, in determining how the antigen would be disposed of once it is bound (opsonization by phagocytes or activating complement), the variable region, with its infinite variety of different forms, allows the antibody to specifically recognize an equally large variety of different antigens, thus providing the diversity required for specific antigen recognition.[62,72]

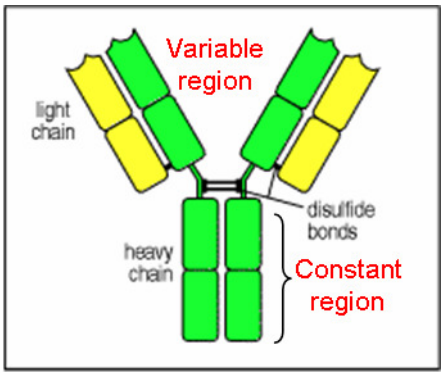

Figure 1-12: Immunoglobulin molecules are composed of two types of protein chain: heavy chains and light chains. Each immunoglobulin molecule (monomer) is made up of two heavy chains (green) and two light chains (yellow) joined by disulfide bonds so that each heavy chain is linked to a light chain and the two

heavy chains are linked together. (Figure published by Garland, http://www.ncbi.nlm.nih.gov/books/bv.fcgi?highlight=light,chains&rid=imm.figgrp.326).

Proteolytic enzymes such as papain, which hydrolyze peptide bonds of polypeptide sequences at particular sites of amino acids are used to dissect the structure of antibody into Fragment antigen binding (Fab; variable region) and Fragment crystallizable (Fc; constant region) (Figure 1-13), where antigen:Fab complexes have intensively been studied to reveal the various interactions between antigen and antibodies.[62,73-77] These analyses have shown that the antibody combining site contacts the antigen over a broad range of its surface that is complementary to the surface recognized on the antigen where electrostatic interactions, hydrogen bonds, van der Waals forces, and hydrophobic interactions can all contribute to binding.[62,73-77]

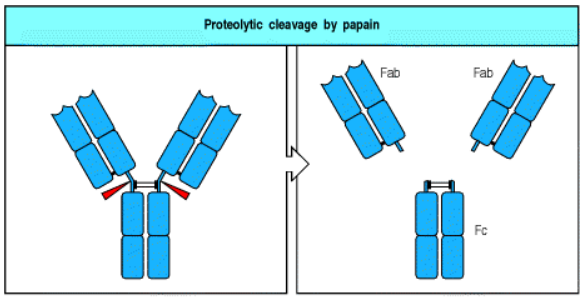

Figure 1-13: Partial digestion of an antibody into Fab and Fc with protease (papain). (Figure published by Garland, http://www.ncbi.nlm.nih.gov/books/bv.fcgi?highlight=papain&rid=imm.figgrp.329).

Igm

IgM antibodies (Figure 1-14) are always the first antibodies to be produced during a humoral immune response to an infection. They are usually made early in immune responses before affinity maturation of B-cells to plasma cells occurs. They are therefore of low affinity and to compensate for the low affinity, IgM consists of multi-site binding, which dramatically improves its overall functional binding strength. IgM, being the largest antibody with 10 antigen-binding sites (pentamers) is normally confined to the blood and is highly potent in activating the complement system, thereby allowing the control and clearance of bloodstream infections before they begin to spread. They are thought to be important in antibody binding to repetitive epitopes such as those expressed by bacterial cell-wall polysaccharides. IgM antibodies make up about 5% to 10% of all the antibodies in the body.[62]

IgG

IgG (Figure 1-14) is the smallest (monomeric) but most abundant antibody (75% to 80%) of all the antibodies in the body. It is produced in large quantities by plasma B-cells in a primary response to clear up an infection, and in much larger amount in subsequent responses by memory B-cells upon re-exposure to the same or related antigens. IgG antibodies, which are made up of four polypeptide chains with two identical light chains and two identical heavy chains, are divided into three equal-sized segments, loosely connected by a flexible tether to form a roughly 'Y' shape. Each polypeptide chain of an IgG antibody comprises a series of similar but not identical amino acid sequences (110 amino acids) where the light chain consists of two such sequences, while the heavy chain is made up of four. Each IgG therefore has two binding sites, one at each amino end of its variable regions. It can bind with very high affinity to surface antigenic epitopes of many kinds of pathogens such as viruses, bacteria, and fungi, and protects the body against them by agglutination and immobilization, complement activation (classical pathway), opsonization for phagocytosis, and neutralization of their toxins. In addition, IgG is the only antibody that can cross the placenta in a pregnant woman, thereby providing protection to the fetus inside the uterus.[62]

IgE

IgE (Figure 1-14) is typically the least abundant isotype of all antibodies (0.05% of IgG) found in the lungs, skin, and mucous membranes, and has only been found in mammals. Its levels are often high in people with allergies since

they are the one that cause the body to react against foreign substances such as pollen, fungus spores, and animal dander, as a consequence of its binding to the two phagocytes, basophils and mast cells. The allergic reactions usually occur after the binding of the allergen to the IgE bound to phagocytes results in the release of various immunological mediators. IgE also plays a role in controlling parasitic diseases such as those caused by helminths, where IgE-coated helminths binding to eosinophils results in the killing of the parasite. IgE cannot fix complement in the clearance of pathogens. Like IgG, IgE exists as a monomer and has an extra domain in the constant region.[62]

IgA

IgA (Figure 1-14) is the second most common serum antibody which makes up 10 to 15% of the antibodies present in the body although a small number of people do not make IgA antibodies. IgA antibodies normally protects the body surfaces that are usually exposed to the outside environment such as the nose, breathing passages, digestive tract, ears, eyes, and vagina. This isotype is also found in secretions including saliva, tears, and blood. While serum IgA is a monomer, IgA found in secretions is a dimer. IgA, when bound to antigen, activates phagocytes of the innate immunity to engulf and destroy the foreign particle, but does not react with complement.[62]

IgD

IgD, which is a monomer, (Figure 1-14) is almost exclusively found on B cell surfaces where it functions as a receptor for antigen. IgD on the surface of B cells has extra amino acids at the C-terminal end for anchoring to the membrane,

and is believed to somehow regulate the activation of the cell. A very small number of this isotype is also found in serum as well as in the tissues that line the belly or chest where its function is not clear.[62]

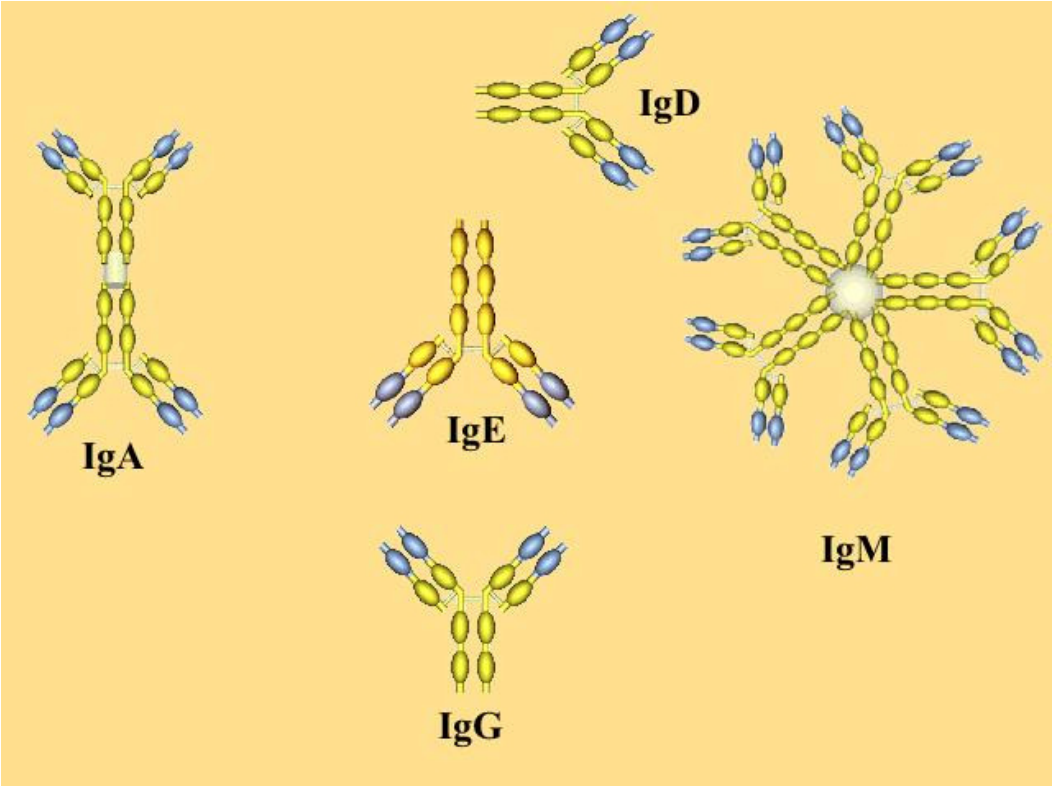

Figure 1-14: The five different isotypes of immunoglobulin. (Figure published by V.V. Klimov, http://www.immunology.klimov.tom.ru/1-1.php).

1.2.2.2 Cell-mediated immunity against bacterial infection

While resisting pathogenic bacteria, which are mainly extracellular, are cleared up by humoral immunity, some bacteria succeed in interfering to some extent with the activities of phagocytes to avoid phagocytosis, or have devised

numerous and diverse strategies to survive and multiply inside phagocytes, for example, by preventing the discharge of lysosomal contents into the phagosome environment or rupturing the early phagosome and escaping into the cytoplasm. Cell-mediated immunity is therefore needed either to destroy the cell, if the bacteria are infecting the cytoplasm (Figure 1-15a), or to reactivate the bactericidal activity of the infected phagocytic cells to enable them to digest the invading bacteria (Figure 1-15b), since antibodies in general are unable to enter cells.[62]

In cell-mediated immunity, infected phagocytes act as antigen presenting cells and travel to the nearest lymphoid organ to activate corresponding T-cells. An infected phagocyte tends to display a peptide fragment of foreign protein that is released by the invading bacteria during their growth as MHC class I antigens, if they are growing in the cytoplasm, while peptide fragments that are derived from protein released from those residing in the phagosome are displayed as MHC class II antigens.[62] The activation phase of cell-mediated immunity begins when a naïve T-cell specifically recognizes a peptide fragment displayed on the surface of an infected phagocytic cell (Figure 1-15a). The displayed peptide fragment on an MHC class I molecule when bound to a matching T-cell receptor, normally activates the T-cell to proliferate and differentiate into effector cytotoxic CD8 T-cells and memory T-cells. These cytotoxic T-cells then travel throughout the body in search of cells bearing that unique MHC Class I peptide complex, and on encountering their target bind to the complex where the binding induces them to release certain potent chemicals that punch holes in the cell membrane

of those infected cells bearing the same displayed MHC class I peptide complex, thereby causing the cells to burst and die (apoptosis) (Figure 1-15a).[62]

A naïve T-cell that recognizes specifically a peptide fragment on an MHC class II molecule derived from bacteria inside the phagosome, on the other hand, is activated to proliferate and differentiate into helper T-cells and memory T-cells (Figure 1-15b). These helper T-cells, on recognizing the same MHC class II peptide complex on infected cells throughout the body, induce the activation of the bactericidal activities of the infected phagocytes or activate the fusion of the lysosome with the phagosome containing the invading bacteria, which then digest the invading pathogen (Figure 1-15b).[62]

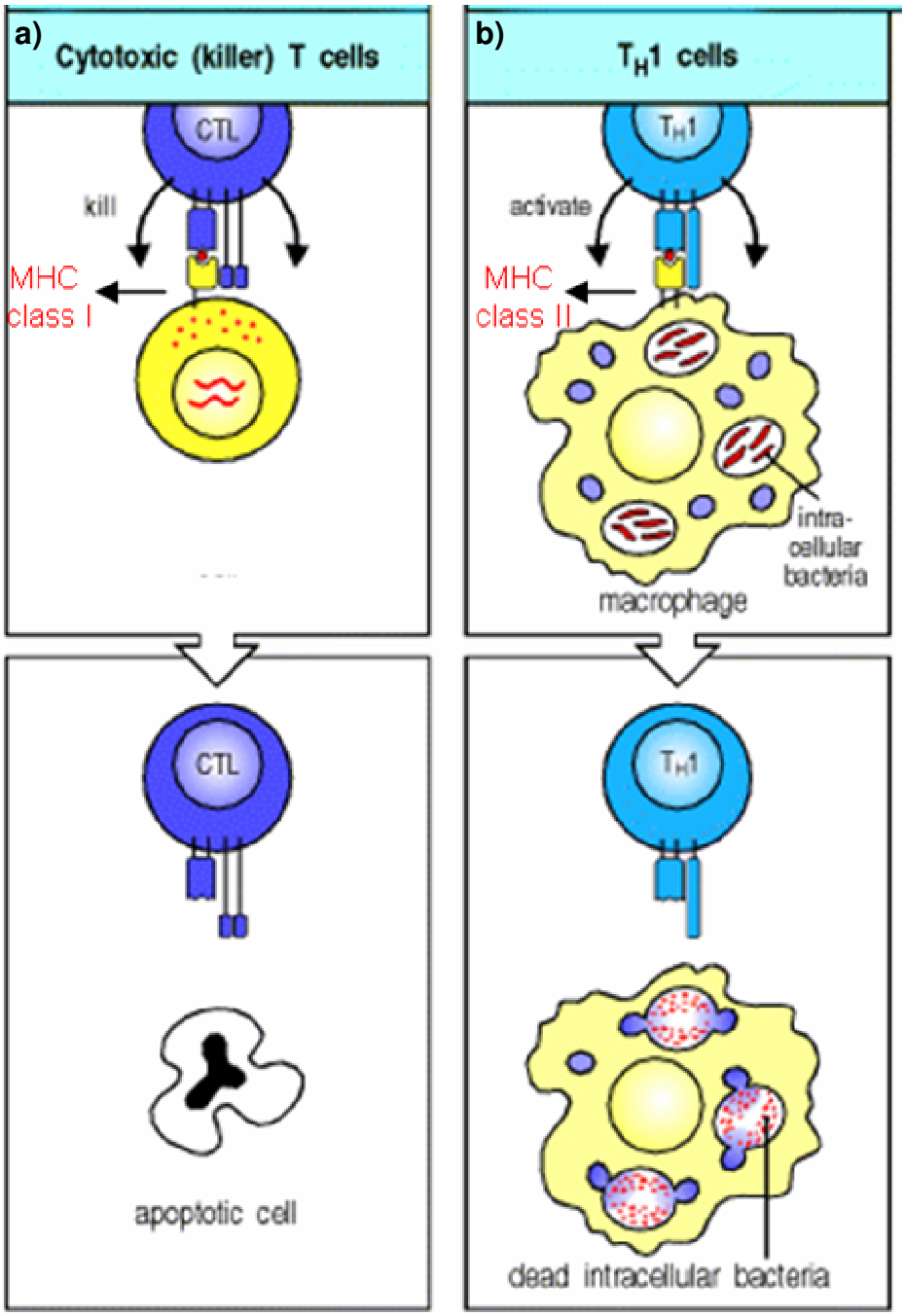

Figure 1-15: Cell-mediated immune response against intracellular bacteria infecting (a) the cytoplasm**,** (b) the phagosome. (Figure originated from that published by Garland, http://www.ncbi.nlm.nih.gov/books/bv.fcgi?rid=imm.figgrp.-1063).

1.2.3 Bacteria that are successful as human pathogens

Just as vertebrates have evolved various types of defenses to defend themselves against all pathogens, so do the pathogens which are constantly evolving, and have therefore developed elaborate strategies to overcome these defenses.[62,78,79] Those successful pathogens are mainly responsible for the leading cause of morbidity and mortality worldwide.[15] The major penalty that the adaptive immunity pays in developing such extraordinary diversity and specificity of the antigen receptors is that, when first encountering pathogens, it requires several days to develop into effector cytotoxic T-cells that kill infected cells, or antibodies that target extracellular pathogens for elimination. During this period, the body is highly dependent on the prolonged inflammatory response of the innate immune system to control and hold the infection while adaptive immunity is being developed.[62] Most of the successful pathogenic bacteria overcome these early induced responses due to their high rate of replication together with their developed virulence factors and cause diseases where their severity depends on the pathogenicity of the bacterial pathogens. While in most cases the growth of the pathogens inside the host is simply enough for damaging tissues and causing diseases, in some cases, the release of endotoxins and/or exotoxins or destructive enzymes by the pathogens is greatly responsible for the resulting infectious diseases that can range from mild to deadly.[62,78,79]

Many others have evolved complex and efficient strategies to successfully evade or subvert the highly evolved adaptive immune surveillance once developed. Among the numerous strategies, one employs antigenic variation

where bacteria constantly vary their surface epitopes (proteins or polysaccharides), to circumvent both humoral and cellular responses, so that the same pathogen can re-infect and cause disease many times, often with higher severity, in the same individual.[80-82] Another successful strategy is to camouflage their surfaces by binding to host molecules, or altering their surface antigenic determinants into non-antigenic components that are present on the host cells, to inactivate the immune system, and avoid detection by the immune cells.[79] There are many reported examples of the very few most virulent bacterial pathogens that are capable of directly interfering with adaptive immunity due to the virulence factor of their LPS, which act as superantigens by neutralizing the activities of dentritic cells, and other antigen presenting cells.[62,79] Other classes of pathogenic bacteria release several proteinaceous toxins that interfere with the development of naïve T-cells into effector cells, as well as block the receptors of antibodies.[62,82] These toxins are also known to enhance the severity of diseases by interfering with other vitally important bodily functions such as transmembrane signaling pathways, altering the membrane permeability; inside cells, these toxins modify the physiological properties of the cytoplasm resulting in cell lysis.[62,82] Furthermore, these superantigens, in high concentration, also function as potent inducers of severe inflammation, and the severe inflammatory response induced often directs the immune response against the host own blood cells resulting in blood sepsis or damaging other host tissues.[83] Many successful intracellular bacteria that multiply in phagocytes as part of their virulence strategies inhibit host cell apoptosis to promote their growth by mechanisms that

are not very well understood.[62,79] They have also devised other successful strategies such as the development of actin-based motility that allows them to spread from cell to cell through the formation of protrusions that extend into a neighboring cell.[84] In some cases, they simply enter a state of latency by temporarily inhibiting their replication and production of toxins that normally signal T-cells of their presence. This state can resume later, which then results in recurrent illness.[80] Most successful human pathogens use one or more of the above common strategies and a few others have developed other unique strategies to cause disease in humans, even in the presence of the highly evolved adaptive immunity.[62,79]

Most bacteria that are human pathogens are Gram-negative mainly due to the presence on their surface of the highly virulent lipopolysaccharides (LPS), together with other virulence factors both surface-associated and secreted to promote colonization, growth, dissemination, and survival of the organism.[65,80,85] A bacterial LPS consists of a toxic Lipid A (endotoxin) anchored in the outer membrane, an immunogenic polysaccharide core, and an antigenic O-linked series of oligosaccharides (Figure 1-16), which are unique to specific bacterial strains and vary depending on serotypes. The O-polysaccharide is responsible for many of the antigenic properties of these strains. In addition to the key association of LPS to the Gram-negative bacteria pathogenicity, LPS also help the bacteria to resist an assortment of drugs, making treatment of infections of Gram-negative bacteria rather challenging.[65,80,85]

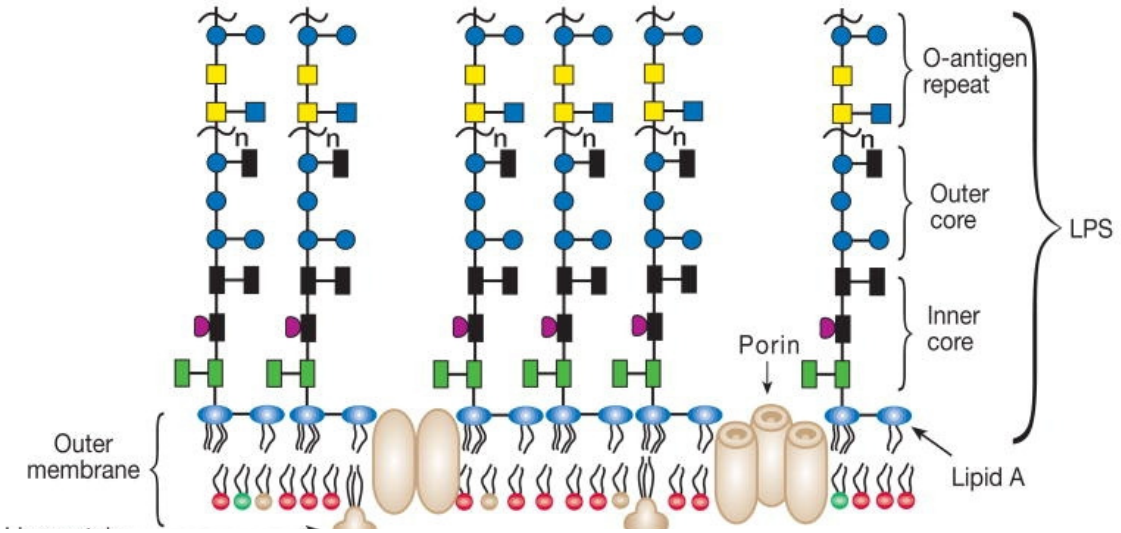

Figure 1-16: Structure of LPS. (Figures published by Cold Spring Harbor Laboratory Press, http://www.ncbi.nlm.nih.gov/bookshelf/br.fcgi?book=glyco2&part=ch20).

The *Streptococcus* and the *Staphylococcus* are the two out of the only six of the human pathogenic Gram-positive species that are cocci (round bacteria) (Figure 1-2), while the remaining organisms are bacilli (rod-shaped bacteria) (Figure 1-2), which can be further subdivided based on their capability to form spores. While the presence of the outer membrane comprising LPS, mainly accounts for the pathogenicity of some successful Gram-negative bacteria once breaching the physical barriers, pathogenic Gram-positive bacteria, on the other hand, rely on the presence of mutated non-antigenic capsules, made up of hyaluronic acid, which are also found on the human cell surfaces, as disguises to

allow the organism to evade both the innate and the adaptive immune responses, as well as release exotoxins as superantigens.[62,79]

Each of these mechanisms used by pathogenic bacteria shows in general how pathogens mobilize their own anti-immune system to successfully attack their hosts including the nature of the immune responses and its weaknesses. This deconstruction of the fundamental properties of microbial pathogenesis provides insights on how to manipulate the immune system to benefit the host.

1.2.3.1 *Streptococcus* Group A (GAS)

The *Streptococcus* Group A (GAS), which is also referred to as *Streptococcus pyogenes* (Figure 1-17a), is an example of a Gram-positive bacterium, which is one of the most frequent pathogens in humans.[86-88] It is a non-motile, non-spore forming coccus, which has a round-to-ovoid shape with a diameter of 0.6-1.0 μm.[89] Since, they normally divide in one plane, they usually appear in pairs of cells, or in chains of varying lengths. It is a catalase-negative aerotolerant anaerobe with a fermentative metabolism, requiring an enriched medium containing blood in order to grow, as well as, exhibiting beta (clear) hemolysis on blood agar.[89,90] The term "Group A" refers to a classification of *Streptococcus* bacteria based upon the structures of the O-polysaccharide of their cell-wall.[91] The cell surface structure of GAS has been studied extensively. Eighteen different group-specific cell-wall polysaccharide antigens were established by Rebecca Lancefield.[91] The GAS cell-wall polysaccharide is a polymer of N-acetylglucosamine and rhamnose sugar units.

GAS is commonly found among the normal flora on the skin and in the throat, where the skin including the mucociliary movement, coughing, sneezing, and epiglottal reflexes provide an effective barrier against invasive GAS from penetrating beyond the superficial epithelium of the upper respiratory tract.[36] However, GAS, which is normally an exogenous secondary invader, possessing all the virulence factors of a pathogenic Gram-positive bacterium such as its surface M protein and lipoteichoic acid for adherence, hyaluronic acid capsule (Figure 1-17b) as an immunological disguise and to inhibit phagocytosis, invasins, exotoxins such as pyrogenic toxin, which causes scarlet fever and systemic shock syndrome, and exoenzymes can infect if it is able to penetrate the constitutive defenses (skin and mucous layers) of healthy humans.[36] This takes place usually following a viral disease, a rupture in the skin, or disturbances in the normal flora due to the excessive use of antibiotics, while being a very common opportunistic pathogen for those with compromised immune defenses, as well as those with long-term illnesses such as cancer, diabetes, and kidney disease. The infections range from relatively mild sore throats, and skin infections to life-threatening invasive diseases such as “flesh-eating disease”.[36,86-88] *Streptococcus pyogenes* owes its major success as a pathogen to its ability to colonize and rapidly multiply and spread throughout its host especially in the respiratory tract, bloodstream, or the skin, and its ability to evade phagocytosis.[87] It is the M protein, where more than 100 types have been identified on the basis of antigenic specificity, which is the major virulent factor in GAS species, since it can rapidly change its antigenic determinants with host

molecules, thus avoiding detection by the immune system.[36,92] In some cases, it also allows survival of the organism by blocking the binding of complement of innate immunity. Furthermore, the M protein together with the peptidoglycan, comprising group-specific cell-wall polysaccharides, possess epitopes that also mimic those of mammalian heart muscles and connective tissues, sometimes leading to autoimmune diseases following an acute infection. Moreover, GAS species, which are always beta-hemolytic, lyse eukaryotic red blood cells and phagocytes allowing their spread among tissues during their invasions.[36,88,92]

Even though GAS has remained sensitive for quite a while to some antimicrobial agents such as penicillin or cephalosporin, which inhibit the enzyme responsible for the formation of their peptidoglycan in the cell-wall of the bacterium, there has been a recent increase in the variety, severity, and sequelae of severe Group A *Streptococcal* infections due to drug-resistance by the bacterium, and has once again become a major global public health problem. There is a now a need for an effective therapeutic drug to prevent this pathogen from causing more severe diseases. The finding that low levels of protective antibodies (passive immunity) specific against either the M-protein or their toxins correlated with invasive GAS in providing protection against these infections suggested the importance of immunoglobulins as a new potential therapy against invasive GAS. Based on these findings, there is a now a growing interest in the search for an effective agent that can be used to induce the immune system to produce naturally functional antibodies with a capacity to target the pathogen.[87]

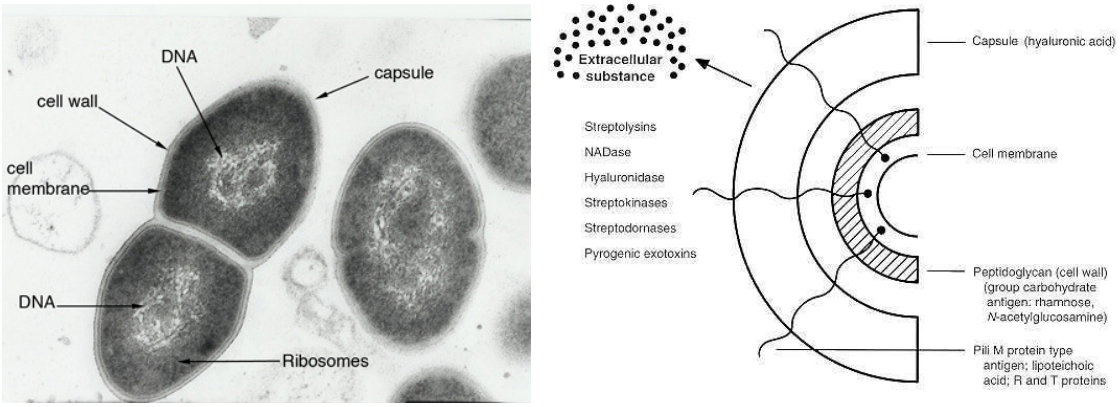

Figure 1-17: (a) *Streptococcus* pyogenes, (b) trans sectional structure of a *Streptococcus* Group A bacterium. (Figures published by Kenneth Todar, http://www.textbookofbacteriology.net/streptococcus_2.html).

1.2.3.2 The *Shigella* bacteria

The *Shigella* bacteria (Figure 1-18a), which were discovered by Shiga, a Japanese scientist 100 years ago,[93] are Gram-negative, non-motile, non-spore forming, rod-shaped pathogenic bacteria that are divided into four serotypes: *Shigella dysenteriae*, *Shigella boydii, Shigella sonnei, Shigella flexneri*, where the last two serotypes are responsible for causing most diseases in humans.[94] *Shigella flexneri* Y (Y is based on the structure of the O-polysaccharide of its LPS; there are 15 different serotypes) normally resides in the human intestine, and causes shigellosis, a major form of bacillary dysentery by invading the large intestinal epithelium, if able to penetrate through the colonic mucous membranes.[94,95] While most of those who are infected by the organism normally develop bloody diarrhea, fever, and stomach cramps, which usually resolve in

less than one week, others, especially young children and the elderly, develop the severe form of shigellosis, including septic shock that very often are fatal. Since the disease can be spread easily through food, or by person-to-person contact, *Shigella*-caused dysentery is endemic in poor countries mainly due to a lack of hygiene, causing an estimated 163 million illness episodes annually, and more than one million deaths worldwide, including several thousand cases in developed countries.[94,96]

Immunological studies showed that this pathogen might be a mutated form of the non-pathogenic *Escherichia* coli of the human colon.[97] The virulence factors that contribute to the pathogenicity of *Shigella flexneri* Y in the human colon may have been acquired by means of horizontal gene transmission from *Escherichia* coli after acquisition of O-antigen genes of their LPS by hypermutation, followed by inactivation of native O-antigen genes of *Escherichia* coli, resulting in virulent LPS of *Shigella* (Figure 1-18b). This O-polysaccharide of *Shigella flexneri* Y is made up of N-acetylglucosamine and L-rhamnose.[97] The virulent LPS (Figure 1-18b) is mainly responsible for the pathogenicity of the bacterium when invading its host by promoting strong inflammation.[98,99]

While shigellosis infection was an example of a new emerging disease by mutated *E*-coli 100 years ago, it is now a growing fear of a re-emerging infectious organism due to the effect of antimicrobial-resistance drugs. Like the GAS system, the new strategies that are being developed to naturally raise antibodies against the *Shigella* species, are likely to come to fruition in the near future.

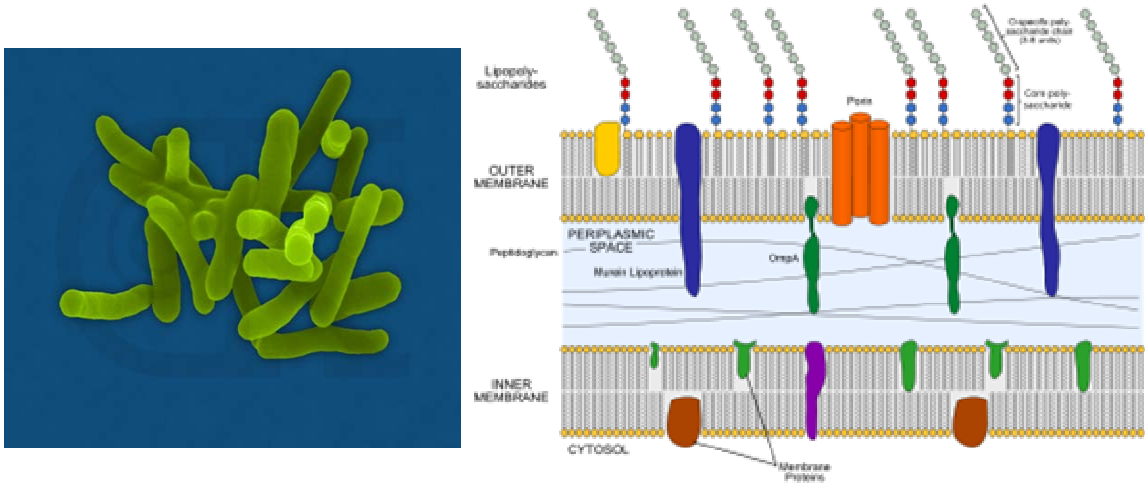

Figure 1-18: (a) *Shigella* species, (b) trans sectional structure of a *Shigella* bacterium. (Figures published by Dennis Kunkel Microscopy, Inc., http://202.114.65.51/fzjx/wsw/newindex/tuku/MYPER/zxj/97304c.htm).

1.3 Vaccines

One of the greatest achievements of the 20th century in preventive medicine is the manipulation of the immune system to artificially stimulate protective immune responses that can then naturally target some pathogenic microbes. This field of science called immunology has originated, and grew from the success of the British microbiologist, Edward Jenner, who discovered in 1796 that cowpox, or vaccina, induced protection against human small pox, which once killed several millions in a year.[100] His procedure, which he called vaccination, describes the inoculation of healthy people with a harmless version of a pathogen or toxin, called a vaccine that stimulates the immune system of the

vaccinated individuals without actually causing the disease to produce protective antibodies, and memory cells. Consequently, if the actual pathogen were encountered in the future, the immune system would be primed to mount a secondary immune response with strong and immediate protection against the pathogen before it is able to establish an infection, and cause disease. Unlike antibiotics, which have instead shifted the equilibrium in favor of the infectious agents by causing resistance to develop, mass vaccination on the other hand, has eradicated small pox from the globe, has eliminated polio from most part of the world,[101] and has marketedly reduced measles,[102] which used to kill millions of children every year, and without causing any such resistance to occur in pathogens.

Currently, there are more than 70 bacteria that are serious human pathogens,[103] and several more are emerging at an alarming rate.[15] Even though, vaccines are available against some of these agents,[104] there have been very few newly developed ones against important diseases for the past 20 years. With the ever increasing range of infectious diseases, which are a continuing menace to the human race, there is now a growing need for new and more effective vaccines to treat not only common diseases, but also reemerging diseases.

Due to the advances in immunology in the past 30 years, such as the detailed understanding of microbial pathogenicity, analysis of the protective host response to pathogenic organisms, and the understanding of the regulation of the immune system to generate effective T- and B-lymphocytes responses, the

design of more specific and better vaccines, incorporating these immunological principles can now be achieved. Since, most bacteria are obligate extracellular agents that live and replicate outside cells (extracellularly), an effective vaccine against such agents would be one that induces a strong humoral response with production of protective antibodies.[62] Furthermore, in order to stimulate artificially a strong and protective humoral response against bacterial agents, an ideal vaccine should contain enough antigenic determinants to be recognized by both the B-cells and the helper T-lymphocytes of the adaptive immune system.[62,83] Finally, the vaccine should not have side effects, not result in any disease in the vaccinated person, and should be sufficiently stable to reach the site of interaction with B cells or T cells necessary to elicit an immune response.[62]

1.3.1 Types of vaccines

Several different types of vaccines have been developed since Pasteur first used live, but attenuated (non-virulent) vaccines over a century ago to treat cholera. The live attenuated vaccines traditionally consist of the whole pathogens or their toxins, which have been either genetically or chemically altered, so that they are unable to replicate and cause disease, but in which their immunogenicity is retained.[105-107] There are many examples of highly successful live attenuated vaccines that have been developed to control diseases such as polio, measles, rubella, varicella, and mumps.[108] However, even though these live attenuated vaccines, which comprise all the antigenic determinants of the pathogen, are generally far more potent and elicit a greater number of relevant

mechanisms, including both humoral and cell-mediated responses, and provoke more durable immunological responses, they are often found to be unsuitable for immunosuppressed or immunodeficient individuals since they generally behave as opportunistic agents in such immunocompromised individuals.[105-107] Moreover, sometimes the live pathogens in the vaccines are not completely attenuated, and there are many cases where they have reverted back to virulent pathogens.[105-107] An alternative to live attenuated vaccines, which is much safer, is to use killed vaccines in which the pathogens are killed by heat or chemicals.[105-107] These vaccines are easier to produce, and have been very useful in the protection against some influenza agents, for example. However, they were found to be less effective in providing protection against highly virulent bacteria, compared to live attenuated ones, since the antigens on dead cells normally are less antigenic, producing only a shorter period of immunity. Reversal to pathogenic organisms was also observed in some killed vaccines.[105-107]

With the advent of genomics, proteomics, and biotechnology, combined with our understanding of pathogenesis, and immune responses to various pathogens, there is now a growing opportunity to develop safer, and more effective vaccines in terms of specific, and long-lasting immunity, while at the same time overcoming the risk of pathogenic reversion. The most recent development in such vaccines is the use of specifically identified antigenic determinants from the surface of pathogens (Figure 1-19) instead of the whole pathogens, or from their secreted toxins or superantigens, to stimulate precise

immune targeting, strong enough to completely clear the whole microbial infection.[62,105-107] Microbial surface proteins such as adhesins (Figure 1-19), or their proteinaceous toxins, which are critically important in determining the success of a bacterial strain in its competition for survival in the world, are excellent component vaccines due to the fact that these proteins are highly antigenic comprising both discontinuous epitopes for recognition by B-cells, as well as excellent continuous T-cells epitopes, which can lead to strong humoral immune responses with the production of memory cells.[62,105-107] However, even though these protein subunit vaccines have demonstrated excellent protection against many bacterial infections, the isolation of such components in large scale and in purified form is cumbersome and expensive.[109] One solution to overcome this problem is to introduce genes coding for surface proteins into plasmids (genetic recombination), which can then express the proteins once injected into the skin or muscle. The proteins produced can then trigger the immune system to produce protective antibodies that will target the encoded proteins on the pathogens.[109-111]

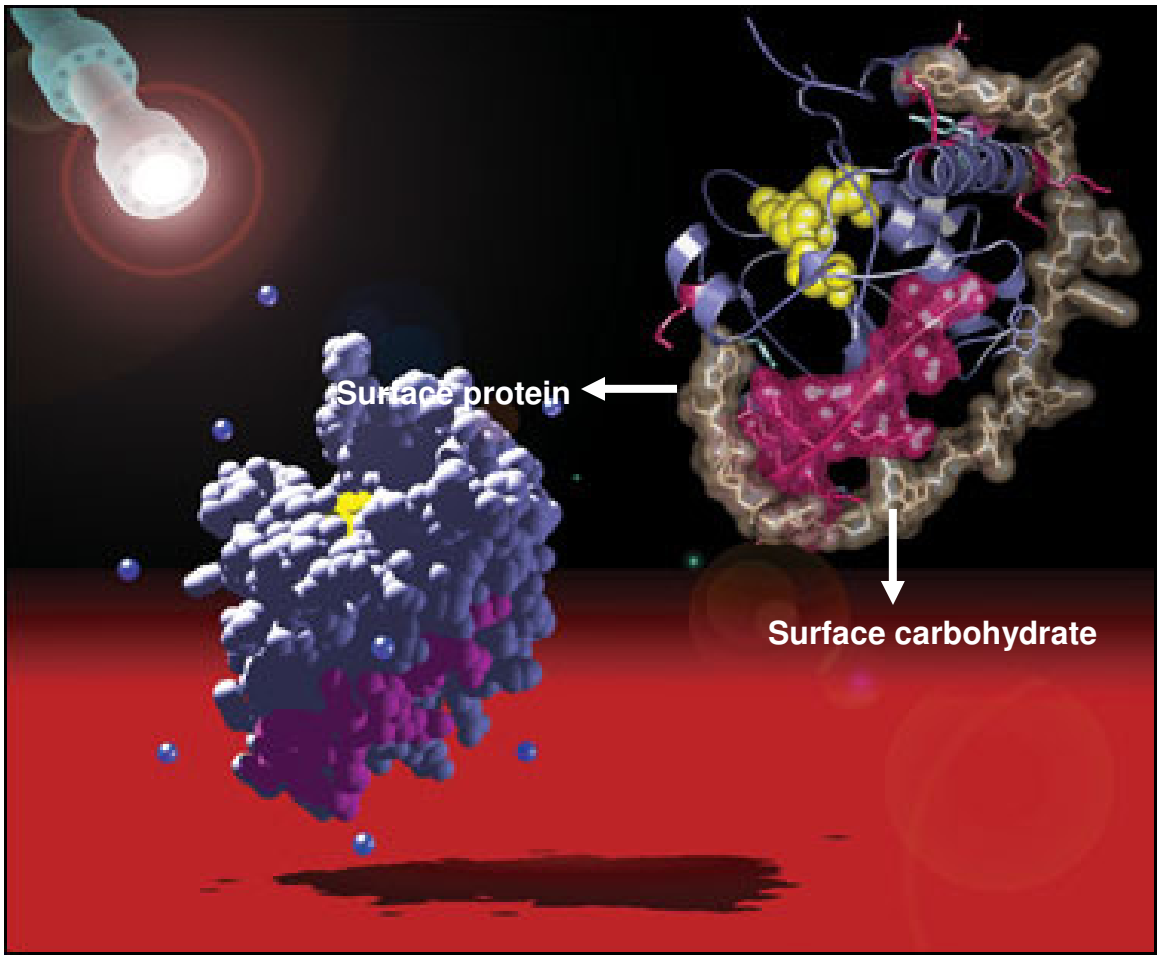

Figure 1-19: Bacterial surface antigens. (http://www.bnl.gov/bnlweb/pubaf/pr/phc2004/DNAbinding300.jpg).

Another novel method in the design of protein subunit vaccines is to identify relevant T-cell epitopes by eluting them directly from MHC class II molecules from B-cells in animal models, which have been infected with the pathogens, or from naturally infected humans. Several peptide sequences originating from bacterial protein antigens have been eluted from MHC II molecules, and while these peptides could not be used on their own as subunit

vaccines, since they do not possess the discontinuous epitopes of the original proteins that were recognized by the B-cell, the genes that code for the original proteins could be revealed and incorporated into plasmid vaccines, by identifying those of the eluted fragmented peptides from the MHC II molecules. Based on this approach, plasmid protein-based vaccines are now being developed against some obligate extracellular pathogens, and one particular example is that developed against *Leishmania*.[62] However, at present, DNA vaccines are only experimental, and may include some potential risk such as the integration of the microbial DNA into the genome of the host cell that might result in transformation or tumorigenic events, as well as the triggering of the production of anti-DNA antibodies, resulting in severe autoimmune diseases. While these remain to be tested, other approaches other than using bacterial proteins are being exploited to develop effective component vaccines against bacterial infections.[103]

As immunogenicity of bacteria often arises in part from such cell-surface elements as polysaccharides (Figure 1-19), which comprise antigenic epitopes recognized by B-cells, they have until recently been extracted, and purified from cultures of intact bacteria by conventional biochemical techniques in order to be exploited as potential component subunit vaccines.[62,112-116] However, while the whole microorganism, or its proteins have multiple antigenic determinants to activate both the B-cells and the T-cells of the adaptive immune system, microbial polysaccharides, on the other hand, are mostly T-cell independent, and the immune response elicited against such polysaccharides are therefore composed of low-affinity IgM antibodies. This is because of the lack of T-cell

involvement, further activation of B-cells into immunological memory cells does not occur, resulting in only short-term immunity.[62,112-118] Most importantly, polysaccharide vaccines fail in children less than two years of age, as their immune systems are not mature enough to generate an effective B-cell immune response, without the interaction of helper T-cells.[62,112-118]

It was observed that the immunogenicity of these polysaccharide vaccines against bacteria could be improved by conjugation to carrier proteins such as tetanus toxoid, bovine serum albumin, or keyhole limpet hemocyanin, which converts the polysaccharide from a T-cell independent to a T-cell dependent antigen.[62,112-116] Upon immunization with these vaccines, some B-cells that bind the antigenic epitopes of the polysaccharide component of the vaccine are activated by helper T-cells that specifically recognize peptide fragments of the linked carrier protein to produce specific antibodies against the polysaccharide (Figure 1-20). In this case, the immune response is stronger, with production of memory cells that results in the production of millions of anti-polysaccharide antibodies against the real pathogen bearing the polysaccharide.[118] While several carbohydrate-protein conjugates vaccines have been developed,[113,119] and have proved successful against both Gram-positive and Gram-negative bacteria, isolation and purification of carbohydrates from the organisms, like the surface protein components of bacteria, are difficult,[120] which make carbohydrate-based vaccines unattractive. Unlike proteins, they are also not directly expressed by genes, which make DNA vaccines targeting bacterial carbohydrates challenging. Although chemical synthesis of carbohydrates may

reduce the problem associated with its isolation and purification,[121,122] this remains rather a limited solution since carbohydrate chemistry in general is complicated, making their synthesis expensive as well as time consuming.

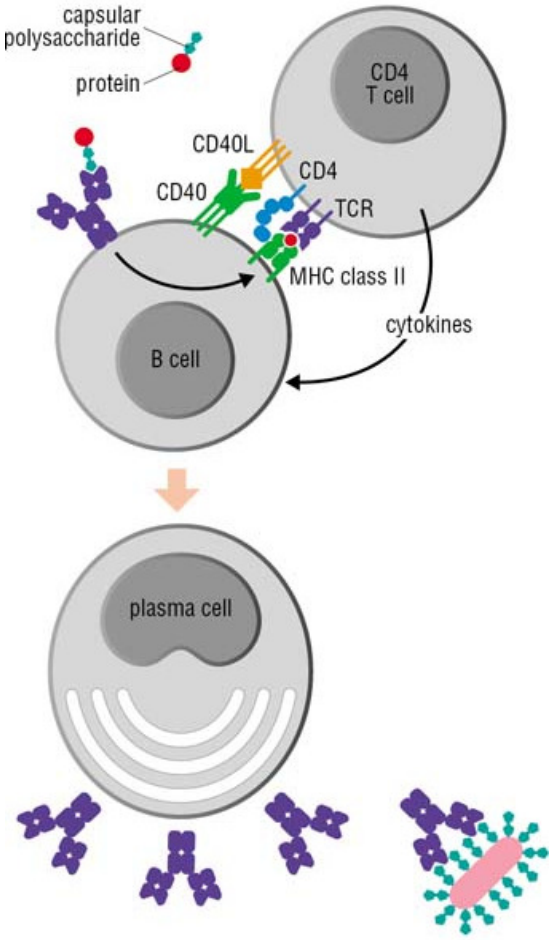

Figure 1-20: (a) Processing of polysaccharide-protein conjugate vaccine by the immune system. (Figure originated from that published by Garland, http://www.ncbi.nlm.nih.gov/books/bv.fcgi?rid=imm.figgrp.1123).

1.3.2 Molecular mimics of carbohydrates as subunit vaccines

Molecular mimics of carbohydrates present an alternative approach to vaccine development that includes the use of more easily available non-carbohydrate molecules that have the potential to mimick the biological activity of the natural carbohydrates, often with greater advantages such as greater specificity or selectivity, or lower toxicity.[73,74,123] The first therapeutic agents exploited as surrogates of bacterial carbohydrate antigens are anti-idiotypic antibodies (Figure 1-10).[124-127] According to Jerne's network theory, anti-idiotypic antibodies, which are normally raised to eliminate excess antibodies in the body, can mimick structurally the antigen that has raised the excess antibodies they are eliminating.[128] This, in turn, has led to the hypothesis that antigenic mimicry of anti-idiotypic antibodies could be used to induce an immune response against the mimicking antigens. Anti-idiotypic antibodies (Figure 1-21) that specifically mimick carbohydrate antigens in their functions, therefore, have potential to elicit cross-reactive anti-carbohydrate immune responses when used as subunit vaccines.[124-127] Since, anti-idiotypic antibodies, like any antibody, can be safely produced, and purified in large quantities,[129] they, therefore, represent promising alternatives to carbohydrate antigens, as well as to many other antigens, especially when the molecules of interest are not appropriate for large-scale production and purification, or are infectious or toxic. While anti-idiotypic antibodies as surrogate antigens are sometimes too big to fit into anti-carbohydrate antibodies, and hence fail as vaccines, some of the successful

ones are currently being exploited in the development of surrogate vaccines against bacterial agents.[124-126,127]

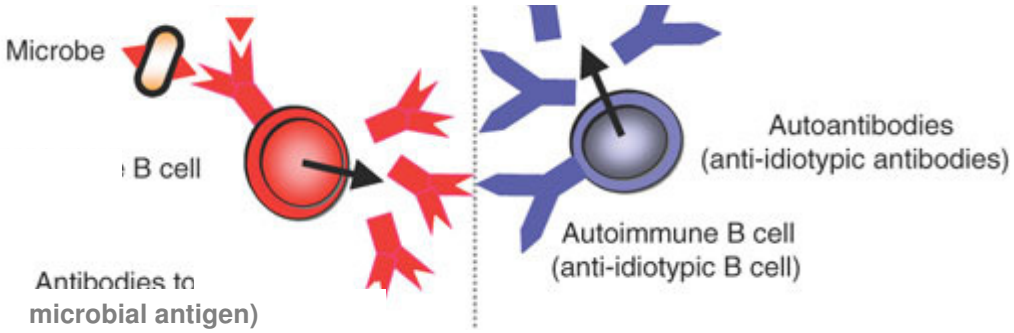

Figure 1-21: Production of anti-idiotypic antibodies targeting microbial-antigen antibodies. (Figure originated from that published by Nature Medicine**,** Nature Medicine **2004**, *10*, 72-79).

Recently, immunological studies have shown that peptide fragments, which are strong epitopes of T-cells of the immune system, have the potential to act as molecular mimics of carbohydrates by inducing strong anti-carbohydrate immune responses.[73,74,123] While the interactions between carbohydrate and protein such as antibody, in general, are characterized by low to moderate affinity, carbohydrate-mimetic peptides, on the other hand, comprise different functionality that allow them to potentially bind to antibody with greater affinity,[73,74,123] and, hence, could be valuable as surrogate therapeutic agents,

either replacing natural carbohydrate ligands, or strengthening existing anti-carbohydrate immune responses. Several carbohydrate-mimetic peptides with reasonable affinity (equivalent or higher than the parent carbohydrate epitopes) have been identified from phage-displayed libraries (Figure 1-22), which is the most widely used method of identification of antigenic carbohydrate-mimetic peptides. The immunogenicity of many of these peptides known as mimotopes has been demonstrated, although antigenicity should not necessarily be expected to lead to immunogenicity.[73,74,123] Furthermore, these mimetic peptides may show greater discrimination than carbohydrates in raising antibodies, and hence could direct the immune system against particular epitopes on the original carbohydrates, especially those that are not found on human tissues, thus avoiding undesirable cross-reactivity with self structures.[73,74,123] Because of the several limitations in the use of carbohydrates as vaccines in contrast to peptide mimotopes, there is now a growing interest in carbohydrate-mimetic peptides, which are easier to produce naturally, as well as, easier to synthesize chemically, as potential surrogate vaccines to target cell-surface polysaccharides of pathogenic bacteria.

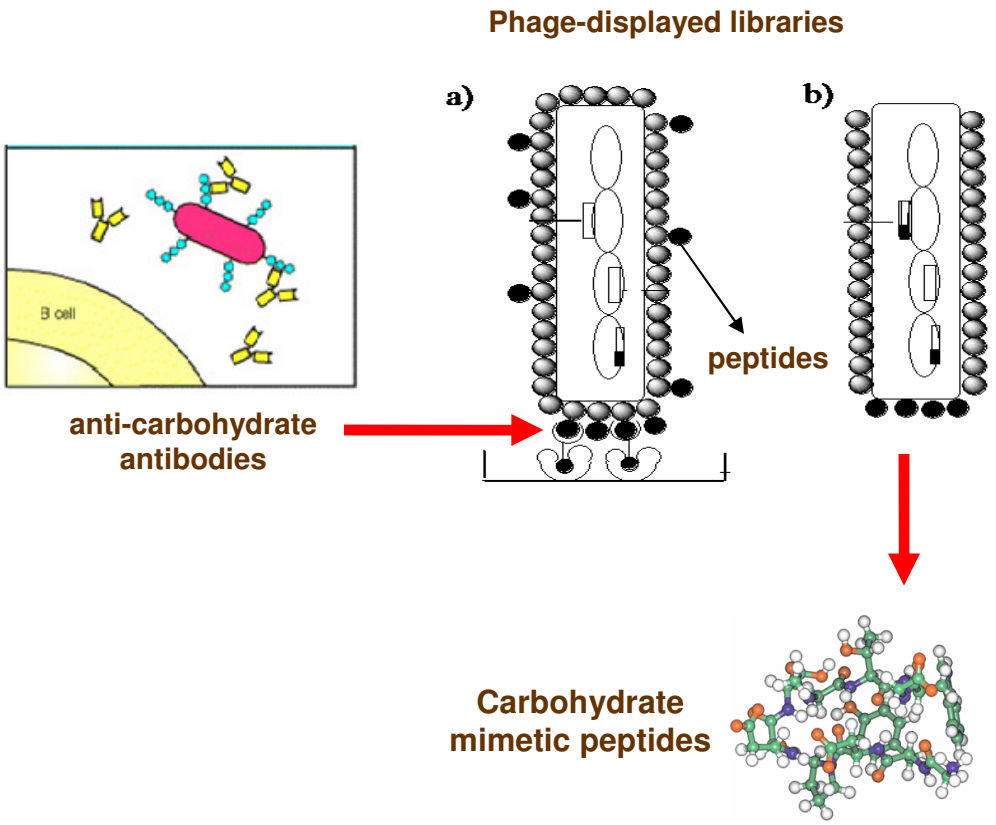

Figure 1-22: Identification of carbohydrate-mimetic peptides from phage-displayed libraries.

NMR spectroscopy, X-ray crystallography, and computational analysis have provided our group and others with powerful tools to investigate at the molecular level, the nature and origin of mimicry of some carbohydrate antigens by peptides to determine bioactive conformations adopted by these mimetic peptides among the multiple conformations of similar energy, including the determination of exact epitope sequences of the carbohydrates mimicked by these peptides.[75,130,131] These findings have provided useful insights into the

requirements for antigenicity by mimetic peptides at the molecular level, and these results could be used to improve their immunogenicity, and hence be important in vaccine development.

1.3.2.1 Peptide-carbohydrate mimicry in the *Shigella flexneri* Y and the *Streptococcus* Group A systems

The cell-wall polysaccharide of the Gram-positive bacterium *Streptococcus* Group A (GAS) (Figure 1-23a), and the polysaccharide of the cell-surface LPS of the Gram-negative bacterium *Shigella flexneri* Y (Figure 1-23b), are important antigens that are excellent targets for vaccine development against these two potential pathogens. From previous immunological studies on the immune responses against these two polysaccharides, monoclonal antibodies against certain epitopes on these two polysaccharide antigens have been developed.[132,133] Using the monoclonal antibody SA-3, which recognizes a hexasaccharide epitope (two repeating units) on the cell-wall polysaccharide of GAS,[134] to screen phage-displayed libraries, several peptides with similar or higher affinity than the hexasaccharide were isolated and a subset among the mimetic peptides contained the conserved sequence DRPVPY (Figure 1-23c).[134] Similarly, a monoclonal antibody SYA/J6, recognizing a pentasaccharide epitope on the cell-surface polysaccharide of *Shigella flexneri* Y,[135] was used to select mimetic peptide sequences from phage-displayed libraries. An octapeptide with sequence MDWNMHAA (Figure 1-23d), was identified as a potential mimic of the O-polysaccharide of the *Shigella flexneri* Y.[134]

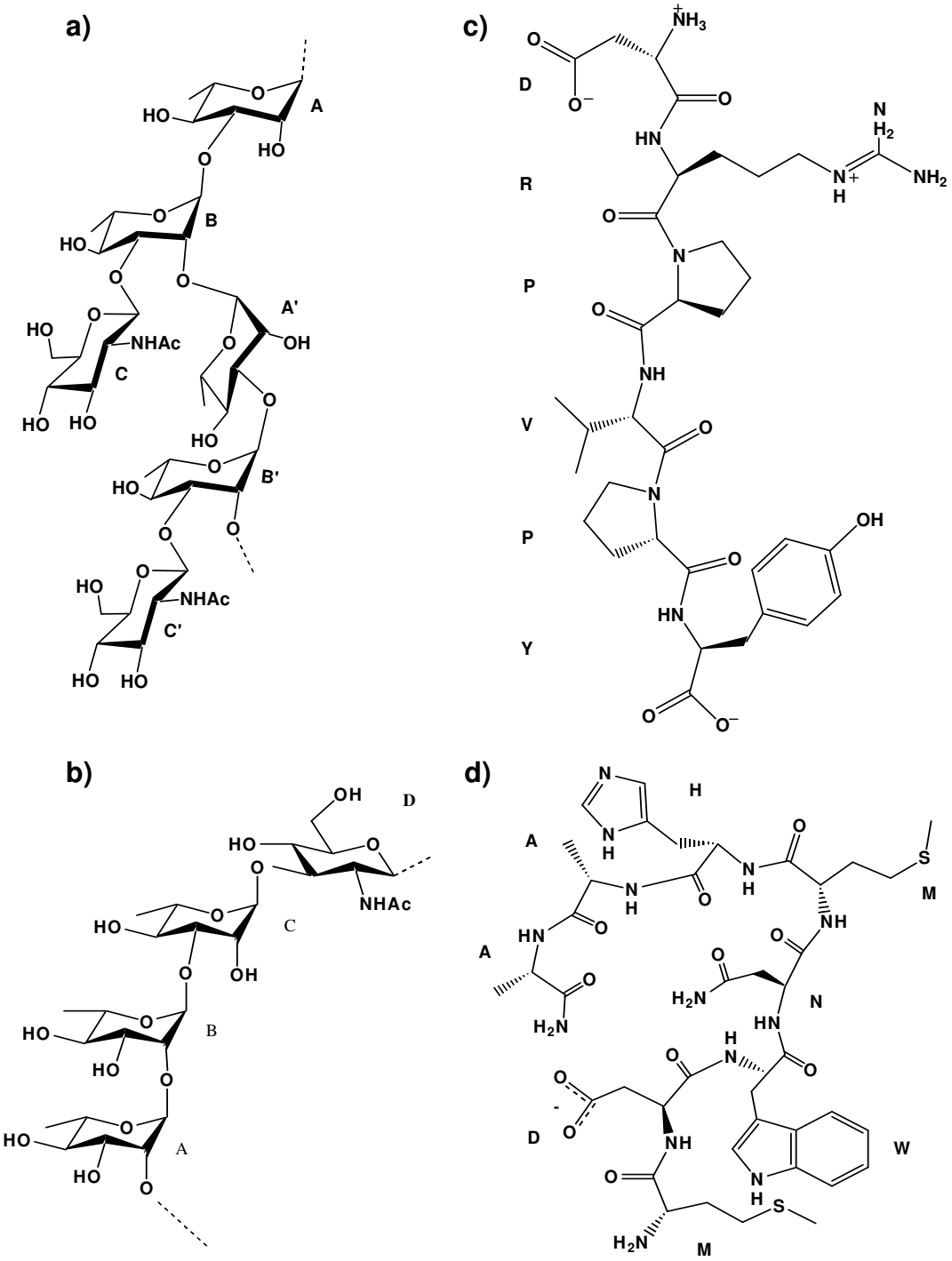

Figure 1-23: Structure of the (a) cell-wall polysaccharide of *Streptococcus* Group A, (b) cell-surface polysaccharide of *Shigella flexneri* Y, (c) peptide mimic DRPVPY, (d) peptide mimic MDWNMHAA.

En route to investigating whether these two identified mimetic peptides would be effective mimotopes, and hence effective surrogate vaccines, their thermodynamics of binding (binding affinity), and the nature of their antigenic mimicry were first extensively studied by our laboratory. In the case of the GAS system, it was found that the mimetic peptide DRPVPY (Figure 1-23c), has a slightly higher affinity in binding to the SA-3 antibody with K_D 625 nM, than the parent hexasaccharide (Figure 1-24a) (K_D 17.5 μM); the peptide binding is entropically more favorable than that of the carbohydrate epitope.[134] Moreover, NMR studies performed recently in our laboratory revealed that antigenically, DRPVPY is a functional mimic of the carbohydrate epitope, in that it does not interact with the same residues in the antibody combining site as does the parent hexasaccharide.[75,76] Interestingly, it was also found by using transferred NOESY experiments that DPRVPY adopts a distinct turn in the VPY region when bound to SA-3 (Figure 1-24c), which are stabilized by hydrophobic contacts between the side chains, and that this tight turn is also present in the average conformations of the free peptide,[75,76] suggesting that if structural mimicry is not required for immunogenicity, DRPVPY could be a potential mimotope of the cell-wall polysaccharide of GAS.

In 2001, the crystal structures of the Fab fragment of an anti-carbohydrate antibody in complex with a mimetic peptide (Figure 1-24e and f), identified from phage-displayed libraries, as well as with the parent carbohydrate epitope (Figure 1-24b) were available for the first time, allowing direct examination of the nature of peptide-carbohydrate mimicry.[131,136,137] These two crystal structures, a

bound pentasaccharide portion of the cell-surface polysaccharide of *Shigella flexneri* Y, and its bound peptide mimic MDWNMHAA to SYA/J6 Fab fragment allow a detailed comparison of specific interactions in the complexes, revealing the nature of peptide-carbohydrate mimicry in this system (Figure 1-24e and f). Overall, while a very few structural mimetic interactions were observed, MDWNMHAA, like DRPVPY, does not structurally mimic the carbohydrate in binding to the anti-carbohydrate antibody.[131] In addition, the peptide involves several ordered water molecules in its binding that bridge between part of the ligand and the active site to provide complementarity, and occupy some deep cavities where some of the oligosaccharide residues resided (Figure 1-24f). The octapeptide also makes more intermolecular contacts (126) to the combining site than the pentasaccharide (74), and hence complements the shape of the active site better than does the parent oligosaccharide. Moreover, the bound peptide (Figure 1-24d) makes a one-turn α-helix, similar to bound DRPVPY, starting from Met-6 to Ala-8, in order to allow the side chains to make important and specific hydrophobic and polar contacts with the combining site. However, in contrast to DRPVPY, MDWNMHAA is deprived of its bioactive conformation in its free state.[131] Moreover, measurement of the thermodynamics of binding of the mimetic MDWNMHAA shows that the high enthalpy of binding of the octapeptide is actually offset by an unfavorable entropy, most probably due to the presence of several water molecules and/or the more ordered α-helix in the bound conformation than in the free peptide, resulting in similar binding affinities of the mimetic octapeptide and the oligosaccharide.[131]

Whether lack of structural mimicry or the insufficient population of the bioactive conformation within the ensemble of conformations averaged by the free octapeptide would affect the immunogenicity of this mimetic peptide, by rendering it a weak mimotope of the cell-surface polysaccharide of *Shigella flexneri* Y, or whether improving the binding affinity of the peptide would improve its immunogenicity remains to be determined.

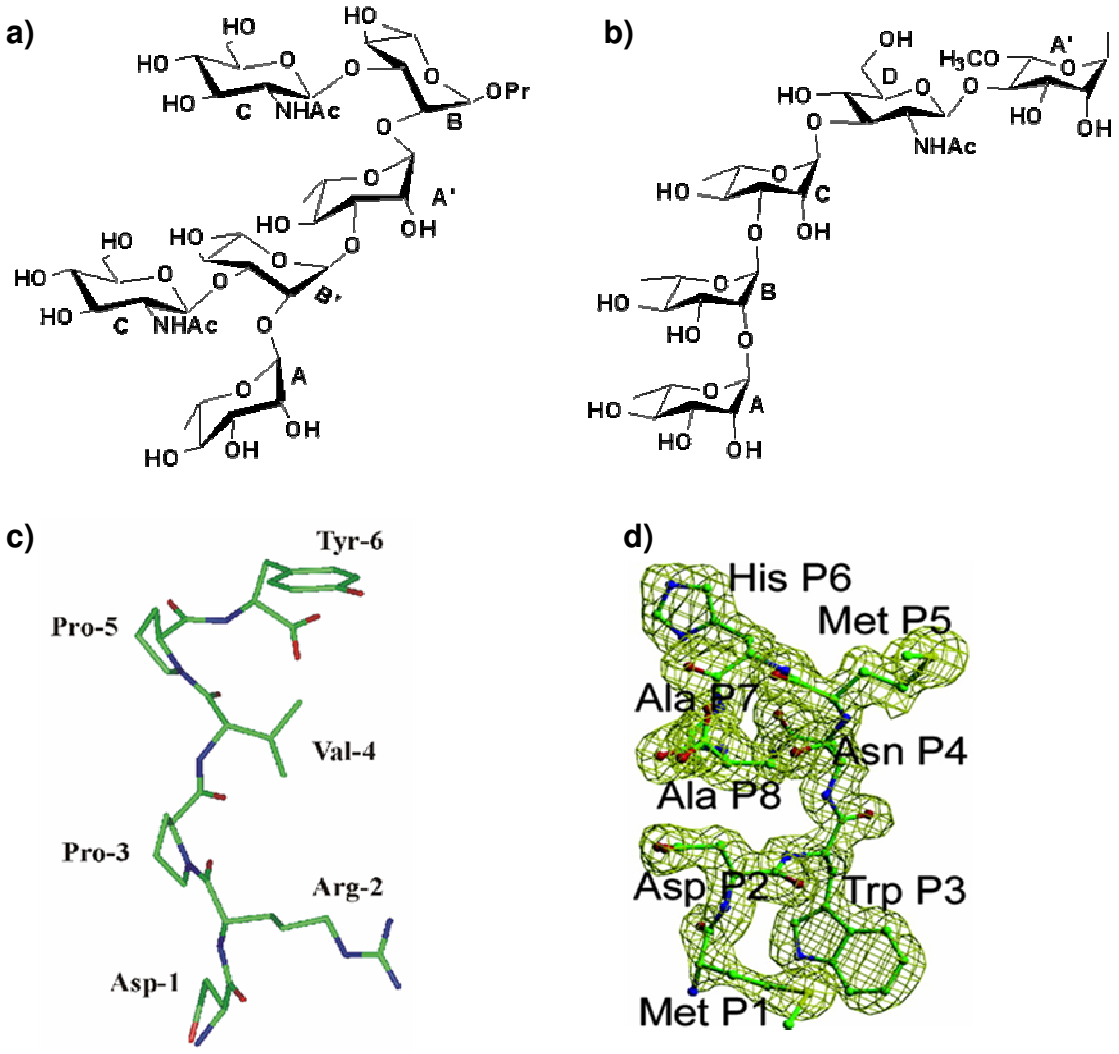

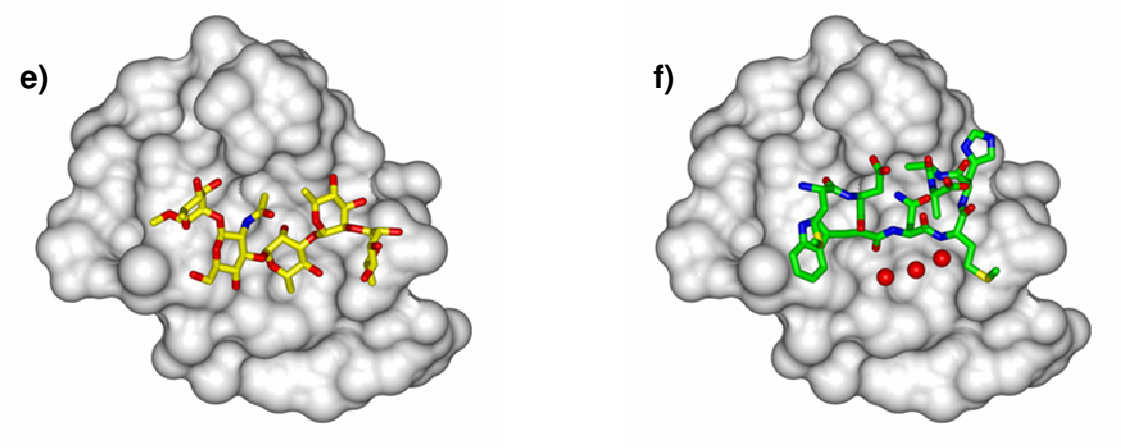

Figure 1-24: Structures of the (a) hexasaccharide fragment corresponding to the O-polysaccharide of the Streptococcus Group A, (b) pentasaccharide fragment of the O-polysaccharide of the S. flexneri Y, (c) average bound conformation of the hexapeptide DRPVPY**,** (d) 1.8-A resolution of the bound conformation of the octapeptide MDWNMHAA**,** (e) Fab fragment of SYA/J6 antibody with bound pentasaccharide, (f) Fab fragment of SYA/J6 antibody with bound octapeptide MDWNMHAA; the red spheres represent three immobilized water molecules.

1.3.3 Glycopeptides as mimics of bacterial carbohydrates

The combination of X-ray crystal structures and computation (specialized programs on molecular modeling) is currently emerging as a powerful tool for designing the second generation of therapeutics agents, possibly with much higher affinity. With the goal of developing efficient vaccines against bacterial infections, this technique is currently being explored to design new classes of compounds as potential ligands that could potentially raise antibodies against

bacterial cell-surface carbohydrates.[73,138,139] One of the well-developed approaches in designing new bioactive compounds, which is the shortest and most successful strategy, is to improve upon initial discoveries. Carbohydrate-mimetic peptides are such compounds that could be modified in an attempt to improve their immunogenicity. Since immunogenicity is normally directly proportional to the strength of binding affinity of the mimetic peptides to their respective anti-carbohydrate antibodies, improving the binding affinity by modifying the structures of the mimetic peptides in order to improve their interactions and complementarity with their respective combining sites of the antibodies, and hence their immunogenicity, is an ideal goal in the design of better ligands for anti-carbohydrate antibodies.

One way of improving the binding affinity of mimetic peptides is to combine the prominent parts of the mimetic peptides with those of their parent oligosaccharides, forming chimeric glycopeptides, which have the advantages of combining important features of both the original carbohydrates, and the mimetic peptides ligands. While several groups have investigated glycopeptides as mimetic ligands for carbohydrate-binding proteins, mainly based on combinatorial libraries comprising variability in both the peptide and carbohydrate portions,[73,138,139] a strategy employing rational design based on crystal structures represents a new challenge in the development of chimeric glycopeptides ligands for anti-carbohydrate antibodies. Based on the knowledge of the properties and characteristic features of the spatial arrangements of both the bound peptide and the bound parent carbohydrate in the combining site, obtained from X-ray

crystallography, the crucial parts of each ligand could be selected, while molecular modeling is used to test the binding modes of the newly designed chimeric ligand since the original peptide and carbohydrate interact with the antibody quite differently. Since structures of the bound chimeric glycopeptides in complex with antibody are not available, it is postulated that the carbohydrate portion, in most cases, would be vital for molecular recognition, occupying the same sub-site of the active site, as it occupies with the original parent carbohydrate.[73] The peptide portion, on the other hand, is expected to provide not only similar interactions as the missing oligosaccharide residues, but also additional favorable interactions other than structural mimicry, which altogether could improve the binding affinity of both the individual parent carbohydrate, and its peptide mimic ligand.[73] Alternatively, the newly designed chimeric glycopeptides could adopt completely different bioactive conformations when bound to their cognate anti-carbohydrate antibodies. If such chimeric glycopeptides with greater binding affinity than the individual carbohydrate or its peptide mimic could be achieved, their immunogenicity could then be studied in order to validate their use as surrogate mimics of bacterial carbohydrates in the development of vaccines against bacterial pathogens.

1.4 Immunochemistry and Immunology

Validating the immunogenicity of new candidate vaccines through functional immunological tests in animal models before proceeding to clinical

trials in humans has high potential. These preclinical testing strategies and rationales in research laboratories, even though are diverse, play an essential role both in contributing to optimize immunogenicity of vaccines based on results obtained, as well as to the understanding of protective immune mechanisms (antibody isotype, T-cell involvement, and specificity), evaluation of the safety and potency of vaccines (immunogenicity), and validating assays prior to clinical tests.[140,141] After several key issues such as the size of the antigen in the novel vaccine, animal models, route of administration, and choice of an appropriate adjuvant are considered, the vaccine candidate is then administered to the animal models following developed protocols, and a detailed analysis of the level and type of antibody responses in the case of antibody humoral immune response is carried out.[62,141]

An antigen with molecular weight less than 10 KDa is too small to be immunogenic.[83,142,143] An effective immunogen is one, which must at least consist of two different epitopes, one to stimulate a B-cell, and a second one to stimulate a helper T-cell.[62,83,143] Smaller molecules, which are referred to as haptens, even though they can effectively bind lymphocytes, cannot display two such clear epitopes, to induce a strong humoral immune response. One of the solutions to this problem is to couple the hapten to macromolecular carrier proteins such as TT, BSA, or keyhole limpet hemocyanin, which were found to be the most potent T-cell immunogens. In this case, the conjugate vaccine comprises a whole range of epitopes to react with both B-cells and T-cells of the immune system, resulting in a vigorous immune response with production of

antibodies targeting epitopes of both the carrier, and the hapten.[62,83,143] Even though the proportion of the antibodies made to the hapten would be small compared to that of the carrier protein, it would be far higher than with the hapten alone.[62,83]

In the design of an efficient hapten-carrier conjugate vaccine, several aspects such as selection of an appropriate carrier protein, the conjugation method, and the number of hapten molecules incorporated on the protein must be considered. In addition to its ability to enhance the immunogenicity of the conjugated hapten, a successful carrier protein must be safe for use in humans, cost effective, as well as, comprise an abundance of sites for hapten couplings.[144] On the other hand, the conjugation method, which is used to covalently link the hapten to the carrier protein, should be high yielding, and manipulation of the functional groups on both the hapten and carrier protein for attachment should not reduce the immunological functionality of the hapten or the carrier protein. The method should also allow optimal number of haptens to be conjugated to the protein since the strength of the immune response, directed against the newly created antigenic determinant, is often directly proportional to the amount of haptens attached to a carrier protein.[145] Furthermore, to preserve the chemical structure and spatial conformation of the hapten, and hence its biological activity when attached to a protein, a suitable linker, which is small in size and weakly immunogenic is normally required.[146] After the hapten is conjugated accordingly, the first preclinical testing of the vaccine includes *in vitro* studying of its immunochemical characterization using Enzyme-linked

Immunosorbent Assay (ELISA),[62] to determine if it is still being recognized by the antibody that originally binds to the hapten. The results obtained then determine if the conjugation method needs modification, whereas if the antigenicity of the hapten has not been suppressed upon conjugation, its immunogenicity is then studied *in vivo*.

During the last decades, there have been intensive efforts to determine animal models permitting an *in vivo* prelude to human studies with the new vaccine candidates. Of several animal models used to study immune responses, inbred mice provide a suitable model of the human immune system to chart all the fundamental pathways of immunity induced by new vaccines.[141] Besides sharing 99% of their genes with humans, mice are small, inexpensive and easier to handle.[147]

The route and frequency of administration of a tested vaccine in animal models should be as close as possible to that proposed for clinical use. While intramuscular or intraosseous mode of injections of vaccines are often used for inducing cellular immunity, targeting obligate intracellular pathogens, intradermal, intravenous, or subcutaneous injections, are those that are used for specifically inducing humoral immunity with production of protective antibodies and memory cells.[141] To further amplify and prolong an immune response to a hapten-carrier conjugate when administered as a vaccine, an appropriate adjuvant is normally added in the formulation. Aluminum salt-based substances, called alum, which are one of the few adjuvants licensed for clinical use in administered vaccines, are thought to adsorb the vaccine molecule, while maintaining a high

concentration near the site where the vaccine has been administered.[148] This then allows a slow release of the vaccine into the body, resulting in the generation of higher levels of antibodies over a longer period of time, thus rendering the vaccine more effective.

After a vaccine candidate with the appropriate adjuvant has been administered via the chosen route to groups of inbred mice, the immune sera collected after each vaccination for the presence and types of antibodies that recognize the antigen in the vaccine, as well as on the whole pathogen are determined by ELISA[62] (Figure 1-25). If active immunity is found to develop in the animal models after the immunization procedures, the efficacy of the vaccine is further tested to determine if it can convey protection in mice challenged with the live bacteria, and at the same time, the toxicity level of the vaccine, if there is any, on different organs of the animal models is also determined. These preclinical immunogenic results are crucial to determine if a new vaccine should move from laboratory to clinical testings in human, or should be altered structurally to improve its immunogenicity.

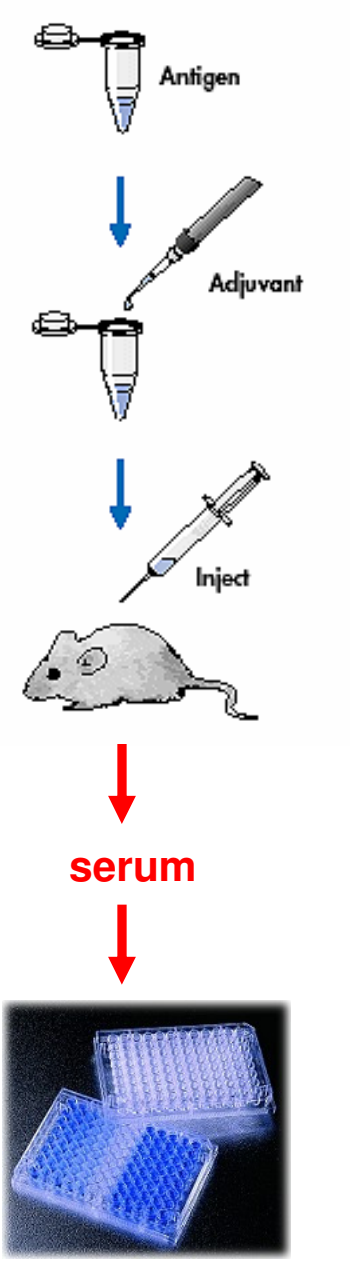

Figure 1-25: Immunological protocol for *in vivo* preclinical testing of a candidate vaccine.

1.5 Aim of research work

Since carbohydrate-mimetic peptide-based vaccines would have many advantages over carbohydrate-based vaccines to target bacterial pathogens, studying the requirements for these antigenic mimetic peptides as strong immunogens is crucial for the development of efficient peptide-based vaccines against bacterial infections. While many of them could raise antibodies against their original carbohydrates, others are not good mimotopes. There is now a growing interest to understand this phenomenon. When this project was initiated, it was not known whether differences in the binding modes of mimetic peptides (functional mimicry) would prevent them from inducing a protective immune response that would cross-react with the original carbohydrates. It was also not known whether mimetic peptides that do not display their bioactive conformations in the conformational ensemble of the free peptides would be able to act as potential mimotopes. The *Streptococcus* Group A and the *Shigella flexneri* Y provide two ideal systems to investigate these hypotheses including the requirements for immunogenicity by mimetic peptides in general. This information would be useful in the determination of carbohydrate-mimetic peptides as surrogate vaccines to target these two bacterial pathogens.

In order to study the immunogenicity of the two mimetic peptides identified for GAS and *Shigella flexneri* Y cell surface, we had to develop synthetic methods to prepare high-density peptide-protein conjugates comprising the two corresponding mimetic peptides, with appropriate chemical linkages, and suitable linker, followed by their immunochemical characterization. Recognition by their

complementary antibodies would then be studied. Should these studies yield positive results, the immunogenicity of the peptide conjugates would then be studied in mice to reveal the potential of these two carbohydrate-mimetic peptide protein conjugates as candidate vaccines against the corresponding bacteria, as well as to provide insight into the requirements for immunogenicity by mimetic peptides.

Since the immunogenicity of a mimetic peptide is dictated by the strength of the binding affinity of the peptide to the antibody, we further proposed to improve the binding affinity of the mimetic peptide, MDWNMHAA, by designing chimeric glycopeptides by molecular modeling, using previous information obtained from NMR, and X-ray crystallography, and to develop synthetic strategies to synthesize the glycopeptides. The immunochemical characterization of the glycopeptides would then be studied and if stronger binding affinity were achieved, the designed chimeric glycopeptides would then be conjugated to carrier proteins, and their immunogenicity studied *in vivo*.

In this thesis work, we were also interested in exploring molecular modeling strategy to design new glycopeptides as a mimic of the cell-wall polysaccharide of GAS in order to study whether conformational epitopes displayed by long sequences of polysaccharides could be simulated. After designing a potential glycopeptide, a synthetic strategy would then be developed.

The thesis is presented in a journal article style, with **Chapter 1** as a general introduction, followed by **Chapter 2**, **3**, **4**, **5** as four journal articles, and **Chapter 6** and **7**, as two unpublished research work.

Chapter 1 of this thesis consists of background information on emerging and re-emerging infectious diseases currently affecting the world population. The emergence of bacteria and their pathogenicity are also described, along with an overview of the two bacteria *Streptococcus* Group A and *Shigella flexneri* Y. The interesting properties of the immune system is also presented to show the different immune mechanisms in response to bacterial infections, as well as, how the immune system could be manipulated by the use of vaccine strategy to combat infectious diseases. The potential of carbohydrate-mimetic peptides as well as of newly designed glycopeptides based on crystal structures and molecular modeling, as vaccines are described, including, how the immunochemical characterization of a new vaccine candidate both *in vitro* and *in vivo* is generally determined.

Chapter 2 presents a manuscript (Hossany, B. R.; Johnson, M. A., Eniade, A. A.; Pinto, B. M. *Bioorg*. *Med. Chem*. **2004**, *12*, 3743-3754) that describes the synthesis and immunochemical characterization of protein conjugates of carbohydrate and carbohydrate-mimetic peptides as experimental vaccines. This chapter describes the synthetic strategy developed to synthesize protein conjugates of the two mimetic oligopeptides DRPVPY and MDWNMHAA, and their immunochemical characterization to determine if the two mimetic peptides are still recognized by their respective antibodies upon conjugation to carrier proteins.

Chapter 3 presents a manuscript (Borrelli, S.; Hossany, B. R.; Findlay, S.; Pinto, B. M. *Am*. *J*. *Immunol*. **2006**, *2*, 77-87) that describes the immunological

evidence for peptide-carbohydrate mimicry with a Group A *Streptococcus* polysaccharide-mimetic peptide. The immunogenicity in mice of the carbohydrate-mimetic peptide DRPVPY attached to tetanus toxoid that was evaluated to address our questions regarding the requirements for immunogenicity of carbohydrate-mimetic peptides, as well as, to determine if the mimetic peptide could effectively promote a strong and rapid thymus-dependent cross-reactive immune response against the original *Streptococcus* polysaccharide, is described.

Chapter 4 presents a manuscript (Borrelli, S.; Hossany, B. R.; Pinto, B. M. *Clin. Vaccine Immunol*. **2008**, *15*, 1106-1114) that describes the immunological evidence for functional versus structural mimicry with a *Shigella flexneri* Y polysaccharide-mimetic peptide. The immunogenicity in mice of the carbohydrate-mimetic peptide MDWNMHAA attached to tetanus toxoid that was evaluated to further address our questions of whether structural mimicry is required for immunogenicity of carbohydrate-mimetic peptides, including the importance of bioactive conformation in the free peptide, is described. The determination if the mimetic peptide could effectively promote a strong and rapid thymus-dependent cross-reactive immune response against the original *Shigella flexneri Y*, is also described.

Chapter 5 presents a manuscript (Hossany, B. R.; Johnston, B. D.; Wen, X.; Borrelli, S.; Yuan, Y.; Johnson, M. A.; Pinto, B. M. *Carbohydr. Res*. **2009**, *344*, 1412-1427) that describes the design, synthesis and immunochemical evaluation of a chimeric glycopeptide corresponding to the *Shigella flexneri* Y O-

polysaccharide and its peptide mimic MDWNMHAA. The chapter describes how molecular modeling and X-ray crystallography were exploited to design two glycopeptides comprising portions of both the O-polysaccharide and its peptide mimic, MDWNMHAA in an attempt to improve the binding affinity of the mimetic peptide. Two methods developed for the synthesis of the first candidate are described including the immunochemical characterization study of the synthesized glycopeptide.

Chapter 6 describes the progress made toward the synthesis of the second chimeric glycopeptide corresponding to the *Shigella flexneri* Y O-polysaccharide and its peptide mimic MDWNMHAA. The synthetic strategies and the progress made toward the total synthesis of the second candidate are described.

Chapter 7 describes the design of a glycopeptide mimic corresponding to the cell-wall polysaccharide antigen of the *Streptococcus* Group A in order to study the importance of conformational epitopes in immunogenicity. The synthetic strategy and the progress made toward the synthesis of the glycopeptide mimic are described.

1.6 References

(1) WHO, In *World Health Organization*; Genève, 2004.

(2) Butler, J. C., Crengle, S., Cheek, J. E. *Emerg. Infect. Dis.* **2001**, *7 (suppl.)*, 554-555.

(3) Guerrant, R. L., Blackwood, B. L. *Clin. Infect. Dis.* **1999**, *28*, 966–986.

(4) Koch, R. *Beiträge zur Biologie der Pflanzen* **1876**, *2*, 277–310.

(5) Porter, R. In *The Greatest Benefit to Mankind: A Medical History of Humanity from Antiquity to the Present* London, 1997.

(6) Worboys, M. In *Spreading Germs: Diseases, Theories, and Medical Practice in Britain*; Cambridge Univ. Press: Cambridge, 2000.

(7) Casadevall, A., Pirofski, L. A. *Infect. Immun.* **2000**, *68*, 6511-6518.

(8) Dorman, C. J. In *Bacterial Virulence: Philosophy and mechanisms*; Blackwell: Oxford, 1994.

(9) Salyers, A. A., Whitt, D. D. In *Bacterial Pathogenesis: a molecular approach* Washington, 1994; Vol. ASM.

(10) Finlay, B. B., McFadden, G. *Cell* **2006**, *124*, 767–782.

(11) Hughes, D., Andersson, D. I. In *Antibiotic Development and Resistance* Taylor and Francis: New York, 2001.

(12) Salyers, A. A., Whitt, D. D. In *Revenge of the microbes*; American Society for Microbiology: Colindale, 2005.

(13) Martinez, J. L. *Proc. R. Soc. B* **2009**, *276*, 2521-2530

(14) WHO, In *World Health Organization Report in Infectious Diseases*; Geneva, 2000.

(15) WHO, In *World Health Report 2007 - A safer future: global public health security in the 21st century*; Geneva, 2007.

(16) McMichael, A. J. In *Environmental and social influences on emerging infectious diseases: past, present, and future*; Oxford University Press: Oxford, 2005.

(17) Paiva de Sousa, C. *Braz. J. Infect. Dis.* **2003**, *7*, 23-31.

(18) Smolinski, M. S., Hamburg, M. A., Lederberg, J. In *Microbial Threats to Health:Emergence, Detection, and Response*; The National Academies Press: Washington, 2003.

(19) Weiss, R. A. *Philos. Trans. R. Soc. Lond. B Biol. Sci.* **2001**, *356*, 957-977.

(20) In *Climate Change: The Scientific Basis. Contribution of Working Group I to the Third Assessment Report of the Intergovernmental Panel on Climate Change*; Cambridge University Press: Cambridge, 2001.

(21) Patz, J. A., Campbell-Lendrum, D., Gibbs, H., Woodruff, R. *Annu. Rev. Public Health* **2008**, *29*, 27-39.

(22) Council, N. R. *Under the Weather: Climate, Ecosystem, and Infectious Disease*; National Academy Press: Washinghton, DC, 2001.

(23) Patz, J. A., Graczyk, T. K., Geller, N., Vittor, A. Y. *Int. J. Parasitol.* **2000**, *30*, 1395-1405.

(24) Wilson, M. L. In *Ecology and infectious disease* Johns Hopkins University Press: Baltimore, 2001.

(25) Marshall, B. J., Armstrong, J. A., McGechie, D. B., Glancy, R. J. *Med. J. Aust.* **1985**, *142*, 436-439.

(26) Toews, G. B. *Eur. Respir. Rev.* **2005** *14*, 62–68.

(27) Knobler, S. L., Mahmoud, A. A. F., Pray, L. A. In *Assessing the Science and response Capabilities, Workshop Summary*; National Academy Press: Washington DC, 2002.

(28) Moxon, E. R., Hood, D. W., Saunders, N. J., Schweda, E. K. H., Richards, J. C. *Philos. Trans. R. Soc. Lond. B Biol. Sci.* **2002**, *357*, 109–116.

(29) WHO, In *World Health Report: State of the Art of Vaccine Research and Development*; Geneva, 2009.

(30) Schopf, J. *Proc. Natl. Acad. Sci. USA 91* **1994**, *15*, 6735-6742.

(31) DeLong, E., Pace, N. *Syst. Biol.* **2001**, *50*, 470-478.

(32) Eldredge, N. In *Life on Earth*; ABC-CLIO: Santa Barbara, 2002.

(33) Srivastava, S., Srivastava, P. S. In *Understanding Bacteria*; Kluwer Academic Publishers: Norwell, 2003.

(34) Whitman, W., Coleman, D., Wiebe, W. *Proc. Natl. Acad. Sci. USA* **1998**, *95*, 6578–6583.

(35) De Marais, D. J. *Science* **2000**, *289*, 1703-1705.

(36) Todar, K. In *The Impact of Microbes on the Environment and Human Activities* 2008.

(37) Francis, J. W. In *Proceedings of the Fifth International Conference on Creationism*; Ivey, R. L. J., Ed.; Creation Science Fellowship: Pittsburgh, Pennsylvania, 2003, p 433–444.

(38) Porter, J. R. *Bacteriological reviews* **1976**, *40*, 260–269.

(39) Schulz, H., Jorgensen, B. *Annu. Rev. Microbiol.* **2001**, *55*, 105–137.

(40) Berg, J. M., Tymoczko, J. L., Stryer, L. In *Molecular Cell Biology*; 5th ed.; Freeman, W. H. & Co.: New York, 2002.

(41) Audesirk, T., Audesirk, G. In *Biology, Life on Earth*; 5th ed.; Prentice-Hall, 1999.

(42) Koch, A. *Clin. Microbiol. Rev.* **2003**, *16*, 673–687.

(43) Gitai, Z. *Cell* **2005**, *120*, 577–586.

(44) Shih, Y. L., Rothfield, L. *Microbiol. Mol. Biol. Rev.* **2006**, *70*, 729–754.

(45) Thanbichler, M., Wang, S., Shapiro, L. *J. Cell. Biochem.* **2005**, *96*, 506–521.

(46) Poehlsgaard, J., Douthwaite, S. *Nat. Rev. Microbiol.* **2005**, *3* 870–881.

(47) Nealson, K. *Orig. Life Evol. Biosph.* **1999**, *29*, 73–93.

(48) Alcamo, I. E. In *Fundamentals of Microbiology*; 5th ed ed.; Benjamin Cumming: Menlo Park, 1997.

(49) Tenaillon, O., Toupance, B., Le Nagard, H., Taddei, F., Godelle, B. *Genetics* **1999**, *152*, 485–493.

(50) Perfeito, L., Fernandes, L., Mota, C., Gordo, I. *Science* **2007**, *317*, 813-815.

(51) Alberts, B., Dennis, B., Lewis, J., Raff, M., Roberts, K., Watsonis, J. D. In *Molecular Biology of the Cell* Garland Publishing, a member of the Taylor & Francis Group: New York, 1994.

(52) Belkum, A. V., Struelens, M., Visser, A. D., Verbrugh, H., Tibayrenc, M. *Clin. Microbiol. Rev.* **2001**, *14*, 547–560.

(53) Vandamme, P. A. R. In *Manual of clinical microbiology* 8th ed.; American Society for Microbiology: Washington, 2003.

(54) Beveridge, T. J. *Int. Rev. Cytol.* **1981**, *72*, 229–317.

(55) Beveridge, T. J. *J. Bacteriol.* **1990**, *172*, 1609–1620.

(56) Hentschel, U., Steinert, M., Hackeret, J. *Trends Microbiol.* **2000**, *8*, 226–231.

(57) Guarner, F., Malagelada, J. R. *Lancet* **2003**, *361*, 512–519.

(58) O'Hara, A. M., Shanahan, F. *EMBO Rep.* **2006**, *7*, 688–693.

(59) Martínez, J. L., Baquero, F. *Clin. Microbiol. Rev.* **2002**, *15* 647-679.

(60) Habicht, G. S. *Ann. N. Y. Acad. Sci.* **1994**, *712*, ix-xi.

(61) Kaufmann, S. H. E., Sher, A., Ahmed, R. In *Immunology of infectious diseases*; American Society For Microbiology Herndon, 2002.

(62) Janeway, C. A., Travers, P. In *Immunobiology: The Immune System in Health and Disease*; 3rd ed.; Garland: New York, 1997.

(63) Medzhitov, R., Janeway, C. A. Jr. *Curr. Opin. Immunol.* **1997**, *9*, 4–9.

(64) Bos, J. D. In *Skin Immune System (SIS): Cutaneous Immunology and Clinical Immunodermatology* CRC LLC: Boca Raton, 2005.

(65) DeFranco, A. L., Locksley, R. M., Robertson, M. *Immunity*; New Science Press: London, 2007.

(66) Janeway, C. A. J., Medzhitov, R. *Annu. Rev. Immunol.* **2002**, *20*, 197-216.

(67) Garcia, K. C., Teyton, L., Wilson, I. A. *Annu. Rev. Immunol.* **1999**, *17*, 369-397.

(68) Novotny, J., Bruccoleri, R., Newell, J., Murphy, D., Haber, E., Karplus, M. *J. Biol. Chem.* **1983**, *258*, 14433-14437.

(69) Litman, G. W., Rast, J. P., Shamblott, M. J. *Mol. Biol. Evol.* **1993**, *10*, 60–72.

(70) Mattu, T., Pleass, R., Willis, A., Kilian, M., Wormald, M., Lellouch, A., Rudd, P., Woof, J., Dwek, R. *J. Biol. Chem.* **1998**, *273*, 2260–2272.

(71) Market, E., Papavasiliou, F. N. *PLoS Biol.* **2003**, *1*, e16.

(72) Edelman, G. M. *Science* **1973**, *180*, 830-840.

(73) Johnson, M. A., Pinto, B. M. *Topics Curr. Chem.* **2008**, *160*, 1001-1011.

(74) Johnson, M. A.; Pinto, B. M. *Aust. J.Chem.* **2002**, *55*, 13-25.

(75) Johnson, M. A.; Pinto, B. M. *Carbohydr. Res.* **2004**, *339*, 907-928.

(76) Johnson, M. A.; Rotondo, A.; Pinto, B. M. *Biochemistry* **2002**, *41*, 2149-2157.

(77) Porter, R. R. *Science* **1973**, *180*, 713-716.

(78) Fleckenstein, J. M., Kopecko, D. J. *J Clin Invest.* **2001**, *107*, 27–30.

(79) Finlay, B. B., Falkow, S. *Microbiol. Mol. Biol. Rev.* **1997**, *61*.

(80) Schaechter, M., Engleberg, N. C., DiRita, V. J., Dermody, T. In *Schaechter's Mechanisms of Microbial Disease*; 4th ed.; Lippincott Williams & Wilkins, 2006.

(81) Lachmann, P. J., Oldstone, M. B. A. In *Microbial Subversion of Immunity*; Caister Academic Press: Norfolk, 2006.

(82) Lukacova, M., Barak, I., Kazar, J. *Clin. Microbiol. Infect.* **2008**, *14*, 200–206.

(83) Engelkirk, P. G., Duben-Engelkirk, J. In *Laboratory Diagnosis of Infectious Diseases: Essential of Diagnosis Mibrobiology*; Lippincott, W.: Texas, 2008.

(84) Welch, M. D. In *Listeria monocytogenes: Pathogenesis and Host Response*; Springer US: Berkeley, 2007, p 197-223.

(85) Munford, R. S. *Infect. Immun.* **2008**, *76*, 454-465.

(86) Bisno, A. L. In *Principles of Infectious Diseases*; Wiley: New York, 1985.

(87) Fong, I. W., Drlica, K. In *Reemergence of Established Pathogens in the 21st Century* Kluwer Academic/Plenum New York, 2003.

(88) Cunningham, M. D. *Clin. Microbiol. Rev.* **2000**, *13*, 470-511.

(89) Facklam, R. *Clin. Microbiol. Rev.* **2002**, *15*, 613-630.

(90) Batzloff, M. R., Sriprakash, K. S., Good, M. F. *Curr. Drug Targets* **2004**, *5*, 57-69.

(91) Lancefield, R. *J. Exp. Med.* **1928**, *47*, 9-10.

(92) Fischetti, V. A. *Clin Microbiol Rev* **1989**, *2*, 285-314.

(93) Keusch, G. T., Acheson, D. W. D. In *Enteric Infections and Immunity*; Plenum: New York, 1996.

(94) Thorpe, C. M., Smith, W. E., Hurley, B. P., Acheson, D. W. *Infect. Immun.* **2001**, *69*, 6140–6147.

(95) Kweon, M. *Curr. Opin. Infect. Dis.* **2008**, *21*, 313–318.

(96) Niyogi, S. K. *J. Microbiol.* **2005**, *43*, 133–143.

(97) Kaper, J. B., Nataro, J. P., Mobley, H. L. T. *Nat. Rev. Microbiol.* **2004**, *2*, 123-140.

(98) Sansonetti, P. J. *Nat. Rev. Immunol.* **2004**, *4*, 953–964.

(99) Lindberg, A. A., Haeggman, S., Karlsson, K., *Bull. World Health Organ.* **1984**, *62*, 597-606.

(100) Jenner, E. In *An Inquiry Into the Causes and Effects of the Variolae Vaccinae, a Disease Discovered in Some of the Western Counties of England, Particularly Gloucestershire, and Known by the Name of the Cow Pox*; Sampson Low: London, 1798.

(101) Fenner, F., Henderson, D. A., Arita, I., Jezek, Z., Ladnyi, I. D. "Smallpox and its eradication," 1988.

(102) WHO In *Weekly Epidemiological Record* 1998; Vol. 50, p 389-393.

(103) Ada, G. L., Ramsay, A. J. *Vaccines, vaccination, and the immune response*; Lippincott-Raven: Philadelphia, 1997.

(104) "Division of Microbiology and Infectious Diseases. Accelerated development of vaccines: the Jordan Report," 2000.

(105) Cruz, S. J. In *Immunotherapy and Vaccines*; VCH: Weinhein, 1997.

(106) Mackett, M. W., J. D. In *Human Vaccine*; Bios Scientific: Oxford, 1995.

(107) Mims, C. A. In *The Pathogenesis of Infectious Disease*; Academic: London, 1976.

(108) Gorda, A. *N. Engl. Med.* **2001**, *345*, 1042-1053.

(109) Rosenberg, I. M. In *Protein analysis and purification: Benchtop Techniques* 2nd ed.; Birkhausser: Boston, 2005.

(110) Davis, H. L. *Curr. Opin. Biotechnol.* **1997**, *8*, 635-640

(111) Robinson, H. L., Pertmer, T. M. *Adv. Virus Res.* **2000**, *55*, 1-74.

(112) Jennings, H. J. *Adv. Exp. Med. Biol.* **1988**, *228*, 495-550.

(113) Jennings, H. J. *Curr. Top. Microbiol. Immunol.* **1990**, *150*, 97-127.

(114) Lindberg, A. A. *Vaccine* **1999**, *17 Suppl. 2*, S28-36.

(115) Mc Cool, T. L., Harding, C. V., Greenspan, N. S., Schreiber, J. R. *Infect. Immun.* **1999**, *67*, 4862.

(116) Weintraub, A. *Carbohydr. Res.* **2003**, *338*, 2539-2547.

(117) Mond, J. J., Lees. A., Snapper, C. M. *Annu. Rev. Immunol.* **1995**, *13*, 655-692.

(118) Parker, D. C. *Annu. Rev. Immunol.* **1993**, *11*, 331-360.

(119) Bencomo, V. V., Fernández-Santana,V., Hardy, E. Toledo, M. E., Rodríguez, M. C., Heynngnezz, L., Rodriguez, A, Baly, A., Herrera, L. Izquierdo, M., Villar, A., Valdés, Y., Cosme, K., Deler, M. L., Montane, M., Garcia, E., Ramos, A., Aguilar, A., Medina, E., Toraño, G., Sosa, I., Hernandez, I., Martínez, R., Muzachio, A., Carmenates, A., Costa, L., Cardoso, F., Campa, C., Diaz, M., Roy, R. *Science* **2004**, *305*, 522 - 525.

(120) Seeberger, P. H. *Carbohydr. Res.* **2008**, *343*, 1889-1896.

(121) Plante, O. J., Palmacci, E. R., Seeberger, P. H. *Science* **2001**, *291*, 1523-1527.

(122) Boons, G. J. *Contemp. Org. Synth.* **1996**, *3*, 173–200.

(123) Monzavi-Karbassi, B., Cunto-Amesty, G., Luo, P., Kieber-Emmons, T. *Trends Biotechnol.* **2002**, *20*, 207-214.

(124) Köhler, H., Kaveri, S., Kieber-Emmons, T., Morrow, W. J. W., Müller, S., Raychaudhuri, S. *Methods Enzymol.* **1989**, *178*, 3–35.

(125) Monafo, W. J., Greenspan, N. S., Cebra-Thomas, J. A., Davie, J. M. *J. Immunol.* **1987**, *139*, 2702–2707.

(126) Stein, K. E., Soderstrom, T. *J. Exp. Med.* **1984**, *160*, 1001-1011.

(127) Westerink, M. A. J., Giardina, P. C., Apicella, M. A., Kieber-Emmons, T. *Proc. Natl. Acad. Sci. USA.* **1995**, *92*, 4021-4025.

(128) Jerne, N. K. *Ann. Immunol.* **1974**, *125C*, 373-387.

(129) Pan, Y., Yuhasz, S. C., Amzel, L. M. *The FASEB Journal* **1995**, *9*, 43-49.

(130) Johnson, M. A.; Pinto, B. M. *Bioorg. Med. Chem.* **2004**, *12*, 295-300.

(131) Vyas, N. K.; Vyas, M. N.; Chervenak, M. C.; Bundle, D. R.; Pinto, B. M.; Quiocho, F. A. *Proc. Natl. Acad. Sci. U. S. A.* **2003**, *100*, 15023-15028.

(132) Carlin, N. I., Gidney, M. A., Lindberg, A. A., Bundle, D. R. *J. Immunol.* **1986**, *137*, 2361-2366.

(133) Harlow, E., Lane, D. In *Antibodies: A Laboratory Manual*; Cold Spring Harbor Laborotory, 1988.

(134) Harris, S. L.; Craig, L.; Mehroke, J. S.; Rashed, M.; Zwick, M. B.; Kenar, K.; Toone, E. J.; Greenspan, N.; Auzanneau, F. I.; MarinoAlbernas, J. R.; Pinto, B. M.; Scott, J. K. *Proc. Natl. Acad. Sci. U. S. A.* **1997**, *94*, 2454-2459.

(135) Carlin, N. I. A.; Lindberg, A. A.; Bock, K.; Bundle, D. R. *Eur. J. Biochem.* **1984**, *139*, 189-194.

(136) Vyas, M. N.; Vyas, N. K.; Meikle, P. J.; Sinnott, B.; Pinto, B. M.; Bundle, D. R.; Quiocho, F. A. *J. Mol. Biol.* **1993**, *231*, 133-136.

(137) Vyas, N. K.; Vyas, M. N.; Chervenak, M. C.; Johnson, M. A.; Pinto, B. M.; Bundle, D. R.; Quiocho, F. A. *Biochemistry* **2002**, *41*, 13575-13586.

(138) St. Hilaire, P. M., Meldal, M. *Angew. Chem. Int. Ed.* **2000**, *39*, 1162-1179.

(139) Tang, Y., Zhu, W., Chen, K., Jiang, H. *Drug Discovery Today: Technologies* **2006**, *3*, 307-313.

(140) Fattom, A. I., Horwith, G., Fuller, S., Propst, M., Naso, R. *Vaccine* **2004**, *22*, 880-887.

(141) Griffin, J. F. T. *Adv. Drug Deliv. Rev.* **2002**, *54*, 851-861.

(142) Sheedy, C., MacKenzie, C. J., Hall, J. C. *Biotech. Adv.* **2007**, *25*, 333-352.

(143) Kuby, J. *Immunology*; Freeman, W. H. and company: New-York, 1997.

(144) Mahender, K. S., Srivastava, S., Raghava, G. P. S., Varshney, G. C. *Bioinformatics* **2006**, *22* 253-255.

(145) Pozsgay, V., Chu, C., Pannell, L., Wolfe, J., Robbins, J. B., Schneerson, R., *Proc. Natl. Acad. Sci. USA* **1999**, *96*, 5194-5197.

(146) Buskas, T., Liao, J., Boons, G.-J. *Chem. Eur. J.* **2004**, *10*, 3517-3524s.

(147) Waterston, R. H., Lindblad-Toh, K., Ewan, B., Jane, R., Abril, J. F.; Agarwal, P., Agarwala, R., Ainscough, R., Alexandersson, M., An, P., Antonarakis, S. E., Attwood, J., Baertsch, R., Bailey, J., Barlow, K., Beck, S., Berry, E., Birren, B., Bloom, T. *nature* **2002**, *420*, 520-562.

(148) Virelizier, J.-L. *Biologicals* **2009**, *37* 139-140.

CHAPTER 2: SYNTHESIS AND IMMUNOCHEMICAL CHARACTERIZATION OF PROTEIN CONJUGATES OF CARBOHYDRATE AND CARBOHYDRATE-MIMETIC PEPTIDES AS EXPERIMENTAL VACCINES

This chapter comprises the manuscript **"*Synthesis and immunochemical characterization of protein conjugates of carbohydrate and carbohydrate-mimetic peptides as experimental vaccines*"** which has been published in Bioorganic and Medicinal Chemistry (**2004**, *12*, 3743-3754).

Rehana B. Hossany, Margaret A. Johnson, Adewale A. Eniade and B. Mario Pinto

Understanding the requirements for immunogenicity (capacity to induce an immune response against the original carbohydrate) of carbohydrate-mimetic peptides is vitally important for improving existing vaccines or for the development of new vaccines to target bacterial pathogens where carbohydrate vaccines have failed or where no vaccines exist. After identification of the two carbohydrate-mimetic peptides DRPVPY and MDWNMHAA, from phage-displayed libraries, we were interested in determining the immunogenicity of the two mimetic peptides.

This would characterize their potential as surrogate vaccines against the two pathogenic bacteria *Streptococcus* Group A and *Shigella flexneri* Y respectively, as well as addressing our questions of whether differences in their mechanism of binding (functional mimicry) from that of the original carbohydrates would allow them to elicit a cross-reactive immune response with their respective carbohydrates. Furthermore, by studying their immunogenicities, we would also be able to test whether well-defined turn conformations adopted by mimetic peptides in the combining site of antibody should be present to a certain extent in the free peptide ensemble to enable a mimetic peptide to be immunogenic.

While carbohydrate-mimetic peptides are capable of effectively reacting with anti-carbohydrate antibodies *in vitro*, they are often too small on their own to induce production of antibodies *in vivo*, since small peptides, typically <2.5 KDa are only epitopes of the B-cells, and do not contain additional motifs required to associate with T-cell receptors. Therefore, in order to study the immunogenicity of the two mimetic peptide haptens, it was first necessary to conjugate them to carrier proteins.

In this chapter, an efficient protocol that has been developed by the thesis author to synthesize protein conjugates of DRPVPY and MDWNMHAA is described. In the preparation of the peptide-protein conjugates, selection of an appropriate carrier protein, the conjugation method, and the number of peptide molecules incorporated on the carrier protein were considered, as discussed in Chapter 1. In this study, we

chose bovine serum albumin (BSA) and tetanus toxoid (TT) as carrier proteins as they are non-toxic and suitable for human use. While BSA was commercially available, TT was provided by Dr. Francis Michon. The conjugation method developed in the curent work represents a new and successful strategy to link peptide haptens to a carrier protein via the *N*-terminus of the peptide. As far as the number of peptide haptens incorporated onto carrier proteins is concerned, the synthesis of high density peptide-protein conjugates were successfully achieved with both the peptides.

The chapter also describes the results obtained after the peptide conjugates were re-evaluated *in vitro* as ligands for their respective antibodies. This was to determine if the two oligopeptides DRPVPY and MDWNMHAA were still recognized by their same respective antibodies upon conjugation to carrier proteins. The immunochemical characterization study was performed by Dr. Margaret A. Johnson.

For the *Shigella flexneri* Y system, a polysaccharide-TT conjugate was also prepared by the thesis author for use as a positive control in the immunochemical characterization study. The polysaccharide used was a gift from Dr. David Bundle of the University of Alberta. Moreover, as a negative control for the same system, a BSA conjugate of the octapeptide MDWNPHAA, in which a methionine at the fifth position of the mimetic octapeptide was substituted by a proline residue, was synthesized by the

thesis author. The peptide MDWNPHAA itself was prepared by Dr. Adewale Eniade.

Overall, it was found that conjugations of the two mimetic peptides DRPVPY and MDWNMHAA to the two carrier proteins did not hamper their ability to bind to their respective monoclonal anti-carbohydrate antibodies directed against their respective bacterial polysaccharides.

The recognition of the prepared peptide-protein conjugates by their cognate antibodies was an initial step toward determining the potential of the two mimetic peptides DRPVPY and MDWNMHAA for use as vaccines to target the two pathogenic bacteria *Streptococcus* Group A and *Shigella flexneri* Y, respectively. Our next step would be to test the immunogenicity of the corresponding peptide-based vaccines in mice to determine if they were capable of inducing production of antibodies that would cross-react with their respective bacterial polysaccharides. This would address our questions and also provide insight into the requirements for immunologically cross-reactive peptide mimics of carbohydrates.

2.1 KEYWORDS

Carbohydrate-mimetic peptides, Protein conjugate vaccines, Polysaccharide-conjugate vaccine, Group A *Streptococcus*, *Shigella flexneri* Y

2.2 ABSTRACT

The peptides DRPVPY and MDWNMHAA, which were identified as mimics of the cell-surface polysaccharides of *Streptococcus* Group A and *Shigella flexneri* Y, respectively, were used in this study to develop experimental vaccines directed against these two bacteria. Both oligopeptides were synthesized employing the Fmoc solid-phase strategy and linked via the amino end to a bifunctional linker, diethylsquarate. These adducts were then conjugated to the two carrier proteins, bovine serum albumin (BSA) and tetanus toxoid (TT) to yield the peptide conjugate vaccines. The average level of incorporation of DRPVPY and MDWNMHAA on TT was 65% and 75%, respectively, whereas that of both peptide haptens on BSA was 100%. A polysaccharide conjugate against *S. flexneri* Y, which comprises about 10 tetrasaccharide repeating units, was also prepared based on reductive amination at the reducing end with 1,3-diaminopropane, followed by coupling of the aminated polysaccharide to diethylsquarate, and subsequent coupling of the adduct to TT. An average incorporation of 73% of polysaccharide haptens was achieved. The glycoconjugate and the oligopeptide conjugates were shown to

bind effectively to the respective monoclonal antibodies directed against the cell-surface polysaccharides.

2.3 INTRODUCTION

Many strategies are being explored to manipulate the immune system to better fight a pathogen.[1] One of the most efficient and cost-effective methods is a prime/boost strategy with vaccines.[2] Several types of vaccines, which comprises either an attenuated strain of the infectious organism, killed organisms, part of the organism, or a weakened form of a toxin that it produces, have been developed and used.[2-4] However, the possibility of infection with these agents has led to their replacement by subunit vaccines, which contain only the antigens that trigger the immune system.[4-5]

Carbohydrates that coat the surfaces of many pathogenic microorganisms, such as bacteria, as well as being important in bacterial survival and virulence within the host, are also one of the main biomolecules that are recognized by the immune system.[6-9] Therefore, targeting carbohydrate antigens is a promising avenue in order to develop efficient vaccines. Some polysaccharide-based vaccines have been successfully developed, but generally show weak immunogenic effects, poor responses in infants, the elderly, and in immunodeficient persons. [6-9] Polysaccharide–protein conjugates, on the other hand, have proven effective in several cases,[9] and well-defined oligosaccharide-conjugate vaccines have also been explored with a view to eliciting discriminating

immune responses.[10] However, the complex structures of polysaccharide conjugates, their production, and characterization,[11,12] make alternative approaches, to drive specific T-cell dependent immune responses against carbohydrate antigens, highly desirable.

Peptide mimics of carbohydrates have potential as surrogate ligands for traditional carbohydrate vaccines.[13] Several studies have successfully identified peptide sequences, through phage-displayed library screening, that specifically mimic certain carbohydrate structures;[13] in certain cases, these peptides could also induce an immune response against the original carbohydrate antigen.[13] Carbohydrate-mimetic peptides, which are easier to synthesize, also have the potential of eliciting a more targeted immune response and therefore present attractive candidates as vaccines, especially in cases involving autoimmune responses.[13]

We have targeted two bacteria to illustrate the potential of the method. The first, the Group A *Streptococcus* (GAS), causes streptococcal pharyngitis (strep throat), some forms of pneumonia, toxic shock syndrome, and necrotizing fasciitis or flesh-eating disease.[14,15] Polysaccharide-conjugate vaccines have been used in immunization of animals and the bactericidal activity of human sera (containing antibodies to GAS polysaccharide) against several strains of GAS in vitro has been demonstrated.[16] The second bacterial strain, *Shigella flexneri* Y is another virulent bacteria that causes bacillary dysentery by invading the colonic mucosa.[17] Although this particular serogroup is not a significant human pathogen, it nevertheless serves as a useful model system. The cell-wall

polysaccharide of GAS is made up of a branched trisaccharide repeating unit, l-Rha-α-(1 → 2)-[d-GlcNAc-β-(1 → 3)]-α-l-Rha [Figure 2-1(a)],[18,19] while the *O*-polysaccharide of *S. flexneri* Y is comprised of the repeating unit (→2)-α-l-Rha-α-(1 → 2)-α-l-Rha-α-(1 → 3)-α-l-Rha-α-(1 → 3)-β-d-GlcNAc-(1 →) [Figure 2-1(c)].[20,21] Screening of a phage-displayed peptide library with the anti-carbohydrate antibody SA-3, directed against GAS polysaccharide yielded the peptide sequence DRPVPY (Figure 2-1b).[22] Similarly, an octapeptide with sequence MDWNMHAA (Figure 2-1d),[22] was identified as a ligand for the anti-*S. flexneri* Y antibody SYA/J6. This antibody is ideally suited for characterizing the conjugates synthesized in the present work against *S. flexneri* Y, since it has been the subject of extensive ligand mapping and crystallography studies by Bundle et al.[23,24]

Both oligopeptides DRPVPY and MDWNMHAA have been found to specifically bind to their corresponding antibodies used to screen peptide libraries.[22] Our long-term objective is to test the immunogenicity of the corresponding peptide-based vaccines and the cross-reactivity of immune sera with the bacterial polysaccharide. Accordingly, it was necessary to first prepare peptide conjugates and characterize them immunochemically.

The method used in the coupling of the immunizing peptide with a carrier protein is an important factor to consider when preparing peptide antigens. This factor is of concern because the flexible peptide may adopt a different preferred conformation when attached to the carrier protein.[25] The position of attachment of a peptide to the carrier protein, dictated by the conjugation method, affects the

reactivity of the resulting conjugated peptide toward its complementary antibody.[26-28] Several reports exist in which peptides were conjugated via the side chain of lysine,[27] cysteine,[27-29] aspartic acid,[28] glutamic acid,[28] threonine[30] or serine.[30]

In the cases at hand, NMR and molecular modeling studies of the bound conformations of DRPVPY[31] and MDWNMHAA,[32] and replacement analysis of MDWNMHAA[33] had indicated that all the amino acids, except aspartic acid in DRPVPY and methionine (1) in MDWNMHAA, formed part of the critical epitopes. We reasoned therefore, that on conjugation of the two oligopeptides DRPVPY and MDWNMHAA to the carrier proteins, bovine serum albumin (BSA) and tetanus toxoid (TT), via the N-termini of the peptides would lead to conjugated oligopeptides that would still be recognized by the respective antibodies.

We thus embarked on a program to synthesize the carbohydrate-mimetic peptide conjugates using the two peptide sequences DRPVPY and MDWNMHAA, and describe here our findings. We chose to explore a strategy that had been very successful for the preparation of oligosaccharide-protein conjugates, namely the use of the bifunctional linker, diethylsquarate.[34-36] The application of this methodology to peptide-protein conjugates is unprecedented, to the best of our knowledge. We report in the present work the synthesis of oligopeptide-ethylsquarate adducts, linked directly via the N-termini of the peptides, followed by their conjugation to the carrier proteins, BSA, and TT. We also report the synthesis of the *S. flexneri* Y *O*-polysaccharide conjugate of TT

for use in a prime/boost vaccination protocol. Finally, the immunochemical evaluation of both the glycoconjugate and the oligopeptide conjugates as ligands for their respective antibodies is described.

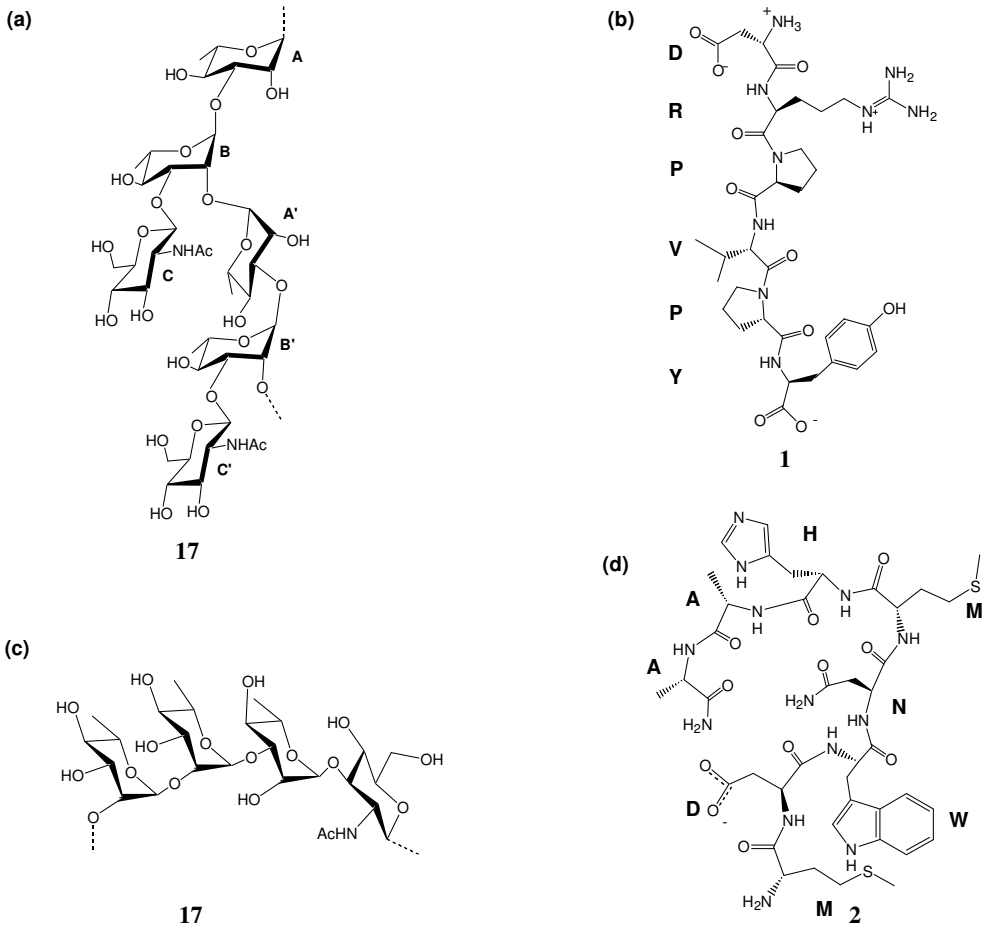

Figure 2-1: Structures of the (a) the cell-wall polysaccharide of Group A Streptococcus, (b) its peptide mimic, (c) the O-polysaccharide of S. flexneri Y, and (d) its peptide mimic.

2.4 RESULTS AND DISCUSSION

2.4.1 Synthesis

Since an amide functionality was desired at the C-termini of the peptides, the peptide sequences were assembled on Rink amide MBHA resin[37,38] employing Fmoc chemistry[39] and the HBTU/HOBt/DIPEA coupling strategy.[40] When the peptide chains were completed, the Fmoc protecting group was removed and cleavage/deprotection was carried out using TFA-triisopropylsilane-CH_2Cl_2, where the triisopropylsilane served as a scavenger.[37] Acid labile side chain protecting groups were utilized so that simultaneous side chain deprotection and cleavage of the peptide could be achieved. The peptides **1**-**3** were purified by HPLC on a C_{18} reverse-phase column (gradient elution CH_3CN/H_2O) and, after lyophilization, they were obtained as white powders, in yield ranging from 44% to 60% (Scheme 2-1).

The hexapeptide H-DRPVPY-NH_2 (**1**) and the octapeptide H-MDWNMHAA-NH_2 (**2**) were then conjugated to the two carrier proteins bovine serum albumin (BSA) and tetanus toxoid (TT), as described below (Scheme 2-2 and Scheme 2-3). The octapeptide H-MDWNPHAA-NH_2 (**3**), which was found to bind with a very low affinity to the anti-carbohydrate antibody SYA/J6 with respect to H-MDWNMHAA-NH_2 (**2**),[33] was also conjugated to BSA (Scheme 2-2 and Scheme 2-3) to provide a negative control in immunochemical experiments.

Scheme 2-1: Solid phase synthesis of the peptides **1**-**3**

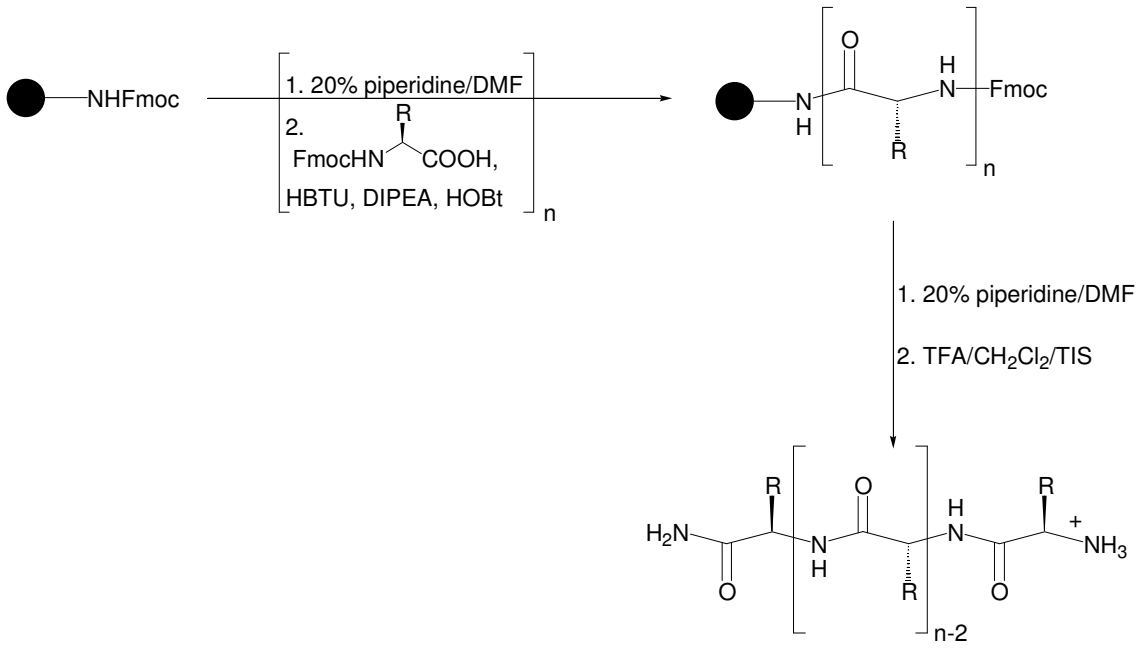

compound	n	peptide	%
1	6	DRPVPY	60
2	8	MDWNMHAA	48
3	8	MDWNPHAA	40

The hexapeptide H-DRPVPY-NH_2 (**1**) and the octapeptide H-MDWNMHAA-NH_2 (**2**) were then conjugated to the two carrier proteins bovine serum albumin (BSA) and tetanus toxoid (TT), as described below (Scheme 2-2 and Scheme 2-3). The octapeptide H-MDWNPHAA-NH_2 (**3**), which was found to bind with a very low affinity to the anti-carbohydrate antibody SYA/J6 with respect to H-MDWNMHAA-NH_2 (**2**),[33] was also conjugated to BSA (Scheme 2-2 and Scheme 2-3) to provide a negative control in immunochemical experiments.

We examined the use of the bifunctional linker, 3,4-diethoxy-3-

cyclobutene-1,2-dione (diethylsquarate), to link the peptides to the carrier proteins BSA and TT; this linker was found to be successful in the coupling of oligosaccharide-squarate adducts with protein carriers.[34-36] When the peptides **1**-**3** were added to diethylsquarate in methanol at room temperature, no reaction occurred, most probably because the amino termini of the peptides were protonated. Addition of small portions of sodium acetate to the reaction mixtures initiated the reactions and after 1 h, there was complete disappearance of the free peptides, as judged by MALDI-TOF mass spectrometry. After purification by HPLC and lyophilization, the peptide-squarate adducts **4**-**6** were obtained as white powders in yields ranging from 55% to 76% (Scheme 2-2). Both the free peptides **1**-**3** and the peptide-squarate adducts **4**-**6** were characterized by 1D and 2D (TOCSY) NMR spectroscopy and MALDI-TOF mass spectrometry. The peptide-squarate adducts **4**-**6** were then coupled to the carrier proteins BSA and TT via the conjugate addition of the ε-amino groups of the lysines of the protein to the monoethyl squarate (Scheme 2-3).

The first coupling reaction was attempted with the squarate-MDWNPHAA-NH_2 (**6**), and BSA, and resulted in the incorporation of an average of three peptide haptens (11%) in the conjugate **9**. The reaction was repeated and the average level of incorporation of the oligopeptide could be improved to 20 (71%) when the volume as well as the molar concentration of the carbonate buffer used in the second trial were reduced. In the coupling of squarate-DRPVPY-NH_2 (**4**) and squarate-MDWNMHAA-NH_2 (**5**) to BSA (Scheme 2-3), similar reaction conditions were applied but the two oligopeptide-squarate adducts **4** and **5** were

added directly to the BSA, dissolved in a minimum volume of buffer. MALDI-TOF mass spectrometry showed an average incorporation of 28 haptens per BSA molecule (100%) for both oligopeptide conjugates **7** and **8**.

The peptide-squarate adducts **4** and **5** were added to tetanus toxoid in carbonate buffer, and the reaction mixtures were stirred for 3-5 days at room temperature and monitored by MALDI-TOF mass spectrometry. When no further increase in the incorporation of the peptides on the protein was observed, the reaction mixtures were dialyzed against distilled water and lyophilized to give the tetanus toxoid-squarate-peptide conjugates **10** and **11** as white powders (Scheme 2-3). The DRPVPY and MDWNMHAA haptens were incorporated on the protein in yields of 65% and 75%, respectively.

Scheme 2-2: Synthesis of the peptide-squarate adducts **4**-**6**

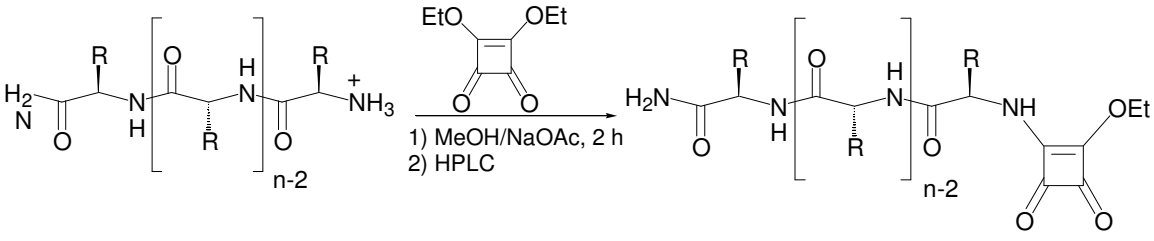

compound	n	peptide-squarate adduct	%
4	6	DRPVPY-squarate	76
5	8	MDWNMHAA-squarate	63
6	8	MDWNPHAA-squarate	55

Scheme 2-3: Synthesis of the peptide protein conjugates **7**-**11**

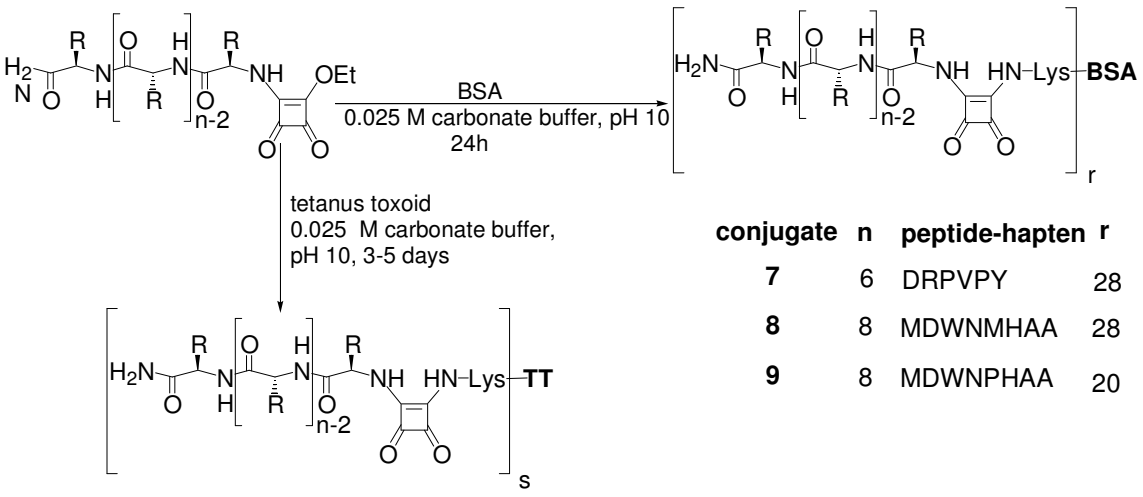

conjugate	n	peptide-hapten	r
7	6	DRPVPY	28
8	8	MDWNMHAA	28
9	8	MDWNPHAA	20

conjugate	n	peptide-hapten	s
10	6	DRPVPY	39
11	8	MDWNMHAA	45

For the immunological studies, a polysaccharide-conjugate antigen of *S. flexneri* Y, which comprises about 10 oligosaccharide repeating units,[41] was prepared from *O*-polysaccharide supplied by D. R. Bundle (University of Alberta). An amino functionality was first introduced to the KDO residue of the core region of the polysaccharide **12** at the reducing end by reductive amination with 1,3-diaminopropane,[42] followed by coupling of the aminated polysaccharide **13** to diethylsquarate and, subsequent coupling of the resulting adduct **14** to the carrier protein TT (Scheme 2-4). The reductive amination reaction was performed for 6 days, as reported in the literature,[42] and after dialysis against water, gave a mixture of aminated polysaccharide **13** and unreacted polysaccharide **12** as a white powder (Scheme 2-4). The aminated product **13** could be purified on a

Biogel P-2 column eluted with 20 mM pyridylacetic acid buffer, pH 5.4,[42] but was used directly in the next step. The presence of the amino group on the aminated polysaccharide **13** was determined using the Kaiser test.[43] The reaction of the aminated polysaccharide **13** with diethylsquarate was carried out in MeOH/H_2O (2:1) at room temperature for 2 h. The reaction mixture was then dialyzed and lyophilized to give the aminated polysaccharide-squarate adduct **14**, containing some of the unreacted polysaccharide **12**, as a white powder (Scheme 2-4). The aminated polysaccharide-squarate adduct **14** was not isolated but was used directly in the coupling reaction with TT in carbonate buffer. The reaction mixture was stirred for 8 days at room temperature, then dialyzed against distilled water to remove the unreacted polysaccharide **12** and the squarate adduct **14**, and lyophilized to give the TT-squarate-polysaccharide adduct **15** as a white powder (Scheme 2-4). The sugar content of the glycoconjugate **15** was assessed by the method of Dubois et al.,[44] and the level of incorporation of the polysaccharide hapten on the protein was determined to be 73% (44 haptens).

Scheme 2-4: Synthesis of the polysaccharide protein conjugate **15**

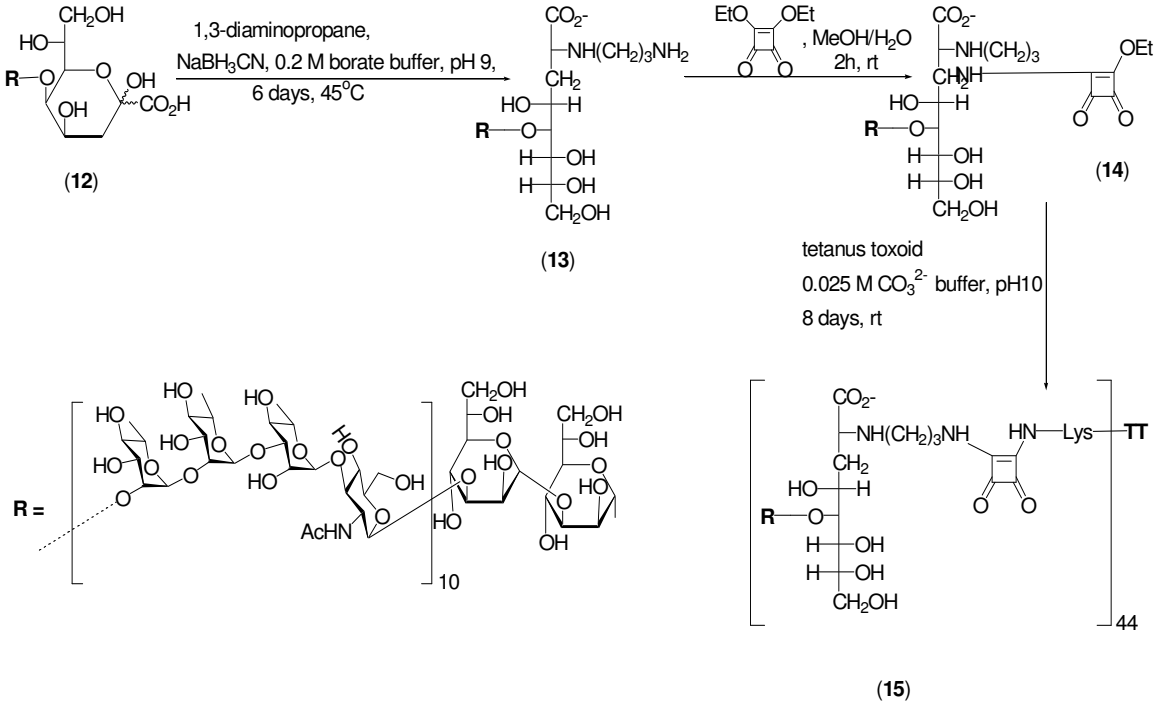

2.4.2 Immunochemistry

The binding affinity of the protein conjugates **8**, **9**, **11**, and **15** was investigated by competitive ELISA, in which these conjugates in solution were allowed to inhibit binding of the antibody SYA/J6 to *S. flexneri* Y lipopolysaccharide (LPS), as the solid phase antigen (both antibody and LPS gifts from D. R. Bundle, University of Alberta). Samples of the antibody were allowed to equilibrate with the peptide conjugates **8**, **9**, and **11**, and for comparison, with the polysaccharide **12**, the polysaccharide conjugate **15**, and octapeptide H-TDWNMHAA-NH_2[33] (**16**), which binds as well as H-MDWNMHAA-

NH_2(**2**).[33] These solutions were then added to a polystyrene plate coated with *S. flexneri* Y lipopolysaccharide. Binding of the conjugates **8**, **9**, **11**, and **15** to the antibody was indicated by a reduction in the amount of antibody bound to the solid phase (measured using a secondary antibody-peroxidase conjugate). No inhibition of binding was observed in control experiments using TT or BSA at concentrations equal to or greater than those of the protein conjugates. The results of the assay are summarized in Table 2-1 and Figure 2-2.

Conjugation of the octapeptide **2** to either tetanus toxoid or BSA resulted in an increase in binding affinity of roughly 10-fold: IC_{50} values of 2.2 and 2.5 μM for **8** and **11**, respectively, in contrast to a value of 19 μM for **2**,[32] or 33.5 μM for **16**. In contrast, the protein-polysaccharide conjugate **15** and the polysaccharide **12** bound with roughly equal affinity. This may reflect the difference between a polyvalent antigen (**12**) and the monovalent octapeptide antigens (**2** and **16**). The 10-fold increase in binding affinity achieved by presenting the octapeptide in a multivalent fashion will likely result in greater immunogenicity of compounds, **8** and **11**, as surrogate anti-*S. flexneri* Y vaccines.

Table 2-1: IC_{50} values for the inhibition of binding of the monoclonal antibody SYA/J6 to *S. flexneri* Y lipopolysaccharide by peptide and polysaccharide ligands, and by their protein conjugates

Compound	IC_{50} (μM)
8	2.2
9	n.d.[a]
11	2.5
12	<0.5
15	1.1
16	33.5

[a] 50% inhibition was not attained.

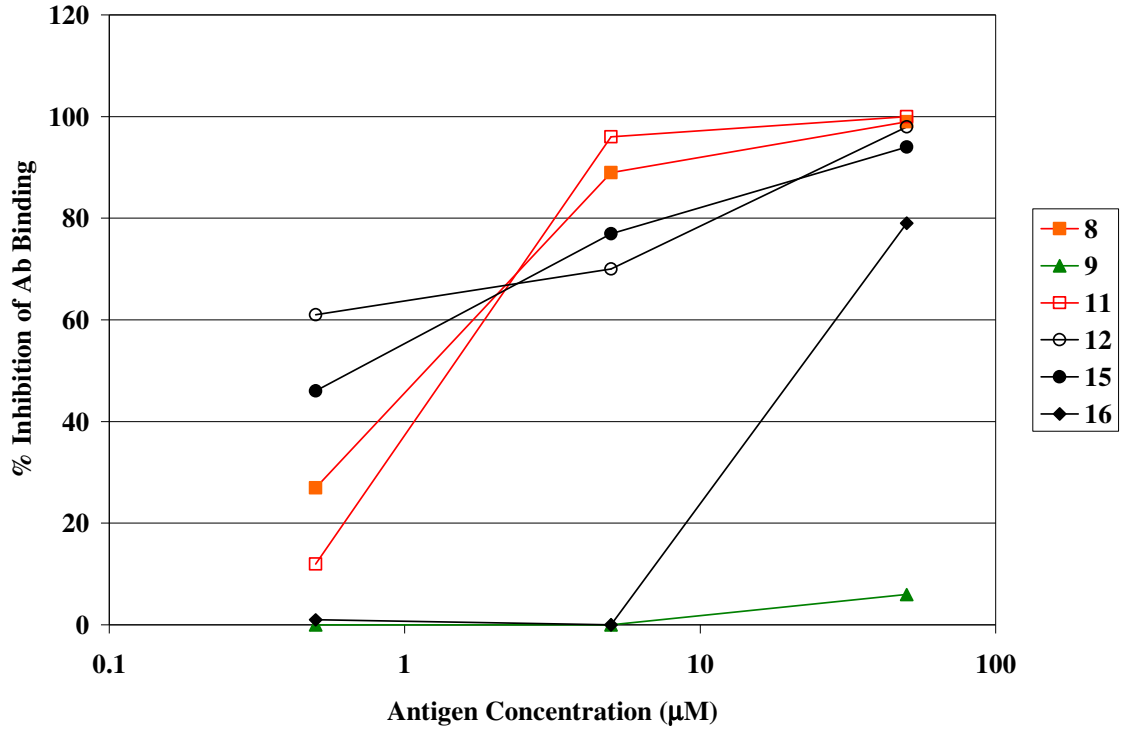

Figure 2-2: Inhibition of antibody binding to *S. flexneri* Y lipopolysaccharide by peptide and polysaccharide antigens, and their protein conjugates. In the case of protein conjugates, concentrations refer to the equivalent molar concentration of the free antigen.

The binding affinity of protein conjugates **7** and **10** of the peptide H-DRPVPY-NH_2 (**1**), the molecular mimic of the Group A *Streptococcus* (GAS) cell-wall polysaccharide, was also investigated by competitive ELISA. However, no solution-phase inhibitors were able to reduce the binding of the anti-*Streptococcus* Group A antibody to killed GAS bacteria on the solid phase. The inhibitors tested included the cell-wall polysaccharide **17**[18,19] [Figure 2-1(a)], the pentasaccharide **18**,[35] corresponding to the cell-wall polysaccharide of Group A

Streptococcus (Figure 2-3a), TT-sq-pentasaccharide conjugate **19** (Figure 2-3b),[45] synthesized in an analogous fashion to that described for a hexasaccharide-tetanus toxoid conjugate,[35] the peptide H-DRPVPY-NH_2 (**1**), as well as the protein conjugates **7** and **10**. The strong binding observed is likely due to high avidity of the multivalent IgM antibody for the bacteria on the solid phase. In test reactions, a small amount of inhibition (5-25%) by GAS cell-wall polysaccharide was observed when the antibody concentration was reduced to 20 or 200 pM and when the plate was coated with GAS cells at 5×10^7 or 5×10^6 cells/mL However, since a strong base-line (complete inhibition) could not be demonstrated, we decided to measure binding of the peptide conjugates **7** and **10** by direct ELISA.

Direct ELISA using plates coated with the peptide conjugates **7** and **10**, as well as the TT-sq-pentasaccharide conjugate **19** (Figure 2-3b), showed that SA-3 bound strongly to **7** and **10**, with nearly equal affinity as that for **19**. The optical density values observed are reported in Table 2-2.

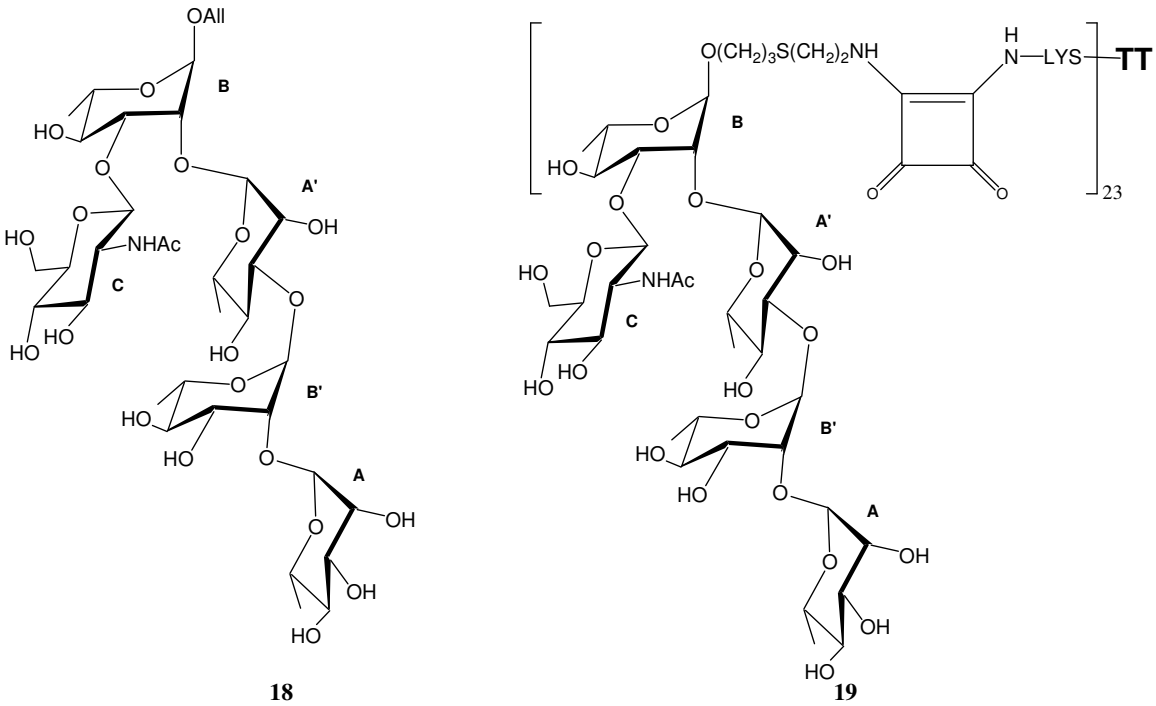

Figure 2-3: (a) Pentasaccharide fragment B(C)A′B′A corresponding to the cell-wall polysaccharide of Group A *Streptococcus*, (b) tetanus toxoid-squarate-pentasaccharide conjugate.

Table 2-2: Optical density values indicating binding of mAb SA-3 to protein conjugates **7**, **10**, and **19** in a solid phase assay

	Solid-phase protein conjugate	ΔOD × 1000a
7	BSA-sq-DRPVPY-NH2	875
10	TT-sq-DRPVPY-NH2	872
19	TT-sq-Pentasaccharide	995
—	TT	4
—	BSA	11

[a] Values are $(A_{405}–A_{490})\times1000$, after subtraction of the background value of 7 for wells coated with skim milk solution.

2.5 CONCLUSIONS

An efficient protocol has been developed to synthesize protein conjugates containing oligopeptides that can mimic the polysaccharides found on the cell surfaces of *Streptococcus* Group A and *S. flexneri* Y. A protein-polysaccharide conjugate corresponding to the *O*-polysaccharide of *S. flexneri* Y was also synthesized. Both the carbohydrate mimetic peptide conjugates and the glycoconjugate were shown to bind effectively to the respective monoclonal

antibodies directed against the cell-surface polysaccharides. These conjugates will now be tested as experimental vaccines.

2.6 EXPERIMENTAL

2.6.1 General methods

The Fmoc amino acids used were purchased from Novabiochem and the other reagents from Aldrich Chemical Co. DMF was freed of amines by concentrating under high vacuum and was then distilled and stored over molecular sieves whereas the other solvents were distilled according to standard procedures.[46] The oligopeptides sequences were synthesized on the Rink Amide [4-(2′,4′-dimethoxyphenyl-Fmoc-aminomethyl)-phenoxyacetamido-norleucyl-MBHA resin[37,38] (Novabiochem) (0.73 mmol/g substitution level), using standard 9-fluorenyl-methoxycarbonyl (Fmoc) chemistry[39] employing 2-[1-H-benzotriazole-1-yl]-1.1.13.3-tetramethyluronium hexafluorophosphate/1-hydroxybenzotriazole (HBTU/HOBt) coupling strategy.[40] The Kaiser ninhydrin[43] (5% ninhydrin in ethanol, 80% phenol in ethanol and 2% 0.001 M aq KCN in pyridine) assay for amino group was used to monitor both the Fmoc-amino acid coupling and the Fmoc deprotection reactions. 1D and 2D NMR spectra were recorded on Bruker AMX 400 and AMX 600 spectrometers, respectively, in 10% D_2O in water. Chemical shifts, which were referred to external DSS [3-(trimethylsilyl)-1-propanesulfonic acid], and coupling constants were obtained from a first-order analysis of one-dimensional spectra and ^1H assignments were

based on TOCSY experiments. MALDI-TOF mass spectra were obtained for some samples dispersed in a 2,5-dihydroxybenzoic acid matrix and others in 3,5-dimethoxy-4-hydroxy cinnamic acid matrix, on a Perseptive Biosystems Voyager DE instrument. High-resolution mass spectra were LSIMS (FAB), run on a Kratos Concept H double focusing mass spectrometer at 10,000 RP.

2.6.1.1 Antibodies and polysaccharide antigens

The purified monoclonal antibody SYA/J6 created and characterized by the group of D. R. Bundle, together with *O*-polysaccharide and lipopolysaccharide (*S. flexneri* Y) samples were generous gifts prepared according to the methods published by this group.[23,24,42] E Altman and D.R Bundle, *Methods Enzym.* **247** (1994), p. 243. Abstract | View Record in Scopus | Cited By in Scopus (6)[42]

2.6.2 Synthesis of the oligopeptides 1-3

2.6.2.1 General procedure

Rink Amide MBHA resin (200 mg, loading=0.73 mmol/g) was swelled in DMF (10 mL) for 2 h. A solution of piperidine (20%) in DMF (10 mL) was added to the suspension and the flask was shaken gently for 1 h using a mechanical shaker. After the suspension was filtered, the resin was washed with DMF (5 × 10 mL). A solution of Fmoc-Ala-OH (140 mg, 0.45 mmol), in the synthesis of the octapeptides **2** and **3** and Fmoc-Tyr(*t*Bu)-OH (207 mg, 0.45 mmol) in the case of H-DRPVPY-NH_2 (**1**) in DMF (10 mL) preactivated with HBTU (160 mg, 0.42 mmol) and HOBT (30.3 mg, 0.44 mmol) was then added to the suspension

followed by the addition of five drops of DIPEA. The flask was shaken with a mechanical shaker. The coupling reaction was monitored by withdrawing a sample of the resin, washing it with DMF and carrying out a Kaiser test. After the reaction was completed, the suspension was filtered and the resin was washed with DMF (5 × 10 mL). Successive deprotection of the Fmoc group and coupling of the appropriate Fmoc-amino acid were repeated until the peptide sequence Fmoc-MDWNMHAA-resin, Fmoc-MDWNPHAA-resin, and Fmoc-DRPVPY-resin were obtained. After removal of the Fmoc group (20% piperidine in DMF) from the N-terminal of the peptide-resin moiety, the latter was washed with DMF (5 × 10 mL), and dichloromethane (3 × 10 mL). A solution of trifluoroacetic acid, dichloromethane, and triisopropylsilane (7:7:1) was added to the peptide-resin and it was shaken with a mechanical shaker for 3 h. After the resin was filtered and washed with fresh 95% TFA (2 × 5 mL), the filtrate was combined and concentrated under vacuum. The peptide residues were then purified by reversed-phase HPLC (Gradient elution, acetonitrile/water) on a C_{18} column. The appropriate fractions of the synthesized peptides **1**-**3** were combined and concentrated under reduced pressure and the remaining solutions were lyophilized to afford the oligopeptides **1**-**3** as white crystals.

2.6.2.2 H-Asp-Arg-Pro-Val-Pro-Tyr-NH_2 (H-DRPVPY-NH_2) (1)

White solid (66 mg, 60% yield). ^{1}H NMR (90% H_2O/10% D_2O) δ 8.77 (d, *J*=6.4 Hz, Arg NH), 8.32 (d, *J*=7.6 Hz, Val NH), 7.96 (d, *J*=7.3 Hz, Tyr NH), 7.21 (t, *J*=5.7 Hz, Arg side chain NH), 7.15 (2H, d, *J*=8.7 Hz, Tyr 2,6-ArH side chain), 6.80 (2H, d, *J*=8.7 Hz, Tyr 3,5-ArH side chain), 4.52-4.43 (3H, m, Arg α-H, Tyr α-

H, Pro-3 α-H), 4.38 (1H, m, Val α-H), 4.31 (1H, m, Pro-5 α-H), 4.21 (1H, t, *J*=7.9 Hz, Asp α-H), 3.83 (2H, m, Pro-3 *δ*-H), 3.65 (2H, m, Pro-5 *δ*-H), 3.21 (2H, dd, *J*=12.8 and 6.56 Hz, Arg-H), 3.03 (2H, m, Tyr β-H), 2.92 (1H, dd, *J*=17.8 and 4.7 Hz, Asp β-H), 2.78 (1H, dd, *J*=17.8 and 8.6 Hz, Asp β-H), 2.28 (1H, m, Pro-3 β-H), 2.22 (1H, m, Pro-5 β-H), 2.10-1.93 (4H, m, Pro-3 γ-H, Val β-H, Pro-3 β-H), 1.90-1.80 (3H, m, Pro-5 γ-H, Pro-5 β-H), 1.78-1.62 (4H, m, Arg β-H, Arg γ-H), 0.96 (3H, d, *J*=7.4 Hz, Val γ-CH_3), 0.93 (3H, d, *J*=7.6 Hz, Val γ-CH_3); MALDI-TOF MS: (*m*/*z*) calcd for $C_{34}H_{54}N_{10}O_9$: 747.86 [M^++H]; Found: 747.48 [M^++H].

2.6.2.3 H-Met-Asp-Trp-Asn-Met-His-Ala-Ala-NH_2 (H-MDWNMHAA-NH_2) (2)

White crystals (68 mg, 47.8% yield). ^{1}H NMR (90% H_2O/10% D_2O) *δ* 10.15 (br s, Trp ring NH), 8.77 (d, *J*=7.4 Hz, Asp NH), 8.59 (s, His H-2), 8.41 (d, *J*=7.6 Hz, His NH), 8.36 (d, *J*=6.5 Hz, Trp NH), 8.32 (d, *J*=5.9 Hz, Ala-8 NH), 8.25 (d, *J*=5.8 Hz, Ala-7 NH), 8.19 (d, *J*=7.5 Hz, Asn NH), 8.05 (d, *J*=6.8 Hz, Met NH), 7.63 (d, *J*=8.0 Hz, Trp H-4), 7.53 (br s, C-terminal Ala amide NH), 7.51 (br s, Asn side chain NH), 7.50 (d, *J*=8.1 Hz, Trp H-7), 7.28 (2H, s, His H-4, Trp H-2), 7.24 (dt, *J*=7.1 and 0.9 Hz Trp, H-6), 7.15 (dt, *J*=7.1 and 0.8 Hz, Trp H-5), 7.05 (br s, C-terminal Ala amide NH), 6.87 (br s, Asn side chain NH), 4.28 (3H, m, Ala α-H, Ala α-H, Met α-H), 4.03 (t, *J*=6.8 Hz, Met α-H), 3.32 (dd, *J*=14.8 and 6.6 Hz, Trp β-H), 3.27 (dd, *J*=15.5 and 5.9 Hz, His β-H), 3.22 (dd, *J*=14.9 and 7.8 Hz, Trp β-H), 3.15 (dd, *J*=15.5 and 8.8 Hz, His β-H), 2.91 (dd, *J*=17.0 and 6.6 Hz, Asp β-H), 2.79 (dd, J=17.0 and 7.3 Hz, Asp β-H), 2.67 (dd J=15.8 and 6.8 Hz, Asn β-H), 2.58 (dd, J=15.8 and 6.9 Hz, Asn β-H), 2.48 (ddd, J=13.7, 8.1 and 5.5 Hz, Met γ-

H), 2.43-2.36 (2H, m, Met γ-H and Met γ-H), 2.27 (td, J=13.7 and 6.8 Hz, Met γ-H), 2.07 (3H, s, Met ε-CH3), 2.03-1.84 (4H, m, Met β-CH2, Met β-CH2), 1.96 (3H, s, Met ε-CH3), 1.41 (3H, d, J=7.1 Hz, Ala-8 β-CH3), 1.38 (3H, d, J=7.3 Hz, Ala-7 β-CH3); MALDI-TOF MS: (m/z) calcd for C41H59N13O11S2: 975.13 [M++H]; Found: 975.25 [M++H]. HRMS: (m/z) Calcd for C41H59N13O11S2: 974.3977 [M++H]; Found: 974.3967 [M^++H].

2.6.2.4 H-Met-Asp-Trp-Asn-Pro-His-Ala-Ala-NH_2 (H-MDWNPHAA-NH_2) (3)

White crystals (60 mg, 43.7% yield). ^{1}H NMR (90% H2O/10% D2O) δ 10.17 (br s, Trp ring NH), 8.84 (d, J=7.3 Hz, Asp NH), 8.61 (d, J=1.4 Hz, His H-2), 8.38 (d, J=6.9 Hz, Trp NH), 8.28 (d, J=6.2 Hz, Ala NH), 8.27(d, J=8.0 Hz, His NH), 8.13 (d, J=8.1 Hz, Asn NH), 7.99 (d, J=5.8 Hz, Ala NH), 7.62 (d, J=7.9 Hz, Trp H-4), 7.57 (br s, Asn side chain NH), 7.52 (br s, C-terminal Ala amide NH), 7.50 (d, J=8.2 Hz, Trp H-7), 7.31 (s, His H-4), 7.25 (d, J=2.22 Hz, Trp H-2), 7.25 (dt, J=7.1 and 1.0 Hz Trp, H-6), 7.16 (dt, J=7.0 Hz and 1.0 Hz, Trp H-5), 7.05 (br s, C-terminal Ala amide NH), 6.94 (br s, Asn side chain NH), 4.28 (dq, J=7.3 and 3.0 Hz, Ala α-H), 4.27 (dq, J=7.2 and 2.5 Hz, Ala α-H), 4.12 (dd, J=8.7 and 3.8 Hz, Pro α-H), 4.08 (t, J=6.7 Hz, Met α-H), 3.58 (2H, ddd, J=9.7 Hz, 7.4 and 5.0 Hz, Pro δ-CH2), 3.31-3.25 (3H, m, Pro δ-H, Trp β-H, His β-H), 3.21 (dd, J=14.5 and 6.9 Hz, Trp β-H), 3.14 (dd, J=15.5 and 9.4 Hz, His β-H), 2.90 (dd, J=17.0 and 6.3 Hz, Asp β-H), 2.79 (dd, J=17.0 and 7.8 Hz, Asp β-H), 2.74 (dd J=15.8 and 8.4 Hz, Asn β-H), 2.55 (dd, J=15.8 and 6.2 Hz, Asn β-H), 2.48 (ddd, J=13.7, 7.8 and 6.7 Hz, Met γ-H), 2.39 (ddd, J=13.7, 7.5 and 6.7 Hz, Met γ-H),

2.14 (br, m, Proβ-H), 2.10-2.01 (2H, m, Met β-CH2), 2.02 (3H, s, Met ε-CH3), 1.84 (br, m, Pro, β-H), 1.72 (2H, m, Pro γ-CH2), 1.41 (3H, d, J=7.3 Hz, Ala β-CH3), 1.38 (3H, d, J=7.1 Hz, Ala β-CH3); MALDI-TOF MS: (m/z) calcd for C41H57N13O11S: 941.06 [M^++H]; Found: 941.06 [M^++H]. HRMS: (m/z) calcd for $C_{41}H_{57}N_{13}O_{11}S$: 940.4099 [$M^+$+H]; Found: 940.4108 [$M^+$+H].

2.6.3 Synthesis of the peptide-squarate adducts 4

2.6.3.1 *N*-(3,4-Dione-2-ethoxycyclobutene)-DRPVPY-NH_2 (sq-DRPVPY-NH_2) (4)

To a solution of diethylsquarate (sq) (17 µL, 1.5 equiv) in freshly distilled MeOH (1 mL), H-DRPVPY-NH_2 (**1**) (57.4 mg, 0.077 mmol), dissolved in MeOH (2 mL), was added followed by the addition of sodium acetate (15 mg). The reaction mixture was stirred at room temperature for 1.5 h. After the reaction was completed, the solution was concentrated under reduced pressure and the residue was purified by reverse-phase HPLC (Gradient elution, acetonitrile/water). After freeze-drying of the appropriate fractions, the sq-DRPVPY-NH_2 adduct (**4**) was obtained as a white powder (51 mg, 76%). ^{1}H NMR (90% H_2O/10% D_2O) δ 8.93 (d, *J*=7.8 Hz, Asp NH), 8.35 (d, *J*=6.9 Hz, Arg NH), 8.16 (d, *J*=7.6 Hz, Val NH), 7.95 (d, *J*=7.5 Hz, Tyr NH), 7.28 (d, *J*=7.2 Hz, Arg side chain NH), 7.10 (2H, d, *J*=8.7 Hz, Tyr 2,6-ArH side chain), 6.79 (2H, d, *J*=8.7 Hz, Tyr 3,5-ArH side chain), 5.34-4.52 (4H, m, Arg α-H, Asp α-H, Tyr α-H, Pro-3 α-H), 4.38 (1H, m, Val α-H), 4.29 (1H, m, Pro-5 α-H), 3.75 (2H, m, Pro-3 δ-H), 3.68-3.50 (4H, m, CH_2-squarate, Pro-5 δ-H), 3.15 (2H, dd, *J*=12.6 and 6.7 Hz,

Arg δ-H), 2.95 (2H, m, Tyr β-H), 2.85 (2H, dd, *J*=17.5 and 8.3 Hz, Asp β-H), 2.25-2.10 (2H, m, Pro-3 β-H, Pro-5 β-H), 2.09-1.85 (4H, m, Pro-3 -H, Val β-H, Pro-3 β-H), 1.87-1.72 (3H, m, Pro-5 γ-H, Pro-5 β-H), 1.70-1.50 (4H, m, Arg -H, Arg γ-H), 1.13 (3H, t, *J*=7.1 Hz, CH_3-squarate), 0.89 (6H, d, *J*=7.4 Hz, Val γ-CH_3); MALDI-TOF MS: (*m*/*z*) calcd for $C_{40}H_{58}N_{10}O_{12}$: 871.96 [M^++H]; Found: 871.73 [M^++H].

2.6.3.2 *N*-(3,4-Dione-2-ethoxycyclobutene)-MDWNMHAA-NH_2 (sq-MDWNMHAA-NH_2) (5) and *N*-(3,4-dione-2-etoxycyclobutene)-MDWNPHAA-NH_2 (sq-MDWNPHAA-NH_2) (6)

The octapeptides H-MDWNMHAA-NH_2 (**2**) (3 mg, 9.2 μmol) and H-MDWNPHAA-NH_2 (**3**) (13 mg, 13.8 μmol) were treated with diethylsquarate (sq) as described above. After purification by HPLC, the peptides-squarate adducts **5** (2.2 mg, 63%) and **6** (8.2 mg, 55%) were obtained as white powders. ^{1}H NMR for *N*-(3,4-dione-2-ethoxycyclobutene)-MDWNMHAA-NH_2 (**5**) (90% H_2O/10% D_2O) *δ* 10.10 (br s, Trp ring NH), 8.61 (s, His H-2), 8.50 (d, *J*=7.6 Hz, Met-1 NH), 8.38 (d, *J*=7.3 Hz, Asp NH), 8.32 (d, *J*=7.7 Hz, His NH), 8.25 (d, *J*=6.5 Hz, Trp NH), 8.21 (d, *J*=5.6 Hz, Ala-8 NH), 8.18 (d, *J*=5.7 Hz, Ala-7 NH), 8.15 (d, *J*=7.5 Hz, Asn NH), 8.02 (d, *J*=6.8 Hz, Met NH), 7.63 (d, *J*=7.9 Hz, Trp H-4), 7.54 (d, s, C-terminal Ala amide NH), 7.53 (br s, Asn side chain NH), 7.51 (d, *J*=8.1 Hz, Trp H-7), 7.31 (s, His H-4), 7.29 (s, Trp H-2), 7.27 (dt, *J*=7.1 and 0.9 Hz Trp, H-6), 7.18 (dt, *J*=7.1 and 0.8 Hz, Trp H-5), 7.06 (br s, C-terminal Ala amide NH), 6.86 (br s, Asn side chain NH), 4.30 (3H, m, Ala α-H, Ala α-H, Met α-H), 3.69-3.60 (m, CH_2-squarate, Met α-H), 3.38 (dd, *J*=14.6 and 6.8 Hz, Trp β-H), 3.29 (dd, *J*=15.7 and 5.9 Hz, His β-H), 3.20 (dd, *J*=14.7 and 7.8 Hz, Trp β-H),

2.60-2.40 (m, His β-H, Asp β-H, Asp β-H, Asn β-H, Met-5 γ-H, Met-1 γ-H), 2.10-2.05 (6H, s, Met-5 ε-CH_3, Met-5 ε-CH_3), 2.04-1.90 (4H, m, Met-1 β-CH_2 and Met-5 β-CH_2), 1.96 (3H, s, Met-1 ε-CH_3, Met-5 ε-CH_3), 1.44 (3H, d, *J*=6.9 Hz, Ala-8 β-CH_3), 1.40 (3H, d, *J*=7.1 Hz, Ala-7 β-CH_3), 1.21 (3H, t, *J*=7.0 Hz, CH_3-squarate); MALDI-TOF MS: (*m*/*z*) calcd for $C_{47}H_{63}N_{13}O_{14}S_2$: 1099.21 [$M^+$+H]; Found: 1099.35 [$M^+$+H].

^{1}H NMR for *N*-(3,4-dione-2-ethoxycyclobutene)-MDWNPHAA-NH_2 (**6**) (90% H_2O/10% D_2O) δ 10.10 (br s, Trp ring NH), 8.59 (d, *J*=7.5 Hz, Asp NH), 8.55 (d, *J*=7.8 Hz, Met-1 NH), 8.53 (d, *J*=1.4 Hz, His H-2), 8.32 (d, *J*=7.2 Hz, Trp NH), 8.28 (d, *J*=5.8 Hz, Ala-8 NH), 8.19 (d, *J*=7.8 Hz, His NH), 8.11 (d, *J*=7.9 Hz, Asn NH), 7.96 (d, *J*=5.8 Hz, Ala-7 NH), 7.55 (d, *J*=7.33 Hz, Trp H-4), 7.48 (br s, C-terminal Ala amide NH), 7.44 (d, *J*=8.1 Hz, Trp H-7), 7.25-7.16 (3H, m, Trp H-2, His H-4, Trp, H-6), 7.10 (dt, *J*=7.2 Hz and 1.1 Hz, Trp H-5), 7.01 (br s, C-terminal Ala amide NH), 6.81 (br s, Asn side chain NH), 5.05 (dq, *J*=7.2 and 3.1 Hz, Ala-8 α-H), 4.85 (dq, *J*=7.2 and 2.3 Hz, Ala-7 α-H), 4.25 (dd, *J*=8.5 and 3.9 Hz, Pro α-H), 4.00 (t, *J*=6.7 Hz, Met α-H), 3.55-3.45 (3H, m, Pro δ-H, CH_2-squarate), 3.31-3.25 (3H, m, Pro δ-H, Trp β-H, His β-H,), 3.15-3.11 (2H, m, Trp β-H, His β-H), 2.83 (dd, *J*=16.8 and 6.5 Hz, Asp β-H), 2.70 (dd, *J*=17.0 and 7.5 Hz, Asp β-H), 2.60 (dd, *J*=15.8 and 8.4 Hz, Asn β-H), 2.53 (dd, *J*=15.8 and 6.2 Hz, Asn β-H), 2.43 (ddd, *J*=13.5, 7.4 and 6.6 Hz, Met γ-H), 2.35 (ddd, *J*=13.6, 7.5 and 6.6 Hz, Met γ-H), 2.22-2.15 (br, m, Proβ-H, Met β-H), 2.01 (3H, s, Met ε-H), 1.94 (br, m, Pro, β-H), 1.84 (2H, m, Pro γ-H), 1.35 (3H, d, *J*=7.2 Hz, Ala-8 β-CH_3), 1.31 (3H,

d, *J*=7.2 Hz, Ala-7 β-H), 1.10 (3H, t, *J*=7.2, CH_3-squarate); MALDI-TOF MS: (*m*/*z*) calcd for $C_{47}H_{62}N_{13}O_{14}S$: 1066.15 [$M^+$+H]; Found: 1066.31 [$M^+$+H].

2.6.4 Preparation of the BSA-sq-peptide conjugates 7-9

2.6.4.1 Synthesis of the BSA-sq-MDWNPHAA-NH_2 conjugate (9)

To a solution of BSA (4.13 mg, 0.0626 µmol) in 0.1 M carbonate buffer pH 10 (0.3 mL) was added sq-MDWNPHAA-NH_2 (**6)** (3 mg, 2.82 µmol) dissolved in the same buffer (0.2 mL). The reaction mixture was stirred at room temperature and the incorporation of the peptide-squarate adduct **6** was monitored by MALDI-TOF mass spectrometry. After 5 days, when no further increase of the peptide haptens was observed, the reaction mixture was dialyzed against distilled water using an Amicon ultrafiltration cell equipped with a Diaflo membrane (NMWL: 3000). The residue dissolved in water was lyophilized to give the BSA-sq-peptide conjugate **9** as a white powder (4.30 mg). The peptide conjugate **9** was shown to contain 3 octapeptide haptens per BSA molecule (11%).

2.6.5 Increasing the number of sq-MDWNPHAA-NH_2 (6) haptens on BSA

2.6.5.1 Synthesis of the BSA-sq-MDWNPHAA-NH_2 conjugate (9)

Sq-MDWNPHAA-NH_2 (6) (1.45 mg, 1.36 µmol) in 0.025 M carbonate buffer pH 10 (3 drops) was added to a solution of BSA (2 mg, 0.0303 µmol) in 0.025 M carbonate buffer (0.15 mL). The reaction mixture was stirred at room

temperature and after 5 days, the level of the incorporation of the peptide haptens was 71%. The BSA-sq-MDWNPHAA-NH_2 conjugate (9) was obtained as white powder after dialysis and lyophilization.

2.6.5.2 Synthesis of the BSA-sq-DRPVPY-NH_2 (7) and BSA-sq-MDWNMHAA-NH_2 (8) conjugates

The two sq-peptide adducts **4** and **5** were conjugated to BSA following the same procedure as described above. The amount of buffer solution used to dissolve the BSA was reduced and the sq-peptide adducts **4** and **5** were added directly to the BSA. The peptide contents of both conjugates **7** and **8** after 24 h stirring were 28 (100% incorporation of the peptides), based on the results obtained from MALDI-TOF mass spectrometry. Both peptide conjugates **7** and **8** were obtained as white powders.

2.6.6 Preparation of the tetanus toxoid-sq-peptide (TT-sq-peptide) conjugates 10 and 11

2.6.6.1 Synthesis of TT-sq-DRPVPY-NH_2 (10)

Tetanus toxoid (2 mL, 3 mg/mL), available in tris buffer, was dialyzed against 0.025 M carbonate buffer pH 10 (3 × 5 mL) and concentrated to a minimum volume of 0.3-0.5 mL. The sq-DRPVPY-NH_2 (**4**) (3 mg, 3.4 mmol) was then added and the reaction mixture was stirred for 3 days at room temperature. The peptide conjugate **10** was then dialyzed against distilled water and after lyophilization, it was obtained as a white powder (1.28 mg). MALDI-TOF mass spectrometry showed an incorporation of 39 peptide haptens (65%).

2.6.6.2 Synthesis of TT-sq-MDWNMHAA-NH_2 (11)

TT-sq-MDWNMHAA-NH_2 (**11**) was prepared as described above for the preparation of the TT-sq-DRPVPY-NH_2(**10**). The peptide conjugate **11** was obtained as a white powder and its peptide content was 45 hapten molecules per TT (75%).

2.6.7 Preparation of the polysaccharide glycoconjugate 15

2.6.7.1 Synthesis of the aminated polysaccharide 13

The *S. flexneri* Y *O*-polysaccharide (**12**) was polydisperse with 7-15 repeating units, as assessed by SDS-gel chromatography;[41] we chose an average value of 10 repeating units for our calculations. To the *O*-polysaccharide **12** (2 mg, 0.267 µmol), dissolved in 0.2 M sodium borate buffer, pH 9, (0.2 mL) was added dropwise a solution of 1,3-diaminopropane dihydrochloride (3.92 mg, 0.027 mmol), in 0.1 mL of the same buffer containing sodium cyanoborohydride (0.257 mg, 3.33 µmol). The reaction mixture was stirred for 6 days at 45 °C. It was then diluted with water and dialyzed to give a mixture of aminated polysaccharide **13** and unreacted polysaccharide **12** as a white powder. The product was assayed for the presence free amino group[43] and sugar.[44] The aminated polysaccharide **13** was not separated from the unreacted polysaccharide **12** but was used directly in the next reaction.

2.6.7.2 Synthesis of the aminated polysaccharide-squarate adduct 14

The mixture of the unreacted polysaccharide **12** and aminated polysaccharide **13** was treated with diethylsquarate (sq) (51 µL, 0.297 µmol) in MeOH/H_2O (2:1) for 2 h at room temperature. It was then dialyzed against distilled water (5 × 5 mL) and the residue dissolved in water was lyophilized to give a mixture of the squarate-aminated polysaccharide **14** and the unreacted polysaccharide **12** as a white powder. The mixture was used directly in the next coupling reaction.

2.6.7.3 Synthesis of the TT-sq-aminated polysaccharide 15

Tetanus toxoid (0.13 mL, 3 mg/mL) in tris buffer was dialyzed against 0.025 M carbonate buffer, pH 10, (3 × 5 mL), concentrated to 0.3 mL and then added to the mixture above. After 8 days stirring at room temperature, the reaction mixture was dialyzed against distilled water (5 × 5 mL) and the residue dissolved in water was lyophilized to give the glycoconjugate **15** as a white powder (1 mg). The polysaccharide content of the conjugate **15** was determined using the method of Dubois et al.[44] and was shown to contain 44 polysaccharide haptens (73%).

2.6.7.4 Dialyzes of the protein conjugates

The dialyzes of the protein-peptide conjugates **7**-**11**, the aminated polysaccharide **13**, the aminated polysaccharide squarate adduct **14**, and TT were carried out using an Amicon ultrafiltration cell equipped with a Diaflo

membrane (NMWL: 3000); for the dialysis of the polysaccharide conjugate **15**, a Diaflo membrane (NMWL: 10,000) was used.

2.6.7.5 Typical analysis of oligosaccharide content

TT-sq-polysaccharide conjugate **15** (1 mg) was dissolved in distilled water (5 mL). To three test tubes, 100, 200, and 300 µL of the conjugate solution were added, respectively. The solutions in each test tube were adjusted with distilled water to 1000 µL. Phenol (25 µL, 80%) was then pipetted into the first test tube followed by rapid addition of concentrated sulfuric acid (2.5 mL). This process was repeated with the other two test tubes. The tubes were allowed to stand for 10 min, before they were shaken and placed in a water bath at 30 °C. The absorbances of the pink color was measured at 490 nm. A blank was also prepared by substituting distilled water for the sugar solution. The amount of sugar was determined by reference to a standard curve prepared using l-rhamnose and *N*-acetylglucosamine.

2.6.8 ELISA binding assays

2.6.8.1 Competitive ELISA binding assay for *S. flexneri* Y antibody

A 96-well polystyrene plate (Fisher) was coated with *S. flexneri* Y LPS (40 µL/well; 1 µg/mL in Tris-buffered saline solution (TBS; 50 mM Tris, 150 mM NaCl, pH 7.5) by incubation overnight at 4 °C with gentle rocking. After washing four times with TBS/0.1% Tween 20, wells were blocked with skim milk solution (200 µL/well; 5% skim milk powder in TBS) for 30 min at 37 °C with gentle shaking, then washed another four times before addition of pre-mixed

antibody/conjugate solutions (40 µL/well). The mAb SYA/J6 (60 nM) and conjugates **8**, **9**, **11**, and **15** (at concentrations equivalent to 0.5-50 µM of the free ligand), in skim milk solution, were allowed to pre-equilibrate by incubation overnight at 4 °C with gentle rocking. The given concentrations are the final concentrations in the assay, and therefore, solutions of the antibody and conjugates **8**, **9**, **11**, and **15** were prepared at twice the final concentration and equal volumes (20 µL) were mixed. These solutions were added to the LPS-coated plate, which was then incubated again overnight at 4 °C with gentle rocking. The wells were washed six times with TBS/0.1% Tween 20. The secondary antibody-horseradish peroxidase conjugate (Pierce, ImmunoPure goat anti-mouse IgG (H+L), mixed with glycerol for long-term storage, and diluted 1:500 in skim milk solution; 40 µL/well) was added and the plate, which was incubated for 30 min at 37 °C with gentle shaking. The plate was washed six times with TBS/0.1% Tween 20. The concentration of bound antibody was measured by a colorimetric assay for horseradish peroxidase, as follows. To the washed plate was added a freshly prepared solution of 2,2′-azino-bis(3-ethylbenzthiazoline-6-sulfonic acid) (0.51 mM) (ABTS; Sigma) in citric acid-phosphate buffer (61.4 mM citric acid, 77.2 mM disodium hydrogen phosphate, pH 4) containing 0.03% H_2O_2. The color was allowed to develop and was measured as the difference between absorbance at 405 and 490 nm ($A_{405} - A_{490}$); the values measured at 20 min, corresponding to maximum intensity, were used.

2.6.8.2 Competitive ELISA binding assay for Group A

Streptococcus antibody

The above procedure was followed for the Group A *Streptococcus* (GAS) carbohydrate-mimetic peptide conjugates **7** and **10**, the cell-wall polysaccharide **17**, the pentasaccharide **18**, corresponding to the cell-surface of Group A *Streptococcus*, with slight modifications as follows. The plate was coated with heat-killed, pepsin-treated GAS cells (40 µL/well, overnight at 4 ℃ with gentle rocking); 5 × 107 cells/mL in 50 mM Na_2CO_3, PH 10) to provide a solid-phase antigen. The mAb SA-3 was used at 20nM concentration. Pre-equilibrium of the antibody/ligand solutions was carried out for 2 h at room temperature, followed by 20 min at 37 ℃ with gentle shaking. The secondary antibody-horseradish peroxidase conjugate (Pierce, goat anti-mouse IgM (µ) was used at 1:1000 dilution in skim milk solution. Unfortunately, no inhibition of binding was observed under these conditions, likely due to high avidity of the multivalent IgM antibody for the solid phase.

In test reactions, a small amount of inhibition (5-25%) by the GAS cell-wall polysaccharide **17** was observed when the antibody concentration was reduced to 20 or 200 pM and when the plate was coated with GAS cells at 5×10^7 or 5×10^6 cells/mL. However, since complete inhibition could not be demonstrated, we decided to measure binding of the peptide conjugates **7** and **10** by direct ELISA.

2.6.8.3 Direct ELISA binding assay

A96-well polystyrene plate (Fisher) was coated with protein solutions (40 µL/well; ~1 µg/well; 0.1-0.2 nM in TBS) by incubation overnight at 4 ^oC with

gentle rocking. The plate was washed with TBS/0.1% Tween 20, blocked with skim milk solution (200 µL/well), and washed another four times with TBS/0.1% Tween 20, as described above. The antibody SA-3 (20 µL, 40 nM in skim milk solution) was added to each well, followed by another 20 µL of skim milk solution with or without GAS cells, 5 × 107 cells/mL, for a final antibody concentration of 20 nM. The plate was incubated for 1 h at 37 ℃ with gentle shaking, washed six times with TBS/0.1% Tween 20. The secondary antibody-horseradish peroxidase conjugate (goat anti-mouse IgM (µ) was allowed to bind (20 min, 37 ℃, with gentle shaking). After washing the plate six times with TBS/0.1% Tween 20, freshly prepared ABTS solution (ABTS concentration 0.36 mM) was added and the color was allowed to develop. The maximum intensity was reached at roughly 20 min and the data recorded at this time point were reported.

The concentrations of the protein conjugates **7** and **10** for coating the plate were chosen as follows. The concentration of the TT-sq-DRPVPY-NH_2 conjugate **10** was set at 1 µg/well (1 µg/40 µL), or 137 nM. The concentrations of the other conjugate **7**, were adjusted based on the molar ratios of incorporation, to provide an equal number of conjugated ligands on the solid phase; therefore, the concentration of the TT-sq-pentasaccharide conjugate **19** (Figure 2-3b), was adjusted by a factor of 39/23 × 137 nM, to 232 nM; the concentration of the BSA-sq-DRPVPY-NH_2 conjugate **7** was adjusted by a factor of 39/28 × 137, or 191 nm. The negative controls TT and BSA were used at 232 and 191 nM, respectively.

2.7 ACKNOWLEDGEMENTS

We are grateful to the Natural Sciences and Engineering Research Council of Canada for financial support, to D. R. Bundle for providing the *S. flexneri* Y LPS, *O*-polysaccharide and the SYA/J6 antibody, and to F. Michon for providing tetanus toxoid.

2.8 References

1. Janeway, C. A.; Travers, P. In *Immunobiology: The Immune System in Health and Disease*, 3rd ed.; Austin, P., Lawrence, E., Robertson, M., Eds.; Garland: New York, 1997.
2. Mackett, M.; Williamson, J. D. *Human Vaccine*; Bios Scientific: Oxford, 1995; Brown, F. *Vaccine Design Chichester*; Wiley, 1993.
3. Cruz, S. J. *Immunotherapy and Vaccines*; Weinhein: VCH, 1997.
4. Mims, C. A. *The Pathogenesis of Infectious Disease*; Academic: London, 1976.
5. Lerner, R. A. *Sci. Am.* **1983**, *248*, 48.
6. Jennings, H. J. *Curr. Top. Microbiol. Immunol.* **1990**, *C 125*, 373.
7. Jennings, H. J. *Adv. Exp. Med. Biol.* **1988**, *228*, 495.
8. Lee, C.-J. *Mol. Immunol.* **1987**, *24*, 1005.
9. Lindberg, A. A. *Vaccine 17 Suppl.* **1999**, *2*, S28.

10. Benaissa-Trouw, B.; Lefeber, D. J.; Kamerling, J. P.; Vliegenthart, J. F. G.; Kraaijeveld, K.; Snippe, H. *Infect. Immun.* 2001, 69, 4698-4701; Pozsgay, V. *Adv. Carbohydr. Chem. Biochem.* **2001**, *56*, 153.

11. Peeters, C. A.; Tenbergen-Meekes, A. M.; Poolman, J. T.; Beurret, M.; Zegers, B. J. M.; Rijkers, G. T. *Infect. Immun.* **1991**, *59*, 3504.

12. Barington, T.; Gyhrs, A.; Kristensen, K.; Heilmann, C. *Infect. Immun.* **1994**, *62*, 9.

13. Johnson, M. A.; Pinto, B. M. *Aust. J. Chem.* **2002**, *55*, 13; Zwick, M. B.; Shen, J.; Scott, J. K. *Curr. Opin. Biotechnol.* **1998**, *9*, 427.

14. Bisno, A. L. In *Principles and Practice of Infectious Diseases*, 2nd ed.; Mandell, G. L., Douglas, R. G., Benett, J. E., Eds.; Wiley: New York, 1985; Chapter 160, p 1133.

15. Read, S. E.; Zabriskie, J. B. In *Streptococcus Diseases and the Immune Response*; Read, S. E., Zabriskie, J. B., Eds.; Academic: New York, 1980; Weiss, K. A.; Laverdiere, M. *Can. J. Surg.* **1997**, *40*, 18; Stevens, D. L. *Immunol. Invest.* **1997**, *26*, 129; Nowak, R. *Science* **1994**, *264*, 1665.

16. Blake, M. S.; Zabriskie, J. B.; Tai, J. Y.; Michon, F. U.S. Patent 5,866,135, 1999.

17. Hale, T. L. In *Topley and Wilson's Microbiology and Microbial Infections*; Hansler, W. J., Shumman, M. , Eds.; Arnold: London, 1998; Vol. 3, p 479.

18. Coligan, J. E.; Kindt, T. J.; Krause, R. M. *Immunochemistry* **1978**, *15*, 755.

19. Huang, D. H.; Krishna, N. R.; Pritchard, D. G. *Carbohydr. Res.* **1986**, *155*, 193.

20. Kenne, L.; Lindberg, B.; Petersson, K.; Romanowska, E. *Carbohydr. Res.* **1977**, *56*, 363; Kenne, L.; Lindberg, B.; Petersson, K.; Katzenellenbogen, E.; Romanowska, E. *Eur. J. Biochem.* **1977**, *76*, 327; Kenne, L.; Lindberg, B.; Petersson, K.; Katzenellenbogen, E.; Romanowska, E. *Eur. J. Biochem.* **1978**, *91*, 279.

21. Carlin, N. I. A.; Lindberg, A. A.; Bock, K.; Bundle, D. R. *Eur. J. Biochem.* **1984**, *139*, 189.

22. Harris, S. L.; Craig, L.; Mehroke, J. S.; Rashed, M.; Zwick, M. B.; Kenar, K.; Toone, E. J.; Greenspan, N.; Auzanneau, F.-I.; Marino-Albernas, J.-R.; Pinto, B. M.; Scott, J. K. *Proc. Natl. Acad. Sci.* U.S.A. **1997**, *94*, 2454.

23. Bundle, D. R.; Gidney, M. A. J.; Josephson, S.; Wessel, H.-P. Synthesis of *Shigella flexneri* O-Antigenic Repeating Units. In *Conformational Probes and Aids to Monoclonal Antibody Production*; Anderson, H.-P., Unger, F. M., Eds.; *ACS Symp. Ser.* 231; American Chemical Society: Washington, 1983; Vol. 83; Bundle, D. R. *Pure Appl. Chem.* **1989**, *61*, 1171; Bundle, D. R.; Altman, E.; Auzanneau, F.-I.; Baumann, H.; Eichler, E.; Sigurskjold, B. W. The Structure of Oligosaccharide-Antibody Complexes and Improved Inhibitors of Carbohydrate-Protein Binding in Complex Carbohydrates in Drugs Research. In *Alfred Benzon Symp. Ser. 36*; Bock, K., Clausen, H., Eds.; Munksgaard: Copenhagen, 1994; *Recognition of Carbohydrate Antigens by Antibody Binding Sites in Carbohydrates*; Hecht, S., Ed.; Oxford University Press Inc.: Oxford, 1998.

24. Vyas, M. N.; Vyas, N. K.; Meikle, P. J.; Sinnott, B.; Pinto, B. M.; Bundle, D. R.; Quiocho, F. A. *J. Mol. Biol.* **1993**, *231*, 133; Vyas, N. K.; Vyas, M. N.; Chervenak, M. C.; Johnson, M. A.; Pinto, B. M.; Bundle, D. R.; Quoicho, F. A. *Biochemistry* **2002**, *41*, 13575.

25. Rhodes, G.; Houghten, R.; Taulane, J. P.; Carson, D.; Vaughan, *J. Molec. Immun.* **1984**, *21*, 1047; Dyson, J. H.; Cross, K. J.; Houghten, R. H.; Wilson, I. A.; Wright, P. E.; Lerner, R. A. *Nature* 1985, 318, 480; Geysen, H. M.; Meloen, R. H.; Barteling, S. J. *Proc. Natl. Acad. Sci. U.S.A.* **1984**, *81*, 3998.

26. Dyrberg, T.; Oldstone, M. B. A. *J. Exp. Med.* **1986**, *164*, 1344.

27. Schaaper, W. M. M.; Lankhof, H.; Puijk, W. C.; Meleon, R. H. *Molec. Immun.* **1989**, *26*, 81.

28. Mezo, G.; Dalmadi, B.; Mucsi, I.; Bosze, S.; Rajnavolgyi, E.; Hudecz, F. *J. Peptide Sci.* **2002**, *8*, 107.

29. Batzloff, M. R.; Hayman, W. A.; Davies, M. R.; Zeng, M.; Pruksakorn, S.; Brandt, E. R.; Good, M. F. *J. Infect. Dis.* **2003**, *187*, 1598; Goetsch, L.; Haeuw, J. F.; Champion, T.; Lacheny, C.; N'Guyen, T.; Beck, A.; Corvaia, N. *Clin. Diagn. Lab. Immunol.* **2003**, *10*, 125.

30. Geoghegan, K. F.; Stroh, J. G. *Bioconjugate Chem.* **1992**, *3*, 138.

31. Johnson, M. A.; Rotondo, A.; Pinto, B. M. *Biochemistry* **2002**, *41*, 2149.

32. Johnson, M. A.; Pinto, B. M. *Bioorg. Med. Chem.* **2004**, *12*, 295.

33. Johnson, M. A.; Eniade, A. A.; Pinto, B. M. *Bioorg. Med. Chem.* **2003**, *11*, 781.

34. Tieze, L. F.; Schroter, C.; Gabius, S.; Brinck, U.; Goerlach-Graw, A.; Gabius, H.-J. *Bioconjugate Chem*. **1991**, *2*, 148.

35. Auzanneau, F.-I.; Pinto, B. M. *Bioorg*. *Med*. *Chem*. **1996**, *4*, 2003.

36. Kamath, V. P.; Diedrich, P.; Hindsgaul, O. *Glycoconj*. *J*. **1996**, *13*, 315.

37. Atherton, E.; Sheppard, R. C. Solid Phase Peptide Synthesis: A Practical Approach; IRL: New York, 1989.

38. Rink, H. *Tetrahedron Lett*. **1987**, *28*, 3787; Bernatowicz, M. S.; Daniels, S. B.; Koster, H. *Tetrahedron Lett*. **1989**, *30*, 4645.

39. Cammish, L. E.; Kates, S. A. In Fmoc Solid Phase Peptide Synthesis: A Practical Approach; Chan, W. C., White, P. D., Eds.; Oxford University Press: Oxford, England, 2000.

40. Dourtoglou, V.; Ziegler, J. C.; Gross, B. *Tetrahedron Lett*. **1978**, *19*, 1269; Dourtoglou, V.; Cross, B.; Lambropoulou, V.; Zioudrou, C. *Synthesis* **1984**, 572; Knorr, R.; Trzeciak, A.; Bannwarth, W.; Gillessen, D. *Tetrahedron Lett*. **1989**, *30*, 1927.

41. Sinnott, B.; Bundle, D. R., unpublished results.

42. Altman, E.; Bundle, D. R. *Methods Enzym*. **1994**, *247*, 243.

43. Colescott, R. L.; Bossinger, C. D.; Cook, P. I.; Kaiser, E. *Anal*. *Biochem*. **1970**, *34*, 595.

44. Dubois, M.; Gilles, K. H.; Hamilton, J. K.; Rebers, P. A.; Smith, F. *Anal*. *Chem*. **1956**, *28*, 1988.

45. Johnston, B. D.; Pinto, B. M., unpublished results.

46. Perrin, D. D.; Armarego, W. L. F. Purification of Laboratory Chemicals, 3rd.; Pergamon: London, 1988.

CHAPTER 3: IMMUNOLOGICAL EVIDENCE FOR PEPTIDE-CARBOHYDRATE MIMICRY WITH A GROUP A *STREPTOCOCCUS* POLYSACCHARIDE-MIMETIC PEPTIDE

This chapter comprises the manuscript **"*Immunological evidence for peptide-carbohydrate mimicry with a Group A Streptococcus polysaccharide-mimetic peptide*"** which has been published in the American Journal of Immunology (**2006**, *2*, 77-87).

Silvia Borrelli, Rehana B. Hossany, Susan Findlay and B. M. Pinto

After the peptide-protein conjugates of the two mimetic peptides DRPVPY and MDWNMHAA were successfully synthesized and were shown to be recognized by their respective antibodies, we first examined the immunogenicity of the Group A *Streptococcus* (GAS)-mimetic peptide conjugate, DRPVPY-TT, in mice. The DRPVPY-BSA was used as a solid-phase antigen in the ELISA assays.

The immunological study was performed by Dr. Silvia Borrelli, assisted by Susan Finlay. The peptides DRPVPY, DRPVP, and the two peptide conjugates DRPVPY-BSA and DRPVPY-TT used in this work were

synthesized by the thesis author. The thesis author also participated in discussions and interpretations of the immunological results. The cell-wall polysaccharide (CWPS), CWPS-TT, heat-killed pepsin-treated GAS bacteria, and TT were provided by Dr. Francis Michon.

In the current study, BALB/c mice were immunized, with the synthesized DRPVPY-TT in both homologous (only DRPVPY-TT) and heterologous (DRPVPY-TT/CWPS-TT or CWPS-TT/DRPVPY-TT) prime/boost strategies. We then looked at how their immune system responded to the different vaccinations by studying the primary (first immunization) and memory immune (after several immunizations) responses. This was achieved by testing the immune sera collected after each vaccination for the presence of anti-DRPVPY and anti-CWPS antibodies (cross-reactivity).

In this work, we effectively demonstrated that the peptide DRPVPY, conjugated to TT, was able to promote a strong and rapid thymus-dependent response to DRPVPY, a requirement for a successful vaccine. More importantly, in addition to the induced production of high anti-DRPVPY antibodies, the peptide conjugate was able to specifically induce a cross-reactive immune response (high antibody titers) against the original *Streptococcus* Group A polysaccharide. This specificity in cross-reactivity of the anti-peptide antibodies with the CWPS epitopes was demonstrated in a competitive inhibition experiment using the immune serum obtained after initial immunization with DRPVPY-TT. The results

obtained from the inhibition assays also proved that the tyrosine moiety in the mimetic peptide DRPVPY plays a critical role in the immunogenicity of the peptide.

Since the mimetic peptide DRPVPY can act as an immunogenic mimic of the *Streptococcus* Group A polysaccharide, this showed evidence that lack of structural mimicry by the peptide does not prevent it from inducing a cross-reactive immune response. Furthermore, the tight turn conformation about the VPY motif in DRPVPY observed in both bound and free peptide might also have contributed to the immunogenicity of the mimetic peptide. This remains to be confirmed by comparing these results with those of the MDWNMHAA-TT (next target), which is a functional mimic of the *Shigella flexneri* Y polysaccharide but lacks the tight turn of the bound peptide in the free peptide.

In contrast to the rapid T-cell dependent response to DRPVPY-TT, when the secondary response (boosting) was examined to test the efficacy of the memory cells formed during the primary response to the peptide conjugate, we observed, however, a loss in binding of the antibodies with the GAS polysaccharide. This short-lasting cross-reactivity was attributed to a carrier-suppression effect, a phenomenon commonly observed with macromolecular carrier proteins. The experiment was then repeated and attempts to enhance the secondary response in both experiments were not successful. With these results in hand, we conclude that there is scope for further modification of the

DRPVPY conjugate to eliminate the carrier-suppression effect, perhaps by conjugation to other moieties, and hence, improve the viability of the peptide in the form of vaccine.

3.1 KEYWORDS

Group A *Streptococcus*, cell-wall polysaccharide, mimetic-peptide, immunology, mouse antisera, peptide-carbohydrate cross-reactivity

3.2 ABSTRACT

The immunogenicity of a peptide-protein conjugate developed by linking a peptide mimic DRPVPY of the Group A *Streptococcus* cell-wall polysaccharide (GAS-CWPS), to tetanus toxoid (TT) was examined.

BALB/c mice were immunized three times subcutaneously following homologous or heterologous prime/boost strategies at 4- or 6- week intervals in two different experiments. DRPVPY-TT, CWPS-TT, heat-killed, pepsin-treated GAS bacteria (with exposed polysaccharide) and TT, were used as immunogens with alum as adjuvant. Antibody titers were determined by ELISA with GAS bacteria (with exposed polysaccharide) and DRPVPY-linked to bovine serum albumin (BSA, DRPVPY-BSA) as solid phase antigens. All mice primed with DRPVPY-TT developed high IgG anti-peptide and anti-GAS titers. The binding

of polyclonal anti-peptide antibodies to GAS could be inhibited by purified CWPS, synthetic oligosaccharides corresponding to CWPS, DRPVPY-BSA, DRPVPY and DRPVP, as assessed by competitive-inhibition ELISA. Anti-oligosaccharide titers were also obtained upon titration of anti-peptide sera with synthetic oligosaccharide-BSA conjugates. All mice primed with CWPS-TT and mice primed and boosted with GAS developed IgG anti-peptide titers. These data demonstrate conclusively the cross-reactivity of the immune responses and support the hypothesis of antigenic mimicry of the GAS-CWPS by the hexapeptide DRPVPY.

However, mice boosted with DRPVPY-TT, after 6-8 weeks, showed a decrease in IgG anti-GAS titers, but an increase in IgG anti-peptide titers, suggesting carrier-induced suppression of the response to polysaccharide. Strategies are outlined for further refinement of a DRPVPY conjugate as a surrogate of the cell-wall polysaccharide for use in vaccines against Group A *Streptococcus*.

3.3 INTRODUCTION

Streptococcus pyogenes (Group A *Streptococcus*, GAS) is a gram-positive extracellular bacterium, which colonizes the throat or skin and is responsible for a number of suppurative infections and their nonsuppurative, immunologically-mediated sequelae including acute rheumatic fever, acute glomerolunephritis and reactive arthritis[1]. GAS has been recognized as a

common cause of bacterial pharyngitis (strep throat), skin abscesses, impetigo and scarlet fever. More recently, GAS has been recognized as the causative agent of toxic shock-like syndrome and necrotizing fasciitis which invades skin and soft tissues and in severe cases leaves infected tissues destroyed[1-4]. Acute rheumatic fever and rheumatic heart disease are the most serious autoimmune sequelae of GAS infection affecting children worldwide. After the advent of antibiotics, diseases caused by S. pyogenes declined in incidence and severity in developed countries[5]. In the last 20 years, these diseases have re-emerged in industrial countries and a dramatic increase of their frequency is observed in developing countries[6,7]. Mass vaccination would therefore be of interest for efficient prevention of these infections[1,8].

The Lancefield classification scheme of serologic typing distinguished the beta-hemolytic *Streptococci* based on their Group A cell-wall polysaccharide (CWPS), composed of *N*-acetylglucosamine linked to a rhamnose polymer backbone (compound **1**, Figure 3-1). Streptococci were also serologically separated into M protein serotypes based on a surface protein. More than 80 M protein serotypes have been identified. Vaccines containing the streptococcal M protein and its component peptides[9-11] as well as CWPS-protein conjugates[12,13] are under investigation, among other antigens[1,14]. The validity of the CWPS as a viable vaccine candidate has been established in a recent study[13].

An alternative approach to vaccine design is the use of molecules that mimic the immunogenic element of interest[15,16]. Carbohydrate-mimetic peptides have potential as surrogate ligands for traditional carbohydrates vaccines

providing more discriminating immune responses[15]. Screening of phage-displayed peptide libraries with carbohydrate-specific antibodies had identified carbohydrate-mimetic peptides with demonstrated antigenic and immunogenic potential in certain cases[15,17-19]. In the present context, a GAS carbohydrate-mimetic peptide, DRPVPY (compound **2**, Figure 3-1), cross-reactive with an anti-CWPS monoclonal antibody, SA-3, was identified[20]. SA-3 recognizes a branched trisaccharide repeating unit L-Rha-α-(1→2)-[D-GlcNAc-β-(1→3)]-α-L-Rha as an epitope[21]. Detailed immunochemical studies of the recognition of DRPVPY by SA-3 showed that the mechanism of peptide binding differs from that of the carbohydrate[20]. The structure of this peptide is worthy of comment. The presence of two prolines adds defined structure to this short peptide. A detailed transferred-NOE NMR study of the antibody-bound conformation of the peptide has been described in detail by Johnson et al.[22,23].

It was clear that a defined tight turn conformation in the VPY region, a likely peptide epitope, is recognized by the SA-3 antibody used to isolate this peptide in the original phage screening protocol. Evidence was presented that this conformation was also present in the ensemble of conformations of the free peptide. STD-NMR experiments also indicated that the D residue did not form contacts within the antibody combining site, a results that is consistent with previous immunochemical studies in which the D residue was modified[24]. These data, taken together, augur well for a presentation of this peptide conformation on the phage surface. The synthesis of DRPVPY-based conjugates, to bovine serum albumin, BSA (compound **4**, Figure 3-2) and to tetanus toxoid, TT,

(compound **5**, Figure 3-2) together with their immunochemical evaluation with SA-3 was reported recently[24]. It is noteworthy that a search of the human genome reveals that the sequence DRPVPY is not present (NCBI's protein database).

We report herein, the immunogenicity of a DRPVPY-TT conjugate (compound **5**, Figure 3-2) in BALB/c mice, the cross-reactivity of the anti-peptide sera with CWPS and the characterization of the specificity of the antibody response observed by competitive-inhibition ELISA. The potential of the conjugate as a surrogate compound in vaccines against GAS and new insights into carbohydrate-peptide antigenic mimicry are presented.

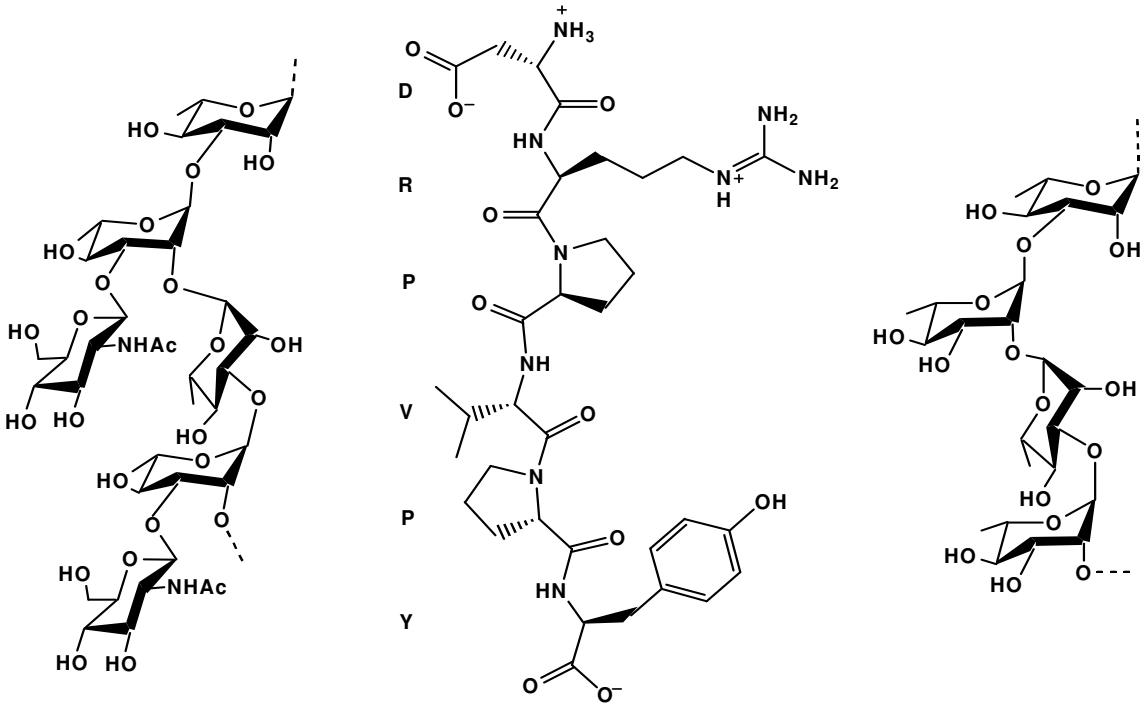

Figure 3-1: Cell-wall polysaccharide (CWPS) of the bacteria *Streptococcus* Group A (compound **1**), CWPS-peptide mimic: DRPVPY (compound **2**) and CWPS variant (CWPSv, compound **3**).

3.4 MATERIALS AND METHODS

3.4.1 Group A *Streptococcus* (GAS) used as solid-phase antigen for ELISA and as immunogen in control mice groups

Streptococcus pyogenes Group A type 4, strain J17A4 bacteria were heat-killed and pepsin-digested to expose the cell-wall polysaccharide, as described[27,28]; kindly provided by J. B. Pitner[29]. The original treatment with

pepsin was reported by Krause et al.[28],to remove most of protein and expose the cell-wall carbohydrate antigens. Immunization with such bacteria in several studies in the past[27,28,29] has shown that a strong anti-polysaccharide response is obtained.

3.4.2 Preparation of Group A polysaccharide and Group A variant polysaccharide used as inhibitors and CWPS-TT conjugate

The cell-wall Group A polysaccharide (CWPS, compound **1**, Figure 3-1) and its variant (CWPSv, compound **3**, Figure 3-1) form were extracted and characterized as described[30]. The CWPS-TT conjugate was obtained by reductive amination using cyanoborohydride as described [30]. These compounds were kindly provided by Dr. Francis Michon (Baxter Vaccines, MD, USA).

3.4.3 Monoclonal Antibody MAb SA3, peptides DRPVPY and DRPVP, DRPVPY-TT and DRPVPY-BSA conjugates

The MAb SA3 (IgM) has been described earlier[27] and was used as an ELISA control after purification from ascites fluid by gel-filtration chromatography. The CWPS-peptide mimetic DRPVPY was synthesized using the Fmoc solid-phase strategy and linked via the amino terminus to a bifunctional linker, diethylsquarate, and then conjugated to tetanus toxoid (TT) or bovine serum albumin (BSA) as immunogenic carriers, as described[31] (compounds **4** and **5**, Figure 3-2). The average level of incorporation of the peptide on TT was 65% while that on BSA was 100% (Figure 3-2). The peptide DRPVP was also

synthesized as described above, and evaluated as an inhibitor in competitive inhibition ELISA assays.

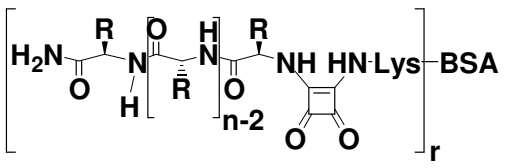

n	peptide hapten	r
6	DRPVPY	28

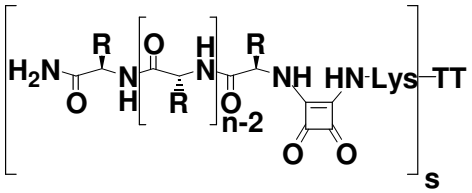

n	peptide hapten	s
6	DRPVPY	39

Figure 3-2: Synthetic peptide conjugates: DRPVPY-BSA (compound **4**, left) and DRPVPY-TT (compound **5**, right) used in this study

3.4.4 Synthetic oligosaccharides and glycoconjugates used as inhibitors and solid-phase antigens in ELISA

The pentasaccharide (compound **6**, Figure 3-3), the branched-trisaccharide (compound **7**, Figure 3-3), and hexasaccharide (compound **8**, Figure 3-3) were available from our previous work[27,28], CWPS-BSA (compound **9**, Figure 3-3), branched-trisaccharide-BSA (compound **10**, Figure 3-3), pentasaccharide-BSA (compound **11**, Figure 3-3), (hexasaccharide)5-BSA (compound **12**, Figure 3-3), $(hexasaccharide)_{16}$-squarate-BSA (compound **13**, Figure 3-3) were also available from our previous work[21,29].

3.4.5 Experimental groups of mice and immunization protocols

Female BALB/c mice (6-8 weeks) were obtained from Charles River Breeding Laboratories, (Montreal, Quebec, Canada) and were maintained in our Animal Facility following the animal care guidelines. Five groups of 4 mice each were injected subcutaneously (s.c.) in week 0, 4 and 10, with the conjugates, Alhydrogel (2%, Superfos Brenntag Biosector, Frederikssund, Denmark), or controls in two different experimental protocols. Mice were bled every 2 weeks, their sera analyzed, and mean reciprocal end-point titers and standard deviation determined.

In experiment 1, Control groups received 100 μl of heat-killed pepsin-treated GAS bacteria (Group 5, G5) or 100 μg of Alhydrogel and 100 μg of TT (Group 4, G4), in weeks 0, 4 and 10. Mice from Group 1 (G1) received 100 μg Alhydrogel and 100 μg of DRPVPY-TT, in weeks 0 and 4. Results obtained in weeks 6 and 8 lead to boost these mice with 50 μg DRPVPY-BSA in week 10.

In Groups 2 (G2) and 3 (G3) a heterologous prime/boost strategy was implemented. Group 2 mice were primed with 1 μg CWPS-TT and boosted with 100 μg DRPVPY-TT in week 4, and results led us to boost with 50 μg of DRPVPY-BSA in week 10. Group 3 mice were primed with 100 μg DRPVPY-TT and boosted with 1 μg CWPS-TT in week 4 and results led to a final boost with 50 μg of DRPVPY-TT in week 10.

In experiment 2, control groups received 100 μg of Alhydrogel and 2 μg of CWPS-TT (Group 4, G4) or 100 μg of TT (Group 5, G5) in weeks 0, 4 and 10. Mice from Group 1 (G1) received 100 μg DRPVPY-TT, once and were then euthanized in week 5. Group 2 (G2) mice were immunized with 100 μg DRPVPY-

TT in weeks 1 and 4. Results from these weeks led us to give a final boost with 2 μg CWPS-TT in week 10. Mice from Group 3 (G3) were primed with 2 μg CWPS -TT and boosted with 100 μg DRPVPY-TT in week 4, and results led to a final boost was with 10 μg DRPVPY-TT in week 10.

---

6. α-L-Rha*p*(1→2) α-L-Rha*p*-(1→3)-α-L-Rha*p*-(1→2) [β-D-Glc*p*NAc(1→3)]α-L-Rha*p*(1→OAll

7. α-L-Rha*p*-(1→2) [β-D-Glc*p*NAc(1→3)]-α-L-Rha*p*(1→OAll

8. α-L-Rha*p*-(1→2) [β-D-Glc*p*NAc(1→3)]-α-L-Rha*p*(1→3))-α-L-Rha*p*-(1→2) [β-D-Glc*p*NAc(1→3)]α-L-Rha*p*(1→OAll

9. CWPS-BSA

10. [-α-L-Rha*p*-(1→2) [β-D-Glc*p*NAc(1→3)]-α-L-Rha*p*-O$(CH_2)_8$CONH]$_{8\text{-}18}$-BSA

11. [[β-D-Glc*p*NAc(1→3)]-α-L-Rha*p*-(1→3)-α-L-Rha*p*-(1→2)[β-D-Glc*p*NAc(1→3)]-α-L-Rha*p*-O$(CH_2)_8$CONH]$_{8\text{-}18}$-BSA

12. [[-α-L-Rha*p*-(1→2) [β-D-Glc*p*NAc(1→3)]-α-L-Rha*p*-(1→3)-α-L-Rha*p*-(1→2)[β-D-Glc*p*NAc(1→3)]-α-L-Rha*p*- O$(CH_2)_3$ S$(CH_2)_2$ NH CO $(CH_2)_2$NH]$_5$-BSA

13. [[-α-L-Rha*p*-(1→2) [β-D-Glc*p*NAc(1→3)]-α-L-Rha*p*-(1→3)-α-L-Rha*p*-(1→2)[β-D-Glc*p*NAc(1→3)]-α-L-Rha*p*.O$(CH_2)_3$S$(CH_2)_2$NH-squarate]$_{16}$-BSA

Figure 3-3: Structures of synthetic oligosaccharide inhibitors and glycoconjugates: pentasaccharide (compound **6**), branched-trisaccharide (compound **7**) and hexasaccharide (compound **8**), a polysaccharide BSA-

conjugate (compound **9**), and other oligosaccharide protein conjugates (compounds **10**-**13**) used as solid-phase antigens in titration ELISA.

3.4.6 ELISA for binding antibody

Antibody titers to DRPVPY and GAS polysaccharide in sera from vaccinated mice were determined before vaccination and 2 weeks after each vaccination by ELISA, as described[32]. ELISAs were performed in 96-well plates (NUNC-MaxiSorp, Rochester, NY), coated overnight with 100 μl/well of DRPVPY-BSA (or TT, 10 μg/ml) or with a suspension of heat-killed, pepsin-treated GAS bacteria corresponding to $A_{595\ nm}$ ~0.25. Wells were blocked by the addition of 1% BSA for 2 h at room temperature. The plates were washed three times with a washing solution of 0.05% Tween 20 and 0.9% NaCl. Antisera, 3-fold-serially diluted in 0.05% Tween PBS (PBS-T) at a starting dilution of 1/50, were added (100 μl per well) and incubated for 3 h at room temperature. After washing four times as before, followed by the addition of 100 μl per well of alkaline phosphatase-labeled goat anti-mouse IgG or IgM (Caltag Laboratories, San Francisco, CA) diluted 1:3000 in PBS-T. The plates were incubated overnight at room temperature, and again washed four times. 100 μl of substrate solution containing p-nitrophenyl phosphate (1 mg/ml, Kirkegaard & Perry lab, Gaithersburg, MD) was added to the wells. After 10 to 60 min at room temperature, the plates were scanned at 405 nm in a SpectraMax 340 microplate reader. The titer was defined as the highest dilution yielding an absorbance ≥0.1

after subtracting twice the average background reading. The negative control consisted of wells without serum. The positive control was the mouse MAb SA-3, appropriately diluted.

3.4.7 Competitive-inhibition ELISA studies with CWPS, CWPSv, DRPVPY, DRPVP, DRPVPY-BSA, and synthetic oligosaccharides corresponding to CWPS as inhibitors

Sera from those mice that had the highest anti-DRPVPY antibody titers cross-reactive to GAS bacteria in week 4 (G1-experiment 2), were used. Sera were incubated in duplicate at a final dilution of 1:100 with two-fold serial dilutions of inhibitors (compounds **1**-**3**, Figure 3-1); (compound **4**, Figure 3-2), (compounds **6**-**8**, Figure 3-3) in PBS-T, starting at an initial concentration of 500 μg/ml, for 1 h at room temperature. Then, 100 μl of the mixtures were transferred to plates coated with antigens and incubated at room temperature for 3 h. The plates were washed and the bound IgG was detected as described for the ELISA above.

3.4.8 Titration ELISA

Microtiter plates (NUNC) were coated overnight at room temperature with CWPS-BSA (compound **9**, Figure 3-3), branched-trisaccharide-BSA (compound **10**, Figure 3-3), pentasaccharide-BSA (compound **11**, Figure 3-3), $(hexasaccharide)_5$-BSA (compound **12**, Figure 3-3) and (hexasaccharide-squarate)16-BSA (compound **13**, Figure 3-3) conjugates (10 μg/ml), diluted in PBS (pH=7.4). Plates were blocked with 100 μl/well of 1% BSA in PBS for 2 h at room temperature.

Mouse antisera were serially diluted (starting dilution of 1/50) in PBS-T and duplicate aliquots (100 µl/well) were added to coated microtiter plates and incubated for 3 h at room temperature. The ELISA was performed as described above.

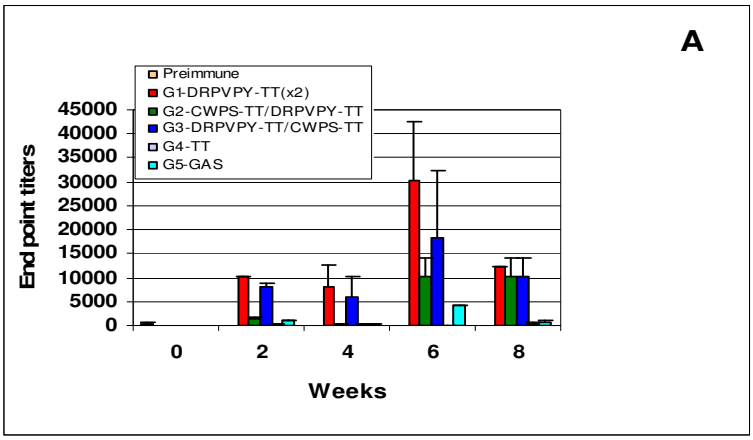

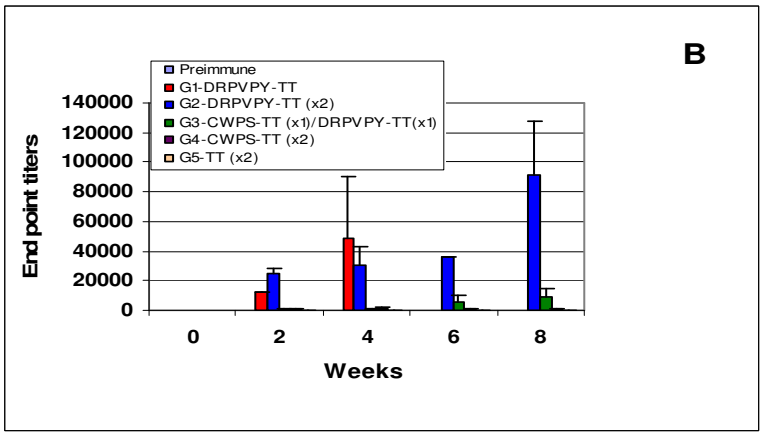

Figure 3-4: Immunogenicity of the peptide conjugates: Antibodies titers (IgG) to DRPVPY. Experiment 1 (A), Experiment 2 (B). Plates were coated with DRPVPY-BSA (compound **4**, Figure 3-2, 10 µg/ml) as described in Materials and Methods.

3.5 RESULTS

3.5.1 Immunogenicity of the peptide conjugates

3.5.1.1 Antibody titers to DRPVPY

The individual mouse antisera (4 mice per group, 5 groups of mice: G1 to G5) were evaluated for the relative amounts of IgG antibody they contained that bound to DRPVPY-BSA. Pre-immune sera screened by ELISA, using DRPVPY-BSA as solid phase antigen, showed low background activity (week 0, Figure 3-4A&B). Mice primed with 100 μg of the DRPVPY-TT conjugate responded with high IgG antibody titers against DRPVPY-BSA (weeks 2 and 4, Figure 3-4A&B). Increases were seen after boosting mice from G1-experiment 1 (Figure 3-4A) and G2-experiment 2 (Figure 3-4B) in weeks 6 and 8. Control groups (G4 and G5) showed much lower mean end-point titers to peptide at all time points. This result indicates that the conjugates effectively promoted a strong and rapid thymus-dependent response to DRPVPY.

3.5.1.2 Cross-reactivity

Anti-peptide antibodies bind to exposed-polysaccharide on Group A *Streptococcus* (GAS) bacteria. Titers against exposed polysaccharide on GAS bacteria were obtained when a high dose of the peptide-experimental vaccine was administered to mice (Fig 5-6). A lower dose of 20-40 μg/mouse did not elicit high cross-reactive titers (data not shown). The subcutaneous immunization with DRPVPY-TT (100 μg/ml) of mice resulted in anti-GAS primary responses (IgM and IgG, weeks 2 and 4, Figure 3-5, 3-6). The response was higher for IgG than

for IgM. Four weeks after priming, the IgG response was higher than that at week 2. The IgM response declined four weeks after priming (Figure 3-5, 3-6). No titer increases against TT, used as control, were seen. These anti-GAS titers, were much lower than those against peptide.

A lack of secondary response (IgG) cross-reactive with GAS bacteria was observed after mice received a booster injection of DRPVPY-TT at equal dose (G1 experiment 1 and G2 experiment 2, respectively, in week 6-8, Figure 3-5, 3-6) or lower (G3 experiment 2, at week 12, Figure 3-6). Attempts to save the cross-reactive response were conducted in week 10 in both experiments. The immunization carrier was changed to BSA and boosting with a lower dose of DRPVPY-BSA were not successful (G1 experiment 1, week 12, Figure 3-5). A booster injection with a 10-fold lower dose of DRPVPY-TT was tried in G3 experiment 2, week 10, or half dose (G3-experiment 1, week 10); however, a secondary-like response (fast, strong and high IgG titers) was not observed at week 12 (Figure 3-5, 3-6).

3.5.2 Heterologous boosting strategies

Priming with DRPVPY-TT and boosting with CWPS-TT (G3 experiment 1-Figure 3-5) resulted in no titer increases against GAS (Figure 3-5-G3, week 6). Priming with CWPS-TT and boosting with DRPVPY-TT at a high (Figure 3-5-G2 experiment 1, week 6) and at a lower dose (Figure 3-6-G3 experiment 2, week 10-12) or even using another carrier, BSA (Figure 3-5-G2 experiment 1, week 10-12), although titers against GAS increased (Figure 3-5-G2-week 8, and Figure

3-6-G3-week 8), did not have a response with the characteristics of a secondary response.

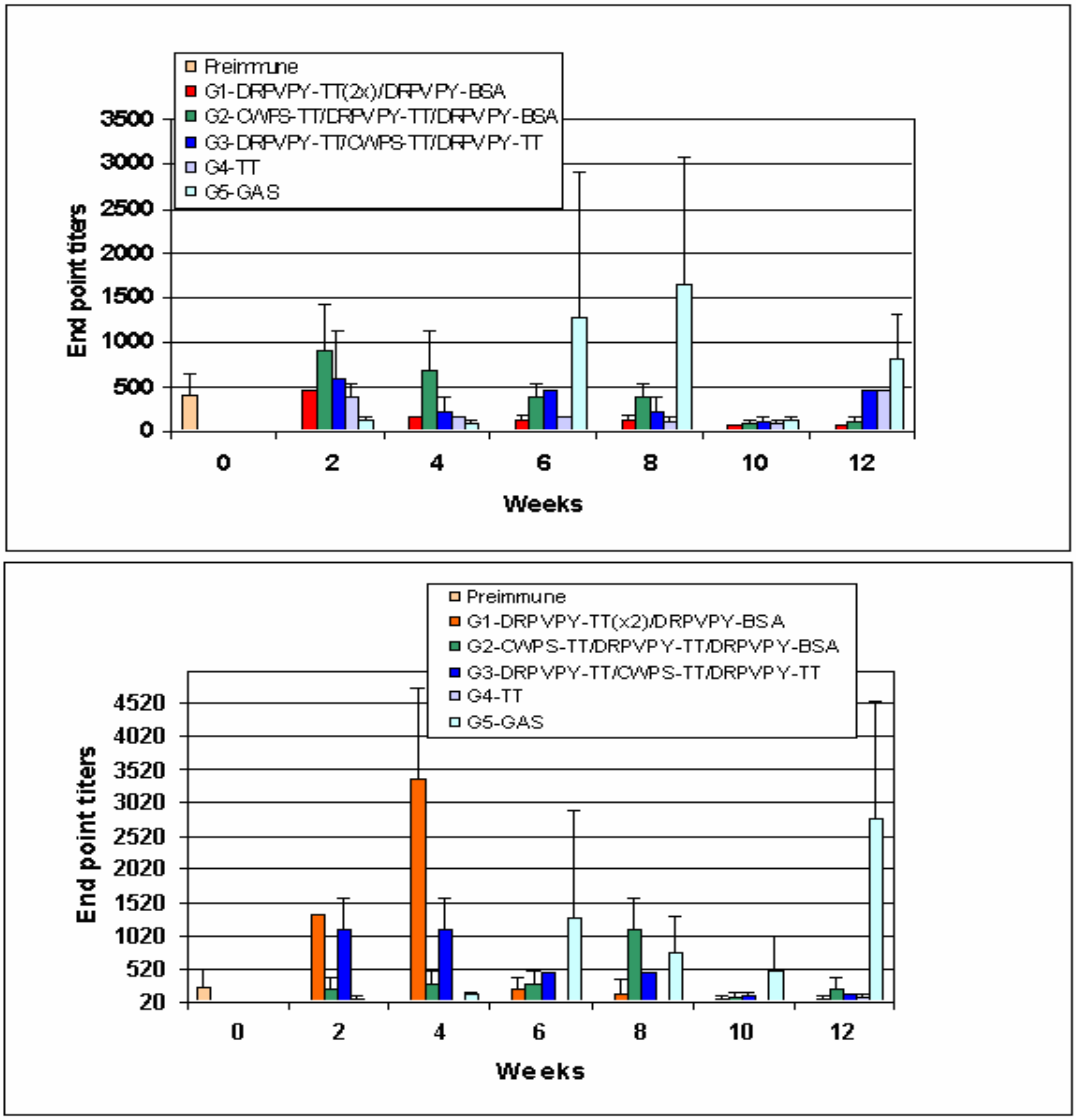

Figure 3-5: Cross-reactivity in Experiment 1: Anti-peptide antibodies binding to heat-killed, pepsin treated Group A Streptococcus (GAS) bacteria as the solid-phase antigen in ELISA (see Materials and Methods). IgM response (top) and IgG response (bottom).

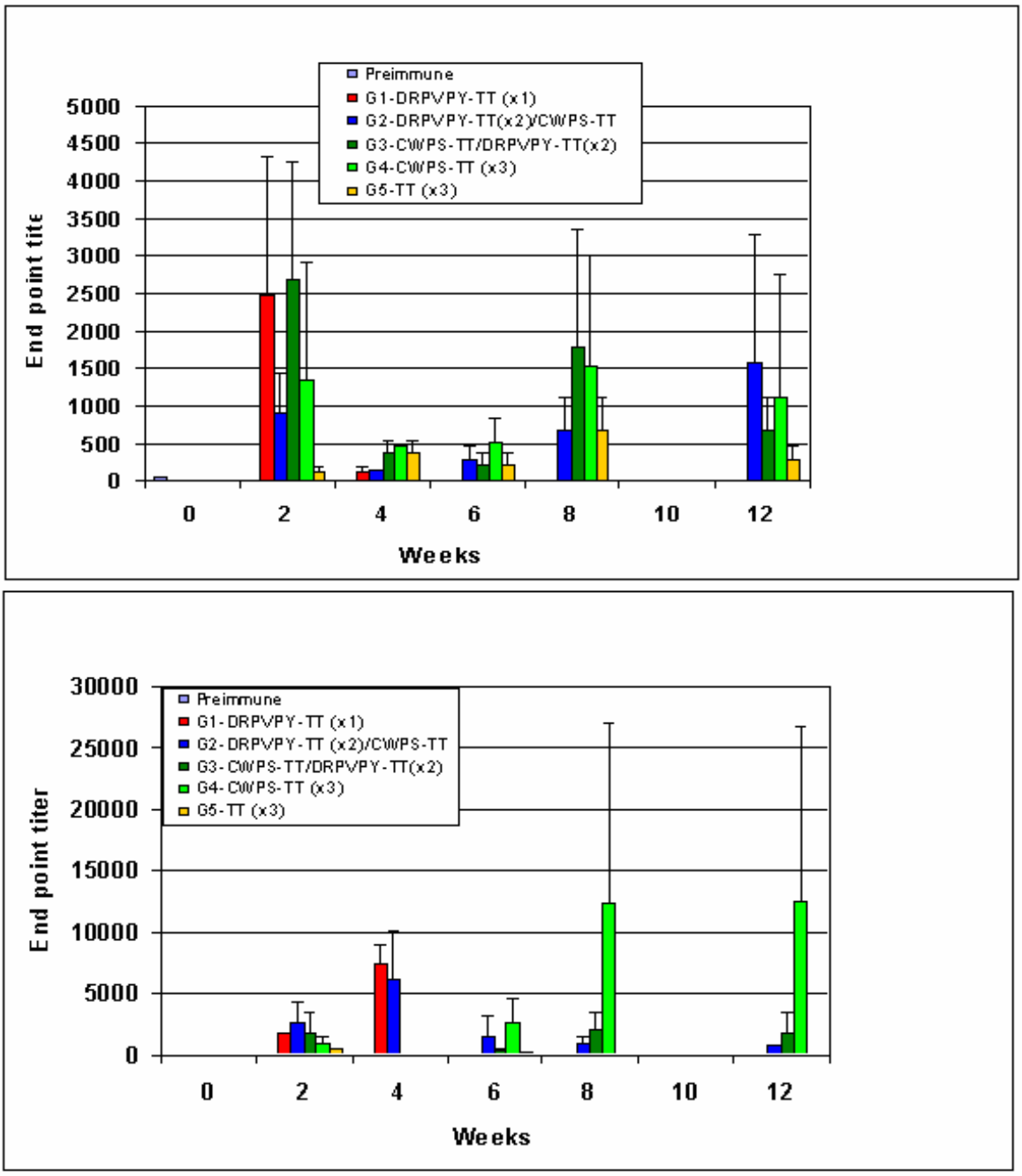

Figure 3-6: Cross-reactivity in Experiment 2: Anti-peptide antibodies binding to heat-killed, pepsin treated Group A *Streptococcus* (GAS) bacteria as the solid-phase antigen in ELISA (see Materials and Methods). IgM response (top) and IgG response (bottom).

3.5.3 Specificity of the primary response to DRPVPY-TT

To investigate the epitope specificities of the anti-DRPVPY polyclonal antibodies, competitive ELISA inhibitions were performed. The antisera with highest endpoint-titers, obtained at week 5 of mice from G1-experiment 2, immunized once with DRPVPY-TT were used in these experiments. Titration experiments of antisera were performed for each experiment and the dilution used corresponded to an A_{405nm} ~1, after 20 min. Heat-killed, pepsin-treated Group A *Streptococcus* (GAS) was used as the solid-phase antigen.

Competitive inhibition ELISA with CWPS and CWPSv were performed with GAS bacteria as the solid-phase antigen. Only the native CWPS inhibited the binding of the anti-DRPVPY polyclonal antibodies (IgG, Figure 3-7I), with greatest inhibitory activity of about 30% at a concentration of 250 μg/ml. No inhibition curve was obtained with the CWPSv under the same conditions. These data confirm the binding of the anti-peptide polyclonal antibodies with GAS and confirm that the GlcNAc moiety, the immunodominant sugar, is a critical part of the GAS-CWPS epitope.

Inhibition ELISA studies with DRPVPY, DRPVP, and DRPVPY-BSA-conjugate as inhibitors of the binding of anti-DRPVPY polyclonal antibodies to GAS bacteria showed that the DRPVPY-BSA conjugate was the best inhibitor, reaching the maximum inhibitory activity, about 70%, at a concentration of 100 μg/ml. DRPVPY and DRPVP showed 35% and 27% inhibition, respectively, and at the same concentration (Figure 3-7II).

Inhibition ELISA studies with synthetic oligosaccharides corresponding to the CWPS (compounds **6**-**8**, Figure 3-3) as inhibitors of the binding of anti-peptide polyclonal antibodies to GAS bacteria, showed a maximum inhibitory activity of about 40%, at a concentration of 250 μg/ml. There was no significant difference between the activities of the three inhibitors: branched trisaccharide, pentasaccharide and hexasaccharide (Figure 3-7III).

Finally, individual mouse sera from G1, experiment 2 (at week 5) were titrated against CWPS-BSA-glycoconjugates, or BSA-peptide-conjugate as antigens (Figure 3-8). The antisera from the four mice reacted best with the $(\text{hexasaccharide})_{16}$-sq-BSA (compound **13**, Figure 3-3), $(\text{hexasaccharide})_{5}$-BSA (compound 12, Figure 3-3), pentasaccharide-BSA (compound **11**, Figure 3-3), and DRPVPY-BSA (compound **4**, Figure 3-2, data not shown); a weaker reaction, was observed with the CWPS-BSA (compound **9**, Figure 3-3) and branched-trisaccharide-BSA (compound **10**, Figure 3-3), with serum from mouse number 2 reacting the weakest (Figure 3-8). These results corroborate the results above on the cross-reactivity observed with the polysaccharide and oligosaccharides.

I

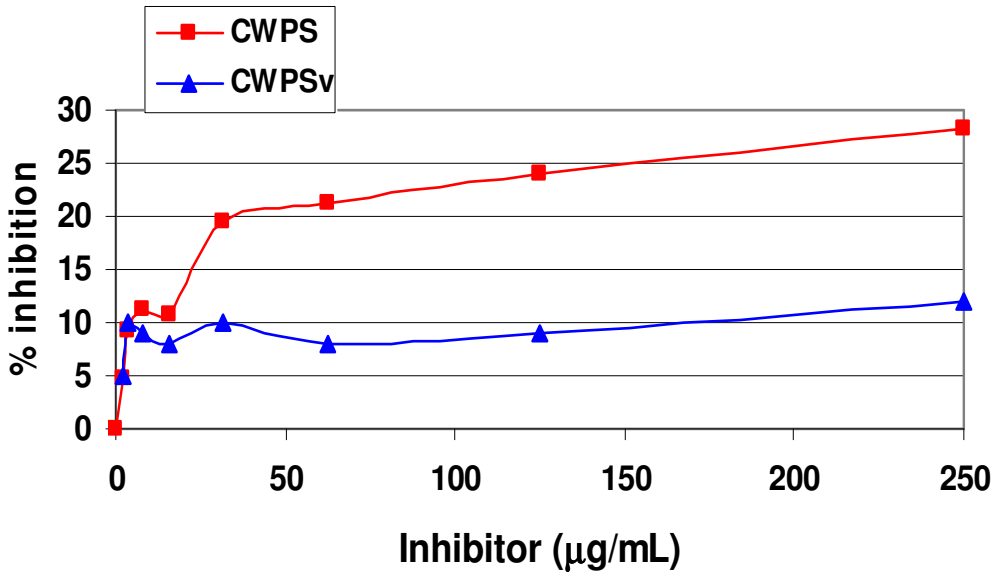
CWPS
CWPSv
% inhibition
30
25
20
15
10
5
0
0
50
100
150
200
250
Inhibitor (µg/mL)

II

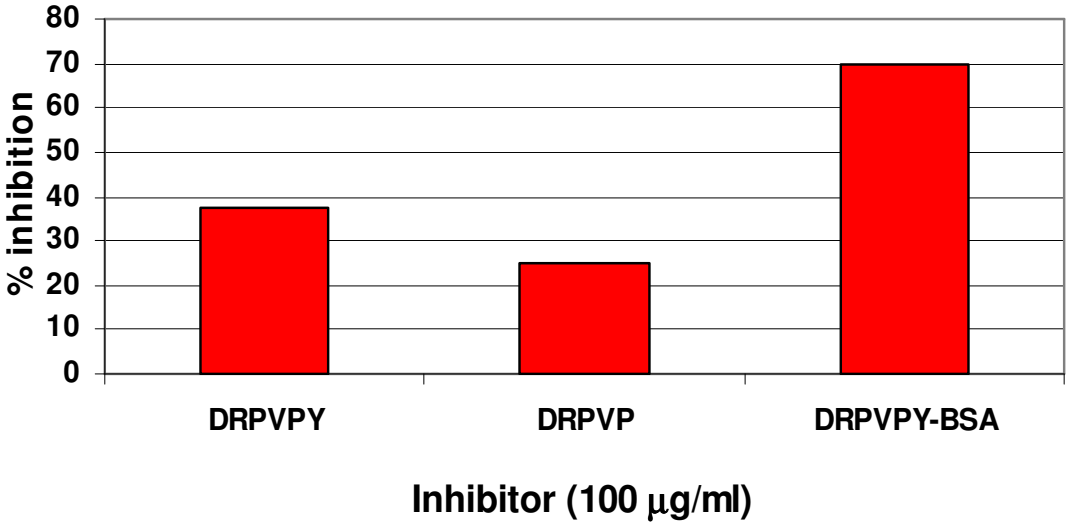
% inhibition
80
70
60
50
40
30
20
10
0
DRPVPY
DRPVP
DRPVPY-BSA
Inhibitor (100 µg/ml)

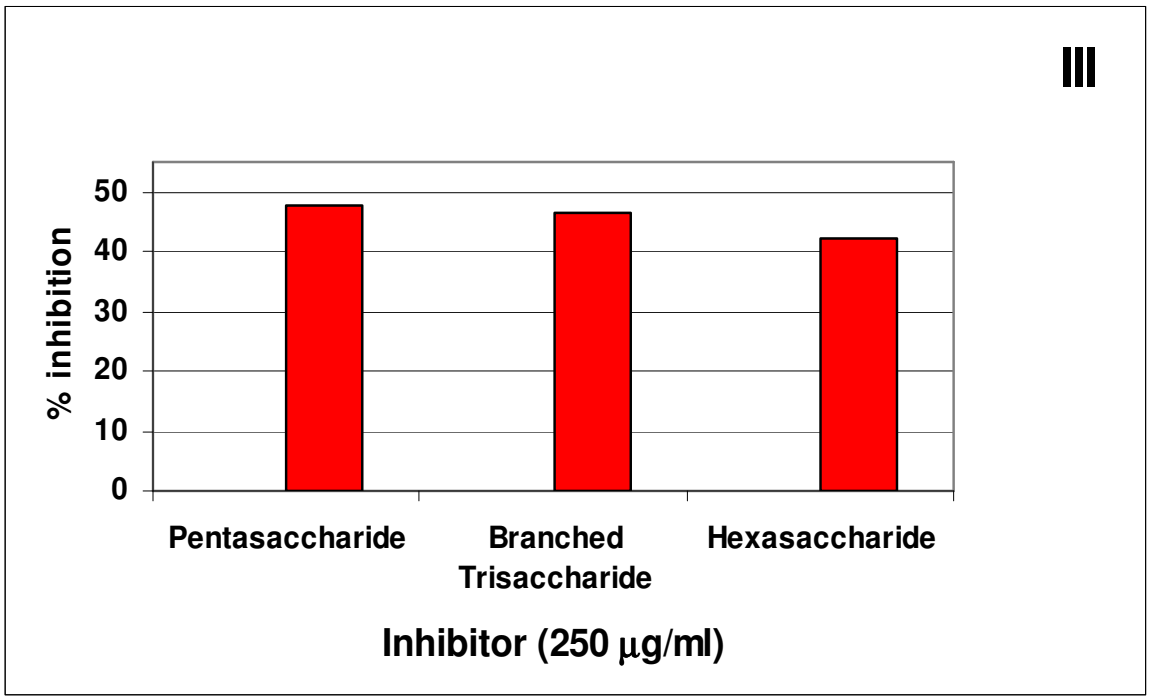

Figure 3-7: Competitive inhibition ELISA using GAS bacteria as the solid-phase antigen and: (I) CWPS and CWPSv, (II) DRPVPY (compound **2**, Figure 3-1), DRPVP and DRPVPY-BSA (compound **4**, Figure 3-2) and (III), Synthetic oligosaccharides corresponding to CWPS (compounds **6**-**8**, Figure 3-3) as inhibitors.

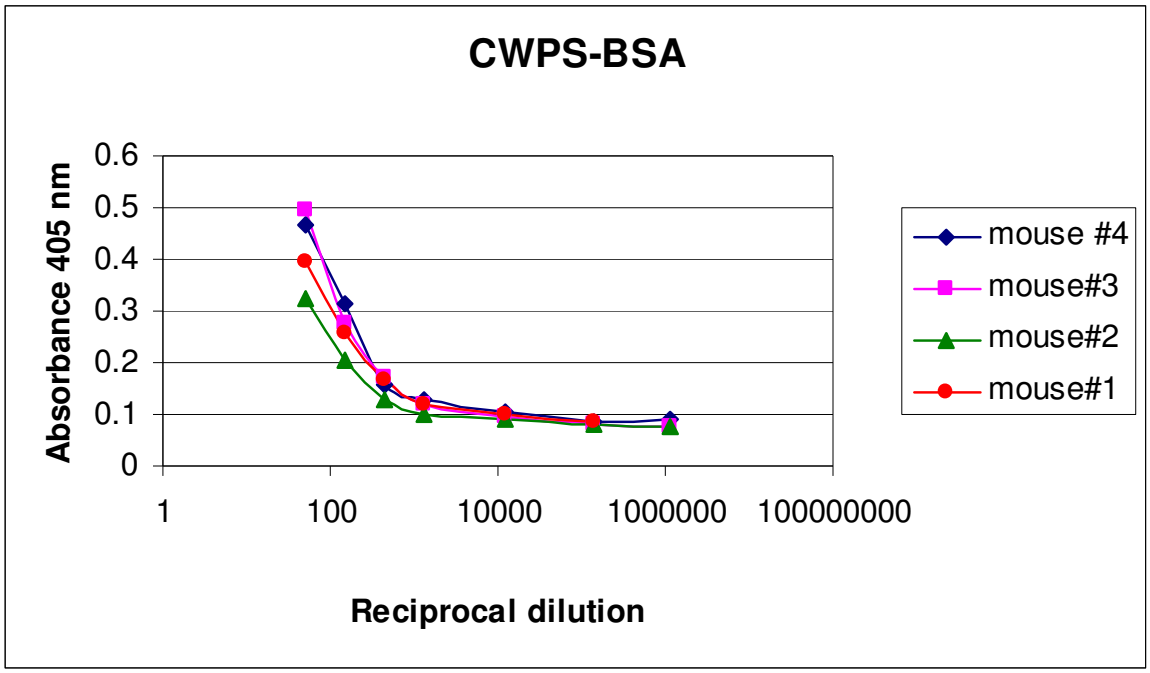
CWPS-BSA
Absorbance 405 nm
0.6
0.5
0.4
0.3
0.2
0.1
0
1
100
10000
1000000
100000000
Reciprocal dilution
mouse #4
mouse#3
mouse#2
mouse#1

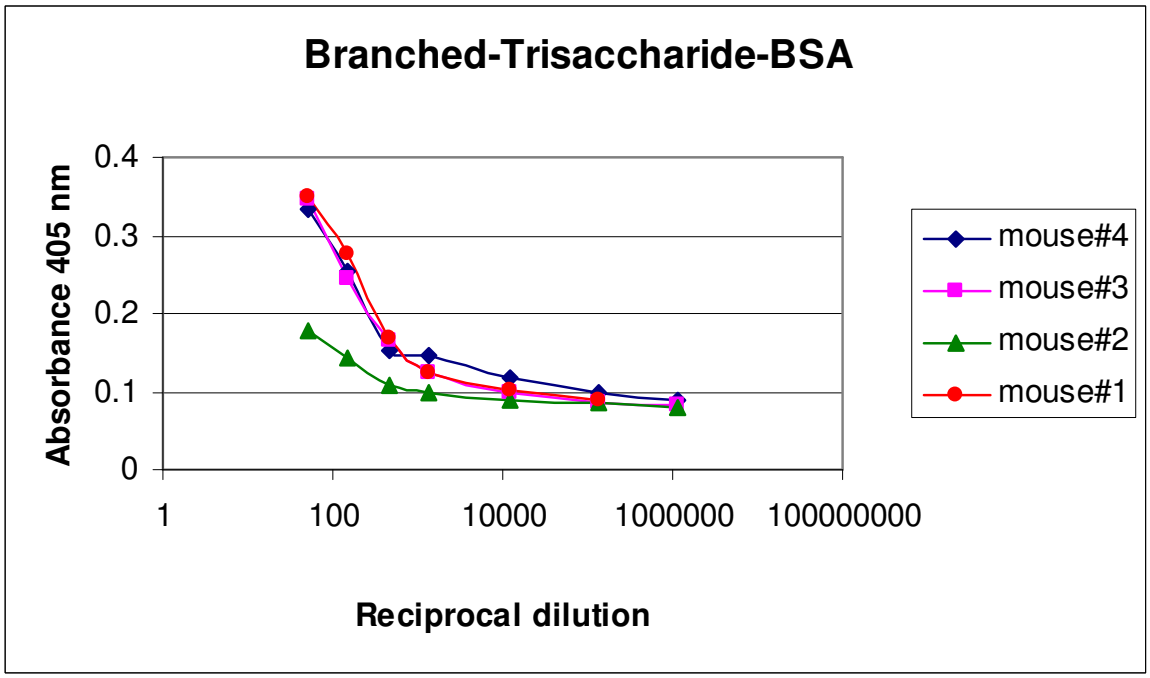
Branched-Trisaccharide-BSA
Absorbance 405 nm
0.4
0.3
0.2
0.1
0
1
100
10000
1000000
100000000
Reciprocal dilution
mouse#4
mouse#3
mouse#2
mouse#1

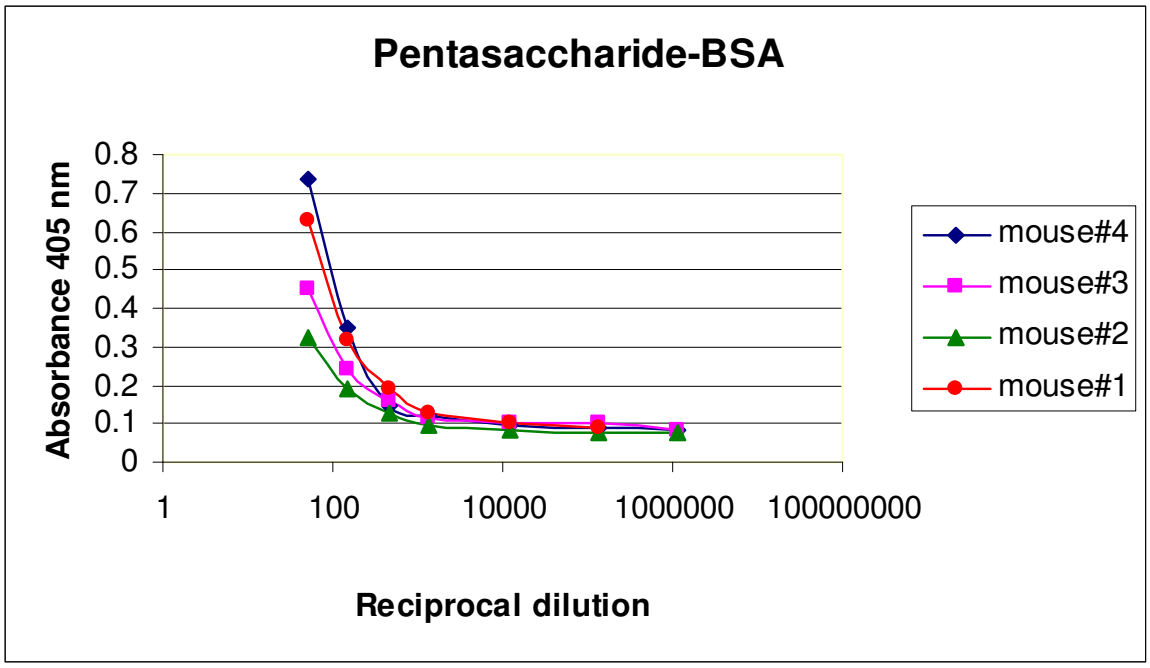
Pentasaccharide-BSA
Absorbance 405 nm
0.8
0.7
0.6
0.5
0.4
0.3
0.2
0.1
0
1
100
10000
1000000
100000000
Reciprocal dilution
mouse#4
mouse#3
mouse#2
mouse#1

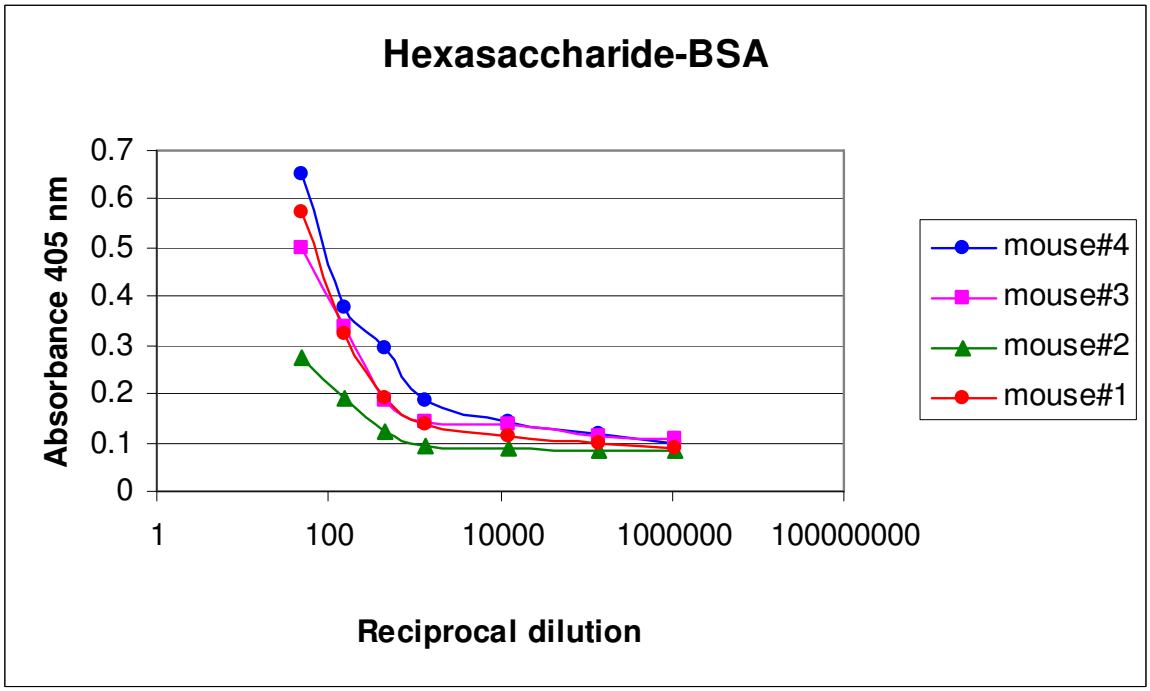
Hexasaccharide-BSA
Absorbance 405 nm
0.7
0.6
0.5
0.4
0.3
0.2
0.1
0
1
100
10000
1000000
100000000
Reciprocal dilution
mouse#4
mouse#3
mouse#2
mouse#1

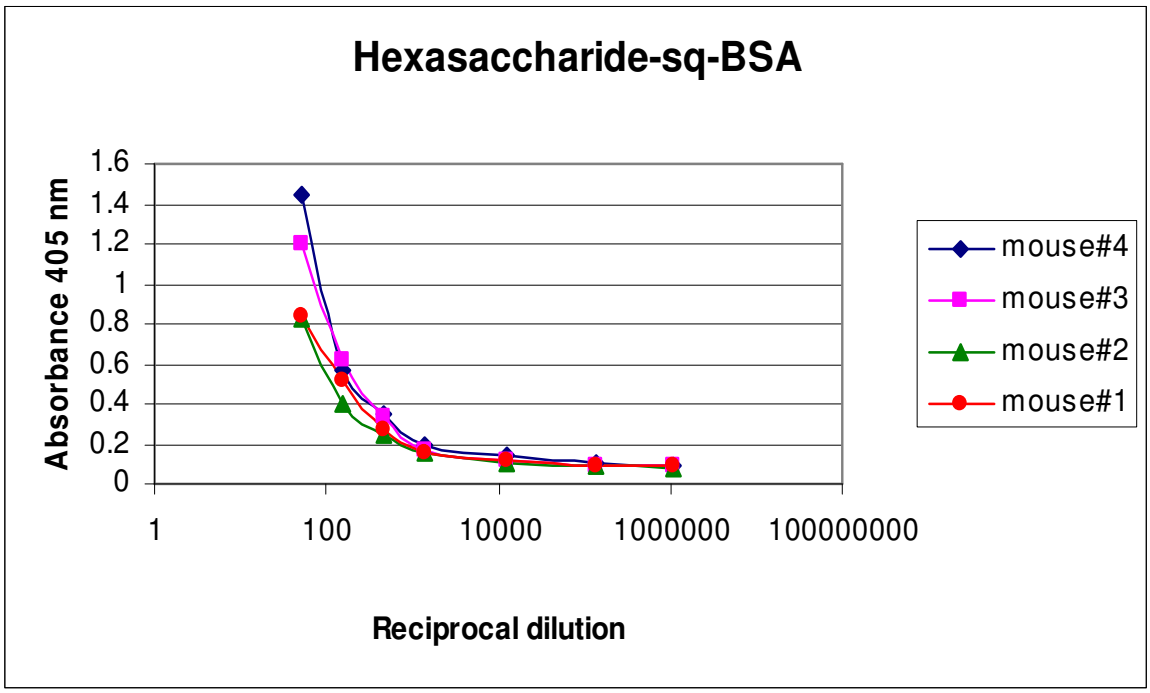

Figure 3-8: Titration ELISA of anti-peptide polyclonal antibodies (IgG) using CWPS (compound **9**, Figure 3-3) and synthetic oligosaccharide-BSA conjugates (compounds **10**-**13**, Figure 3-3) as solid-phase antigens (see Materials and Methods).

3.5.4 Cross-reactivity

3.5.4.1 Anti-polysaccharide (GAS and CWPS) antibodies bind to DRPVPY-BSA

Mice immunized subcutaneously with heat-killed, pepsin treated GAS ($1x10^8$ bact. /mouse) at weeks 0 and 4, responded with titers against DRPVPY-BSA. A high secondary IgG response was observed at week 6 (Figure 3-9A). Mice primed with a low dose of CWPS-TT (1 µg/mouse) responded with low titers

to DRPVPY-BSA, but with higher titers than those from control mice (100 μg/mouse TT, Figure 3-9A). Mice immunized twice with CWPS-TT (2 μg/mouse, weeks 0 and 4) responded with IgG titers against DRPVPY-BSA after priming (weeks 2 and 4, Figure 3-9B). However, no secondary response was seen after subsequent boosting (weeks 6 and 8, Figure 3-9B).

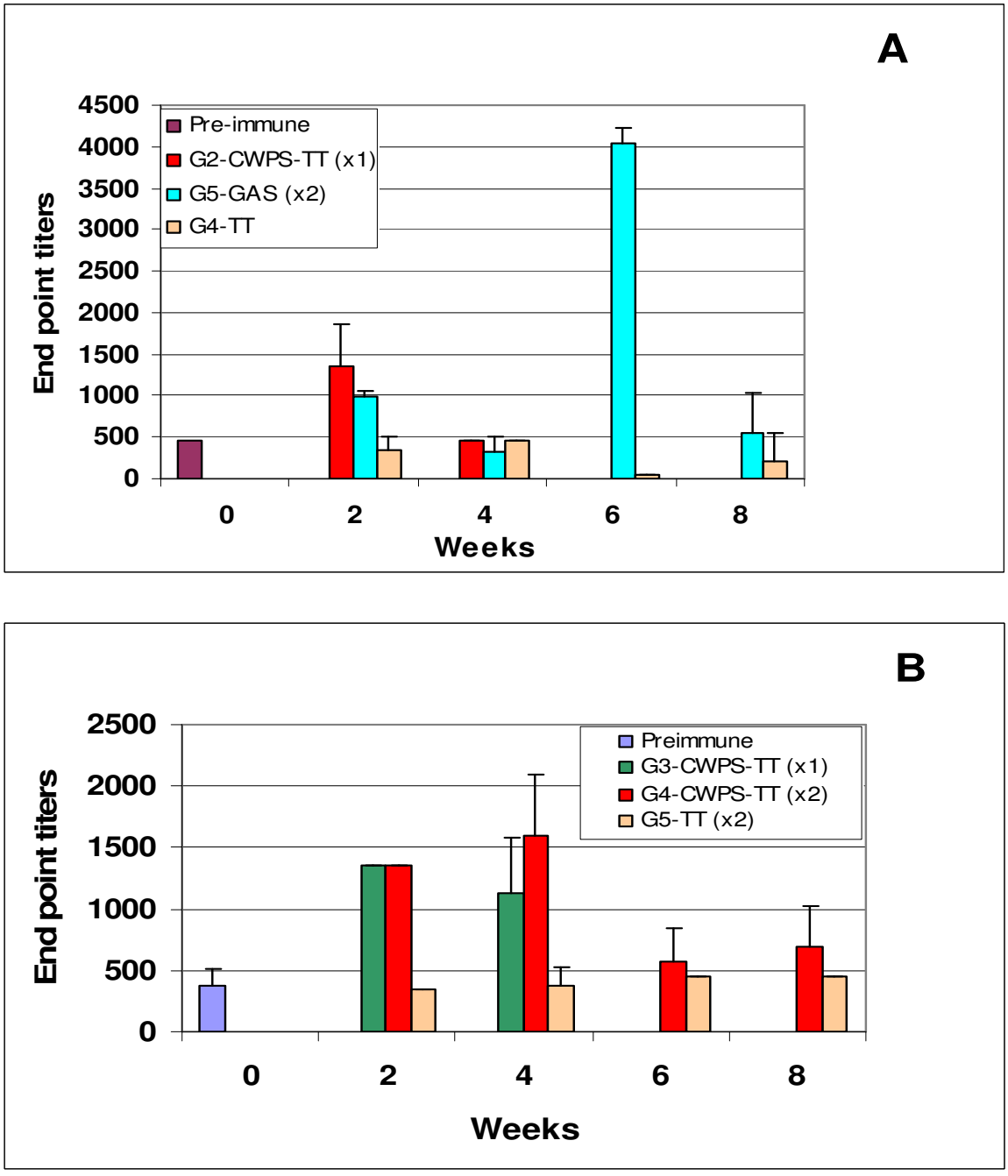

Figure 3-9: Cross-reactivity. Anti-polysaccharide (GAS and CWPS-TT) antibodies (IgG) binding to DRPVPY-BSA (compound **4**, Figure 3-2) as the solid phase antigen; (A): Experiment 1; (B): Experiment 2.

3.6 DISCUSSION

The major impact of this study is the demonstration of the carbohydrate cross-reactivity of the antisera elicited by immunization of mice with the synthetic peptide DRPVPY linked to protein-carrier, a peptide that mimics carbohydrate epitopes of the *Streptococcus* Group A[33]. Thus, the DRPVPY-TT conjugate[31] when used in immunization of BALB/c mice elicited antibodies whose specificity at different time points, as probed by ELISA, was also directed against oligosaccharide epitopes.

The immunogenicity of the DRPVPY-conjugates was evident from primary and secondary antibody responses (immunological memory) with high anti DRPVPY titers, which increased after booster immunizations (IgG) (Figure 3-4A&B). This result indicates that the conjugates effectively promoted a strong and rapid thymus-dependent response to DRPVPY.

Furthermore, and more remarkably, the results demonstrate that the peptide DRPVPY can act as an immunogenic mimic when attached to a carrier-protein, and can induce anti-carbohydrate antibodies. Titers against exposed polysaccharide on GAS bacteria were evident when a high dose of the peptide vaccine was administered to mice (Figure 5-6). A lower dose of 20-40 μg/mouse did not elicit high cross-reactive titers (data not shown). These anti-GAS titers, despite the fact that they were much lower than those against peptide, were specific to carbohydrates. Antigenic cross-reactivities between the peptide and CWPS-epitopes were demonstrated by CWPS-specific inhibition of the anti-

peptide polyclonal antibodies binding to GAS bacteria with serum obtained after initial immunization (Figure 3-7I). The role of the GlcNAc residue as the immunodominant sugar[30,34] in the antibody response was evident since CWPSv, lacking the GlcNAc moiety, (compound 3, Figure 3-1) was not able to inhibit the binding of the anti-peptide polyclonal to GAS (Figure 3-7I). The fact that DRPVP was a poorer inhibitor than DRPVPY (Figure 3-7II) may suggest a role of the tyrosine moiety in the antibody response; we had hypothesized previously that the VPY turn conformation might be necessary for effective immunogenicity[35,36]; experiments with antibodies of higher affinity will be essential for a critical test of this hypothesis. The multivalency effect was evident since the DRPVPY-BSA was able to cause up to 70% of inhibition while DRPVPY caused only about 35% inhibition (Figure 3-7II).

The presence of antibodies cross-reactive with carbohydrate was further demonstrated by the reactivity observed in the titration ELISA. Titers against all five antigens (compounds **9**-**13**, Figure 3-3) were observed (Figure 3-8), although much lower than those against peptide (not shown). The sera reacted more weakly with the branched-trisaccharide conjugate, and the strongest binding was with the pentasaccharide-BSA and $(hexasaccharide)_5$-BSA. Higher titers were observed with the $(hexasaccharide)_{16}$-squarate-BSA conjugate, sharing the linker with the immunogen and having 16 oligosaccharide units. This result indicates the dominance in the polyclonal specificity of an extended epitope, as observed earlier[30]. The specificity of the immune response for GAS oligosaccharides was corroborated by the inhibition observed with the branched-trisaccharide

(compound **7**, Figure 3-3), pentasaccharide (compound **6**, Figure 3-3) and hexasaccharide (compound **8**, Figure 3-3), although no significant difference in inhibition among the inhibitors was observed (Figure 3-7III).

The combined evidence leads us to conclude that (i) DRPVPY is an immunological mimic of CWPS, since high titers of cross-reactive antibodies were obtained by immunization of mice with DRPVPY-TT and (ii) the immune response is specific for the GAS oligosaccharide epitopes since the oligosaccharides and CWPS inhibit antibody binding to GAS.

However, a lack of secondary response (IgG) cross-reactive with GAS bacteria was observed after mice received a booster injection of DRPVPY-TT at equal dose (G1 experiment 1 and G2 experiment 2, respectively, in week 6-8, Figure 3-5, 3-6) or lower (G3 experiment 2, at week 12, Figure 3-6). This lack of response may be the result of a carrier-induced suppression effect, which can decrease the production of antigen-specific antibodies[37], so-called incomplete T-cell dependent[38]. While an increase in anti-DRPVPY titers after the booster injections was observed (Figure 3-4A-G1 and 4B-G2, weeks 6-8), indicating the activation of DRPVPY-specific memory cells overall, we suggest that only a sub-population of these memory cells gives rise to carbohydrate cross-reactive antibodies that was not effectively activated. These results may arise from competition between populations of memory cells to peptide and carrier epitopes, the latter being better represented due to the relative sizes of the molecules. This effect has been noted in similar immunization strategies wherein the size and dose of the carrier molecule overwhelm that of the hapten of interest[39,40].

Some strategies have been successful in minimizing the suppression effect. Thus, the change of carrier to a different protein, or use of smaller regions of the same carrier, or use of T-cell peptide epitopes have been shown to remove epitopes that activate the carrier-specific population of memory B-cells upon subsequent immunizations[39,40]. In our case, attempts to save the cross-reactive response were conducted in week 10 in both experiments. First, by changing the immunization carrier to BSA and boosting with a lower dose of DRPVPY-BSA were not successful (G1 experiment 1, week 12, Figure 3-5). Alternatively, a balance in activation of hapten- and carrier-specific immune responses have been obtained through repeated immunization with different concentrations of the same immunogen[39]. In our hands, a booster injection with a 10-fold lower dose of DRPVPY-TT was tried in G3 experiment 2, week 10, or half dose (G3-experiment 1, week 10); however, a secondary-like response (fast, strong and high IgG titers) was not observed at week 12 (Figure 3-6). In future work, the use of multiple antigen peptide (MAP) system, which directs a specific immune response to a localized concentration of peptide epitopes and avoids the use of carrier proteins[14], or an universal 13 amino acid helper T-lymphocyte epitope AKXVAAWTLKAAA (Pan HLA-DR Epitope, PADRE), might present alternative strategies to solve this carrier effect[41].

Mice vaccinated with heat-killed, pepsin treated GAS bacteria three times responded, as expected, with a delayed response due to the low density of antigenic determinants, with IgM titers dominating the primary response, and higher IgG titers in the secondary responses (G5 experiment 1, Figure 3-5). The

booster effect was observed with repeated injections (G5 experiment 1, Figure 3-5). Similarly, vaccination with low doses of the conjugate CWPS-TT (G4 experiment 2, Figure 3-6) increased IgM titers after priming, and subsequently IgG titers after the booster injections (G4 experiment 2, Figure 3-6). It is also worth noting the differences in the mouse responses obtained after immunizations with the two experimental vaccines, DRPVPY-TT and CWPS-TT, indicative of their different immunogenicities. The DRPVPY-TT seemed able to induce a quicker and stronger primary response with higher IgG titers than the CWPS-TT, although a 50-fold higher dose/mouse was required, leading then to a carrier-suppression effect when a booster injection was given (Figure 3-6). The CWPS-TT elicited an expected response for polysaccharide-protein conjugate vaccines[42].

The existence of carbohydrate-peptide mimicry was further demonstrated by the increase in IgG titers to DRPVPY elicited by immunization with GAS (Figure 3-9A). Immunization with CWPS-TT resulted in an increase in titers but no booster effect was observed (Figure 3-9B). This behavior can be explained by a carrier-effect, in which anti-TT antibodies overwhelm the anti-CWPS antibodies cross-reactive with peptide, probably a very small population within the anti-CWPS antibodies.

It is relevant that one comment on the standard deviations. These are not unusually high for using 4 mice/group. The results can be compared to those in analogous studies. Thus, Beenhouwer *et al.*[43] have shown a similar distribution of anti-peptide titers as in the present study, although standard deviations were

not shown, and Fleuridor *et al.*[38] and Maitta *et al.*[44] obtained similar standard deviations for the anti-peptide titers, although with lower titer values. The higher standard deviation observed for the anti-carbohydrate titers derives from the fact that one mouse in each control group did not respond, the other mice giving very similar titers. Nevertheless, the overall conclusions of cross-reactivity are justified.

The facts (i) that repeated administration of the same DRPVPY-TT experimental vaccine (homologous boosting) did not lead to effective boosting of humoral responses, (ii) that DRPVPY is also an immunological mimic of CWPS and (iii) that both experimental vaccines DRPVPY-TT and CWPS-TT were available, led us to circumvent the problem by trying two heterologous boosting strategies[45]. This strategy has been successfully applied for carbohydrate peptide mimics and carbohydrates in the *Cryptococcus neoformans* system[43].

The two strategies consisted of: (i) priming with DRPVPY-TT and boosting with CWPS-TT (G3 experiment 1-Figure 3-5) or (ii) priming with CWPS-TT and boosting with DRPVPY-TT (G2 experiment 1-Figure 3-5 and G3 experiment 2-Figure 3-6). No titer increases against GAS were observed with the first strategy (Figure 3-5-G3, week 6). With the second strategy, boosting with DRPVPY-TT at a high (Figure 3-5-G2, week 6) and at a lower dose (Figure 3-6-G3, week 10-12) or even using another carrier, BSA (Figure 3-5-G2, week 10-12), although titers against GAS increased (Figure 3-5-G2-week 8, and Figure 3-6-G3-week 8), did not have a response with the characteristics of a secondary response (fast, strong and high IgG titers). This behavior can be explained as a cross-reactive

late primary response to the peptide, as supported by the increase in IgG titers to DRPVPY (Figure 3-4A-G2, and Figure 3-4B-G3) observed in weeks 6 and 8, following boosting with DRPVPY-TT.

In conclusion, promising results from the study of the immunogenicity of a peptide-mimic of the Group A *Streptococcus* (GAS) cell-wall polysaccharide (CWPS) have been obtained. The primary response to the peptide immunogen had high titers of mature antibody isotype, IgG, showing participation of both cellular and humoral immune responses. The antibodies generated were cross-reactive with carbohydrate epitopes displayed on GAS bacteria, and this interaction was inhibited by CWPS and oligosaccharide fragments thereof, showing conclusively that the peptide DRPVPY is an antigenic mimic of the GAS CWPS. Conversely, immunization with GAS displaying CWPS led to a cross-reactive response against DRPVPY. However, a long term, stable response against GAS, could not be maintained for groups immunized with DRPVPY-TT due to the carrier-suppression-effect. Further investigation of the effects resulting from boosting with different peptide-conjugates will likely be required for the design of effective anti-GAS vaccines based on mimetic-peptides.

Survival and challenge studies will be conducted when an appropriate vaccine formulation is defined, that is, one with a response that can be reliably boosted. The present study was intended to serve as a prelude to define the parameters; the results obtained are of importance because they do show reliably that peptide-carbohydrate cross-reactivity exists upon immunization.

3.7 ACKNOWLEDGEMENTS

This work was supported by a grant from the Natural Sciences and Engineering Research Council of Canada.

3.8 REFERENCES

1. Cunningham, M.D., 2000. Pathogenesis of Group A Streptococcal Infections Clin. Microbiol. Rev., 13: 470-511.
2. Stevens, D.L., 1997. The toxins of Group A *Streptococcus*, the flesh eating bacteria Immunological Investigations, 26: 129-150.
3. Stevens, D.L., 2003. Skin and soft tissue infections Infect. Med., 20: 483-
4. Bisno, A.L., In *Principles and Practice of Infectious Diseases*; Mandell, G.L., R.G. Douglas andJ.E. Bennet, Eds. p. Pages|; Wiley: New York. 1985; Vol.
5. Quinn, R.W., 1989. Comprehensive review or morbidity and mortality trends for rheumatic fever, strptococcal disease, and scarlet fever: the decline of rheumatic fever. Rev. Infect. Dis., II: 928-952.
6. Stevens, D.L., M.H. Tanner, J. Winship, R. Swarts, K.M. Ries, P.M. Schlievert and E. Kaplan, 1989. Severe group A streptococcal infections associated with a toxic shock-like syndrome and scarlet fever toxin. A. N. Engl. J. Med., 321: 1-7.

7. Stollerman, G.H., 1988. Changing group A streptococci: the reappearance of streptococcal toxic shock. Arch. Intern. Med., 148: 1268-1270.

8. Kehoe, M.A., 1991. Group A streptococcal antigens and vaccine potential. Vaccine, 9: 797-806.

9. Hall, M.A., S.D. Stroop, M.C. Hu, M.A. Walls, M.A. Reddish, D.S. Burt, G.H. Lowell and J.B. Dale, 2004. Intranasal Immunization with Multivalent Group A Streptococcal Vaccines Protects Mice against Intranasal Challenge Infections. Infect. Immun., 72: 2507-2512.

10. Hu, M.C., M.A. Walls, S.D. Stroop, M.A. Reddish, B. Beall and J.B. Dale, 2002. Immunogenicity of a 26-Valent Group A Streptoccocal Vaccine. Infect. Immun., 70: 2171-2177.

11. Kotloff, K.L., M. Corretti, K. Palmer, J.D. Campbell, M.A. Reddish, M.C. Hu, S.S. Wasserman and J.B. Dale, 2004. Safety and Immunogenicity of a Recombinant Multivalent group A Streptococcal Vaccine in Healthy Adults. JAMA, 292: 709-715.

12. Michon, F., S.L. Moore, J. Kim, M.S. Blake, F.-I. Auzanneau, B.D. Johnston, M.A. Johnson and B.M. Pinto, 2005. The doubly-branched hexasaccharide epitope on the cell-wall polysaccharide of Group A *Streptococcus.* recognized by human and rabbit antisera Infect. Immun., 73: 6383-6389.

13. Sabharwal, H., F. Michon, D. Nelson, W. Dong, K. Fuchs, R. Carreno-Manjarrez, A. Sarkar, C. Uitz, A. Viteri-Jackson, R.S. Rodriguez-Suarez,

M.S. Blake and J.B. Zabriskie, 2006. Group A *Streptococcus* (GAS) Carbohydrate as an Immunogen for Protection against GAS Infection J. Infect. Dis., 193: 129-135.

14. Ji, Y., B. Carlson, A. Kondagunta and P.P. Clearly, 1997. Intranasal Immunization with C5a Peptidase Prevents Nasopharyngeal Colonization of Mice by the Group A *Streptococcus*. Infect. Immun., 65: 2080-2087.
15. Johnson, M.A. and B.M. Pinto, 2002. Molecular mimicry of carbohydrates by peptides Aust. J. Chem., 55: 13-25.
16. Roy, R., 2004. New trends in carbohydrate-based vaccines. Drug Discovery Today: Technologies, 1: 327-336.
17. Beenhouwer, D.O., R.J. May, P. Valadon and M.D. Scharff, 2002. High affinity mimotope of the polysaccharide capsule of Cryptococcus neoformans identified from an evolutionary phage peptide library J. Immunol., 169: 6992-6999.
18. Cunto-Amesty, G., P. Luo, B. Monzavi-Karbassi, A. Lees, J. Alexander, M.F. Del Guercio, M.H. Nahm, C. Artaud, J. Stanley and T. Kieber-Emmons, 2003. Peptide mimotopes as prototypic templates of broad-spectrum surrogates of carbohydrate antigens Cell. Mol. Biol., 49: 245-254.
19. Maitta, R.W., K. Datta, A. Lees, S.S. Belouski and L.A. Pirofski, 2004. Immunogenicity and efficacy of Cryptococcus neoformans capsular polysaccharide glucuronoxylomannan peptide mimotope-protein

conjugates in human immunoglobulin transgenic mice Infect. Immun., 72: 196-208.

20. Harris, S.L., L. Craig, J.S. Mehroke, M. Rashed, M.B. Zwick, K. Kenar, E.J. Toone, N. Greenspan, F.I. Auzanneau, J.R. MarinoAlbernas, B.M. Pinto and J.K. Scott, 1997. Exploring the basis of peptide-carbohydrate crossreactivity: Evidence for discrimination by peptides between closely related anti-carbohydrate antibodies Proc. Natl. Acad. Sci. U.S.A., 94: 2454-2459.

21. Reimer, K.B., M.A.J. Gidney, D.R. Bundle and B.M. Pinto, 1992. Immunochemical Characterization of Polyclonal and Monoclonal *Streptococcus* Group-A Antibodies by Chemically Defined Glycoconjugates and Synthetic Oligosaccharides Carbohydr. Res., 232: 131-142.

22. Johnson, M.A., A. Rotondo and B.M. Pinto, 2002. NMR studies of the antibody-bound conformation of a carbohydrate-mimetic peptide Biochemistry, 41: 2149-2157.

23. Johnson, M.A. and B.M. Pinto, 2004. NMR spectroscopic and molecular modeling studies of protein-carbohydrate and protein-peptide interactions Carbohydr. Res., 339: 907-928.

24. Hossany, R.B., M.A. Johnson, A.A. Eniade and B.M. Pinto, 2004. Synthesis and immunochemical characterization of protein conjugates of carbohydrate and carbohydrate-mimetic peptides as experimental vaccines Bioorg. Med. Chem., 12: 3743-3754.

25. Krause, R.M., 1970. The search for antibodies with molecular uniformity Adv. Immunol., 12.

26. Pitner, J.B., W.F. Beyer, T.M. Venetta, C. Nycz, M.J. Mitchell, S.L. Harris, J.R. Marino-Albernas, F.I. Auzanneau, F. Forooghian and B.M. Pinto, 2000. Bivalency and epitope specificity of a high-affinity IgG3 monoclonal antibody to the *Streptococcus* Group A carbohydrate antigen. Molecular modeling of a Fv fragment Carbohydrate Research, 324: 17-29.

27. Auzanneau, F.I., F. Forooghian and B.M. Pinto, 1996. Efficient, convergent syntheses of oligosaccharide allyl glycosides corresponding to the *Streptococcus* Group A cell-wall polysaccharide Carbohydr. Res., 291: 21-41.

28. Hoog, C., A. Rotondo, B.D. Johnston and B.M. Pinto, 2002. Synthesis and conformational analysis of a pentasaccharide corresponding to the cell-wall polysaccharide of the Group A *Streptococcus* Carbohydr. Res., 337: 2023-2036.

29. Auzanneau, F.I. andB.M. Pinto, 1996. Preparation of antigens and immunoadsorbents corresponding to the *Streptococcus* Group A cell-wall polysaccharide Bioorg. Med. Chem., 4: 2003-2010.

30. Zou, W., S. Borrelli, M. Gilbert, T. Liu, R.A. Pon and H.J. Jennings, 2004. Bioengineering of surface GD3 ganglioside for immunotargeting human melanoma cells. J. Biol. Chem., 279: 25390-25399.

31. Malkiel, S., L. Liao, M.W. Cunningham and B. Diamond, 2000. T-cell-dependent antibody response to the dominant epitope of Streptococcal

polysaccharide, N-acetyl-glucosamine, is cross-reactive with cardiac myosin. Infect. Immun., 68: 5803-5808.

32. Peeters, C.A.M., A.J. Tenbergen-Meekes, J.T. Poolman, M. Beurret, B.J.J. Zegers and G.T. Rijkers, 1991. Effect of carrier priming on immunogenicity of saccharide-protein conjugate vaccines. Infect. Immun., 59: 3504.

33. Fleuridor, R., A. Lees and L.A. Pirofski, 2001. A cryptococcal capsular polysaccharide mimotope prolongs the survival of mice with Cryptococcus neoformans infection J. Immunol., 166: 1087-1096.

34. Herzenberg, L.A., T. Tokuhisa and K. Hayakawa, 1983. Epitope-Specific Regulation Ann. Rev. Immunol., 1: 609-632.

35. Herzenberg, L.A. andT. Tokuhisa, 1980. Carrier-Priming Leads to Hapten-Specific Suppression Nature, 285: 664-667.

36. Putz, M.M., W. Ammerlaan, F. Schneider, G. Jung and C.P. Muller, 2004. Humoral immune responses to a protective peptide-conjugate against measles after different prime-boost regimens Vaccine, 22: 4173-4182.

37. Schutze, M.P., E. Deriaud, G. Przewlocki and C. Leclerc, 1989. Carrier-Induced Epitopic Suppression Is Initiated through Clonal Dominance J. Immunol., 142: 2635-2640.

38. Schutze, M.P., C. Leclerc, M. Jolivet, F. Audibert and L. Chedid, 1985. Carrier-Induced Epitopic Suppression, a Major Issue for Future Synthetic Vaccines J. Immunol., 135: 2319-2322.

39. Monzavi-Karbassi, B., S. Shamloo, M. Kieber-Emmons, F. Jousheghany, P. Luo, K.Y. Lin, G. Cunto-Amesty, D.B. Weiner and T. Kieber-Emmons, 2003. Priming characteristics of peptide mimotopes of carbohydrate antigens Vaccine**,** 21: 753-760.

40. Alexander, J., M.F. del Guercio, A. Maewal, L. Qiao, J. Fikes, R. Chesnut, J. Paulson, D. Bundle, S. DeFrees and A. Sette, 2000. Linear PADRE T helper epitope and carbohydrate B cell epitope conjugates induce specific high titer IgG antibody responses J. Immunol.**,** 164: 1625-1633.

41. Alexander, J., M.F. del Guercio, B. Frame, A. Maewal, A. Sette, M.H. Nahm and M.J. Newman, 2004. Development of experimental carbohydrate-conjugate vaccines composed of *Streptococcus* pneumoniae capsular polysaccharides and the universal helper T-lymphocyte epitope (PADRE((R))) Vaccine**,** 22: 2362-2367.

42. Alexander, J., M.F. del Guercio, B. Frame, A. Maewal, A. Sette, G. Newman and M. Newman, 2001. Pneumococcal conjugate vaccines comprised of PADRE T helper epitope and capcular polysaccharides induce specific high titer IgG antibody responses Faseb J.**,** 15: A1189-A1189.

43. Lindberg, A.A., 1999. Glycoprotein conjugate vaccines Vaccine**,** 17: S28-S36.

44. Woodland, D.L., 2004. Jump-starting the immune system: prime-boosting comes of age Trends Immunol.**,** 25: 98-104.

CHAPTER 4: IMMUNOLOGICAL EVIDENCE FOR FUNCTIONAL VS. STRUCTURAL MIMICRY WITH A *SHIGELLA FLEXNERI* Y POLYSACCHARIDE-MIMETIC PEPTIDE

This chapter comprises the manuscript **"*Immunological Evidence for Functional vs Structural Mimicry with a Shigella Flexneri Y Polysaccharide-Mimetic Peptide*"** which has been published in Clinical Vaccine Immunology (**2008**, *15*, 1106-1117).

Silvia Borrelli, Rehana B. Hossany and B. M. Pinto

We have previously shown that the mimetic peptide DRPVPY in the form of a peptide-protein conjugate is an immunological mimic of the GAS polysaccharide, indicating that structural mimicry by mimetic peptide is not required for immunogencity while secondary structure adopted by the mimetic peptide in both the combining site of antibody and the free peptide might be one of the prominent features required for immunogenicity. In order to further test this hypothesis, we embarked on a program to study the immunogenicity in mice of the carbohydrate mimetic peptide MDWNMHAA (attached to TT), which is a functional mimic (confirmed by

X-ray) of the *Shigella flexneri* Y polysaccharide similar to DRPVPY, but lacks bound secondary structure in the free peptide, in constrast to DRPVPY.

The immunological study was conducted by Dr. Silvia Borrelli while the peptide MDWNMHAA and three peptide conjugates $(MDWNMHAA)_{28}$-BSA, $(MDWNMHAA)_{32}$-TT, and $(MDWNMHAA)_{50}$-TT were prepared by the thesis author. The thesis author also participated in discussions and interpretations of the immunological data.

The immunogenicity of MDWNMHAA-TT was examined by immunizing BALB/c mice following similar homologous and heterologous prime/boost strategies that were used to study the immunogenicity of the DRPVPY-TT in the previous work. In a second study, to determine the effect of higher peptide density on carrier protein on immune responses, mice were vaccinated with a MDWNMHAA-TT containing 30% more copies of MDWNMHAA per TT.

Interestingly, it was demonstrated that in addition to structural mimicry not being required for immunogenicity of a carbohydrate-mimetic peptide, lack of bound secondary structure in the free-peptide also does not prevent a carbohydrate-mimetic peptide from inducing a cross-reactive immune response against the bacterial polysaccharide, since MDWNMHAA attached to TT, was found in the current work to be an immunogenic mimic of the *Shigella flexneri* Y polysaccharide. Moreover, on increasing the number of peptide haptens by 30% on the carrier protein

TT, the immune response, specific for the *Shigella flexneri* Y polysaccharide, was faster and stronger. This showed that peptide density on the carrier protein could greatly improve the immunogenicity of peptide haptens.

In addition to addressing our questions regarding the requirements for the immunogenicity of carbohydrate-mimetic peptides, these promising results have provided sufficient evidence for the MDWNMHAA-TT to move from a research phase (initial studies) to a higher developmental phase which is to determine if it can convey protection in mice challenged with live *Shigella flexneri* Y bacteria. This will characterize it further as a potential vaccine against this pathogen.

4.1 KEYWORDS

Shigella flexneri Y, peptide-carbohydrate mimicry, mimetic-peptide, immunogenicity, immunological cross-reactivity, functional vs. structural mimicry

4.2 ABSTRACT

An approach to vaccine design is the use of molecules that mimic the immunogenic element of interest. In this context, the interaction of MDWNMHAA, a peptide mimic of the *Shigella flexneri* Y O polysaccharide (PS), with an anti-carbohydrate monoclonal antibody, as studied previously by X-ray crystallography, suggested the presence of functional rather than structural mimicry and a bound peptide conformation that was not represented significantly in the free-ligand ensemble. The antibody response elicited by an MDWNMHAAcarrier protein (tetanus toxoid [TT]) conjugate has now been investigated in BALB/c mice. The mice were immunized following a homologous prime/boost strategy using MDWNMHAA-TT as the immunogen. The mice showed anti-peptide antibody (immunoglobulin G [IgG]) titers that increased after being boosted. High anti-lipopolysaccharide (LPS) (IgG) titers were observed after the last boost. A faster immune response, with cross-reactive titers, was observed with a peptide conjugate with 30% more copies of the peptide. The binding of anti-peptide polyclonal antibodies to LPS could be inhibited by LPS, PS, MDWNMHAA, and MDWNMHAA-bovine serum albumin, as assessed by

inhibition enzyme-linked immunosorbent assay. Conversely, mice immunized with PS-TT showed IgG anti-peptide titers. These data demonstrate the cross-reactivity of the antibody response and support the hypothesis that functional, as opposed to structural, mimicry of the *S. flexneri* Y O PS by MDWNMHAA or the underrepresentation of the bound ligand conformation in the free-ligand ensemble does not compromise immunological cross-reactivity.

Prime/boost strategies were performed with a heterologous boost of PS-TT or MDWNMHAA-TT. They led to high anti-LPS titers after only three injections, suggesting alternatives to improve the immunogenicity of the carbohydrate-mimetic peptide and confirming the antigenic mimicry.

4.3 INTRODUCTION

Shigellosis, caused by *Shigella* species (gram negative), is a prominent, and the most infectious, diarrheal disease. *Shigella flexneri* Y, the species responsible for the highest mortality rate, is endemic in most developing countries (23). The 13 serotypes of *S. flexneri*, with the exception of serotype 6, result from structural modifications of the O-antigen polysaccharide (PS), the outer portion of the lipopolysaccharide (LPS) on the bacterial surface, which is both an essential virulence factor and a protective antigen (10). The basic O-antigen PS repeat, common to the 12 serotypes, is referred to as serotype Y. A murine immunoglobulin G3 (IgG3) monoclonal antibody, SYA/J6, specific for the PS O antigen of the *S. flexneri* Y LPS, was developed by Bundle (7) and Carlin

and coworkers (8). The O-antigen Y PS is a linear heteropolymer with a tetrasaccharide repeating unit [→2)-α-L-Rha*p*-(1→2)-α-L-Rha*p*-(1→3)-α-L-Rha*p*-(1→3)-β-D-Glc*pN*Ac-(1→] and is recognized by the monoclonal antibody SYA/J6 (7, 9). The oligosaccharides of *S. flexneri* serotype Y have been well studied by nuclear magnetic resonance techniques, which have provided a three-dimensional model of the determinant in solution (4, 30, 31, 32) and the identity of the biological repeating unit (9).

Glycoconjugate vaccines to prevent shigellosis, focused on oligosaccharide analogues related to *Shigella flexneri* 2a and other serotypes, have been synthesized and evaluated (3, 10, 29, 38). An interesting approach to vaccine design is the use of molecules that mimic the immunogenic element of interest (11, 20, 28). Carbohydrate-mimetic peptides have potential as surrogate ligands for traditional carbohydrate vaccines, providing more discriminating immune responses (19, 20, 28). However, there are few examples of immunological responses with peptide-based PS mimics (18, 20, 28). Therefore, the requirements for cross-reactivity are not fully understood and are certainly not predictable, because of the limited data set available.

In order to further exploit this principle, a carbohydratemimetic peptide of the *S. flexneri* Y O-antigen PS, MDWNMHAA, cross-reactive with the anti-*S. flexneri* Y O-PS monoclonal antibody, SYA/J6, was identified by phage library screening (15). The structures of complexes of the antibody SYA/J6 Fab fragment with synthetic deoxytrisaccharide and pentasaccharide ligands, related to the *S. flexneri* Y O antigen, and with the carbohydrate-mimetic peptide have

been determined by X-ray crystallography (17, 33, 34, 35). The structure of the Fab complex with MDWNMHAA revealed differences, and few similarities, with respect to the oligosaccharide complexes (34), providing the first evidence that the modes of binding of the pentasaccharide and octapeptide differ considerably and that few aspects of structural mimicry exist (34).

Furthermore, for a peptide to be immunogenic, it might be necessary that a sufficient population of a bound conformation be displayed in the conformational ensemble of the free peptide (20). Since the α-helix adopted by NMHAA in the C terminus of MDWNMHAA is present only in the bound conformation and not in the free peptide, we questioned whether immunization with an MDWNMHAA conjugate would lead directly to a cross-reactive response against the corresponding PS. We questioned further whether prime/boost strategies would strengthen the immune responses already induced by the PS epitopes, as shown recently with a peptide mimic of the capsular PS of *Cryptococcus neoformans* (2). Therefore, it was of interest to test the immunogenicities and cross-reactivities of antibodies elicited by immunizations with MDWNMHAA conjugates to probe the hypothesis that predisposition of the α-helix motif in the free-peptide conformational ensemble might be necessary for immunological peptide-carbohydrate cross-reactivity.

The synthesis of MDWNMHAA-based conjugates to bovine serum albumin (BSA) and to tetanus toxoid (TT) and of the *S. flexneri* O-PS glycoconjugate (PS-TT), together with their immunochemical evaluation with SYA/J6, was reported recently (16). It is noteworthy that a search of the human

genome revealed that the sequence MDWNMHAA is not present (NCBI protein database). We now report the investigation of the immunogenicities of these conjugates in mice, together with the cross-reactivity of the immune sera with PS. The results are compared to those from our previous study of peptide-carbohydrate cross-reactivity with a peptide mimic of the cell-wall PS of Group A *Streptococcus* (6). Evidence is presented that cross-reactive immunological responses can be elicited even with functional rather than structural peptide mimics, where the former refers to binding of the two ligands using different functional groups on the antibody and the latter to the engagement of the two ligands using the same functional groups (19).

4.4 MATERIALS AND METHODS

4.4.1 PS antigens, monoclonal antibody SYA/J6, and synthesis of peptide MDWNMHAA, MDWNMHAA-TT and MDWNMHAA-BSA conjugates, and O-PS-TT conjugate

The *S. flexneri* Y LPS, used as a solid-phase antigen for enzyme-linked immunosorbent assay (ELISA), and the *S. flexneri* Y O PS (Figure 4-1, compound **1**), used to generate the TT conjugate and as an inhibitor, were generous gifts from D. R. Bundle, prepared and purified as previously described (1). The monoclonal antibody SYA/J6 was also generated, characterized, purified, and provided by D. R. Bundle (7, 8) and was used as an ELISA control.

The PS-mimetic peptide MDWNMHAA (Figure 4-1, compound **2**) was synthesized using the 9-fluorenylmethoxy carbonyl solid-phase strategy and linked via the amino terminus to a bifunctional linker, diethylsquarate, and then conjugated to TT or BSA as an immunogenic carrier, as described previously (16) (Figure 4-1, compounds **3** and **4**). The levels of incorporation of the peptide on TT were 53% for the batch of conjugate used in the first study, $(MDWNMHAA)_{32}$-TT, and 83% for the batch used in the second study, $(MDWNMHAA)_{50}$-TT, while that on BSA was 100% (Figure 4-1). The peptide MDWNMHAA and its conjugates bound to the antibody SYA/J6, as evaluated by ELISA (16).

The *S. flexneri* Y O-PS glycoconjugate (PS-TT) (Figure 4-1, compound **5**), which comprises 10 repeating units (tetrasaccharide), was prepared based on a reductive amination of the PS at the reducing end with 1,3-diaminopropane, followed by linking the aminated PS to diethylsquarate to form an adduct that was subsequently conjugated to TT (16) and used as an immunogen in this study.

4.4.2 Experimental groups of mice and immunization protocols

Female BALB/c mice (6 to 8 weeks old) were obtained from the Charles River Breeding Laboratories (Montreal, Quebec, Canada) and were maintained in our Animal Care Facility following the animal care guidelines. Groups of five mice each were injected subcutaneously with the conjugates, Alhydrogel (2%; Superfos Brenntag Biosector, Frederikssund, Denmark), or controls. The mice

were bled every 2 weeks for 8 weeks, their sera were analyzed, and mean reciprocal endpoint titers and standard deviations were determined.

4.4.2.1 Study 1

Control groups received 0.5 µg of PS-TT (group 4 [G4]) and 100 _g of Alhydrogel or 100 µg of TT (G5) plus 100 µg Alhydrogel, in weeks 0, 2, 4, and 6. Mice from G1 received 100 µg Alhydrogel and 100 µg of $(MDWNMHAA)_{32}$-TT in weeks 0, 2, 4, and 6 (homologous prime/boost strategy).

In G2 and G3, a heterologous-homologous prime/boost strategy was implemented. G2 mice were primed with 100 µg $(MDWNMHAA)_{32}$-TT and boosted with 0.5 µg PS-TT in week 2 and received a final boost with 100 _g of $(MDWNMHAA)_{32}$-TT in week 6. G3 mice were primed with 0.5 µg PS-TT and boosted with 100 µg $(MDWNMHAA)_{32}$-TT in week 2 and were given a final boost with 0.5 µg of PS-TT in week 6. Mice from both groups received 100 µg Alhydrogel per immunization.

4.4.2.2 Study 2

Control groups received 2 µg of PS-TT (G5) and 100 µg of Alhydrogel or 100 µg of TT (G6) plus 100 µg Alhydrogel in weeks 0, 2, 4, and 6. Mice from G1 received 100 µg Alhydrogel and 100 µg of $(MDWNMHAA)_{50}$-TT, in weeks 0, 2, 4, and 6 (homologous prime/boost strategy). Mice from G2 received 100 µg of $(MDWNMHAA)_{50}$-TT and 100 µg Alhydrogel in weeks 0, 2, and 6 (homologous prime/boost strategy).

In G3 and G4, an extended heterologous prime/boost strategy was implemented. G3 mice were primed with 100 µg $(MDWNMHAA)_{50}$-TT and boosted with 0.5 µg PS-TT in weeks 2 and 6. G4 mice were primed with 0.5 µg PS-TT and boosted with 100 µg $(MDWNMHAA)_{50}$-TT in weeks 2 and 6. Mice from both groups received 100 µg Alhydrogel per immunization.

4.4.3 ELISA

Antibody titers to MDWNMHAA and LPS in sera from mice were determined before vaccination and 2 weeks after each vaccination by ELISA as described previously (39). The titer was defined as the highest dilution yielding an absorbance of ≥0.1 after twice the average background reading was subtracted. The negative control consisted of wells without serum. The positive control was the mouse SYA/J6, appropriately diluted.

4.4.3.1 Competitive ELISA with LPS, PS, MDWNMHAA, and MDWNMHAA-BSA as inhibitors

Sera from those mice that had the highest anti-MDWNMHAA antibody titers cross-reactive to LPS in week 8 (mice 1 from G1, G2, and G3 from study 1 or mouse 3 from G1, 4 from G2, 3 from G3, and 2 from G4 from study 2) were used. The sera were incubated in duplicate at a final dilution of 1:200 with two fold serial dilutions of inhibitors: *S. flexneri* Y PS and MDWNMHAA (Figure 4-1, compounds **1** and **2**), MDWNMHAA-BSA (Figure 4-1, compound **3**), and LPS in phosphate-buffered saline–Tween 20, starting at an initial concentration of 200 µg/ml, for 1 h at room temperature. Then, 100 µl (each) of the mixtures was

transferred to plates coated with antigens and incubated at room temperature for 3 h. The plates were washed, and the bound IgG was detected by ELISA.

4.4.3.2 Statistical Analysis

Within groups, comparisons of titers at different times were analyzed with the Wilcoxon matched-pairs test (36). Between groups, comparisons were analyzed with the Mann-Whitney *U* test (26). The *P* values were corrected for multiple comparisons (5). A *P* value of <0.05 was considered to indicate a significant difference.

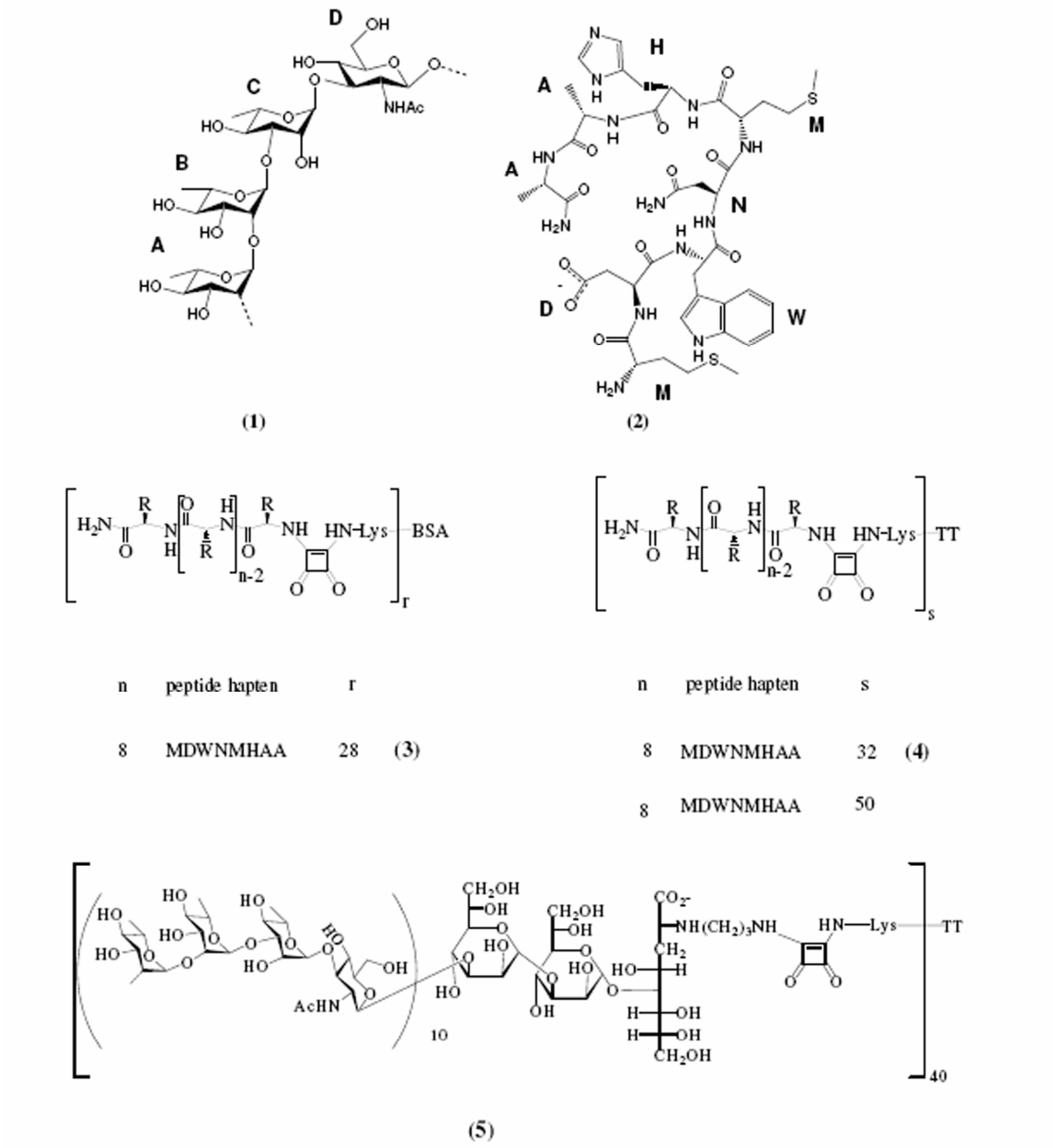

Figure 4-1: Structures of compounds. Shown are the structures of the O PS of *S. flexneri* Y (compound **1**, with monosaccharide residues of the repeating unit labeled A, B, C, and D) and its peptide mimic, the octapeptide MDWNMHAA (compound **2**, with single-letter amino acid code), as well as the synthetic peptide

conjugates MDWNMHAA-BSA (compound **3**) and MDWNMHAA-TT (compound **4**) and the *S. flexneri* Y O-PS conjugate (compound **5**).

4.5 RESULTS

The individual mouse antisera (study 1, five mice per group and five groups of mice, G1 to G5; study 2, five mice per group and six groups of mice, G1 to G6) were evaluated for the relative amounts of IgG antibody they contained that bound to MDWNMHAA-BSA (immunogenicity) and to LPS (cross-reactivity). Preimmune sera screened by ELISA, using MDWNMHAA-BSA or LPS as a solid-phase antigen, showed low background activity (Figure 4-2 and 3, studies 1 and 2, week 0). The immunization schedules are described in Tables 4-1 and 4-2.

Table 4-1: Immunization schedule for study 1

Immunization strategy	Mice Group (*n=5*)	Prime (wk 0) (μg/mouse)	First boost (wk 2) (μg/mouse)	Second boost (wk 4) (μg/mouse)	Second or third boost (wk 6) (μg/mouse)
Homologous	G1	MDWNMHAA-TT (100)	MDWNMHAA-TT (100)	MDWNMHAA-TT (100)	MDWNMHAA-TT (100)
Heterologous /homologous	G2	MDWNMHAA-TT (100)	PS-TT (0.5)	-	MDWNMHAA-TT (100)
Heterologous /homologous	G3	PS-TT (0.5)	MDWNMHAA-TT (100)	-	PS-TT (0.5)
Homologous	G4	PS-TT (0.5)	PS-TT (0.5)	PS-TT (0.5)	PS-TT (0.5)
Homologous	G5	TT (100)	TT (100)	TT (100)	TT (100)

Table 4-2: Immunization schedule for study 2

Immunization strategy	Mice Group (*n=5*)	Prime (wk) 0 (μg/mouse)	First boost (wk 2) (μg/mouse)	Second boost (wk 4) (μg/mouse)	Second or third boost (wk 6) (μg/mouse)
Homologous	G1	MDWNMHAA-TT (100)	MDWNMHAA-TT (100)	MDWNMHAA-TT (100)	MDWNMHAA-TT (100)

Homologous	G2	MDWNMHAA-TT (100)	MDWNMHAA-TT (100)	-	MDWNMHAA-TT (100)
Extended Heterologous	G3	MDWNMHAA-TT (100)	PS-TT (0.5)	-	PS-TT (0.5)
Extended Heterologous	G4	PS-TT (0.5)	MDWNMHAA-TT (100)	-	MDWNMHAA-TT (100)
Homologous	G5	PS-TT (2)	PS-TT (2)	PS-TT (2)	PS-TT (2)
Homologous	G6	TT (100)	TT (100)	TT (100)	TT (100)

4.5.1 Immunogenicity of the peptide conjugates

4.5.1.1 Antibody titers to MDWNMHAA after homologous prime/boost strategy (Studies 1 and 2)

Mice primed with 100 µg of the $(MDWNMHAA)_{32}$-TT conjugate responded with IgG antibody titers against MDWNMHAA-BSA (P = 0.03; week 2) (Figure 4-2, study 1, G1, week 2). Increases were seen after repeated boosting of mice from G1 (Figure 4-2) in weeks 2, 4, and 6 (P = 0.05; week 8). Control groups (G4 and G5) showed much lower mean endpoint titers to peptide at all time points, although titers against peptide were observed after boosting with PS-TT (G4) in weeks 6 and 8 (P = 0.03) and were higher than G5 (P = 0.04; week 6) (Figure 4-2, study 1). Similar results were observed after the $(MDWNMHAA)_{50}$-TT conjugate was injected into the mice, although higher anti-peptide titers appeared in week 2 in study 2 (P = 0.03), and increases were observed after each of the booster injections (P = 0.03; weeks 2, 6, and 8) (Figure 4-2, study 2,

G1 and G2). The titers observed in mice from G1 were not significantly different from those from G2 in week 8 (corrected P = 1.0) for study 2. These results indicate that the conjugates effectively promoted a strong and rapid thymusdependent response to MDWNMHAA and showed a stronger response to $(MDWNMHAA)_{50}$-TT.

4.5.2 Immunogenicity of the peptide conjugate

4.5.2.1 Antibody titers to MDWNMHAA after heterologous-homologous prime/boost strategies (Study 1)

In order to improve the immune response to the weakly immunogenic peptide MDWNMHAA, we altered the immunization schedule with a PS-TT or $(MDWNMHAA)_{32}$-TT booster combined with the corresponding heterologous primer (Table 4-1). Thus, mice primed with 100 µg of the $(MDWNMHAA)_{32}$-TT conjugate (G2, study 1) responded with IgG antibody titers against MDWNMHAA-BSA (P = 0.03; week 2) (Figure 4-2, study 1, G2, week 2). Increases in titers were seen after boosting of mice from G2 with 0.5 µg/mouse of PS-TT in week 2 (P = 0.03; week 4) (Figure 4-2, study 1, G2, weeks 4 and 6). Titers were observed after a homologous last boost of G2 mice with 100 µg/ml $(MDWNMHAA)_{32}$-TT in week 6 but were not significantly higher than those from week 6 (P = 0.14) (Figure 4-2, study 1, G2, week 8). Titers observed for G2 mice were not significantly different from those from G1 (corrected P = 1.0) in week 8.

Mice primed with 0.5 µg of the PS-TT conjugate (G3, study 1) responded with IgG antibody titers against MDWNMHAA-BSA (P = 0.03; week 2) (Figure 4-

2, study 1, G3, week 2). Increases in titers were seen after boosting of mice from G3 with 100 µg/mouse of MDWNMHAA-TT in week 2 (P = 0.03; weeks 4 and 6) (Figure 4-2, study 1, G3, weeks 4 and 6). Titers were observed after a homologous last boost of G3 mice with 0.5 µg/ml PS-TT in week 6 but were not significantly higher than those from week 6 (P = 0.30) (Figure 4-2, study 1, G3, week 8). Titers observed in mice from G3 were not different from those from G1 (corrected P = 0.25) and G2 (corrected P = 0.1) mice in week 8.

4.5.2.2 Antibody titers to MDWNMHAA after extended heterologous prime/boost strategies (Study 2)

In study 2, extended heterologous prime/boost strategies were implemented (Table 4-2). Thus, mice primed with $(MDWNMHAA)_{50}$-TT conjugate (G3) responded with IgG antibody titers against MDWNMHAA-BSA (P = 0.03; week 2) (Figure 4-2, study 2, G3, week 2). Increases in titers were observed after boosting of mice twice with 0.5 µg PS-TT (P = 0.03; weeks 6 and 8) (Figure 4-2, study 2, weeks 6 and 8).

Mice primed with 0.5 µg of the PS-TT conjugate (G4) did not respond with titers against MDWNMHAA-BSA (P = 0.79; week 2) (Figure 4-2, study 2, G4, week 2). Increases in titers were seen after these mice were boosted twice with 100 µg/mouse $(MDWNMH\ AA)_{50}$-TT (P = 0.03; weeks 4, 6, and 8) (Figure 4-2, study 2, weeks 4, 6, and 8). Titers from G3 mice were significantly lower than those from G1 (corrected P = 0.04), G2 (corrected P = 0.04), and G4 (corrected P = 0.03) mice in week 8.

4.5.3 Cross-reactivity

4.5.3.1 Anti-peptide antibodies bind to *S. flexneri* Y LPS after homologous prime/boost strategy (studies 1 and 2)

In study 1, titers against *S. flexneri* Y LPS were obtained when high doses of the $(MDWNMHAA)_{32}$-TT were administered four times to mice, i.e., after four homologous prime/boost immunizations (P = 0.03) (Figure 4-3, study 1, G1, week 8). The subcutaneous immunization of mice with $(MDWNMHAA)_{32}$-TT (100 µg/ml) resulted in a late anti-LPS IgG response (Figure 4-3, week 8).

In study 2, IgG titers against *S. flexneri* Y LPS were observed after two injections of 100 µg/mouse of $(MDWNMHAA)_{50}$-TT (P = 0.03; week 4) (Figure 4-3, study 2, G1 and G2, week 4). These titers increased after the last boosting in week 6 (P = 0.03; week 8). No titer increases against TT, used as control, were seen in any of the studies (Figure 4-3, G5, study 1, and G6, study 6, weeks 2, 4, 6, and 8). The anti-LPS IgG titers appeared lower than those against peptide at the same time point in both studies (Figure 4-2 and 3, week 8 for study 1 and weeks 4, 6, and 8 for study 2).

4.5.4 Cross-reactivity

4.5.4.1 Polyclonal antibodies bind to *S. flexneri* Y LPS after heterologous-homologous prime/boost strategies (study 1)

In study 1, priming with a high dose of $(MDWNMHAA)_{32}$-TT and boosting with a low dose of PS-TT (Figure 4-3, study 1, G2, week 2) resulted in no IgG titer increases against LPS (Figure 4-3, G2, weeks 4 and 6). A high anti-LPS IgG

response resulted after homologous boosting with a high dose of $(MDWNMHAA)_{32}$-TT in week 6 (P = 0.03; week 8) (Figure 4-3, study 1, G2, week 8). These anti-LPS IgG titers were not different from those from G1 (corrected P = 0.1) and G3 (corrected P = 0.08) mice and appeared similar to those against peptide at the same time point (week 8).

Priming with a low dose of PS-TT and boosting with a high dose of $(MDWNMHAA)_{32}$-TT in study 1 (Figure 4-3, study 1, G3, week 2) did not increase the IgG anti-LPS titers. In contrast, an anti-LPS IgG response resulted after homologous boosting with a low dose of PS-TT in week 6 (P = 0.03; week 8) (Figure 4-3, study 1, G3, week 8). These anti-LPS IgG titers were not significantly different from those from G1 (corrected P = 1.0) and G2 (corrected P = 0.08) and appeared similar to those against peptide at the same time point (Figure 4-2 and 4-3, week 8).

4.5.4.2 Polyclonal antibodies bind to *S. flexneri* Y LPS after extended heterologous prime/boost strategies (study 2)

In study 2, priming with a high dose of $(MDWNMHAA)_{50}$-TT and boosting with a low dose of PS-TT (Figure 4-3, study 2, G3, week 2) resulted in IgG titer increases against LPS (P = 0.03; week 4) (Figure 4-3, G3, weeks 4 and 6). Small increases in anti-LPS titers were observed in week 8 (P = 0.05) after a second heterologous boost (in week 6) with a low dose of PS-TT (Figure 4-3, study 2, G3, week 8). G3 anti-LPS titers were not significantly different from those from G1 (corrected P = 0.4), G2 (corrected P = 0.7), and G4 (corrected P = 0.35) in week 8.

In contrast, priming with a low dose of PS-TT and boosting twice with a high dose of $(MDWNMHAA)_{50}$-TT (G4 in study 2) resulted in IgG anti-LPS titers (P = 0.03; weeks 6 and 8) (Figure 4-3, study 2, G4, weeks 6 and 8). These IgG anti-LPS titers were not significantly different from those obtained after repeated homologous prime/boost immunizations, G1 (corrected P = 0.4) and G2 (corrected P = 1.0), in this study.

4.5.4.3 Anti-PS (PS-TT) antibodies bind to MDWNMHAA-BSA (studies 1 and 2)

Mice immunized subcutaneously with 0.5 µg/mouse of PS-TT in weeks 0, 2, 4, and 6 responded with titers against MDWNMHAA-BSA in study 1 (P = 0.03; weeks 2, 6, and 8) (Figure 4-2, study 1, G4, weeks 6 and 8). The titers increased after repeated boosting. The titers were higher than those corresponding to mice immunized with 100 µg TT in week 6 (P = 0.04), but not in week 8 (P = 0.12) (Figure 4-2, study 1, G5). Similarly, in study 2, mice immunized with 2 µg/mouse of PS-TT in weeks 0, 2, 4, and 6 responded with titers against MDWNMHAA-BSA (P = 0.03, weeks 6 and 8) (Figure 4-2, study 2, G5, week 8); these titers appeared higher than those obtained in study 1 but were not significantly different from those corresponding to a high dose of TT (100 µg/mouse) (Figure 4-2, study 2, G6, week 8) (corrected P = 0.45; week 8). However, these titers were correlated with anti-LPS titers that were greater than those from G6 (TT) in week 8 (corrected P = 0.03) (Figure 4-3, study 2, G5 and G6, week 8).

4.5.5 Specificity of the polyclonal antibodies

4.5.5.1 Study 1

In order to investigate the epitope specificities of the polyclonal antibodies, competitive-inhibition ELISAs were performed. The antisera with the highest endpoint titers, obtained at week 8 for one mouse from each group, G1, G2, and G3, immunized three or four times (Table 4-1), were used in these experiments. Titration of the antisera was performed for each experiment, and the dilution used corresponded to an A_{405} of ~0.5 after 30 min (see Figure 4-S1A in the supplemental material). *S. flexneri* Y LPS was used as the solid-phase antigen.

Competitive-inhibition ELISA with *S. flexneri* Y LPS, PS (Figure 4-1, compound **1**), free MDWNMHAA (Figure 4-1, compound **2**), and MDWNMHAA-BSA (Figure 4-1, compound **3**) as inhibitors was performed with *S. flexneri* Y LPS as the solid-phase antigen. All of the inhibitors inhibited the binding of the anti-MDWNMHAA polyclonal antibodies from mouse no. 1 serum from G1 (IgG) (see Figure 4-S1B in the supplemental material), with the greatest inhibitory activity at about 30% at a concentration of 100 µg/ml for LPS, PS, and MDWNMHAA-BSA. A lower inhibition value (20%) was obtained with the free peptide under the same conditions. These data confirm the binding of the anti-peptide polyclonal antibodies with LPS and PS.

The best inhibitors of the binding of polyclonal antibodies from mouse no. 1 from G2 (IgG) (see Figure 4-S1C in the supplemental material) were LPS and MDWNMHAA-BSA, with the greatest inhibitory activity at 25 to 33% at a concentration of 100 µg/ml. A lower inhibition value was obtained with the PS and the free peptide under the same conditions (7% and 4%, respectively).

The best inhibitors of the binding of polyclonal antibodies from mouse no. 1 from G3 (IgG) (see Figure 4-S1D in the supplemental material) were LPS, PS, and MDWNMHAA-BSA, with the greatest inhibitory activity at 20 to 30% at a concentration of 100 µg/ml. A lower inhibition value was obtained with the free peptide under the same conditions (10%).

4.5.5.2 Study 2

The antisera with highest endpoint titers, obtained at week 8 for one mouse from each group, G1, G2, G3, and G4, immunized three or four times (Table 4-2), were used in these experiments. Titration of antisera was performed for each experiment, and the dilution used corresponded to an A_{405} of ~0.6 after 30 min (see Figure 4-S2A in the supplemental material). *S. flexneri* Y LPS was used as the solid-phase antigen.

All the inhibitors inhibited the binding of the anti-MDWNMHAA polyclonal antibodies from mouse no. 3 serum from G1 (IgG) (see Figure 4-S2B-G1 in the supplemental material), with the greatest inhibitory activity at about 50% at a concentration of 100 µg/ml for MDWNMHAA-BSA. A lower inhibition value (40%) was obtained with the LPS and the free peptide under the same conditions. The isolated PS was the poorest inhibitor (10%) at 100 µg/ml. These data confirm the binding of the anti-peptide polyclonal antibodies with LPS and PS.

The best inhibitors of the binding of polyclonal antibodies from mouse no. 4 from G2 (IgG) (see Figure 4-S2B-G2 in the supplemental material) were LPS and MDWNMHAA-BSA, with the greatest inhibitory activity at 35 to 40% at a concentration of 100 µg/ml. A lower inhibition value (10%) was obtained with PS.

No inhibition of the binding of polyclonal antibodies to LPS with the free peptide was observed under the same conditions.

The best inhibitors of the binding of polyclonal antibodies from mouse no. 3 from G3 (IgG, see Figure 4-S2B-G3 in the supplemental material) were LPS, PS, and MDWNMHAA-BSA, with the greatest inhibitory activity at 20 to 25% at a concentration of 100 µg/ml. A lower inhibition value (7%) was obtained with the free peptide under the same conditions.

The best inhibitors of the binding of polyclonal antibodies from mouse no. 2 from G4 (IgG) (see Figure 4-S2B-G4 in the supplemental material) were LPS, PS, and MDWNMHAABSA, with the greatest inhibitory activity at 30 to 70% at a concentration of 100 µg/ml. A lower inhibition value (22%) was obtained with the free peptide under the same conditions.

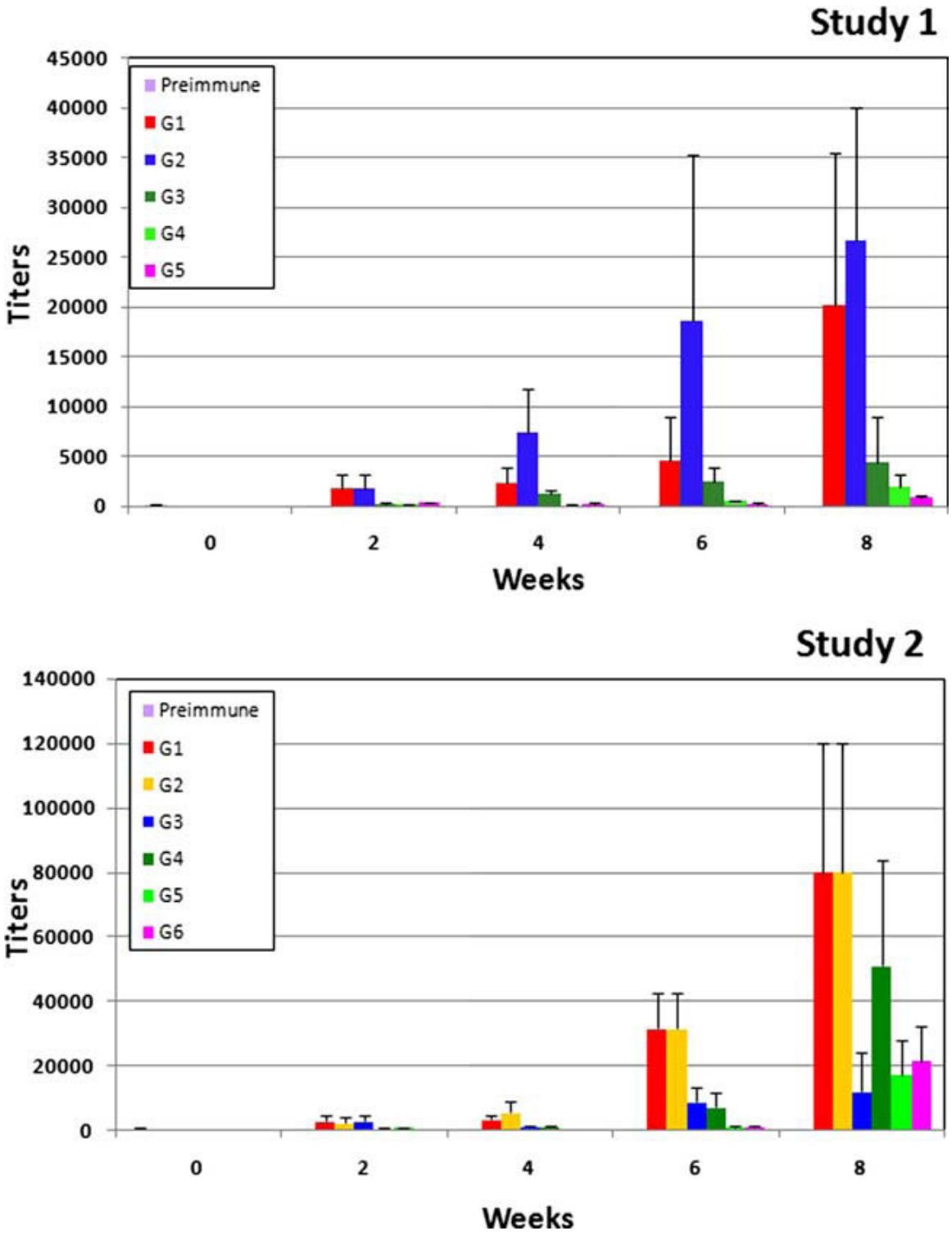

Figure 4-2: Immunogenicities of the peptide conjugates: antibody titers (IgG) to MDWNMHAA. Plates were coated with MDWNMHAA-BSA (compound 3 in

Figure 4-1) (10 μg/ml). Study 1 (Table 4-1 shows a detailed immunization schedule): G1, homologous prime/boost with $(MDWNMHAA\text{-}TT)_{32}$ (four times); G2, heterologous-homologous prime/boost (Table 4-1); G3, heterologous-homologous prime/boost (Table 4-1); G4, homologous prime/boost with PS-TT (four times); G5, TT (four times). Study 2 (Table 4-2 shows a detailed immunization schedule: G1, homologous prime/boost with $(MDWNMHAA)_{50}$-TT (four times); G2, homologous prime/boost with $(MDWNMHAA)_{50}$-TT (three times); G3, extended heterologous prime/boost (Table 4-2); G4, extended heterologous prime/boost (Table 4-2); G5, homologous prime/boost with PS-TT (four times); G6, TT (four times). The error bars represent standard deviations.

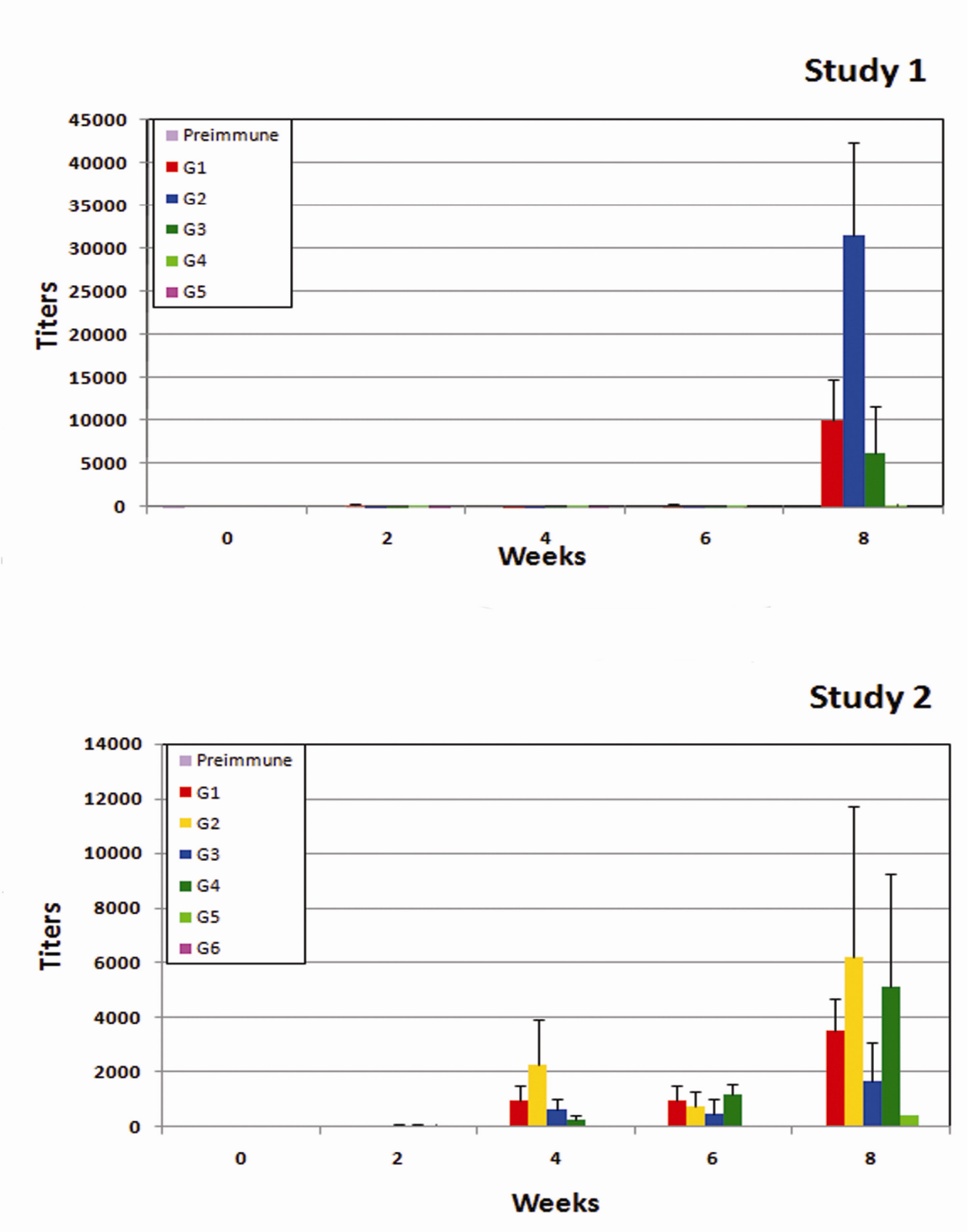

Figure 4-3: Cross-reactivity: polyclonal antibodies (IgG) binding to LPS as the solid phase-antigen in ELISA (10 µg/ml). Study 1 (Table 4-1 shows a detailed immunization schedule): G1, homologous prime/boost with $(MDWNMHAA\text{-}TT)_{32}$

(four times); G2, heterologous-homologous prime/boost (Table 4-1); G3, heterologous-homologous prime/boost (Table 4-1); G4, homologous prime/boost with PS-TT (four times); G5, TT (four times). Study 2 (Table 4-2 shows a detailed immunization schedule): G1, homologous prime/boost with $(MDWNMHAA)_{50}$-TT (four times); G2, homologous prime/boost with $(MDWNMHAA)_{50}$-TT (three times); G3, extended heterologous prime/boost (Table 4-2); G4, extended heterologous prime/boost (Table 4-2); G5, homologous prime/boost with PS-TT (four times); G6, TT (four times). The error bars represent standard deviations.

4.6 DISCUSSION

This study illustrates the concept of peptide-carbohydrate mimicry with an *S. flexneri* Y O-PS-mimetic peptide using an immunological approach. Thus, an MDWNMHAA-TT conjugate used in immunizations of BALB/c mice elicited antibodies directed against the O-PS of the *S. flexneri* Y LPS. Conversely, antisera elicited by immunizations of mice with an *S. flexneri* Y O-PS-TT conjugate cross-reacted with MDWNMHAA-BSA, as probed by ELISA at different time points.

The immunogenicity of MDWNMHAA-TT was manifested in primary and secondary antibody responses (immunological memory), with MDWNMHAA titers that increased after the three booster immunizations given to mice in both of the studies (Figure 4-3, G1). However, these titers were much lower than those

observed in a similar immunological study (6) with a PS-mimetic peptide, DRPVPY, of the *Streptococcus* Group A cell wall PS (15). Interestingly, DRPVPY adopts secondary (turn) structures in the VPY region in both the free and antibody-bound forms (22), in contrast to MDWNMHAA, which lacks defined structure in the free peptide (21). The display of peptide secondary structures (turn conformations) was also observed with another immunogenic *Streptococcus* Group B carbohydrate-mimetic peptide (18). This led us to postulate that defined turn structures in carbohydrate-mimetic peptides are immunodominant elements (epitopes) and thus associated with immunogenicity (20), a hypothesis that has been reinforced in this study. Similar results were also observed by Dyson et al. (13) and Craig et al. (12) for peptides derived from proteins.

The results also demonstrate that the peptide MDWNMHAA can act as an antigenic mimic when attached to a carrier protein and can induce anti-carbohydrate antibodies. However, in study 1, high titers against the O-PS region of the *S. flexneri* Y LPS were evident only after an 8-week period in which a high dose of the peptide conjugate had been administered to mice four times (G1). This result indicates that the kinetics of the immune response are slow and that several homologous immunizations are required for memory to develop and to raise high antibody titers. This time point (week 8) also corresponds to the highest anti-peptide titer obtained, perhaps a prerequisite for the presence of cross-reactive antibodies, as observed earlier (6). These anti-LPS titers, despite the fact that they were 0.5-fold lower than those against the peptide, were

specific to carbohydrates and of similar or higher magnitude than those reported previously (2, 6, 14, 25). Antigenic cross-reactivities between the peptide and the O-PS were demonstrated by the LPS- and PS-specific inhibition of the anti-peptide polyclonal antibodies binding to LPS with serum obtained after the fourth immunization (G1). The fact that MDWNMHAA and PS were poorer inhibitors than MDWNMHAA-BSA and LPS, respectively, is likely due to the presentation of multiple copies of the critical epitopes.

However, when a conjugate containing 30% more copies of peptide per TT was administered at the same doses to mice (G1 and G2, study 2), IgG-anti-LPS titers were observed 2 weeks earlier than in study 1, corresponding to high antipeptide titers. This result suggests that $(MDWNMHAA)_{50}$-TT is a more immunogenic conjugate than $(MDWNMHAA)_{32}$-TT. However, anti-LPS titers obtained with $(MDWNMHAA)_{50}$- TT appeared lower than with $(MDWNMHAA)_{32}$-TT in week 8, despite the higher anti-peptide titers (G1, week 8). This may be the result of a carrier-induced suppression effect, which can decrease the production of antigen-specific antibodies, as observed earlier in a similar immunological study with a strongly immunogenic PS-mimetic peptide conjugate [$(DRPVPY)_{39}$-TT] (6). No clear difference in the LPS-cross-reactive antibody response was observed when $(MDWNMHAA)_{50}$-TT was administered to mice three times (G2) instead of four (G1), suggesting that when a more immunogenic mimetic peptide conjugate is used, fewer injections are required. These anti-LPS titers were also specific to carbohydrate (G1 and G2).

The combined results led us to conclude that (i) MDWNMHAA is an antigenic mimic of the O-PS of *S. flexneri* Y, since high titers of cross-reactive antibodies were obtained after immunizations of mice with MDWNMHAA-TT; (ii) MDWNMHAA is a poorly immunogenic peptide, suggesting the importance of predisposed secondary structures for immunogenicity; and (iii) the anti-peptide antibodies were specific for the PS of *S. flexneri* Y, since this compound inhibits the binding of antibodies to LPS. Nevertheless, the results reported here indicate that the lack of predisposition of the α-helix turn in the free-peptide conformational ensemble does not preempt a cross-reactive immune response. In addition, functional mimicry, as opposed to structural mimicry, of the PS by the peptide is also clearly sufficient to elicit a cross-reactive immune response.

The facts outlined above led us to implement a heterologous prime/boost immunization strategy in order to improve the immune response to the MDWNMHAA peptide. These strategies have recently shown promising results, enhancing both cellular and humoral immune responses against a variety of viral and bacterial pathogens (27, 37). Accordingly, we altered the immunization schedule (Table 4-1) with a heterologous boost in week 2. The following strategies were attempted in study 1: (i) priming with $(MDWNMHAA)_{32}$-TT and boosting with PS-TT (G2) and (ii) priming with PS-TT and boosting with $(MDWNMHAA)_{32}$-TT (G3).

Increases in the anti-MDWNMHAA titers were seen after the heterologous booster in mice and were stronger after boosting with PS-TT (study 1, G2, weeks 4 and 6), indicating immunological memory and antigenic mimicry between the

immunogens. In contrast, boosting with $(MDWNMHAA)_{32}$-TT (study 1, G3, weeks 4 and 6) led to a response that more closely resembled the primary response observed for G1 in week 2 after priming with peptide conjugate. Comparison of the results of priming with $(MDWNMHAA)_{32}$-TT and PS-TT suggests that activation of naı̈ve B cells, and possibly T helper cells, is enhanced when $(MDWNMHAA)_{32}$-TT is given as a primer vaccine. On the other hand, PS-TT appears to be a more effective booster vaccine. This may be due to a different mechanism of processing and presentation of the antigens, considering the different chemical natures of the immunogens, and also due to the antigen availability, since very different doses of immunogens were required. In any event, no cross-reactive anti-LPS (IgG) titers were observed in week 4 or 6 in spite of a small increase in the anti-LPS IgM response in week 4 (not shown).

Remarkably, a last homologous boost (Table 4-1) resulted in few or no significant increases in titers against MDWNMHAA but very high anti-LPS (IgG) titers (study 1, G2 and G3, week 8), evidence of a booster effect leading to a fast, strong response with high IgG titers and clearly confirming the presence of memory B cells and plasma cells that had been effectively restimulated. These anti-LPS antibodies were also specific to carbohydrate. The inhibition results also indicate the effect of multivalent presentation and differences in the polyclonal specificities, and perhaps avidities, among G1, G2, and G3 polyclonal antibodies, as expected, since they were developed after different immunization strategies.

The implementation of extended heterologous prime/boost strategies, with an additional heterologous boost to focus the response, was performed in study 2. This strategy had been successfully applied in the case of a *Neisseria meningitidis* outer membrane vesicle vaccine (24). The following immunization schedules were attempted in study 2: (i) priming with $(MDWNMHAA)_{50}$-TT and boosting twice with PS-TT (G3) and (ii) priming with PS-TT and boosting twice with $(MDWNMHAA)_{50}$-TT (G4).

An increase in the anti-MDWNMHAA titers was seen after the first heterologous booster was given to the mice (study 2, G3 and G4, weeks 4 and 6) with similar titers, indicating immunological memory and antigenic mimicry between the immunogens. Cross-reactive anti-LPS (IgG) titers were observed. Increases in titers against MDWNMHAA after a last heterologous boost (Table 4-2, G3 and G4, week 8) confirmed the presence of memory B cells and plasma cells that had been effectively restimulated. These antibodies bound specifically to LPS. The effect of multivalent presentation and the differences in the polyclonal specificities among G3 and G4 polyclonal antibodies were evident, as expected, since they were developed after different immunization strategies. In G3, the anti-PS response seemed to dominate, while in G4, the anti-peptide response appeared to be the dominant response (G3 and G4).

The existence of immunological carbohydrate-peptide mimicry was further demonstrated by the increase in IgG titers to MDWNMHAA elicited by repeated immunization with PS-TT (G4, study 1, and G5, study 2, weeks 6 and 8), evidence of the booster effect. However, only IgM anti-LPS titers were observed

when a low dose of PS-TT was given four times (not shown); presumably, IgG titers would have risen at a later time. When the dose of PS-TT was 2 _g/mouse (study 2, G5, week 8), IgG anti-LPS titers were observed in week 8.

In conclusion, a peptide mimic of *S. flexneri* Y O-PS, when used as an immunogen, elicited good titers of mature antibody of isotype IgG, with immunological memory. The antibodies generated were cross-reactive with the O-PS, as evaluated by an LPS ELISA binding study, and this interaction was inhibited by LPS and PS, leading us to conclude that the peptide MDWNMHAA is an antigenic mimic of the *S. flexneri* Y O-PS. However, several immunizations were necessary in order to achieve a cross-reactive response, an indication of the low immunogenicity of the peptide. Taken together, previous results (6, 18) and those reported here suggest that predisposition of antibody-bound epitopes in the free-peptide conformational ensemble leads to a more rapid cross-reactive anti-PS response. Nonetheless, a cross-reactive response does develop when these epitopes are not present, suggesting that amplification of the B-cell clones requires longer immunization with multiple boosts. In addition, functional, as opposed to structural, mimicry of the PS by the peptide does not appear to compromise the ability of the peptide to elicit a cross-reactive response. Conversely, immunizations with PS-TT resulted in a cross-reactive response against MDWNMHAA, also confirming the antigenic mimicry. Our goal was to test whether prime/boost strategies would have any competitive advantage here. Extended heterologous and heterologous-homologous prime/boost strategies provided some advantage, since they led to high anti-peptide titers and high

cross-reactive responses after only three injections, suggesting that these schedules might provide an effective approach to increase the immunogenicity of a carbohydrate-mimetic peptide. The present work is significant because it clearly demonstrates such cross-reactivity in an immunological sense and sets the stage for the next phase of the study aimed at probing the protective response, and thus for vaccine development. The data presented address our initial questions and, in combination with other information on peptide-carbohydrate mimicry in the literature, lend credence to the use of carbohydrate-mimetic peptides as vaccine candidates for *Shigella flexneri* Y, as well as for other pathogens.

4.7 ACKNOWLEDGEMENTS

We are grateful to the Natural Sciences and Engineering Research Council of Canada for financial support.

We are grateful to D. R. Bundle for providing the *S. flexneri* Y LPS, the O-PS, and the SYA/J6 monoclonal antibody. We thank F. Michon for providing the TT.

4.8 REFERENCES

1. **Altman, E., and D. R. Bundle.** 1994. Polysaccharide affinity columns for purification of lipopolysaccharide-specific murine monoclonal antibodies. Methods Enzym. **247:**243-253.
2. **Beenhouwer, D. O., R. J. May, P. Valadon, and M. D. Scharff.** 2002. High affinity mimotope of the polysaccharide capsule of Cryptococcus neoformans identified from an evolutionary phage peptide library. J. Immunol. **169:**6992-6999.
3. **Belot, F., C. Guerreiro, F. Baleux, and L. A. Mulard.** 2005. Synthesis of two linear PADRE conjugates bearing a deca- or pentadecasaccharide B epitope as potential synthetic vaccines against *Shigella flexneri* serotype 2a infection. Chem.-Eur. J. **11:**1625-1635.
4. **Bock, K., S. Josephson, and D. R. Bundle.** 1982. Lipopolysaccharide Solution Conformation - Antigen Shape Inferred from High-Resolution H-1 and C-13 Nuclear Magnetic-Resonance Spectroscopy and Hard-Sphere Calculations. J. Chem. Soc. Perkin Trans. 2**:**59-70.
5. **Bonferroni, C. E.** 1935. Il calcolo delle assicurazioni su gruppi di teste, p. 13-60. *In* Studi in onore del professore Salvatore Ortu Carboni. Casa
6. **Borrelli, S., R. B. Hossany, S. Findlay, and B. M. Pinto.** 2006. Immunological evidence for peptide-carbohydrate mimicry with a Group A *Streptococcus* polysaccharide-mimetic peptide. Am. J. Immunol. **2:**73-83.

7. **Bundle, D. R.** 1989. Antibody combing sites and oligosaccharide determinants studied by competitive binding, sequencing and X-ray crytallography. Pure Appl. Chem. **61:**1171-1180.

8. **Carlin, N. I., M. A. Gidney, A. A. Lindberg, and D. R. Bundle.** 1986. Characterization of *Shigella flexneri*-specific murine monoclonal antibodies by chemically defined glycoconjugates. J. Immunol. **137:**2361-2366.

9. **Carlin, N. I., A. A. Lindberg, K. Bock, and D. R. Bundle.** 1984. The *Shigella flexneri* O-antigenic polysaccharide chain. Nature of the biological repeating unit. Eur. J. Biochem. **139:**189-194.

10. **Chowers, Y., J. Kirschner, N. Keller, I. Barshack, S. Bar-Meir, S. Ashkenazi, R. Schneerson, J. Robbins, and J. H. Passwell.** 2007. Specific polysaccharide conjugate vaccine-induced IgG antibodies prevent invasion of *Shigella* into Caco-2 cells and may be curative. Proc. Natl. Acad. Sci. USA **104:**2396-2401.

11. **Clement, M. J., A. Fortune, A. Phalipon, V. Marcel-Peyre, C. Simenel, A. Imberty, M. Delepierre, and L. A. Mulard.** 2006. Toward a better understanding of the basis of the molecular mimicry of polysaccharide antigens by peptides - The example of *Shigella flexneri* 5A. J. Biolog. Chem. **281:**2317-2332.

12. **Craig, L., P. C. Sanschagrin, A. Rozek, S. Lackie, L. A. Kuhn, and J. K. Scott.** 1998. The role of structure in antibody cross-reactivity between peptides and folded proteins. J. Mol. Biol. **281:**183-201.

13. **Dyson, H. J., M. Rance, R. A. Houghten, P. E. Wright, and R. A. Lerner.** 1988. Folding immunogenic peptide fragments of proteins in water solution. II. The nascent helix. J. Mol. Biol. **201:**201-217.

14. **Fleuridor, R., A. Lees, and L. A. Pirofski.** 2001. A cryptococcal capsular polysaccharide mimotope prolongs the survival of mice with Cryptococcus neoformans infection. J. Immunol. **166:**1087-1096.

15. **Harris, S. L., L. Craig, J. S. Mehroke, M. Rashed, M. B. Zwick, K. Kenar, E. J. Toone, N. Greenspan, F. I. Auzanneau, J. R. MarinoAlbernas, B. M. Pinto, and J. K. Scott.** 1997. Exploring the basis of peptide-carbohydrate crossreactivity: Evidence for discrimination by peptides between closely related anti-carbohydrate antibodies. Proc. Natl. Acad. Sci. U.S.A. **94:**2454-2459.

16. **Hossany, R. B., M. A. Johnson, A. A. Eniade, and B. M. Pinto.** 2004. Synthesis and immunochemical characterization of protein conjugates of carbohydrate and carbohydrate-mimetic peptides as experimental vaccines. Bioorg. Med. Chem. **12:**3743-3754.

17. **Johnson, M. A., A. A. Eniade, and B. M. Pinto.** 2003. Rational design and synthesis of peptide ligands for an anti-carbohydrate antibody and their immunochemical characterization. Bioorg. Med. Chem. **11:**781-788.

18. **Johnson, M. A., M. Jaseja, W. Zou, H. J. Jennings, V. Copie, B. M. Pinto, and S. H. Pincus.** 2003. NMR studies of carbohydrates and carbohydrate-mimetic peptides recognized by an anti-group B *Streptococcus* antibody. J. Biol. Chem. **278:**24740-24752.

19. **Johnson, M. A., and B. M. Pinto.** 2007. Bioactive Conformations II *In* T. Peters (ed.), Topic in Current Chemistry, vol. 273. Springer Berlin, Heidelberg.

20. **Johnson, M. A., and B. M. Pinto.** 2002. Molecular mimicry of carbohydrates by peptides. Aust. J. Chem. **55:**13-25.

21. **Johnson, M. A., and B. M. Pinto.** 2004. NMR spectroscopic and molecular modeling studies of protein-carbohydrate and protein-peptide interactions. Carbohydr. Res. **339:**907-928.

22. **Johnson, M. A., A. Rotondo, and B. M. Pinto.** 2002. NMR studies of the antibody-bound conformation of a carbohydrate-mimetic peptide. Biochemistry **41:**2149-2157.

23. **Kotloff, K. L., J. P. Winickoff, B. Invanoff, J. D. Clemens, D. L. Swerdlow, and P. J. Sansonetti.** 1999. Global burden of *Shigella* infections: implications for vaccine development and implementation of control strategies. Bull. World Health Organ. **77:**651-665.

24. **Luijkx, T., H. van Dijken, C. van Els, and G. van den Dobbelsteen.** 2006. Heterologous prime-boost strategy to overcome weak immunogenicity of two serosubtypes in hexavalent *Neisseria meningitidis* outer membrane vesicle vaccine. Vaccine **24:**1569-1577.

25. **Maitta, R. W., K. Datta, A. Lees, S. S. Belouski, and L. A. Pirofski.** 2004. Immunogenicity and efficacy of Cryptococcus neoformans capsular polysaccharide glucuronoxylomannan peptide mimotope-protein

conjugates in human immunoglobulin transgenic mice. Infect. Immun. **72:**196-208.

26. **Mann, H. B., and D. R. Whitney.** 1947. On a test of whether one of two random variables is stochastically larger than the other. . Ann. Math. Stat. **18:**50-60.

27. **Moe, G. R., P. Zuno-Mitchell, S. N. Hammond, and D. M. Granoff.** 2002. Sequential immunization with vesicles prepared from heterologous *Neisseria meningitidis* strains elicits broadly protective serum antibodies to group B strains. Infect. Immun. **70:**6021-6031.

28. **Monzavi-Karbassi, B., G. Cunto-Amesty, P. Luo, and T. Kieber-Emmons.** 2002. Peptide mimotopes as surrogate antigens of carbohydrates in vaccine discovery. Trends Biotechnol. **20:**207-214.

29. **Phalipon, A., C. Costachel, C. Grandjean, A. Thuizat, C. Guerreiro, M. Tanguy, F. Nato, B. V. L. Normand, F. Belot, K. Wright, V. Marcel-Peyre, P. J. Sansonetti, and L. A. Mulard.** 2006. Characterization of functional oligosaccharide mimics of the *Shigella flexneri* serotype 2a O-antigen: Implications for the development of a chemically defined glycoconjugate vaccine. J. Immunol. **176:**1686-1694.

30. **Pinto, B. M., D. G. Morissette, and D. R. Bundle.** 1987. Synthesis of Oligosaccharides Corresponding to Biological Repeating Units of Shigella-*Flexneri* Variant Y-Polysaccharide .1. Overall Strategy, Synthesis of a Key Trisaccharide Intermediate, and Synthesis of a Pentasaccharide. J. Chem. Soc. Perkin Trans. 1**:**9-14.

31. **Pinto, B. M., K. B. Reimer, D. G. Morissette, and D. R. Bundle.** 1989. Oligosaccharides Corresponding to Biological Repeating Units of Shigella-*Flexneri* Variant-Y Polysaccharide .2. Synthesis and Two-Dimensional Nmr Analysis of a Hexasaccharide Hapten. J. Org.Chem. **54:**2650-2656.

32. **Pinto, B. M., K. B. Reimer, D. G. Morissette, and D. R. Bundle.** 1990. Synthesis and 2d-Nmr Analysis of a Pentasaccharide Glycoside of the Biological Repeating Units of Shigella-*Flexneri* Variant-Y Polysaccharide and the Preparation of a Synthetic Antigen. Carbohydr. Res. **196:**156-166.

33. **Vyas, M. N., N. K. Vyas, P. J. Meikle, B. Sinnott, B. M. Pinto, D. R. Bundle, and F. A. Quiocho.** 1993. Preliminary crystallographic analysis of a Fab specific for the O-antigen of *Shigella flexneri* cell-surface lipopolysaccharide with and without bound saccharides. J. Mol. Biol. **231:**133-136.

34. **Vyas, N. K., M. N. Vyas, M. C. Chervenak, D. R. Bundle, B. M. Pinto, and F. A. Quiocho.** 2003. Structural basis of peptide-carbohydrate mimicry in an antibody-combining site. Proc. Natl. Acad. Sci. U.S.A. **100:**15023-15028.

35. **Vyas, N. K., M. N. Vyas, M. C. Chervenak, M. A. Johnson, B. M. Pinto, D. R. Bundle, and F. A. Quiocho.** 2002. Molecular recognition of oligosaccharide epitopes by a monoclonal fab specific for *Shigella flexneri* Y lipopolysaccharide: X-ray structures and thermodynamics. Biochemistry **41:**13575-13586.

36. **Wilcoxon, F.** 1945. Individual comparisons by ranking methods. Biometrics **1:**80-83.

37. **Woodland, D. L.** 2004. Jump-starting the immune system: prime-boosting comes of age. Trends Immunol. **25:**98-104.

38. **Wright, K., C. Guerreiro, I. Laurent, F. Baleux, and L. A. Mulard.** 2004. Preparation of synthetic glycoconjugates as potential vaccines against *Shigella flexneri* serotype 2a disease. Org. Biomol. Chem. **2:**1518-1527.

39. **Zou, W., S. Borrelli, M. Gilbert, T. Liu, R. A. Pon, and H. J. Jennings.** 2004. Bioengineering of surface GD3 ganglioside for immunotargeting human melanoma cells. J. Biol. Chem. **279:**25390-25399.

4.9 SUPPORTING INFORMATION

Immunological evidence for functional vs. structural mimicry with a *Shigella flexneri* Y polysaccharide-mimetic peptide

Silvia Borrelli, Rehana B. Hossany and B. Mario Pinto

Department of Chemistry, Simon Fraser University, Burnaby, BC, Canada, V5A 1S6

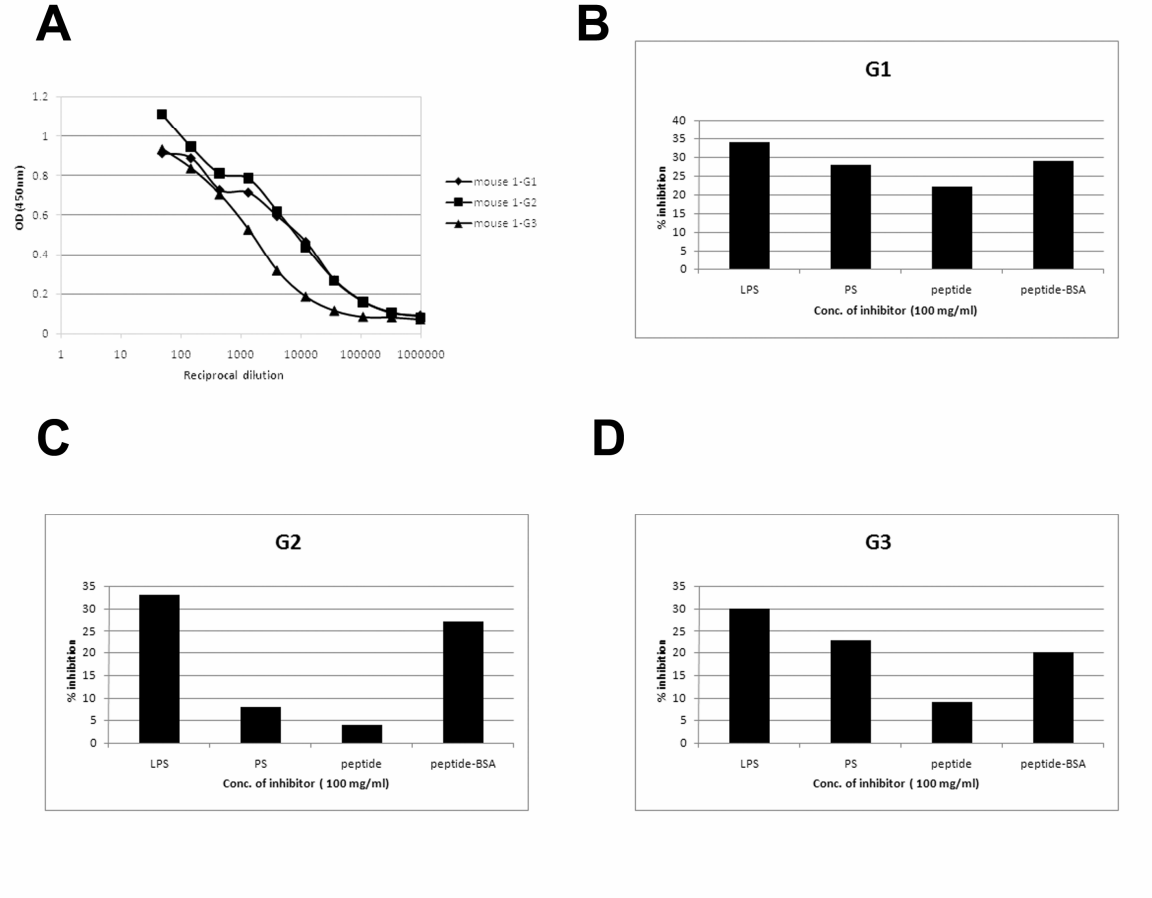

Figure 4-S 1: Titration ELISA of polyclonal antibodies (IgG) from Study 1 using *S. flexneri* Y LPS as a solid-phase antigen (10 μg/ml) (A), and competitive inhibition ELISA using *S. flexneri* Y LPS as a solid-phase antigen (10 μg/ml): (G1) using serum from immunization of Group 1, mouse number 1 (B); (G2) using serum from immunization of Group 2, mouse number 1 (C); (G3) using serum from immunization of Group 3, mouse number 1 (D).

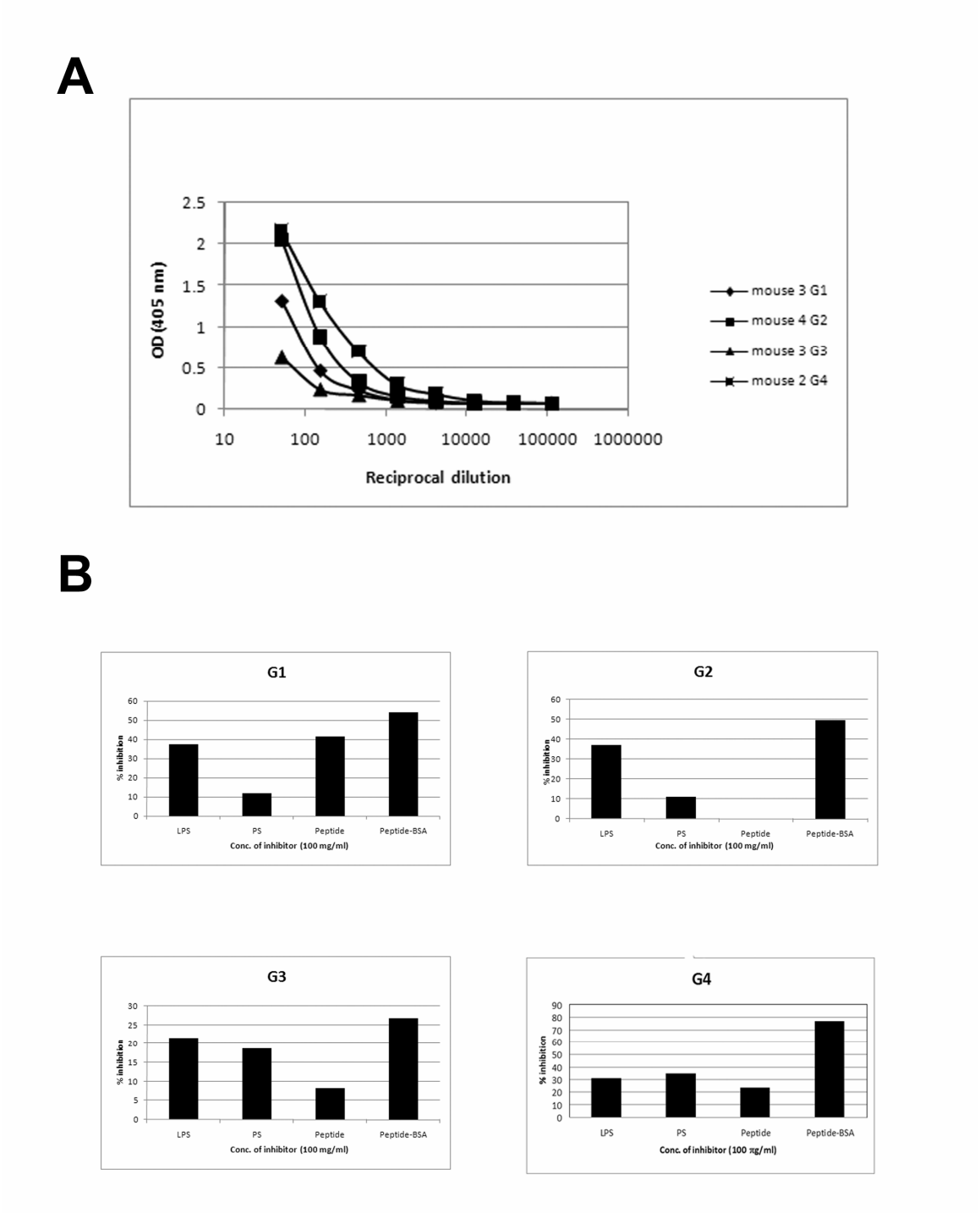

Figure 4-S 2: Titration ELISA of polyclonal antibodies (IgG) from Study 2 using *S. flexneri* Y LPS as a solid-phase antigen (10 μg/ml) (A), and competitive inhibition ELISA using *S. flexneri* Y LPS as a solid-phase antigen (10 μg/ml) (B):

(G1) using serum from immunization of Group 1, mouse number 3; (G2) using serum from immunization of Group 2, mouse number 4; (G3) using serum from immunization of Group 3, mouse number 3; (G4) using serum from immunization of Group 4, mouse number 2.

CHAPTER 5: DESIGN, SYNTHESIS AND IMMUNOCHEMICAL CHARACTERIZATION OF A CHIMERIC GLYCOPEPTIDE CORRESPONDING TO THE SHIGELLA FLEXNERI Y O-POLYSACCHARIDE AND ITS PEPTIDE MIMIC MDWNMHAA

This chapter comprises the manuscript "***Design, Synthesis, and Immunochemical Characterization of a Chimeric Glycopeptide Corresponding to the Shigella flexneri Y O-Polysaccharide and Its Peptide Mimic MDWNMHAA***" which has been published in Carbohydrate Research (**2009**, *344*, 1412-1427).

B. Rehana Hossany, Blair D. Johnston, Xin Wen, Silvia Borrelli, Yue Yuan, Margaret A. Johnson, and B. Mario Pinto

Recently, we have shown that the mimetic peptide MDWNMHAA, identified from a phage-displayed library, is an immunogenic mimic of the *Shigella flexneri* Y polysaccharide. We hypothesize that its immunogenicity could still be improved if its binding affinity (only 2-fold higher than the parent oligosaccharide) to the anti-*Shigella flexneri* Y polysaccharide antibody SYA/J6 is improved. In an effort to improve its

binding affinity, we have used the technique of molecular modeling to design two chimeric molecules, based upon the three-dimensional information obtained previously on the mimetic octapeptide from X-ray crystallography and NMR spectroscopy. In the design, we have targeted the unfavorable entropy of binding suffered by the mimetic octapeptide by replacing the NMHAA portion (which adopts a more ordered α-helix as well as engaging several water molecules) with a trisaccharide A-B-C from the parent pentasaccharide. Docking results revealed two chimeric molecules with either an α- or β-thioglycosidic linkage might be reasonable surrogate ligands for the anti-*Shigella flexneri* Y polysaccharide antibody SYA/J6.

This chapter describes the design of the two chimeric glycopeptides, and the synthesis and immunochemical characterization of the first candidate which is the α-glycopeptide. Dr. Xin Wen, Dr. Yue Yuan and Dr. Margaret A. Johnson performed the molecular modeling studies. The immunochemical evaluation of the glycopeptide was conducted by Dr. Silvia Borrelli. The initial method of synthesizing the α-glycopeptide entirely in solution was accomplished by Dr. Blair D. Johnston. An improved method of synthesizing the glycopeptide, using both solution and solid-phase strategies, was achieved by the thesis author.

The immunochemical study showed that the newly designed α-glycopeptide did not bind to the anti-*Shigella flexneri* Y polysaccharide antibody SYA/J6. It would be of interest next to examine the antigenicity

of the second candidate, β-glycopeptide, as the molecular modeling study showed that this ligand complements the shape of the combining site of the *Shigella flexneri* Y antibody better.

5.1 KEYWORDS

Shigella flexneri Y O-polysaccharide, Carbohydrate-mimetic peptide, Glycopeptide chimera, Molecular modeling, Synthesis, Immunochemistry

5.2 ABSTRACT

Two glycopeptide chimeras corresponding to the *Shigella flexneri* Y O-polysaccharide and its peptide mimic were designed in an attempt to improve the binding affinity by increasing the entropy of binding relative to the original octapeptide mimic of the O-polysaccharide. The design was based on the X-ray crystal structures of a monoclonal antibody SYA/J6 in complex with its cognate ligands, a pentasaccharide corresponding to the *S. flexneri* Y O-polysaccharide and the octapeptide mimic, MDWNMHAA. Both chimeric molecules consist of a rhamnose trisaccharide linked through an α- or β-thioglycosidic linkage to a MDW moiety in which the W unit has been modified. We predicted that omission of the NMHAA moiety would obviate the bound water molecules that provided complementarity with the antibody combining site, and the conformational

restriction resulting from imposition of an α-turn at the C-terminus of the peptide. The glycopeptides were then docked into the active site of SYA/J6 using the program AUTODOCK 3.0, and the structures were optimized. The best models obtained in each case showed that the chimeric molecules, with either an α- or β-thioglycosidic linkage, might be reasonable surrogate ligands for the antibody. We report here the synthesis of the α-glycopeptide employing solution and solid-phase strategies. Immunochemical characterization indicated that the α-glycopeptide unfortunately did not inhibit binding of SYA/J6 to the *S. flexneri* Y lipopolysaccharide.

5.3 INTRODUCTION

Antigens that can stimulate both humoral and cellular immune responses, are crucial in the development of effective vaccines against pathogenic bacteria.[1] While carbohydrates that coat the surfaces of bacteria are capable of inducing an immune response that can recognize whole bacteria,[2-8] polysaccharide vaccines fail to provide protection in infants, the elderly, and in immunodeficient persons since the immune response induced might not involve the T-helper cells of the immune system.[2-11] Conversion of some of these cell-surface polysaccharides into T-cell dependent antigens, by conjugation to carrier proteins, has resulted in potential vaccines that could successfully target infectious bacteria in humans.[5,8,11] However, progress in this field is challenging because the complex structures of the polysaccharide-protein conjugates make them difficult to be

synthesized and characterized.[12,13] Consequently, to drive T-cell-dependent immune responses against carbohydrate antigens, other vaccination strategies need to be explored in order to overcome some of the limitations of carbohydrate vaccines.

Molecular mimics of carbohydrates that have the potential to raise antibodies that cross-react with the natural structures have been identified, and there is now a growing interest in carbohydrate-mimetic peptides as vaccines to target cell-surface polysaccharides of infectious bacteria.[14-17] In addition to their ability to elicit carbohydrate-binding antibody responses, these peptide mimics should focus the immune responses on particular epitopes since greater discrimination of the peptides for the corresponding antibody-combining sites has been observed,[18] thus minimizing auto-immune reactions with self structures where the original carbohydrate antigens would pose a threat as immunogens.[17-19]

Shigella flexneri Y is a virulent bacterium that causes bacillary dysentery by invading the colonic mucosa.[20] Screening of a phage-displayed peptide library with an anti-carbohydrate antibody SYA/J6, directed against the O-polysaccharide (Fig. 5-1a) of *S. flexneri* Y yielded the peptide sequence MDWNMHAA (Fig. 5-1b).[18] The X-ray structures and the thermodynamics of binding of the Fab complexes of SYA/J6 with a pentasaccharide portion [→2)-α-L-Rha-(1→2)-α-L-Rha-(1→3)-α-L-Rha-(1→3)-β-D-GlcNAc-(1→2)-α-L-Rha-(1→] of the O-polysaccharide (Fig. 5-1a) and with the octapeptide mimic,

MDWNMHAA (Fig. 5-1b) have been studied in detail, and interesting similarities and differences between the two complexes have been revealed.[21,22]

Although, the octapeptide (Fig. 5-1b) complements the shape of the combining site groove much better than the pentasaccharide, and makes greater contacts with the antibody-combining site, the binding affinity of the peptide is only twofold higher than that of the pentasaccharide, potentially compromising the immunogenicity of the peptide.[21,22] The affinity can be attributed to the considerable unfavorable entropy that arises from a more ordered bound peptide and the immobilization of several water molecules.[17,22] Furthermore, for a peptide to be immunogenic, it might be necessary that a sufficient population of the bound conformation be displayed in the conformational ensemble of the free peptide.[14,15,17] Since the α-helix adopted by NMHAA in the C-terminus of MDWNMHAA is only restricted to the bound conformation and not to that of the free peptide, we hypothesized that MDWNMHAA might not lead directly to a cross-reactive response against the corresponding polysaccharide.[14,15,17] Nevertheless, we believed it could still be used in prime-boost strategies to strengthen the immune responses already induced by the polysaccharide epitopes, as shown with a peptide mimic of the capsular polysaccharide of *Cryptococcus neoformans*.[23] In order to test these hypotheses, we synthesized protein conjugates of the octapeptide,[24] and recently evaluated their immunogenicities.[16] Indeed, we found that, although the kinetics of the immune response in mice were slow, cross-reactivity was observed, and an effective prime-boost strategy was developed.[16]

We now report the design, of two chimeric glycopeptides (Fig. 5-1), that might serve as surrogate haptens against *S. flexneri* Y, and the synthesis and immunochemical evaluation of the first candidate.

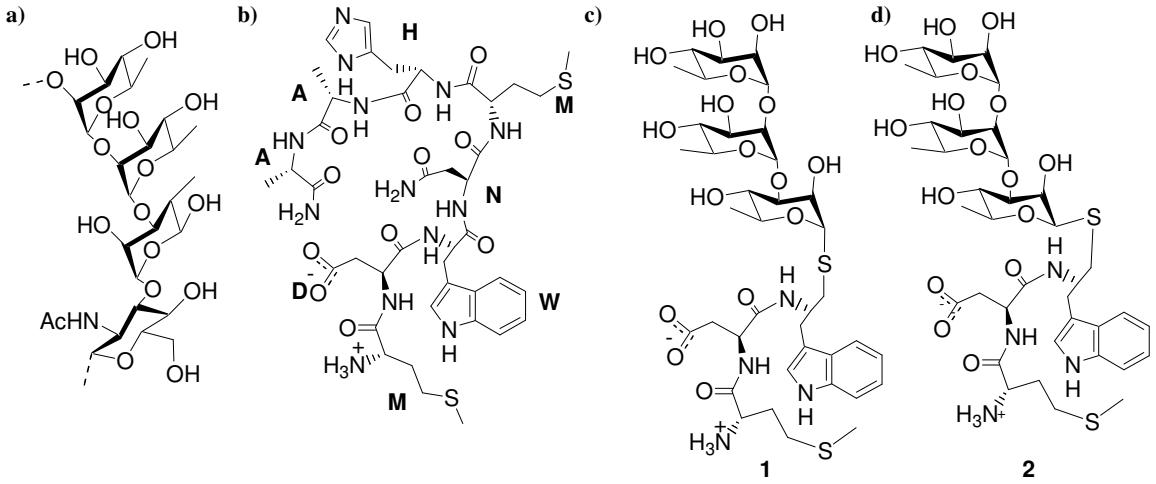

Figure 5-1: Structures of the (a) the O- polysaccharide of *Shigella flexneri* Y, (b) its peptide mimic (c) the chimeric α-glycopeptide **1**, and d) the chimeric β-glycopeptide **2**.

5.4 RESULTS AND DISCUSSION

5.4.1 General

Based on the information gained from the X-ray structures of the antibody-pentasaccharide and antibody-octapeptide complexes,[21,22] and by molecular modeling, we have designed two chimeric molecules (Fig. 5-1c and d) that

contain certain elements of both the oligosaccharide and the octapeptide mimic, and this should lead to increased binding affinity by increasing the entropy of binding relative to the parent octapeptide. The glycopeptides **1** and **2** comprise the two fragments, MDW and the rhamnose trisaccharide (A-B-C), derived from the parent octapeptide and pentasaccharide, respectively, and linked as a thioglycoside; the two glycopeptides differ in the α- or β-configuration at the thioglycosidic linkage (Fig. 5-1). We chose to retain the MDW portion of the octapeptide to maintain the favorable hydrophobic interaction of the W moiety within the combining site. Replacement of the NMHAA unit specifically by the rhamnose trisaccharide (A-B-C) in the glycopeptides **1** and **2**, was done firstly to ensure that ring C penetrates the deep hole at the bottom of the binding site, thus obviating the engagement of water molecules that provide complementarity with the antibody-combining site in binding of the peptide MDWNMHAA, and secondly, to reduce any conformational entropy differences that result from imposition of the α-turn at the C-terminus of the parent octapeptide upon binding. The incorporation of a thioglycosidic linkage between the trisaccharide moiety and the tripeptide in the glycopeptides **1** and **2** was done to increase their stabilities compared to those of the corresponding *O*-glycosides.[25]

5.4.2 Molecular Modeling

In order to validate the choice of the glycopeptides **1** and **2** (Fig. 5-1), they were each docked into the Fab fragment of SYA/J6 using AUTODOCK[26] starting from the coordinates of the two corresponding moieties in the complexes Fab-

ABCDA' and Fab-MDWNMHAA (Fig. 5-2a and b).[21,22] The most favored mode of binding in each case, with the lowest docked energy, showed that both **1** and **2** could fit into the binding groove without steric clashes (Fig. 5-2c and d). Superposition of the two binding modes of **1** and **2** on the parent octapeptide (Fig. 5-3a and c) and the parent pentasaccharide (Fig. 5-3b and d) indicated that both glycopeptides **1** and **2** superimposed well on the parent ligands; furthermore, the favorable hydrophobic interaction of the W moiety with the active site, as well as the penetration of ring C into the deep hole at the bottom of the binding site were preserved in both molecules. The interaction of the W moiety with the hydrophobic pocket within the Ab-combining site was more pronounced in the β-glycopeptide (Fig. 5-2c and d). Thus, the docking experiments justify the choice of **1** and **2** as reasonable surrogate ligands for the antibody SYA/J6. We report here the synthesis and immunochemical evaluation of the first candidate, namely the α-glycopeptide **1**, which lent itself to a more facile synthesis.

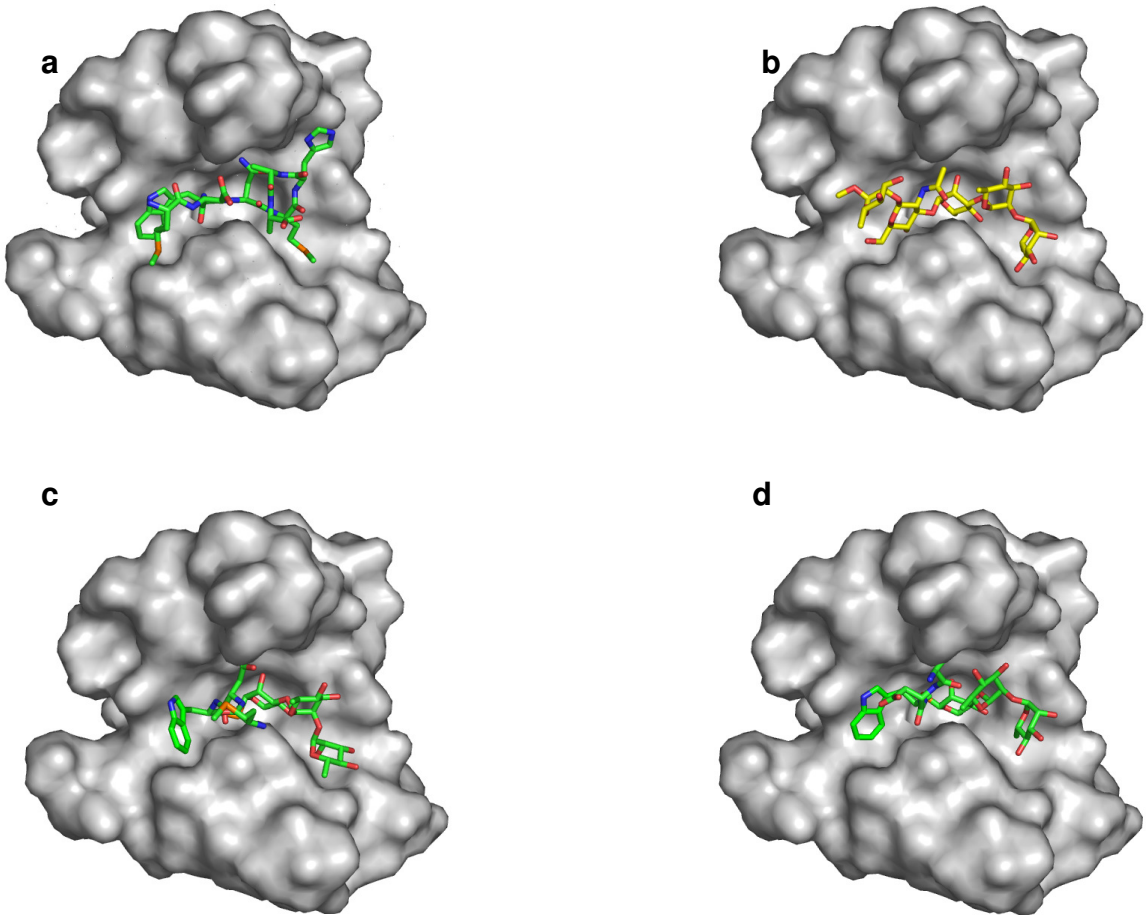

Figure 5-2: Structures of the Fab fragment of SYA/J6 antibody with (a) bound octapeptide MDWNMHAA, (b) bound pentasaccharide, (c) bound α-glycopeptide **1**, and (d) bound β-glycopeptide **2**.

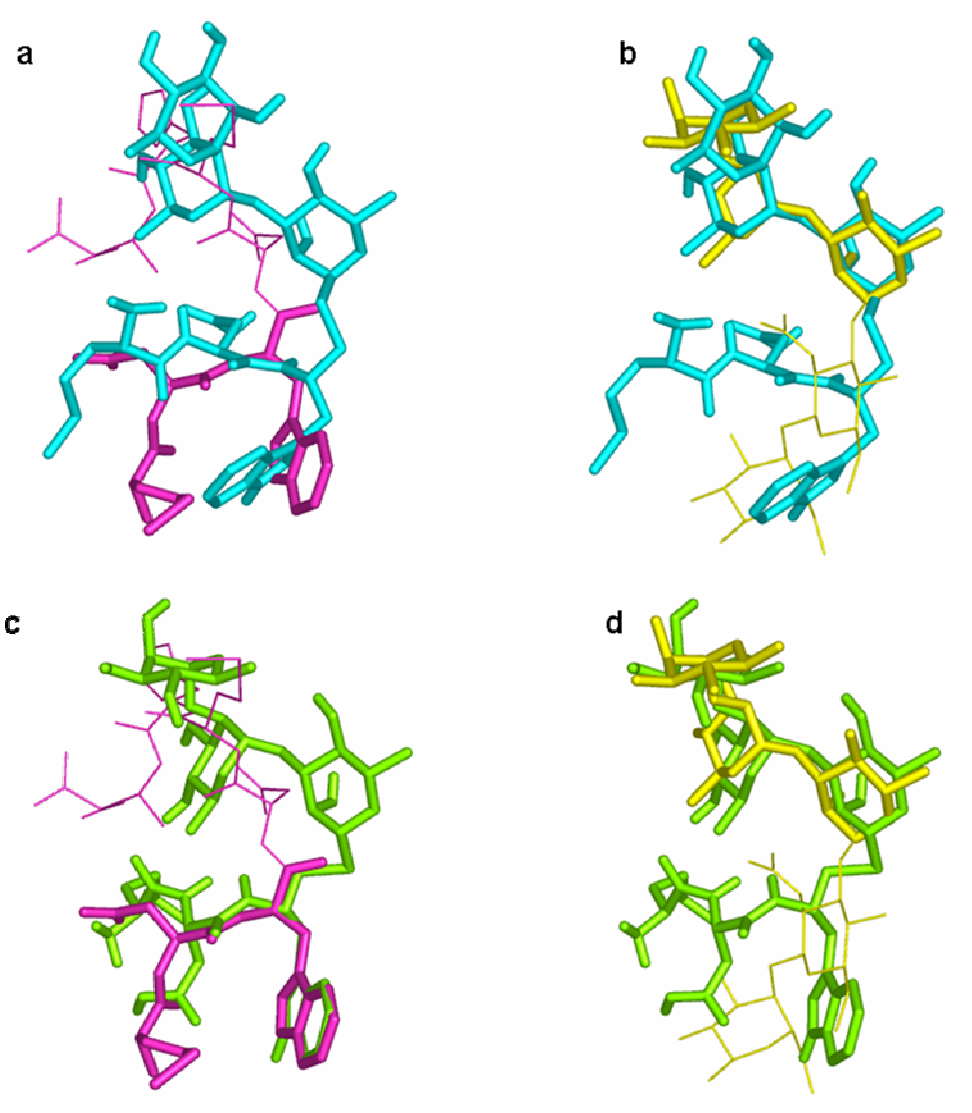

Figure 5-3: Superposition of the (a) α-glycopeptide **1** (cyan) on the parent octapeptide (pink), (b) α-glycopeptide **1** (cyan) on the parent pentasaccharide (yellow), (c) β-glycopeptide **2** (green) on the parent octapeptide (pink), and (d) β-glycopeptide **2** (green) on the parent pentasaccharide (yellow).

5.4.3 Synthesis

Retrosynthetic analysis indicated that the α-glycopeptide **1** could be obtained by deprotection of the glycopeptide **3**, which, in turn, could be derived from the trisaccharide **4** and the tripeptide bromide **5** (Scheme 5-1).

Scheme 5-1: Retrosynthetic analysis of the α-glycopeptide **1**

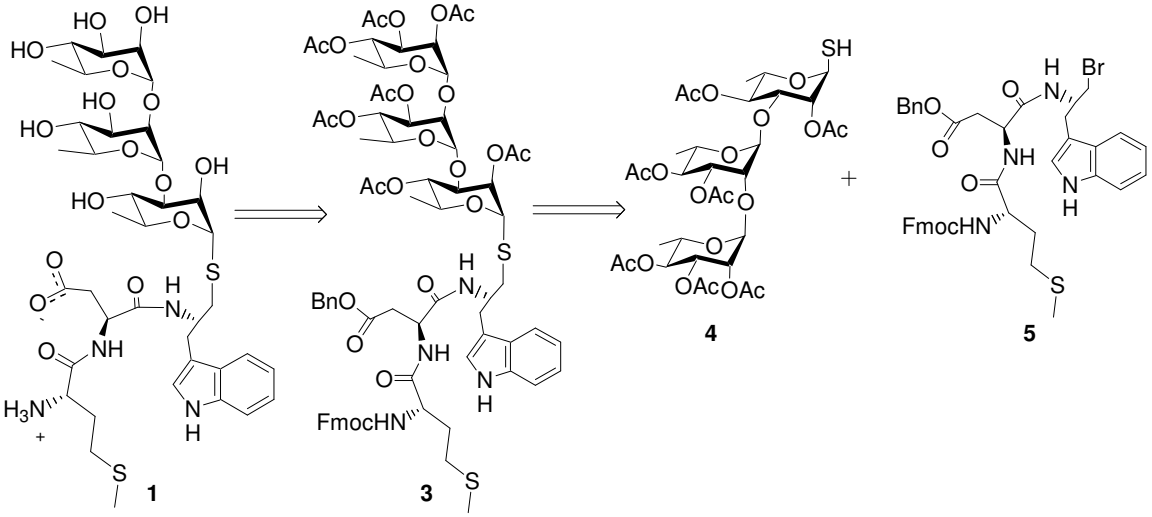

The trisaccharide **4** was prepared by methods analogous to those that we had previously developed[27,28] to prepare oligosaccharides containing α(1→2) and α(1→3)-L-rhamnopyranosidic linkages. In the present case (Scheme 5-2), the reducing terminal rhamnose unit was introduced as a thioglycoside in order to facilitate later conversion to a 1-thiol via the corresponding glycosyl bromide. Thus, the known 2,4-dibenzoylated rhamnose thioglycoside **6**[29] was glycosylated

at the 3-position with the rhamnose trichloroacetimidate donor **7**[28] to give the disaccharide derivative **8** in >90% yield. Selective methanolysis of the 2'-*O*-acetate using HCl-MeOH gave the disaccharide glycosyl acceptor **9** in only moderate yield due to an unusually low selectivity for reaction of the acetate over the benzoate esters. A second glycosylation reaction with donor **7** gave the trisaccharide **10** in 79% yield. The benzoates were replaced by acetates through base-catalyzed methanolysis, followed by acetylation under standard conditions to give the acetylated phenylthio trisaccharide **11**, in quantitative yield for the two steps. The phenylthio group was replaced by SH in a three-step procedure that was carried out without purification of intermediates. Thus, the phenylthio group was first replaced by a bromide by treatment of the thioglycoside **11** with IBr[30] to yield the glycosyl bromide **12**. Nucleophilic displacement of the bromide gave the isothiouronium salt **13**, which was immediately hydrolyzed to the thiol **4**. Compound **4** was obtained as the pure α-anomer by crystallization of the crude α/β product mixture from EtOAc-hexanes. Analysis by ^{1}H NMR spectroscopy indicated that the α-anomer **4**, in $CDCl_3$ did not undergo significant anomerization over several days at ambient temperature.

Scheme 5-2: Synthesis of the precursor **4**

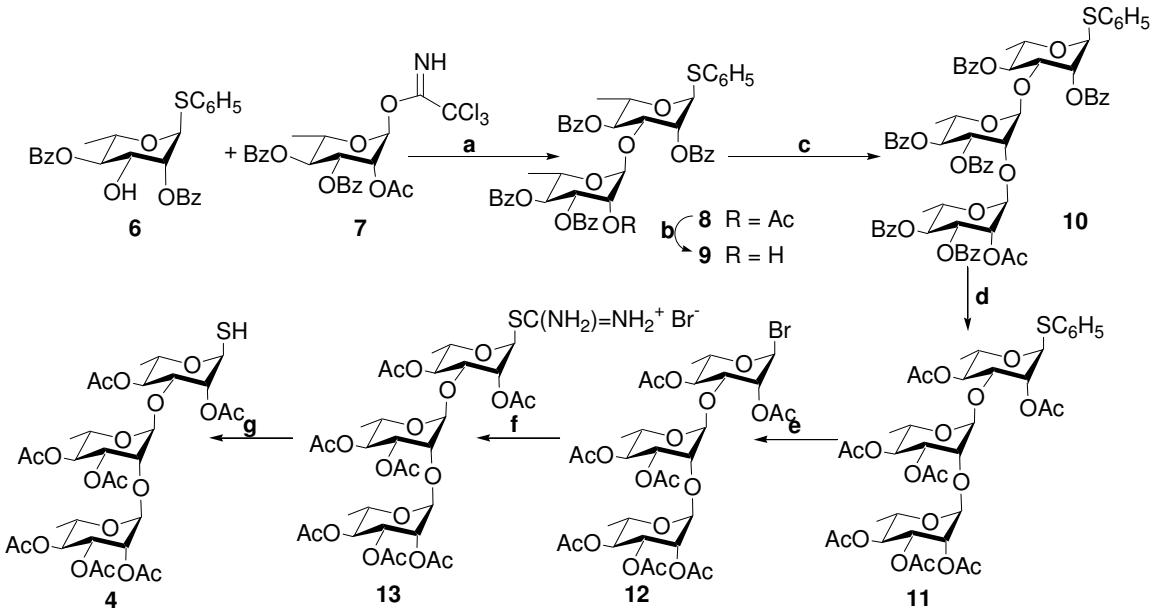

Reagents and conditions: a) TMSOTf, CH_2Cl_2, -40 ^{0}C→rt, >90%, b) CH_3COCl, MeOH, pyridine, 45 ^{0}C→rt, 58%, c) **7**, TMSOTf, CH_2Cl_2, -40 ^{0}C→rt, 79%, d) NaOMe-MeOH, MeOH, Ac_2O, Pyr, quantitative, e) IBr, CH_2Cl_2, f) thiourea, CH_3CN, reflux, g) $Na_2S_2O_5$, CH_2Cl_2-H_2O, reflux, 56% over 3 steps.

The tripeptide **5** was prepared from the alcohol **14** by a bromination reaction using triphenylphosphine and carbon tetrabromide (Scheme 5-3). The alcohol **14** was assembled using standard solution-phase peptide assembly techniques from L-tryptophanol,[31] BOC-Asp(OBn)-OH, and Fmoc-Met-OH, with dicyclohexylcarbodiimide (DCC)-1-hydroxybenzotriazole (HOBt) as the coupling agent (Scheme 5-3). The aspartate side-chain carboxyl group was protected as a benzyl ester, while the *N*-terminal methionine was protected as the α-*N*-Fmoc derivative since it was envisioned that a single, basic deprotection step would

suffice for removal of all protecting groups from both the peptide and trisaccharide portions of the target molecule **1**.

The crude bromide **5** was then coupled with the trisaccharide thiol **4** using a two-phase reaction (Scheme 5-4), with the phase-transfer protocol that was recently reported to be effective for the synthesis of thio-linked glycopeptide derivatives.[32] In the present application, however, the phase-transfer reaction suffered from several competing reaction pathways and provided the glycopeptide **3** in low yield as mixtures with side products. If the processing did not involve acidic conditions, such as an aqueous citric acid wash, purification by flash chromatography gave the α-glycopeptide **3**, which was contaminated by sizeable portions of two impurities. One impurity was made up entirely of carbohydrate, and was tentatively identified as the disulfide **15** resulting from air-oxidation of thiol **4** (Fig. 5-4). The other impurity was entirely peptidic in character, and was assigned to be the oxazoline derivative **16** (Fig. 5-4), resulting from intramolecular displacement of the primary bromide by nucleophilic attack of the oxygen atom of the neighboring amide. These impurities could be removed by HPLC, but it was eventually determined that this was not necessary. Implementation of a citric acid wash in the processing resulted in ring-cleaving hydrolysis of the oxazoline to give a product that was tentatively assigned the ester structure **17** (Fig. 5-4) . This was much more polar than the initial peptide impurity, and was then easily separable from the glycopeptide by flash chromatography. The other acetylated-carbohydrate impurity **15** was unchanged

by this modified workup, and was still not removed by flash chromatography. The mixture was then used without further purification in the deprotection step.

Treatment of the protected glycopeptide **3** with NaOMe in MeOH resulted in formation of a more polar product as shown by TLC analysis of the reaction mixture. Isolation of this material by flash chromatography and analysis by HPLC, and by NMR and MALDI spectroscopy, made it apparent that the product was a mixture of several similar compounds, none of which appeared to be the desired glycopeptide **1**. The mass spectrum indicated that the major components of the mixture had masses of 18 mass units less than that of the expected glycopeptide **1**. It was concluded that the strongly basic deprotection conditions had resulted predominantly in aspartimide formation; and that partial hydrolysis must have occurred during the subsequent HPLC analysis to give mixtures comprising both α- and β-amide linkages between the aspartate and tryptophan units (Scheme 5-5). This is a well known side-reaction,[33] in peptide synthesis and has often been observed when peptides containing aspartate side-chain esters are deprotected by treatment with base.

The aspartimide problem was eventually avoided by the preparation of the glycopeptide **18** in which the benzyl ester was replaced by a *tert*-butyl ester (O*t*Bu), giving a protecting-group for the aspartate side chain that could be selectively removed under acidic conditions. The glycopeptide **18** was prepared by the coupling of the crude tripeptide bromide **19** with the thiol **4** (Scheme 5-4), using the phase-transfer protocol,[32] but the glycopeptide **18** was obtained in low yield, and the side products **15** and **16** were also detected. The bromo

compound **19** was obtained by the bromination of tripeptide **20**, which in turn, was prepared from L-tryptophanol,[34] Fmoc-Met-OH, and Fmoc-Asp(OtBu)-OH amino acids, following the same strategy that was used to prepare the tripeptide **14** (Scheme 5-3)

Scheme 5-3: Synthesis of the tripepides **5** and **19**

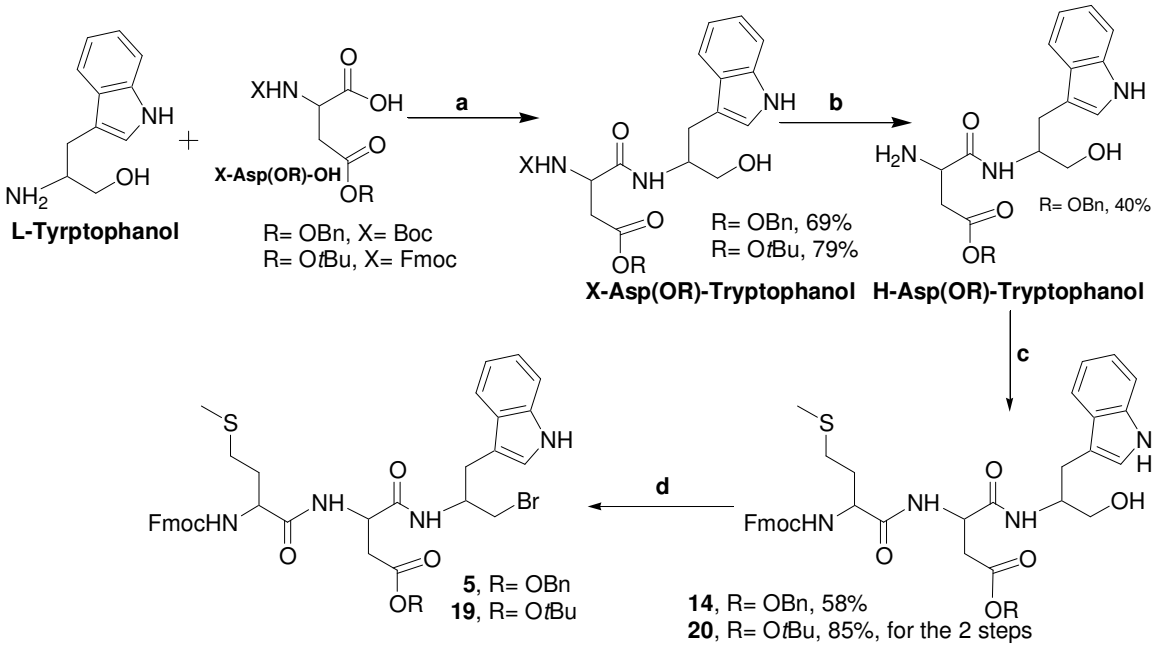

Reagents: a) DCC, HOBt, b) TFA, or piperidine, c) Fmoc-Met-OH, DCC, HOBt, d) CBr_4, PPh_3, CH_2Cl_2.

Scheme 5-4: Synthesis of the protected glycopeptide **3**

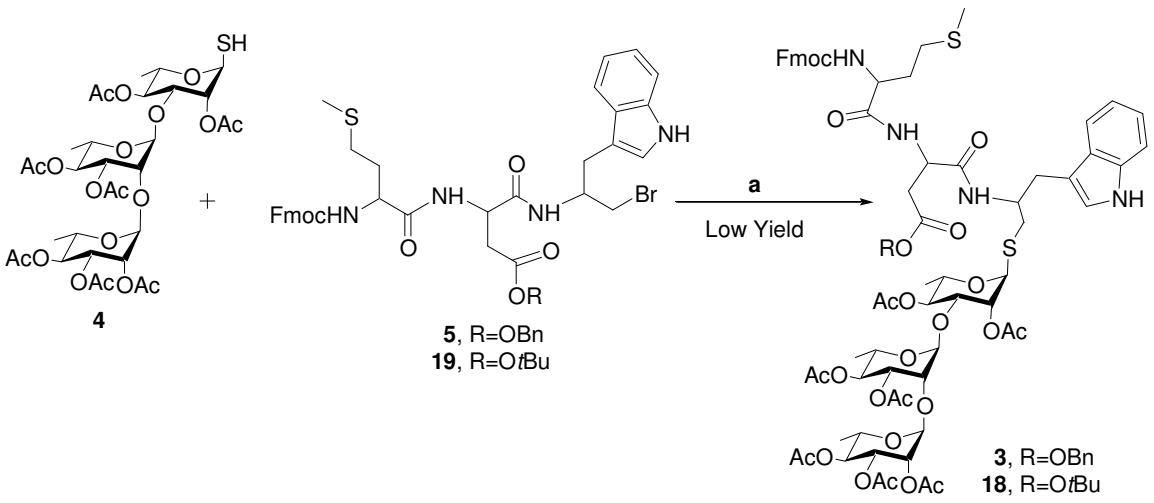

Reagents: a) $NaHCO_3$, Bu_4NHSO_4, $EtOAc/H_2O$, ~16%, after HPLC.

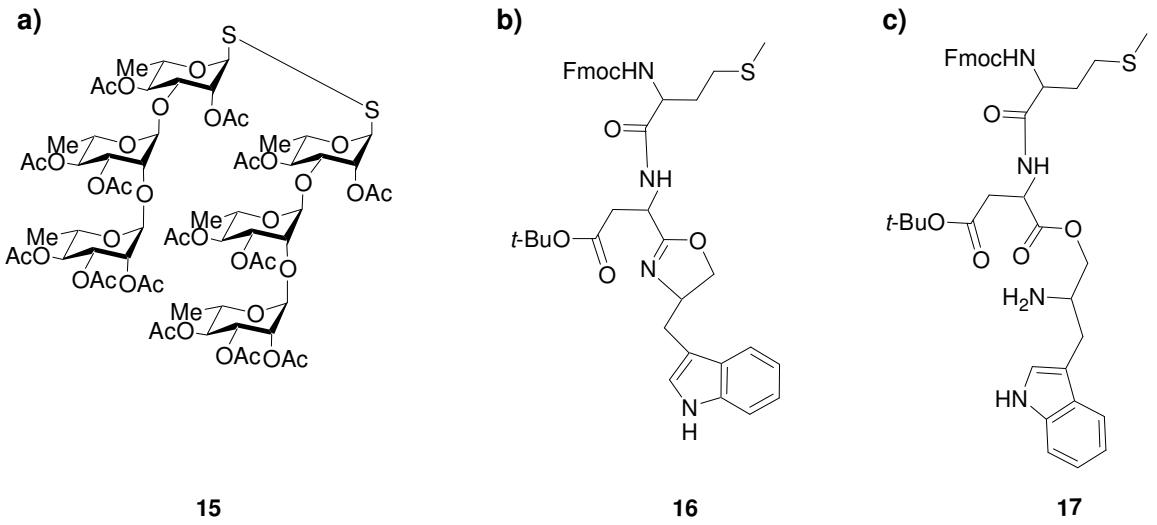

Figure 5-4: Structures of the (a) disulfide **15**, (b) oxazoline derivative **16**, and (c) ester **17**.

Scheme 5-5: Aspartimide formation in the deprotection of the protected glycopeptide **3**

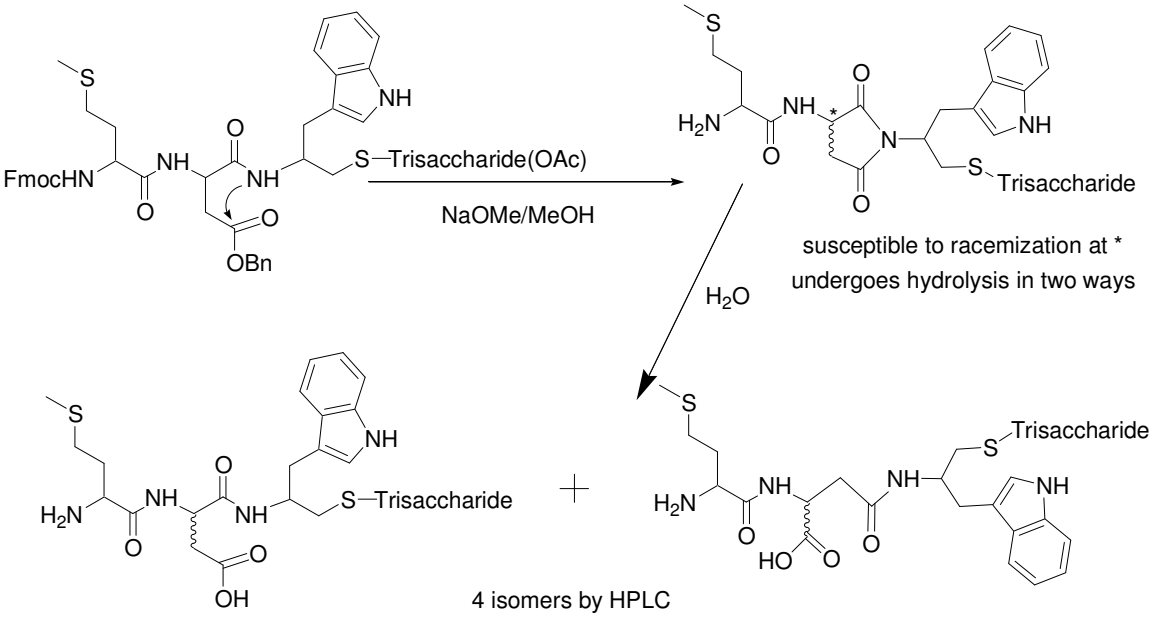

In the deprotection of the glycopeptide **18**, when the -O*t*Bu group was first removed using TFA-TIPSiH, the intermediate free aspartate carboxyl was converted to a carboxylate salt by subsequent NaOMe treatment. It therefore became resistant to aspartimide formation, while the other protecting groups were smoothly removed (Scheme 5-6). The selective cleavage of the aspartate ester also meant that the acetylated-carbohydrate disulfide impurity **15** in the glycopeptide was then considerably less polar than the free aspartate glycopeptide, and it could be readily separated in the early fractions during chromatographic purification of the partially deprotected glycopeptide. Nevertheless, after the base-catalyzed deprotection that followed, a considerable amount of sodium acetate (which was formed by neutralization of the reaction mixture with acetic acid) did co-elute with the glycopeptide **1** fraction during the final chromatographic purification.

Scheme 5-6: Deprotection of 18 to the α-glycopeptide **1**

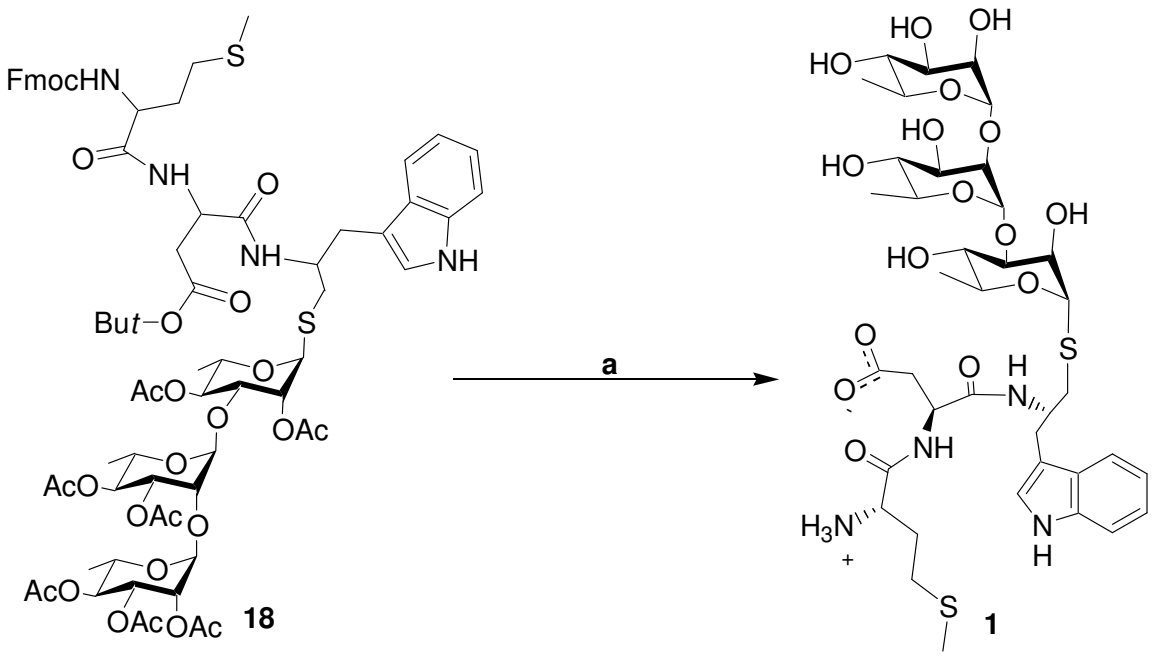

Reagents: a) (i) TFA/TIPSiH, (ii) NaOMe/MeOH, 32%.

We next examined a more efficient synthesis of the glycopeptide **18**. We reasoned that an alternative disconnection was desirable, in particular, one that avoided the presence of the aspartate and methionine moities in the coupling reaction with **4**. Accordingly, the thiol **4** was coupled with the Fmoc-tryptophanol bromide derivative **21**; here, the two-phase reaction proceeded smoothly to give the glycopeptide **22** as the sole product in excellent yield (Scheme 5-7).

The bromide **21** was prepared from L-tryptophanol[34] in two steps (Scheme 5-7). L-tryptophanol was first treated with Fmoc-succinimide to yield Fmoc-tryptophanol. Bromination of the Fmoc-tryptophanol was then carried out using

PPh_3-CBr_4 to afford the bromide **21** in 65% yield. Compound **21** was obtained even more efficiently (95%) when Fmoc-tryptophanol was converted into its mesylate and subsequently treated with lithium bromide (Scheme 5-7).

The Fmoc protecting group in **22** was then removed using DBU-octanethiol[35] to form the amine **23**, which was coupled to the dipeptide **24** using *N*-hydroxybenzotriazole (HOBt) as coupling agent to afford the protected glycopeptide **25**, with a minor peptide impurity that was readily removed by HPLC to afford the protected glycopeptide **25** (Scheme 5-7).

Scheme 5-7: Synthesis of the protected glycopeptide **25**

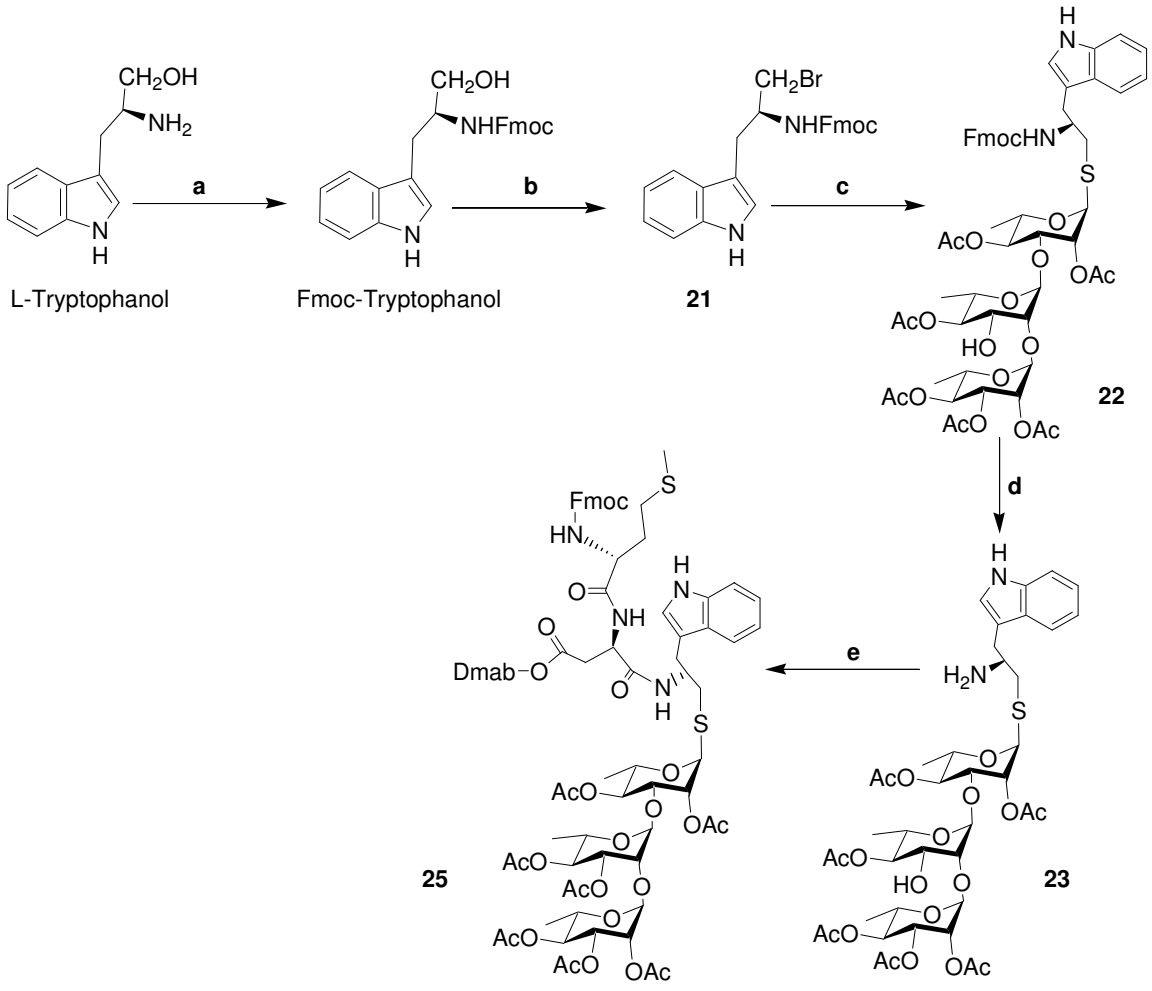

Reagents: a) Fmoc-OSu, $NaHCO_3$, acetone-H_2O, 95%, b) (i) MsCl-py, (ii) LiBr, refluxed, 95% for the 2 steps, c) **4**, $NaHCO_3$, Bu_4NHSO_4, EtOAc-H_2O, 92%, d) DBU, octanethiol, THF, quantitative, and e) 24, HOBt, THF, 72%.

The dipeptide **24**, in turn, was constructed on solid support employing Fmoc chemistry[36] and an HBTU-HOBt-DIPEA coupling strategy[37-39] as shown in Scheme 5-8. In this method, we chose the protecting group *N*-[1-(4,4-dimethyl-

2,6-dioxocyclohexylidene)-3-methylbutyl]-amino benzyl ester (Dmab)[40] on the side chain of Fmoc-aspartic acid because it is stable to piperidine, one of the requirements for the solid phase synthesis of dipeptide **24**. Fmoc-Asp(ODmab)-OH (**27**) and the commercially available Fmoc-Met-OH were used in the solid-phase synthesis, and since a free carboxylic acid group was required at the C-terminus in the synthesis of the dipeptide **24**, a 2-chlorotrityl resin[41] was chosen as the solid support. The Fmoc-Asp(ODmab)-OH (**27**) was successfully prepared in two steps starting from the commercially available Fmoc-Asp-O*t*Bu (Scheme 5-8). The Dmab protecting group was first introduced on the side chain of Fmoc-Asp-O*t*Bu by reacting the amino acid with Dmab-OH in the presence of 2,6-di-*tert*-butyl-4-methylpyridine (DTBMP), HOBt and DIC, to afford the product **26** in 71% yield. Treatment of **26** with 50% TFA in CH_2Cl_2 gave the desired product **27** in nearly quantitative yield (Scheme 5-8).

After cleavage from the resin with dilute acid, and purification by column chromatography, the dipeptide **28** was obtained in 80% yield (Scheme 5-8). The conversion of the carboxylic acid of **28** to the more active pentafluorophenol ester **24** was done to increase the coupling efficiency between the precursors **23** and **24**.

Scheme 5-8: Synthesis of the dipeptide **24**

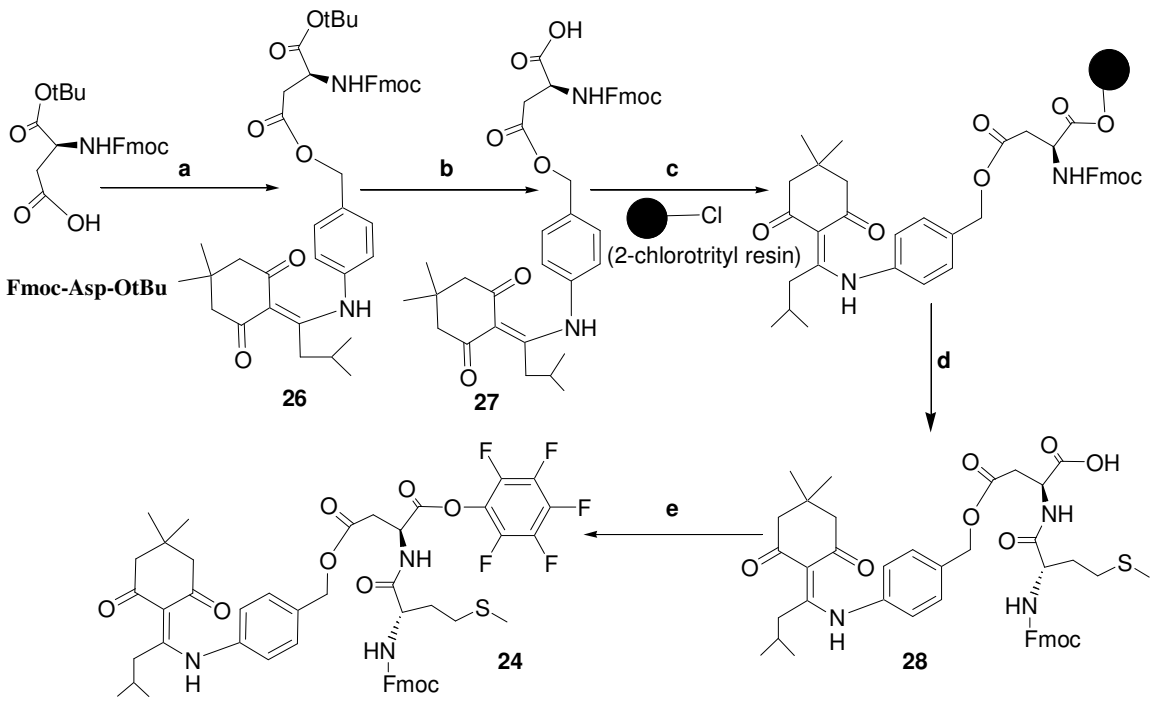

Reagents: a) Dmab-OH, DTBMP, HOBt, DIC, 71%, b) 50% TFA in CH_2Cl_2, 97%, c) DIPEA, DMF, d) (i) 25% Piperidine/DMF, (ii) Fmoc-Met-OH, HBTU/HOBt/DIPEA, DMF, iii) 5% TFA in CH_2Cl_2, 80%, e) Pentafluorophenol, DIC, 73%.

The Fmoc protecting group on the fully protected glycopeptide **25** was then removed selectively using DBU-octanethiol[35] so that the side product dibenzofulvene that formed could be scavenged by the octanethiol, and the complex that formed could be easily removed in ether to give **29** (Scheme 5-9). Treatment of the amine **29** with NaOMe-MeOH, however, did not afford the desired glycopeptide **1** (Scheme 5-9), but resulted in the formation of the same

aspartimide side product that was formed in the deprotection of the glycopeptide **3**.

However, when the Dmab and the acetate protecting groups in **29** were sequentially removed, using 2% hydrazine-THF to first afford **30**, followed by NaOMe-MeOH, the desired glycopeptide **1** was obtained in 68% yield, after treating the mixture first with Rexyn 101 H+ to make it slightly basic, followed by further neutralization with acetic acid, and purification by HPLC (Scheme 5-10).

Scheme 5-9: Aspartimide formation in the deprotection of the glycopeptide **25**

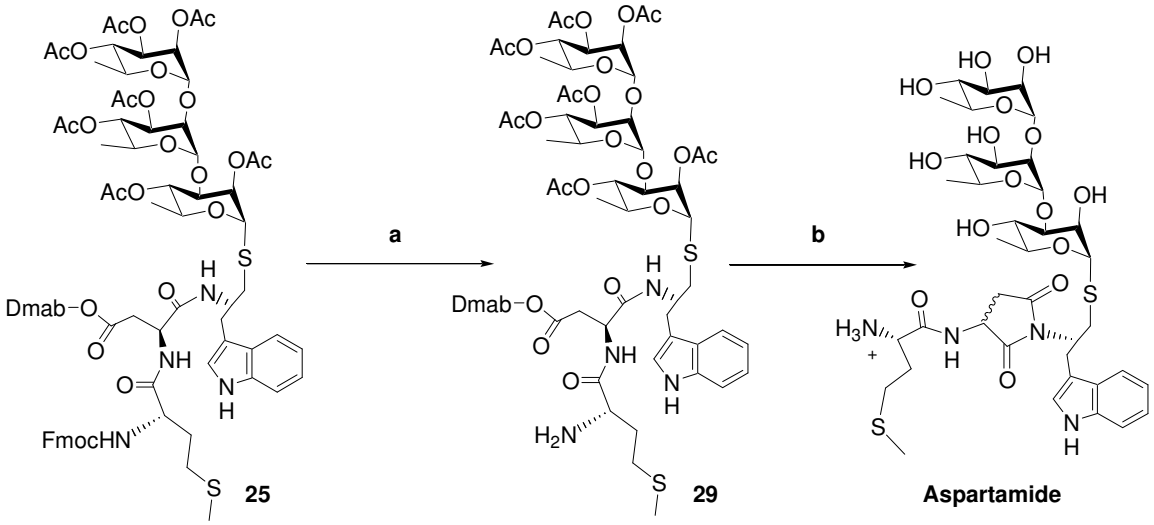

Reagents: a) DBU-octanethiol, THF, quantitative, b) NaOMe, MeOH, 88%.

Scheme 5-10: Deprotection of **29** to the α-glycopeptide **1**

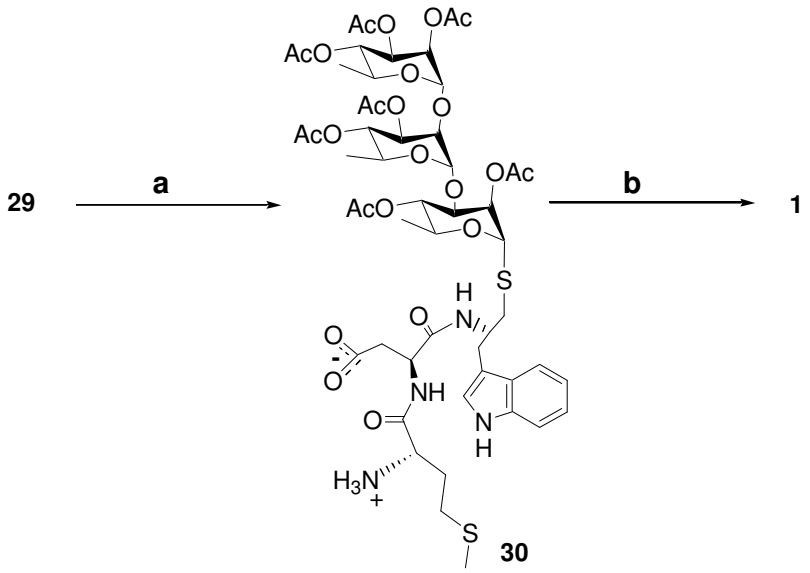

Reagents: a) 2% hydrazine, THF, quantitative, b) NaOMe-MeOH, 68%.

5.4.4 Immunochemistry

The binding of the glycopeptide to the monoclonal antibody SYA/J6 was investigated by competitive inhibition ELISA studies, using *S. flexneri* Y LPS as coating antigen. The purified glycopeptide was analyzed as an inhibitor of the binding of monoclonal antibody SYA/J6, while the LPS, the purified O-polysaccharide and the mimetic-octapeptide, were used as control inhibitors. No inhibitory activity was observed with the glycopeptide even at the highest concentration tested (200 μg/mL). Both the LPS and O-polysaccharide showed IC_{50} values of <0.7 μg/mL and the mimetic-octapeptide showed an IC_{50} value of 6.25 μg/mL (data not shown). The relative inhibitory activities of multivalent

carbohydrate ligand and monovalent peptide ligand differ from those obtained by microcalorimetry for monovalent pentasaccharide and octapeptide ligands (twofold difference);[21,22] we attribute these differences to the effect of multivalent presentation of carbohydrate ligands. The reason for the disappointing lack of inhibition by the glycopeptide is not at all obvious and will require further investigation through synthesis and immunochemical evaluation of its stereoisomer, the β-linked glycopeptide.

5.5 EXPERIMENTAL

5.5.1 Synthesis

5.5.1.1 General methods

The Fmoc amino acids that used were purchased from Novabiochem, and the other reagents were purchased from Aldrich Chemical Co. DMF was freed of amines by concentrating it under high vacuum, and it was then distilled and stored over 4 Å molecular sieves, whereas the other solvents were distilled according to standard procedures.[42] The dipeptide **3** was synthesized on 2-chlorotrityl resin[41] (Novabiochem) (1.64 mmol/g substitution level), using standard 9-fluorenyl-methoxycarbonyl (Fmoc) chemistry[36] employing the 2-[1-H-Benzotriazole-1-yl]-1.1.13.3-tetramethyluronium hexafluorophosphate-1-hydroxybenzotriazole (HBTU-HOBt) coupling strategy.[37-39] The Kaiser ninhydrin (5% ninhydrin in ethanol, 80% phenol in ethanol, and 2% 0.001 M aqueous KCN

in pyridine) assay for the amino group[43] was used to monitor both the Fmoc-amino acid coupling and the Fmoc deprotection reactions. 1D- and 2D-NMR spectra were recorded on 400-, and 500-, and 600-MHz spectrometers. Chemical shifts were referred to internal $CHCl_3$ or external DSS [3-(trimethylsilyl)-1-propanesulfonic acid] and were reported in d units relative to tetramethylsilane. Coupling constants were obtained from a first-order analysis of one-dimensional spectra, and spectral assignments were based on COSY, HMQC and TOCSY experiments. MALDI-TOF mass spectra were obtained for samples dispersed in a 2,5-dihydroxybenzoic acid matrix on a Perseptive Biosystems Voyager-DE instrument. High resolution mass spectra were obtained using LSIMS (FAB), run on a Kratos Concept H double focusing mass spectrometer at 10,000 RP and by the electrospray ionization method, using an Agilent 6210 TOF LC/MS high resolution magnetic sector mass spectrometer.

5.5.1.2 Phenyl 2-*O*-acetyl-3,4-di-O-benzoyl-α-L-rhamnopyranosyl-(1→3)-2,4-di-O-benzoyl-1-thio-α-L-rhamnopyranoside (8)

A mixture of the thioglycoside **6**[29] (1.33 g, 2.86 mmol) and the trichloroacetimidate **7**[28] (1.52 g, 2.72 mmol) in anhydrous CH_2Cl_2 (30 mL) was stirred with freshly activated, crushed 4 Å molecular sieves (1.3 g) under N_2 for 10 min at room temperature. The mixture was cooled in a -40° C bath and trimethylsilyl triflate (40 μL, 0.22 mmol) was added. After 15 min, the cooling bath was removed and the mixture was allowed to warm to room temperature over a period of 40 min. Et_3N (0.2 mL) was added and the molecular sieves were removed by filtration through Celite, with the aid of additional CH_2Cl_2 (100 mL).

The filtrate was washed with saturated $NaHCO_3$ (30 mL), dried over $MgSO_4$, and concentrated to a syrup. Flash chromatography (hexanes-EtOAc; 3:1 to 2:1) gave the disaccharide **8** (2.25 g, >90%) as a colorless, hard foam containing approximately 10 mol % of the by-product trichloroacetamide (^{1}H NMR, broad singlet at δ 6.6 ppm). The mixture was used directly in the next reaction. ^{1}H NMR (400 MHz, $CDCl_3$): δ (ppm) 8.25-7.25 (25 H, m, Ar), 5.74 (1H, dd, $J_{1,2}$ = 1.9, $J_{2,3}$ 3.3 Hz, H2), 5.71 (1H, d, H1), 5.63 (1H, t, $J_{3,4}$ = $J_{4,5}$ = 9.7 Hz, H4), 5.47 (1H, dd, $J_{2',3'}$ = 3.4, $J_{3',4'}$ = 9.9 Hz, H3'), 5.36 (1H, t, $J_{4',5'}$ = 9.8 Hz, H4'), 5.11 (1H, dd, $J_{1',2'}$ = 2.0 Hz, H2'), 5.08 (1H, d, H1'), 4.54 (1H, dq, H5), 4.42 (1H, dd, H3), 4.06 (1H, dq, H5), 1.95 (3H, s, OAc), 1.37 (3H, d, $J_{5,6}$ = 6.3 Hz, H6), 1.33 (3H, d, $J_{5',6'}$ = 6.3 Hz, H6'). ^{13}C NMR (150 MHz, $CDCl_3$): δ (ppm) 169.4 (1C, OAc), 166.0-164.7 (4C, 4 × OBz), 133.6-127.9 (30C, C_{Ar}), 99.4 (1C, C1'), 85.6 (1 C, C1), 76.6 (1C, C3), 73.8 (1C, C2), 73.2 (1C, C4), 71.46 (1C, C4'), 69.9 (1C, C2'), 69.3 (1C, C3'), 68.3 (1C, C5), 67.6 (1C, C5'), 20.6 (1C, *C*H_3-OAc), 17.6 (1C, C6), 17.3 (1C, C6'). MALDI-TOF MS: *m/e* 883.3 (M+Na).

5.5.1.3 Phenyl 3,4-di-O-benzoyl-α-L-rhamnopyranosyl-(1→3)-2,4-di-O-benzoyl-1-thio-α-L-rhamn-opyranoside (9)

The disaccharide **8** (8.15 g, 9.95 mmoL) was dissolved in MeOH (250 mL) and the solution was stirred rapidly. Acetyl chloride (4 mL) was added dropwise and the mixture was stirred for 4 h at rt and then at 45° C for 3.5 h. The solution was cooled to rt and neutralized by the dropwise addition of pyridine. The solvents were evaporated and the residue was partitioned between dichloromethane (200 mL) and saturated $NaHCO_3$ solution (100 mL). The

organic phase was dried over $MgSO_4$ and concentrated to give a syrup. Purification by column chromatography (hexanes:EtOAc; 2:1) gave the disaccharide hemiacetal **9** (4.54 g, 58%) as a colorless foam containing a trace of the starting 2'-*O*-acetate by TLC. ^{1}H NMR (500 MHz, $CDCl_3$): δ (ppm) 8.25-7.25 (25H, m, Ar), 5.75 (1H, dd, $J_{1,2}$ = 1.5, $J_{2,3}$ = 2.4 Hz, H2), 5.71 (1H, d, H1), 5.62 (1H, t, $J_{3,4}$ = $J_{4,5}$ = 9.7 Hz, H4), 5.42 (1H, t, $J_{3',4'}$ = $J_{4',5'}$ = 9.5 Hz, H4'), 5.37 (1H, dd, $J_{2',3'}$ = 2.9 Hz, H3'), 5.09 (1H, d, $J_{1',2'}$ = 1.5 Hz, H1'), 4.56 (1H, dq, H5), 4.45 (1H, dd, H3), 4.08 (1H, dq, H5'), 3.98 (1H, br s, H2'), 2.05 (1H, br s, 2'-O*H*) 1.35 (3H, d, $J_{5,6}$ = 6.4 Hz, H6), 1.17 (3H, d, $J_{5',6'}$ = 6.4 Hz, H6'). ^{13}C NMR (100 MHz, $CDCl_3$): δ (ppm) 166.0, 165.5 (2C) and 164.9 (4C, 4 × OBz), 133.5-127.9 (30C, Ar), 101.5 (1C, C1'), 85.6 (1C, C1), 76.1 (1C, C3), 73.9 (1C, C2), 73.4 (1C, C4), 72.1 (1C, C4'), 71.2 (1C, C2'), 69.4 (1C, C3'), 68.1 (1C, C5), 67.5 (1C, C5'), 17.6 (1C, C6), 17.3 (1C, C6'). MALDI-TOF MS: *m/e* 841.3 (M+Na). Anal. Calcd. for $C_{46}H_{42}O_{12}S$: C, 67.46; H, 5.17. Found C, 67.67; H, 5.11.

5.5.1.4 Phenyl 2-O-acetyl-3,4-di-O-benzoyl-α-L-rhamnopyranosyl-(1→2)-3,4-di-O-benzoyl-α-L-rhamnopyranosyl-(1→3)-2,4-di-O-benzoyl-1-thio-α-L-rhamnopyranoside (10)

A mixture of the disaccharide **9** (4.54 g, 5.54 mmol) and the trichloroacetimidate **7** (3.34 g, 5.98 mmol) in anhydrous CH_2Cl_2 (90 mL) was stirred with freshly activated, crushed 4 Å molecular sieves (4 g) under N_2 for 10 min at room temperature. The mixture was cooled in a -40° C bath and trimethylsilyl triflate (80 μL, 0.45 mmol) was added. After 30 min, the cooling bath was removed and the mixture was allowed to warm to room temperature

over a period of 0.5 h. Triethylamine (0.3 mL) was added and the sieves were removed by filtration through Celite, with the aid of additional CH_2Cl_2 (100 mL). The filtrate was washed with saturated $NaHCO_3$ (50 mL), dried over $MgSO_4$, and concentrated to a syrup. Purification by column chromatography (toluene:EtOAc; 20:1) gave the trisaccharide **10** (5.36 g, 79%) as a colorless, hard foam. ^{1}H NMR (600 MHz, CD_2Cl_2): δ (ppm) 8.25-7.29 (40H, m, Ar), 5.79 (1H, dd, $J_{1,2}$ = 1.8, $J_{2,3}$ = 3.4 Hz, H2), 5.73 (1H, d, H1), 5.67 (1H, dd, $J_{2'',3''}$ = 3.5, $J_{3'',4''}$ = 10.0 Hz, H3''), 5.59 (1H, t, $J_{3,4}$ = $J_{4,5}$ = 9.6 Hz, H4), 5.56 (1H, dd, $J_{2',3'}$ = 3.3 , $J_{3',4'}$ = 10.1 Hz, H3'), 5.46 (1H, t, $J_{4',5'}$ = 9.8 Hz, H4'), 5.45 (1H, dd, $J_{1'',2''}$ = 1.7, Hz, H2''), 5.37 (1H, t, $J_{4'',5''}$ = 9.9 Hz, H4''), 5.23 (1H, d, $J_{1',2'}$ = 1.8 Hz, H1'), 4.60 (1H, d, H1''), 4.58 (1H, dq, H5), 4.50 (1H, dd, H3), 4.11 (1H, dq, H5'), 4.04 (1H, dq, H5''), 3.98 (1H, dd, H2'), 2.00 (3H, s, C*H*$_3$-OAc), 1.34 (3H, d, $J_{5,6}$ = 6.3 Hz, H6), 1.23 (3H, d, $J_{5',6'}$ = 6.3 Hz, H6'), 1.11, (3H, d, $J_{5'',6''}$ = 6.3 Hz, H6''). ^{13}C NMR (100 MHz, CD_2Cl_2): δ (ppm) 169.6 (1C, *C*=O-OAc), 166.3-165.3 (6C, 6 × *C*=O-OBz), 133.9-128.4 (42C, Ar), 100.9 (1C, C1'), 99.5 (1C, C1''), 86.2 (1C, C1), 76.8 (1C, C2'), 76.3 (1C, C3), 74.1 (1C, C2), 73.8 (1C, C4), 71.7 (1C, C4'), 71.6 (1C, C4''), 70.9 (1C, C3'), 69.9 (1C, C3''), 69.8 (1C, C2''), 68.5 (1C, C5), 68.1 (1C, C5'), 67.8 (1C, C5''), 20.8 (1C, *C*H$_3$-OAc), 17.8, 17.6 and 17.5 (3C, C6, C6', C6''). MALDI-TOF MS: *m/e* 1237.4 (M+Na). Anal. Calcd. for $C_{68}H_{62}O_{19}S$: C, 67.20; H, 5.15. Found C, 67.11; H, 5.13.

5.5.1.5 Phenyl 2,3,4-tri-O-acetyα-L-rhamnopyranosyl-(1→2)-3,4-di-O-acetyl-α-L-rhamnopyrano-syl-(1→3)-2,4-di-O-acetyl-1-thio-α-L-rhamnoside (11)

A solution of NaOMe-MeOH (1 M, 10 mL) was added to a suspension of trisaccharide **10** (3.71 g, 3.05 mmol) in anhydrous MeOH (100 mL) and the mixture was stirred at room temperature until the starting material had dissolved (~1 h). The solution was kept in a closed flask for 20 h and then neutralized by stirring with Rexyn 101 H^+ ion-exchange resin. The resin was removed by filtration, and the filtrate was concentrated by rotary evaporation to give a syrupy residue. The residue was extracted by triturating with hexanes (3 × 50 mL) to remove MeOBz. The insoluble trisaccharide was acetylated with acetic anhydride (20 mL) and pyridine (40 mL) for 3 h at rt. The excess reagents were removed by rotary evaporation under high vacuum. The gummy residue was dissolved in Et_2O (150 mL) and washed with saturated $NaHCO_3$ (50 mL), dried over $MgSO_4$, and concentrated to give the trisaccharide **11** as a hard foam (2.72 g, quantitative). ^{1}H NMR (600 MHz, CD_2Cl_2): δ (ppm) 7.51-7.29 (5H, m, Ar), 5.44-5.39 (2H, m, H1, H2), 5.28 (1H, dd, $J_{2'',3''}$ = 3.5, $J_{3'',4''}$ = 10.0 Hz, H3''), 5.25 (1H, dd, H2''), 5.10 (1H, t, $J_{3,4}$ = $J_{4,5}$ = 9.8 Hz, H4), 5.06-4.99 (3H, m, H3', H-', H4''), 4.96 (1H, d, $J_{1',2'}$ = 1.8 Hz, H1'), 4.79 (1H, d, H1''), 4.27 (1H, dq, H5), 4.10 (1H, dd, $J_{2,3}$ = 3.1 Hz, H3), 3.97 (1H, dq, $J_{4'',5''}$ = 9.9 Hz,H5''), 3.92 (1H, dd, $J_{2'3'}$ = 1.9 Hz, H2'), 3.86 (1H, dq, $J_{4',5'}$ = 9.9 Hz, H5'), 2.16, 2.13, 2.11, 2,05, 2.04, 2.03, 1.97 (each 3 H, 7 s, 7 × CH_3-OAc), 1.22 (3 H, d, $J_{5'',6''}$ = 6.3 Hz, H6''), 1.20 (3H, d, $J_{5,6}$ = 6.2 Hz, H6), 1.19 (3H, d, $J_{5',6'}$ = 6.3 Hz, H6'); ^{13}C NMR (100 MHz, CD_2Cl_2):

δ (ppm) 170.5-170.1 (7C, 7 × *C*=O-OAc), 133.7-128.3 (6C, Ar), 100.5 (1C, C1'), 99.9 (1C, C1''), 86.2 (1C, C1), 77.7 (1C, C2'), 75.4 (1C, C3), 73.1 (2C, C2, C4), 71.1, 71.0 and 70.5 (3C, C3', C4' and C4''), 70.1 (1C, C2'), 69.0 (1C, C3''), 68.3 (1C, C5), 67.8 (1C, C5'), 67.6 (1C, C5''), 21.1-20.9 (7C, 7 × *C*H_3-OAc), 17.66, 17.59 and 17.48 (3C, C6, C6', C6''). MALDI-TOF MS: *m*/*e* 865.2 (M+Na). Anal. Calcd. for $C_{38}H_{50}O_{19}S$: C, 54.14; H, 5.98. Found C, 54.02; H, 6.24.

5.5.1.6 2,3,4-Tri-O-acetyl-α-L-rhamnopyranosyl-(1→2)-3,4-di-O-acetyl-α-L-rhamnopyranosyl-(1→3)-2,4-di-O-acetyl-1-thio-α-L-rhamnopyranose (4)

A solution of the trisaccharide phenyl thioglycoside **11** (2.99 g, 3.17 mmol) in CH_2Cl_2 (60 mL) was cooled in an ice-bath while a 1 M solution of IBr in CH_2Cl_2 (40 mL) was added dropwise. The mixture was stirred for 20 min, then diluted with additional cold CH_2Cl_2 (60 mL), and washed with cold 5% aqueous $Na_2S_2O_3$ solution (60 mL) and cold saturated $NaHCO_3$ solution (50 mL). The organic phase was dried over $MgSO_4$, and was then filtered and evaporated to give the trisaccharide glycosyl bromide **12** as a colorless foam. The bromide **12** was immediately dissolved in anhydrous CH_3CN (40 mL) and was slowly warmed to reflux along with thiourea (0.41 g, 5.4 mmol). After 1.5 h at reflux temperature under an N_2 atmosphere, the mixture was cooled and concentrated by rotary evaporation. This yielded the crude isothiouronium salt **13** as a mixture, together with the by-product (diphenyl disulfide) and excess thiourea. Without further purification, the crude product was dissolved in a two-phase mixture of CH_2Cl_2 (40 mL) and water (10 mL) containing $Na_2S_2O_5$ (1.5 g). Hydrolysis of the

isothiouronium salt **13** over 0.5 h was brought about by rapid stirring of the heterogeneous reaction mixture while refluxing under N_2. The mixture was cooled to rt and was diluted with additional CH_2Cl_2 (100 mL). The organic phase was washed with water (50 mL) and saturated NaCl solution (50 mL), dried over $MgSO_4$, and concentrated to give a syrupy residue. Purification by chromatography on silica gel (hexanes-EtOAc; 1:1) gave an α/β mixture of the trisaccharide glycosyl thiol **4** as a colorless syrup (1.52 g, 56% for 3 steps). Selective crystallization of the α-anomer from EtOAc-hexanes gave pure **4** (857 mg) as colorless fine needles. Mp 202-204 °C; $[\alpha]^{25}_D$ -63 (*c* 1.1, $CHCl_3$). ^{1}H NMR (600 MHz, $CDCl_3$): δ (ppm) 5.50 (1H, dd, $J_{1,2}$ = 1.6, $J_{1,SH}$ = 7.0 Hz, H1), 5.32 (1H, dd, $J_{2'',3''}$ = 3.5, $J_{3'',4'}$ 10.1 Hz, H3''), 5.27-5.25 (2H, m, H2, H2''), 5.09 (1H, t, $J_{3,4}$ = $J_{4,5}$ = 9.8 Hz, H4), 5.06 (1H, t, $J_{3'',4''}$ = $J_{4'',5''}$ = 9.8 Hz, H4''), 5.06-5.01 (2H, m, H3, H4), 4.91 (1H, d, $J_{1',2'}$ = 1.8 Hz, H1'), 4.76 (1H, d, $J_{1'',2''}$ = 1.8 Hz, H-1''), 4.25-4.08 (2H, m, H-3, H-5), 3.96 (1H, dq, H-5''), 3.92 (1H, dd, $J_{2'3'}$ = 2.1 Hz, H-2'), 3.83 (1H, dq, $J_{4',5'}$ = 9.9 Hz, H5'), 2.21 (1H, d, S*H*), 2.20, 2.13, 2.12, 2.07, 2.06, 2.04 and 2.00 (each 3H, 7 s, 7 × C*H*$_3$-OAc), 1.22 (3H, d, $J_{5'',6''}$ = 6.3 Hz, H6''), 1.20 (3H, d, $J_{5,6}$ = 6.3 Hz, H6), 1.19 (3H, d, $J_{5',6'}$ = 6.3 Hz, H6'). ^{13}C NMR (150 MHz, $CDCl_3$): δ (ppm) 170.3, 170.3, 170.1, 169.8, 169.8, 169.6, 169.6 (7C, 7 × *C*=O-OAc), 99.9 (1C, C1'), 99.6 (1C, C1''), 77.5 (1C, C2'), 76.6 (1C, C1), 73.8 (1C, C2''), 73.7 (1C, C3), 72.8 (1C, C4), 70.9 (1C, C4''), 70.8 (1C, C4') 70.02 (1C, C3'), 70.0 (1C, C3'), 68.8 (1C, C2'), 68.5 (1C, C3''), 67.9 (1C, C5), 67.4 (1C, C5'), 67.2 (1C, C5''), 20.9, 20.8 (2C), 20.8 (3C), 20.7 and 20.7 (7C, 7 × *C*H$_3$-OAc),

17.4, 17.4 and 17.3 (3C, C6, C6', C6''). MALDI-TOF MS: *m/e* 789.2 (M+Na). Anal. Calcd. for $C_{32}H_{46}O_{19}S$: C, 50.12; H, 6.05. Found C, 50.24; H, 6.17.

5.5.1.7 Fmoc-Met-Asp(OBn)-tryptophanol (14)

L-Tryptophanol[34] (1.97 g, 10.4 mmol), BOC-Asp(OBn)-OH (3.23 g, 10.0 mmol), and HOBt (1.35 g, 10.0 mmol) were combined in dry THF (60 mL). DCC (2.06 g, 10.0 mmol) was added, and the mixture was stirred at rt for 1 h. After filtration to remove dicyclohexylurea (DCU), the solvent was removed by rotary evaporation, and the residue was partitioned between EtOAc (150 mL) and saturated aqueous $NaHCO_3$ (50 mL). The organic phase was washed with 10% citric acid (50 mL), and then with saturated aqueous $NaHCO_3$ (2 × 50 mL) and saturated aqueous NaCl (30 mL). The solution was dried over $MgSO_4$ and was evaporated to an amorphous solid. The crude product was purified by flash chromatography on silica gel (hexanes-EtOAc; 1:2) to give compound BOC-Asp(OBn)-tryptophanol as a colorless hard foam (3.42 g, 69%). ^{1}H NMR (400MHz, $CDCl_3$): δ (ppm) 8.07 (1H, br s, NH ring-Trp), 7.65 (1H, br d, $J_{4,5}$ = 7.9 Hz, H4-Trp), 7.40-7.28 (6H, m, H7-Trp and ArH-Bn), 7.20 (1H, ddd, $J_{6,7}$ = 8.0, $J_{5,6}$ = 7. 1 , $J_{4,6}$ = 1.2 Hz, H6-Trp), 7.13 (1H, ddd, $J_{4,5}$ = 8.0 , $J_{5,7}$ = 1.1 Hz, H5-Trp), 7.06 (1H, d, $J_{1,2}$ = 2.3 Hz, H2-Trp), 6.65 (1H, br d, $J_{NH,\alpha}$ = 7.7 Hz, NH-Trp), 5.54 (1H, br d, $J_{NH,\alpha}$ = 7.8 Hz, NH-Asp), 5.12 and 5.07 (1H each, 2d, $J_{A,B}$ = 12.3 Hz, -OC*H*$_2$- Bn), 4.47 (1H, br m, αH-Asp), 4.23 (1H, m, αH-Trp), 3.66 (1H, dd, $J_{A,B}$ = 11.2 , $J_{A,\alpha}$ = 3.8 Hz, βCH$_2$-Trp), 3.58 (1H, dd, $J_{B,\alpha}$ = 5.3 Hz, βCH$_2$- Trp), 3.06-2.94 (3H, m, βC*H*$_2$- Asp, and C*H*$_2$OH-Trp), 2.73 (1H, dd, $J_{A,B}$ = 17.0 , $J_{B,\alpha}$ = 6.5 Hz, βC*H*$_2$-Asp), 2.45 (1H, br s, OH), 1.40 (9H, s, 3 × BOC). ^{13}C NMR (125

MHz, DMSO-d6): δ 170.6 (2C, 2 × *C*=O), 155.5 (1C, *C*=O-BOC), 136.4-111.3 (14C, C_{Ar}), 78.7 (1C, -O*C*$(CH_3)_3$-BOC), 65.9 (1C, O*C*H_2-Bn), 62.1 (1C, O*C*H_2-Trp), 52.0 (1C, Cα-Trp), 51.4 (1C, Cα-Asp), 36.7 (1C, β*C*H_2-Asp), 28.4 (1C, OC(*C*$H_3)_3$-BOC), 26.6 (1C, β*C*H_2-Trp). HRMS Calcd for $C_{27}H_{33}N_3O_6$: 496.2447. Found: 496.2458.

Dipeptide BOC-Asp(OBn)-Tryptophanol (2.30 g, 4.64 mmol) was dissolved in TFA (20 mL) and was left at rt for 10 min. The TFA was removed by rotary evaporation, and the residue was partitioned between EtOAc (100 mL) and saturated aqueous $NaHCO_3$ solution. The EtOAc phase was again washed with saturated aqueous $NaHCO_3$ solution (30 mL) and then with saturated aqueous NaCl solution (20 mL). The solution was dried over $MgSO_4$ and evaporated to give a colorless syrup.

The crude product H-Asp(OBn)-tryptophanol (0.730 g) was dissolved in dry THF (20 mL). Fmoc-Met (0.693 g, 1.87 mmol) was added, followed by HOBt (0.253 g, 1.87 mmol) and DCC (0.386 g, 1.87 mmol). The mixture was stirred at rt for 1 h and then filtered to remove DCU. The THF was removed to leave a residue, which was only sparingly soluble in EtOAc. Most of the material was brought into solution by rapid stirring with a mixture of EtOAc (150 mL) and saturated aqueous $NaHCO_3$ solution for 0.5 h. The EtOAc layer was then separated and washed with 10% citric acid (30 mL), saturated $NaHCO_3$ solution (30 mL) and saturated NaCl solution (20 mL). The solution was dried ($MgSO_4$) and concentrated to give the crude tripeptide as a pale-yellow solid. Attempted purification by flash chromatography (hexanes-EtOAc; 1:2 to EtOAc) resulted in

only a marginal improvement in purity with the major contaminant (DCU) co-eluting with the product. A suitable solvent for recrystallization could not be found, but eventually a jelly-like solid, with acceptable purity, was obtained by slow cooling of a hot EtOH solution. Pumping of the gel on high vacuum gave the tripeptide **14** as a white solid (0.810 g, 58%). ^{1}H NMR (400 MHz, DMSO-d6): δ 10.8 (1H, br s, NH ring-Trp), 8.35 (1H , d, $J_{\alpha,NH}$ = 8.0 Hz, NH-Asp), 7.90-7.24 (17H, m, 13 ArH-[Fmoc and Bn], H4-, H7-Trp, NH-Met, NH-Trp), 7.10 (1H, d, $J_{1,2}$ = 1.9 Hz, H2-Trp), 7.04 (1H, br t, $J_{5,6} \approx J_{6,7} \approx$ 7.5 Hz, H6-Trp), 6.95 (1H, br t, $J_{5,6} \approx J_{4,5} \approx$ 7.5 Hz, H5-Trp), 5.06 (2H, br s, OCH_2 -Bn), 4.68 (1H, t, J = 5.5 Hz, O*H*-Trp), 4.64 (1H, m, αH-Asp), 4.34-4.16 (3H, m, CH_2-Fmoc and, H9-Fmoc), 4.08 (1H, m, αH-Met), 3.92 (1H, m, αH-Trp), 3.32 (2H, m, βCH_2-Trp), 2.86 (2H, br dd, βCH_2-Trp, βCH_2-Asp), 2.74 (1H, dd, $J_{A,B}$ = 14.4, $J_{\alpha,B}$ = 5.9 Hz, βCH_2 -Trp), 2.66 (1H, dd, $J_{A,B}$ = 11.1, $J_{\alpha,B}$ = 8.3 Hz, βCH_2-Asp), 2.49 (2H, br t, J = 7.4 Hz, SCH_2-Met), 2.01 (3H, s, SCH_3-Met), 1.84 (2H, m, βCH_2-Met). ^{13}C NMR (100 MHz, DMSO-d6): δ 171.5, 170.1 169.6 (3C, 3 × C=O), 156.1 (1C, C=O-Fmoc), 143.9-111.0 (26C, C_{Ar}), 65.7 (2C, O*C*H$_2$-Fmoc, O*C*H$_2$-Bn), 61.8 (1C, O*C*H$_2$-Trp), 54.0 (1C, Cα-Met), 51.9 (1C, Cα-Trp), 49.6 (1C, Cα-Asp), 46.6 (1C, C9-Fmoc), 36.1 (1C, Cβ-Asp), 31.4 (1C, t, Cβ-Met), 29.5 (1C, S*C*H$_2$-Met), 26.3 (1C, Cβ-Trp), 14.6 (1C, S*C*H$_3$-Met). HRMS Calcd for $C_{39}H_{46}N_4O_7S$: 749.3008. Found: 749.3014.

5.5.1.8 Fmoc-Met-Asp(OBn)-tryptophanyl bromide (5)

The tripeptide alcohol **14** (0.157 g, 0.210 mmol) was dispersed with stirring in CH_2Cl_2 (5 mL). Triphenylphosphine (0.121 g, 0.461 mmol) and CBr_4

(0.163 g, 0.491 mmol) were added, which resulted in the peptide dissolving within 10 min to give a homogeneous yellow solution. After a further 10 min, the solvent was removed to yield the crude product as a sticky yellow gum. This was purified by flash chromatography on silica gel (hexanes-EtOAc; 1:1 to 1:2) to provide the bromide **5** as a pale yellow solid. This material was only of limited stability at rt and was generally used immediately in the next step. ^{1}H NMR (400 MHz, $CDCl_3$): δ (ppm) 8.13 (1H, br s, NH ring-Trp), 7.78-7.22 (17H, m, ArH-[Fmoc and Bn], H4-, H7-Trp, NH-Met, NH-Asp), 7.19 (1H, ddd, $J_{6,7}$ = 8.0, $J_{5,6}$ = 7.1, $J_{4,6}$ = 1.2 Hz, H6-Trp), 7.13 (1H, ddd, $J_{4,5}$ = 8.0, $J_{4,6}$ = 1.0 Hz, H5-Trp), 7.05 (1H, d, $J_{1,2}$ = 2.3 Hz, H2-Trp), 6.81 (1H, br d, $J_{NH,\alpha}$ = 7.7 Hz, NH-Trp), 5.34 (1H, br d, $J_{NH,\alpha}$ = 7.7 Hz, NH-Met), 5.10 (2H, br s, OCH_2-Bn), 4.79 (1H, m, αH-Asp), 4.48-4.37 (3H, m, CH_2-Fmoc, αH-Trp), 4.27-4.17 (2H, m, H9-Fmoc, αH-Met), 3.51 (1H, dd, $J_{A,B}$ = 10.3, $J_{\alpha,A}$ = 4.8 Hz, CH_2Br-Trp), 3.39 (1H, dd, $J_{\alpha,B}$ = 4.1 Hz, CH_2Br-Trp), 3.11-2.99 (3H, m, βCH_2-Trp, βCH_2-Asp), 2.71 (1H, dd, $J_{A,B}$ = 17.2, $J_{\alpha,B}$ = 6.4 Hz, Asp βCH_2-Asp), 2.45 (2H, br m, SCH_2-Met), 2.07 (4H, br s, βCH_2-Met, SCH_3-Met), 1.84 (1H, m, βCH_2-Met). MALDI-TOF MS: *m/e* 833.4 (M+Na).

5.5.1.9 Protected glycopeptide 3

The trisaccharide thiol **4** (0.098g, 0.13 mmol) and the tripeptide bromide **5** (0.103 g, 0.127 g) were combined in EtOAc (15 mL) and stirred with saturated aqueous $NaHCO_3$ (2 mL). Bu_4NHSO_4 (0.032 g) was added, and the mixture was stirred rapidly at rt for 5 h. The reaction mixture was diluted with EtOAc (50 mL) and water (20 mL), and the separated aqueous phase was further extracted with EtOAc (30 mL). The combined extracts were dried over $MgSO_4$ and were

concentrated to dryness. The residue was purified by flash chromatography on silica gel (hexanes-EtOAc; 1:2) to give the product as a colorless solid (43 mg). Analysis by ^{1}H NMR spectroscopy indicated a purity of approximately 80%, along with one major, unidentified contaminant that exhibited only peptide resonances. Further purification by preparative HPLC (C-18 reverse phase, 80:20 to 5:95 H_2O-CH_3CN over 30 min) gave the pure glycopeptide **3** as a colorless solid (30 mg, 16%). ^{1}H NMR (400 MHz, CD_2Cl_2): δ (ppm) 8.31 (1H, br s, NH ring-Trp), 7.81-7.28 (15H, m, 13 ArH-[Fmoc and Bn], H4-, H7-Trp), 7.20 (1H, br d, $J_{\alpha,NH}$ = 8.5 Hz, NH-Asp), 7.15 (1H, ddd, $J_{6,7}$ = 8.1, $J_{5,6}$ = 7.3, $J_{4,6}$ = 1.0 Hz, H6-Trp), 7.08 (1H, ddd, $J_{4,5}$ = 7.9, $J_{4,6}$ = 0.9 Hz, H5-Trp), 7.01 (1H, d, $J_{1,2}$ = 2.2 Hz, H2-Trp), 6.72 (1H, br d, $J_{\alpha,NH}$ = 8.0 Hz, NH-Trp), 5.38 (1H, br d, $J_{\alpha,NH}$ = 7.1 Hz, NH-Met), 5.29-5.20 (4H, m, H2-, H2''-, H3'-, H3''-rha), 5.11-4.99 (6H, m, OCH_2-Bn, H1-, H4-, H4'-, H4''-rha), 4.92 (1H, d, $J_{1,2}$ = 1.6 Hz, H1'-rha), 4.77 (1H, d, $J_{1,2}$ = 1.5 Hz, H1''-rha), 4.70 (1H, m, αH- Asp), 4.47 (1H, dd, $J_{A,B}$ = 10.5, $J_{A,9}$ = 6.7 Hz, CH_2-Fmoc), 4.41-4.29 (2H, m, CH_2-Fmoc, αH-Trp), 4.22 (1H, t, J = 6.7 Hz, H9-Fmoc), 4.17 (1H, m, αH-Met), 4.10 (1H, m, H5-rha), 4.02 (1H, dd, $J_{2,3}$ = 3.4, $J_{3,4}$ = 9.8 Hz, H3-rha), 3.95 (1H, m, H5-rha), 3.89 (1H, dd, $J_{1',2'}$ = 1.6, $J_{2'3'}$ = 3.4 Hz, H2'-rha), 3.83 (1H, m, H5-rha), 3.04-2.92 (3H, m, βCH_2-Trp, βCH_2-Asp), 2.80-2.69 (3H, m, SCH_2-Trp, βCH_2-Asp), 2.44 (2H, br t, J = 6.8 Hz, SCH_2-Met), 2.16 (3H, s, CH_3-OAc), 2.12 (3H, s, CH_3-OAc), 2.08 (3H, s, CH_3-OAc), 2.06 (3H, s, SCH_3- Met), 2.07 (9H, s, 3 × CH_3-OAc), 2.01 (1H, m, βCH_2-Met), 1.98 (3H, s, CH_3-OAc), 1.77 (1H, m, βCH_2-Met), 1.19 (3H, d, J = 6.3 Hz, H6-rha) 1.16 (3H, d, J = 6.3 Hz, H6-rha) 1.13 (3H, d, J = 6.2 Hz, H6-rha). ^{13}C NMR (100 MHz, CD_2Cl_2): δ 171.9-

169.8 (11C, 11 × C=O), 156.8 (1C, C=O-Fmoc), 144.2-111.2, (26C, C_{Ar}), 100.4 (1C, C1''-rha), 99.9 (1C, C1'-rha), 83.5 (1C, C1-rha) , 77.8 (1C, C2'-rha), 75.4 (1C, C3'-rha), 73.3 (1C, C2-rha), 73.2 (1C, C3'-rha), 71.1 (2C, 2 × C4-rha), 70.5 (1C, C4-rha), 70.1 (1C, C2''-rha), 69.1(1C, C3''-rha) , 67.8 (2C, 2 × C5-rha), 67.6 (1C, C5-rha), 67.5 (1C, *C*H_2-Fmoc), 67.1 (1C, O*C*H_2-Bn), 55.0 (1C, Cα-Met), 50.6 (1C, Cα-Trp), 50.0 (1C, Cα-Asp), 47.6 (1C, C9-Fmoc), 36.0 (1C, S*C*H_2-Trp), 35.7 (1C, Cβ-Asp), 31.1 (1C, Cβ-Met), 30.5 (1C, S*C*H_2-Met), 29.4 (1C, Cβ-Trp), 21.1-20.9 (7C, 7 × OAc) 17.7, 17.6, 17.4, (3C, 3 × C6-rha), 15.5 (1C, S*C*H_3-Met). MALDI-TOF MS: *m/e* 1519.9 (M+Na).

5.5.1.10 Attempted deprotection of glycopeptide 3

The protected glycopeptide **3** (30 mg) was treated with 0.1 M NaOMe in MeOH (4 mL) for 5 h at rt. The reaction mixture was neutralized by addition of HOAc, filtered, and concentrated to a solid residue. Flash chromatography on silica gel (EtOAc-MeOH-H_2O; 4:2:1) and combining of those fractions that appeared as a single spot on TLC gave a product free from protecting-group remnants. However, analysis by HPLC showed this to be a mixture of four closely eluting compounds with a ratio of 2:2:1:1. The MALDI mass spectrum of the mixture showed a single, major mass corresponding to loss of 18 mass units from the expected glycopeptide **1** (Calcd for $C_{38}H_{58}N_4O_{16}S_2Na$ (M+Na) 913.31, Found 895.15). The ^{1}H NMR spectrum in CD_3OD also indicated a mixture of compounds, as judged by the presence of several SC*H*$_3$ singlets near δ 2.0 as well as a complicated pattern of overlapping rhamnose C*H*$_3$ resonances near δ 1.3.

5.5.1.11 Fmoc-Met-Asp(OtBu)-tryptophanol 20

L-Tryptophanol[34] (3.77 g, 19.8 mmol), Fmoc-Asp(O*t*-Bu)-OH (8.09 g, 19.7 mmol), and HOBt (2.67 g, 19.7 mmol) were combined in dry THF (70 mL). DCC (4.07 g, 19.7 mmol) was added, and the mixture was stirred at rt for 1 h. After filtration to remove DCU, the solvent was removed by rotary evaporation, and the residue was partitioned between EtOAc (250 mL) and saturated aqueous $NaHCO_3$ (50 mL). The organic phase was washed with 10% citric acid (50 mL), then with saturated aqueous $NaHCO_3$ (2 × 50 mL) and saturated aqueous NaCl (50 mL). The solution was dried over $MgSO_4$ and evaporated to an amorphous solid. The crude product was purified by flash chromatography on silica gel (hexanes-EtOAc; 1:2) to give Fmoc-Asp(O*t*Bu)-Tryptophanol as a colorless hard foam (9.11 g, 79%). ^{1}H NMR (400MHz, $CDCl_3$): δ (ppm) 8.07 (1H, br s, NH-Trp ring),), 7.82-7.22 (10H, m, H4-, H7-Trp, ArH-Fmoc), 7.16 (1H, br t, $J_{5,6} \approx J_{6,7} \approx$ 7.4 Hz, H6-Trp), 7.13 (1H, ddd, $J_{4,5}$ = 7.9, $J_{5,7}$ = 0.8 Hz, H5-Trp), 7.06 (1H, d, $J_{1,2}$ = 1.5 Hz, H2-Trp), 6.61 (1H, br d, $J_{NH,\alpha}$ = 7.0 Hz, NH-Trp), 5.76 (1H, br d, $J_{NH,\alpha}$ = 8.4 Hz, NH-Asp), 4.47 (1H, br m, αH-Asp), 4.40 (1H, dd, $J_{A,B}$ = 10.5, $J_{A,9}$ = 7.2 Hz, CH_2-Fmoc), 4.33 (1H, dd, $J_{B,9}$ = 7.0 Hz, CH_2-Fmoc), 4.23 (1H, m, αH-Trp), 4.19 (1H, br t, $J \approx$ 7.0 Hz, H9-Fmoc), 3.70 (1H, dd, $J_{A,B}$ = 11.2, $J_{A,\alpha}$ = 3.4 Hz, CH_2OH- Trp), 3.61 (1H, dd, $J_{B,\alpha}$ = 5.6 Hz, CH_2OH-Trp), 3.03 (1H, dd, $J_{A,B}$ = 17.4, $J_{A,\alpha}$ = 7.0 Hz, βCH_2-Trp), 2.98 (1H, dd, $J_{B,\alpha}$ = 7.0 Hz, βCH_2-Trp), 2.84 (1H, dd, $J_{A,B}$ = 17.1, $J_{A,\alpha}$ = 7.1 Hz, βCH_2-Asp), 2.61 (1H, dd, $J_{B,\alpha}$ = 6.8 Hz, βCH_2-Asp), 2.02 (1H, br s, OH), 1.41 (9H, s, *t*Bu). ^{13}C NMR (125 MHz, DMSO-d6): δ 170.5, 169.7 (2C, 2 × C=O), 156.1 (1C, C=O-Fmoc), 144.1-111.4 (20C, C_{Ar}), 80.4 (1C,

O*C*(CH_3)$_3$- *t*Bu), 66.1 (1C, O*C*H_2-Fmoc), 62.3 (1C, O*C*H_2-Trp), 52.1 (1C, Cα-Trp), 51.9 (1C, Cα-Asp), 46.9 (1C, C9-Fmoc), 38.2 (1C, β*C*H_2-Asp), 28.0 (1C, OC(*C*H_3)$_3$- *t*Bu), 26.6 (1C, β*C*H_2-Trp). HRMS Calcd for $C_{34}H_{37}N_3O_6$: 584.2760. Found: 584.2758.

The Fmoc-protected dipeptide Fmoc-Asp(OtBu)-Tryptophanol (8.31 g, 14.2 mmol) was dissolved in dry DMF containing 20% v/v piperidine (100mL). After 10 min at rt, the solvents were removed by rotary evaporation under high vacuum to give the free amino compound H-Met-Asp(OtBu)-Tryptophanol as a crystalline solid residue. This was dissolved in dry THF (100 mL) and Fmoc-Met-OH (5.34 g, 14.3 mmol) was added, followed by HOBt (1.90 g, 14.1 mmol) and DCC (2.97 g, 14.3 mmol). The mixture was stirred at rt for 15 h and then filtered to remove DCU. The THF was removed to leave a residue that was partitioned between EtOAc (250 mL) and saturated aqueous $NaHCO_3$ (50 mL). The EtOAc layer was separated and washed with 10% citric acid (50 mL), saturated aqueous $NaHCO_3$ (2 × 50 mL) and saturated aqueous NaCl (50 mL). The solution was dried ($MgSO_4$) and concentrated to give the crude tripeptide as a pale-yellow solid. Purification by flash chromatography (EtOAc) gave the protected tripeptide **20** as a white solid (8.65 g, 85%). ^{1}H NMR (500 MHz, $CDCl_3$): δ (ppm) 8.12 (1H, br s, NH ring-Trp), 7.80-7.28 (11H, m, 8 × ArH-Fmoc, H4-, H7-Trp, NH-Asp), 7.17 (1H, br t, $J_{5,6} \approx J_{6,7} \approx 7.5$ Hz, H6-Trp), 7.10 (1H, br t, $J_{5,6} \approx J_{4,5} \approx 7.5$ Hz, H5-Trp), 7.04 (1H, br s, H2-Trp), 6.84 (1H, d, $J_{\alpha,NH} = 8.0$ Hz, NH-Trp), 5.57 (1H, d, $J_{\alpha,NH} = 6.8$ Hz, NH-Met), 4.70 (1H, m, αH-Asp), 4.46 (1H, dd, $J_{A,B} = 10.7$, $J_{A,9} = 6.9$ Hz, CH_2-Fmoc), 4.42 (1H, dd, $J_{B,9} = 6.9$ Hz, CH_2-Fmoc), 4.28-4.18 (3H, m, αH-Met,

αH-Trp, H9-Fmoc), 3.70 (1H, dd, $J_{A,B}$ = 11.4, $J_{A,\alpha}$ = 3.4 Hz, CH_2OH- Trp), 3.60 (1H, dd, $J_{B,\alpha}$ = 5.3 Hz, CH_2OH- Trp), 3.02 (1H, dd, $J_{A,B}$ = 14.7, $J_{\alpha,A}$ = 7.5 Hz, βCH_2-Trp), 2.97 (1H, dd, $J_{\alpha,B}$ = 6.4 Hz, βCH_2-Trp), 2.90 (1H, dd, $J_{A,B}$ = 16.8, $J_{\alpha,A}$ = 4.3 Hz, βCH_2-Asp), 2.59 (1H, dd, $J_{\alpha,B}$ = 6.4 Hz, βCH_2-Asp), 2.48 (2H, m, SCH_2-Met), 2.30 (1H, br s, OH), 2.08 (3H, s, SCH_3-Met), 2.05 (1H, m, βCH_2-Met), 1.86 (1H, m, βCH_2-Met), 1.37 (9H, s, O*t*Bu). ^{13}C NMR (125 MHz, DMSO-d6): δ 171.4, 169.7 169.4 (3C, 3 × C=O), 156.1 (1C, C=O-Fmoc), 143.9-111.1 (20C, Ar), 80.5 (1C, O*t*Bu), 65.7 (1C, *C*H_2-Fmoc), 61.9 (1C, O*C*H_2-Trp), 54.0 (1C, Cα-Met), 51.9 (1C, Cα-Trp), 49.7 (1C, Cα-Asp), 46.6 (1C, C9-Fmoc), 37.3 (1C, β*C*H_2-Asp), 31.5 (1C, β*C*H_2-Met), 29.5 (1C, S*C*H_2-Met), 27.6 (1C, O*t*Bu), 26.3 (1C, β*C*H_2-Trp), 14.6 (1C, S*C*H_3-Met). HRMS Calcd. for $C_{39}H_{46}N_4O_7S$: 715.3165. Found: 715.3159.

5.5.1.12 Glycopeptide 18

The protected tripeptide **20** (1.08 g, 1.51 mmol) was dissolved in CH_2Cl_2 (30 mL) and stirred at rt while triphenylphosphine (0.550 g, 1.10 mmol) and CBr_4 (0.709 g, 2.14 mmol) were added. After 1 h, additional CH_2Cl_2 (50 mL) was added and the solution was washed with saturated aqueous $NaHCO_3$ (20 mL), dried over $MgSO_4$, and concentrated. The residue was purified by flash chromatography (hexanes-EtOAc; 1:2) to give the tripeptide bromide **19** as a pale-yellow foam (1.24 g). This material was only of limited stability at rt and was used immediately in the next step.

The bromide (1.24 g, 1.59 mmol) was combined with the trisaccharide thiol **4** (0.771 g, 1.01 mmol) in EtOAc (50 mL) and was stirred with saturated

aqueous $NaHCO_3$ (20 mL). Bu_4NHSO_4 (0.223 g) was added, and the mixture was stirred rapidly at rt for 6 h. The reaction mixture was diluted with EtOAc (50 mL) and water (20 mL), and the separated aqueous phase was further extracted with EtOAc (30 mL). The combined extracts were washed with 10% citric acid (30 mL), and saturated aqueous $NaHCO_3$ (2 × 30 mL), were then dried over $MgSO_4$ and concentrated to dryness. The residue was purified by flash chromatography on silica gel (hexanes-EtOAc; 1:2 to 100% EtOAc) to give the product as a colorless, hard foam (1.01g). Analysis by ^{1}H NMR spectroscopy indicated that this material was a mixture of the expected glycopeptide **18** (>80%) along with a single impurity that exhibited only typical rhamnose resonances. An analytical sample was further purified by preparative HPLC (C-18 reverse phase, 95:5 to 5:95 H_2O-CH_3CN over 40 min) to give first, an impurity, a compound that was tentatively identified as the disulfide **15** resulting from oxidation of the trisaccharide thiol **4**, and then, the pure glycopeptide **18** as a pure colorless solid (16%). ^{1}H NMR (500 MHz, CD_2Cl_2): δ (ppm) 8.34 (1H, br s, NH ring-Trp), 7.82-7.30 (10H, m, 8× ArH-Fmoc, H4-, H7-Trp), 7.26 (1H, br d, $J_{\alpha,NH}$ = 8.3 Hz, NH-Asp), 7.16 (1H, br t, $J_{5,6} \approx J_{6,7} \approx$ 7.5 Hz, H6-Trp), 7.09 (1H, br t, $J_{5,6} \approx J_{4,5} \approx$ 7.5 Hz, H5-Trp), 7.05 (1H, d, $J_{1,2}$ = 2.1 Hz, H2-Trp), 6.77 (1H, br d, $J_{\alpha,NH}$ = 8.2 Hz, NH-Trp), 5.50 (1H, br d, $J_{\alpha,NH}$ = 7.2 Hz, NH-Met), 5.30-5.23 (3H, m, H2-, H2''-, H3''-rha), 5.22 (1H, br s, H1-rha), 5.11-4.99 (4H, m, H-3', H4-, H4'-, H4''-rha), 4.93 (1H, d, $J_{1,2}$ = 1.5 Hz, H1'-rha), 4.78 (1H, d, $J_{1,2}$ = 1.4 Hz, H1''-rha), 4.65 (1H, m, αH-Asp), 4.47 (1H, dd, $J_{A,B}$ = 10.5, $J_{A,9}$ = 7.1 Hz, CH_2-Fmoc), 4.41 - 4.33 (2H, m, CH_2-Fmoc, αH-Trp), 4.26-4.19 (2H, m, H9-Fmoc, αH-Met), 4.11 (1H, m, H5-

rha), 4.03 (1H, dd, $J_{2,3}$ = 3.4, $J_{3,4}$ = 9.8 Hz, H3-rha), 3.96 (1H, m, H5-rha), 3.90 (1H, br m, H2'-rha), 3.84 (1H, m, H5-rha), 3.02 (2H, d, J = 6.3 Hz, βCH_2-Trp), 2.83 (1H, dd, $J_{A,B}$ = 16.8, $J_{\alpha,A}$ = 4.8 Hz, βCH_2-Asp), 2.78 (2H, d, J = 6.4 Hz, SCH_2-Trp), 2.60 (1H, dd, $J_{\alpha,B}$ = 6.1 Hz, βCH_2-Asp), 2.49 (2H, br t, J = 6.8 Hz, SCH_2-Met), 2.17 (3H, s, CH_3-OAc), 2.13 (3H, s, CH_3-OAc), 2.10 (3H, s, CH_3-OAc), 2.08 (3H, s, -SCH_3-Met), 2.05 (1H, m, βCH_2-Met), 2.04 (9H, s, 3 × CH_3-OAc), 1.99 (3H, s, CH_3-OAc), 1.85 (1H, m, βCH_2- Met), 1.41 (9H, s, O*t*Bu), 1.21 (3H, d, J = 6.3 Hz, CH_3-rha) 1.18 (3H, d, J = 6.3 Hz, CH_3-rha) 1.14 (3H, d, J = 6.2 Hz, CH_3-rha). ^{13}C NMR (100 MHz, CD_2Cl_2): δ 171.3-169.7 (11C, 11×C=O), 156.5 (1C, C=O- Fmoc), 144.0-111.2, (20C, C_{Ar}), 100.2 (1C, C1''-rha), 99.8 (1C, C1'-rha), 83.4 (1C, C1-rha) , 77.7 (1C, C2'-rha), 75.3 (1C, C3'-rha), 73.2 (1C, C2-rha), 73.1 (1C, C3'-rha), 71.0 (2C, 2 × C4-rha), 70.5 (1C, C4-rha), 70.1 (1C, C2''-rha), 69.0 (1C, C3''-rha), 67.8 (1C, C5-rha), 67.7 (2C, 2 × C5-rha), 67.6 (1C, *C*H_2-Fmoc), 54.9 (1C, Cα-Met), 50.5 (1C, Cα-Trp), 49.9 (1C, Cα-Asp), 47.5 (1C, C9-Fmoc), 36.7 (1C, β-*C*H_2-Asp), 35.9 (1C, S*C*H_2-Trp), 31.3 (1C, β*C*H_2-Met), 30.5 (1C, S*C*H_2-Met), 29.4 (1C, β*C*H_2-Trp), 28.1 (1C, O*t*Bu), 21.1-20.8 (7C, 7 × CH_3-OAc) 17.7, 17.6, 17.4, (3C, 3 × C6-rha), 15.5 (1C, S*C*H_3-Met). HRMS Calcd for $C_{71}H_{90}N_4O_{25}S_2$: 1463.5413. Found: 1463.5393.

5.5.1.13 Deprotection of glycopeptide 18

The partially purified glycopeptide **18** (>80% pure, 0.510 g, ≈0.279 mmol) was dissolved in CH_2Cl_2 (20 mL). Tri-isopropylsilane (0.3 mL) and TFA (6.0 mL) were added, and the mixture was kept at rt for 2.5 h. The solvents were evaporated, and the residue was partitioned between CH_2Cl_2 (80 mL) and

saturated aqueous $NaHCO_3$ (30 ml). The emulsified organic phase was separated and washed with 2 M HCl (30 mL) and saturated aqueous NaCl (2 × 30 mL). The solvents were removed and the residue was purified by flash chromatography (EtOAc-MeOH; 10:1 to 4:1) to give the purified, free β-carboxylic acid-aspartate, glycopeptide. At this stage the impurity that was present in the protected glycopeptide was easily separated as a faster running component and was characterized as the acetylated trisaccharide 1,1'-disulfide **15** by NMR and MALDI spectra (data not shown).

The glycopeptide fraction was dissolved in 0.2M NaOMe in MeOH (12 mL) and was kept at rt for 6 h. The base was neutralized by addition of acetic acid and the volatile material was removed under reduced pressure. Purification by flash chromatography (EtOAc-MeOH-H_2O; 4:2:1) gave the glycopeptide **1** as a colorless solid. Analysis of the product by ^1H NMR indicated the presence of NaOAc (19 wt %, singlet at δ 1.78). This led, after allowing for this impurity, to an estimate of 32% for the yield of the deprotection sequence. ^1H NMR (500 MHz, D_2O): δ (ppm) 7.69 (1H, d, $J_{4,5}$ = 7.5 Hz, H4-Trp), 7.47 (1H, d, $J_{6,7}$ = 8.0 Hz, H7-Trp), 7.24 (1H, br s, H2-Trp), 7.21 (1H, br t, $J_{5,6} \approx J_{6,7} \approx$ 8.0 Hz, H6-Trp), 7.14 (1H, br t, H5-Trp), 5.13 (2H, br s, 2 × H1-rha), 4.93 (1H, d, $J_{1,2}$ = 1.5 Hz, H1-rha), 4.63 (1H, dd, α-H Asp), 4.26 (1H, m, αH Trp), 4.08-4.01 (4H, m, 3 × H2-rha, αH-Met), 3.96 (1H, m, H5-rha), 3.89 (1H, dd, $J_{2,3}$ = 3.4, $J_{3,4}$ = 9.9 Hz, H3-rha), 3.76 (1H, dd, $J_{2,3}$ = 3.4, $J_{3,4}$ = 9.8 Hz, H3-rha), 3.73 (1H, m, H5-rha), 3.69 (1H, dd, $J_{2,3}$ = 3.3, $J_{3,4}$ = 9.7 Hz, H3-rha), 3.67 (1H, m, H5-rha), 3.51(t, 1H, J = 9.6, H4-rha), 3.45 (1H, t, J = 9.7 Hz, H4-rha), 3.41(1H, t, J = 9.7 Hz, H4-rha), 3.09 (1H, dd, $J_{A,B}$

= 14.7 Hz, $J_{A,\alpha}$ = 5.8 Hz, β-CH_2 Trp), 2.96 (1H, dd, $J_{B,\alpha}$ = 7.3 Hz, β-CH_2 Trp), 2.92 (1H, dd, $J_{A,B}$ = 13.7, $J_{A,\alpha}$ = 4.3 Hz, -SCH_2 Trp), 2.79 (1H, dd, $J_{B,\alpha}$ = 9.2 Hz, -SCH_2 Trp), 2.63 (1H, dd, $J_{A,B}$ = 16.0, $J_{\alpha,A}$ = 4.6 Hz, β-CH_2 Asp), 2.49 (1H, dd, $J_{\alpha,B}$ = 9.9 Hz, β-CH_2 Asp), 2.44 (1H, dt, $J_{A,B}$ = 13.5, $J_{\beta,A}$ = 7.4 Hz, SCH_2-Met), 2.33 (1H, dt, $J_{\beta,B}$ = 7.2 Hz, SCH_2-Met), 2.02 (2H, m, βCH_2-Met), 1.96 (3H, s, SCH_3-Met), 1.25 (3H, d, J = 6.3 Hz, CH_3-rha) 1.23 (3H, d, J = 6.4 Hz, CH_3-rha) 1.22 (3H, d, J = 6.3 Hz, CH_3-rha). ^{13}C NMR (125 MHz, D_2O): δ 177.3, 172.2, 168.7 (each 1C, 3 × C=O), 136.2, 127.3, 124.4, 121.9, 119.4, 118.7, 112.0, 110.3 (each, 1C, 8 × C_{Ar}-Trp), 102.4 (1C, C1''-rha), 100.9 (1C, C1'-rha), 86.6 (1C, C1-rha), 78.2 (1C, C2'-rha), 77.8 (1C, C3-rha), 72.2, 72.1, 71.9 (each 1C, 3 × C4-rha), 70.2, 70.1, 70.0 (each 1C, 2 × C3-, C2-rha), 69.5, 69.4, 69.3 (each 1C, 3 × C5-rha), 52.3 (1C, Cα Met), 52.0 (1C, Cα-Asp), 51.3 (1 C, Cα-Trp), 39.4 (1C, βCH$_2$-Asp), 36.1 (1C, SCH$_2$-Trp), 30.0 (1C, βCH$_2$-Met), 29.4 (1C, βCH$_2$-Trp), 28.2 (1C, SCH$_2$-Met), 16.8, (2C, 2 × C6-rha), 16.7 (1C, C6-rha), 14.2 (1C, SCH$_3$-Met). MALDI MS: Calcd for $C_{38}H_{58}N_4O_{16}S_2Na$ (M+Na) 913.31. Found 913.11.

5.5.1.14 Bromide 21

To a stirred mixture of L-tryptophanol[34] (3.04g, 16 mmol) and $NaHCO_3$ (1.34 g) in water and acetone (50 mL, 1:1) was added Fmoc-OSu (5.3 g, 16 mmol). After 5 min, a thick white precipitate formed, and the reaction was stirred at rt for 1 h. The solid was then collected by filtration, and was washed with hot water (100 mL) and hot ether (100 mL) to afford Fmoc-tryptophanol (6.3 g, 95%) as a white solid. ^{1}H NMR (500 MHz, acetone-d_6): δ (ppm) 10.02 (1H, br s, NH ring-Trp), 7.85 (2H, d, J = 7.6 Hz, H4-, H5-Fmoc), 7.72 (1H, d, J = 7.7 Hz, H4-

Trp), 7.68 (2H, d, *J* = 6.9 Hz, H1-, H8-Fmoc), 7.41 (2H, d, H3-, H6-Fmoc), 7.36 (1H, d, *J* = 7.8 Hz, H7-Trp), 7.30 (2H, dd, H2-, H7-Fmoc), 7.20 (1H, br s, H2-Trp), 7.09 (1H, br t, *J* = 7.3 Hz, H6-Trp), 7.02 (1H, br t, *J* = 7.3 Hz, H5-Trp), 6.31 (1H, d, *J* = 8.4 Hz, NH-Trp), 4.34 (1H, dd, *J* = 11.0, 7.3 Hz, C*H*$_2$-Fmoc), 4.27 (1H, dd, C*H*$_2$-Fmoc), 4.20 (1H, dd, H9-Fmoc), 4.08-3.96 (1H, m, αH-Trp), 3.68-3.58 (2H, m, C*H*$_2$OH-Trp), 3.09 (1H, dd, *J* = 13.9, 6.9 Hz, βC*H*$_2$-Trp), 3.00 (1H, dd, *J* = 7.3 Hz, βC*H*$_2$-Trp), 2.89 (1H, br s, CH$_2$O*H*-Trp). ^{13}C NMR (150 MHz, acetone-d$_6$): δ (ppm) 156.3 (1C, C=O-urethane), 144.5 (2C, C8a-, C9a-Fmoc), 141.4 (2C, C4a-, C4b-Fmoc), 137.0 (1C, C3a-Trp), 128.3 (1C, C7a-Trp), 127.8 (2C, C3-, C6-Fmoc), 127.2 (2C, C2-, C7-Fmoc), 125.5 (2C, C1-, C8-Fmoc), 123.4 (1C, C2-Trp), 121.4 (1C, C5-Trp), 120.1 (2C, C4-, C5-Fmoc), 118.9 (1C, C4-Trp), 118.8 (1C, C6-Trp), 112.1 (1C, C3-Trp), 111.4 (1C, C7-Trp), 66.1 (1C, *C*H$_2$-Fmoc), 63.5 (1C, *C*H$_2$OH), 54.2 (1C, Cα-Trp), 47.6 (1C, C9-Fmoc), 27.1 (1C, β*C*H$_2$-Trp). MALDI-TOF MS: *m*/*e* 435.7 (M+Na), 413.4 (M+H). Anal. Calcd. for $C_{26}H_{24}N_2O_3$: C, 75.71; H, 5.86; N 6.79. Found: C, 76.02; H, 5.93; N 6.54.

Method 1: To a stirred mixture of Fmoc-tryptophanol (0.98 g, 2.4 mmol) and CBr_4 (1.34g, 4 mmol) in dry CH_2Cl_2 at 0 °C was added PPh_3 (1.25 g, 4.8 mmol) in portions. The reaction mixture was stirred at 0 °C for 2 h and was then concentrated under reduced pressure at rt. The residue was then purified by flash chromatography (Hexanes-EtOAc; 3:1) to afford the bromide **21** as a pale-yellow powder (0.79 g, 65%). The spectral data were the same as for the compound obtained with *method 2* (see below).

Method 2: To a stirred solution of Fmoc-tryptophanol (3g, 7.3 mmol) in pyridine (150 mL) at 0 ^{o}C under a N_2 atmosphere was added MsCl (0.7 mL, 11 mmol). The reaction mixture was stirred at 0 ^{o}C for 1 h and at rt for 4 h. The reaction was then quenched with ice and the solvent was evaporated. The residue was then dissolved in EtOAc (500 mL) and washed with water (300 mL), saturated aqueous $NaHCO_3$ (300 mL), dried over Na_2SO_4, and the solvent was evaporated. The crude material containing LiBr (5.1g, 58.4 mmol) in THF (75 mL) was refluxed under a N_2 atmosphere for 4 h. The solvent was then evaporated, and the mixture was diluted with EtOAc (500 mL), washed with water (5 $\times$ 300 mL), brine (200 mL), dried over Na_2SO_4, and the solvent was evaporated. The residue was then purified by column chromatography (hexanes-EtOAc; 3:1) to give the bromide **21** (3.3g, 95% over the 2 steps), as a pale-yellow solid. ^{1}H NMR (500 MHz, acetone-d_6): δ (ppm) 10.10 (1H, br s, NH ring-Trp), 7.87 (2H, d, *J* = 7.8 Hz, H4-, H5-Fmoc), 7.68 (1H, d, *J* = 6.3 Hz, H4-Trp), 7.67 (2H, d, *J* = 7.3 Hz, H1-, H8-Fmoc), 7.43-7.38 (2H, m, H3-, H6-Fmoc, H7-Trp), 7.31 (2H, dd, H2-, H7-Fmoc), 7.26 (1H, br s, H2-Trp), 7.12-7.07 (1H, br t, *J* = 7.3 Hz, H6-Trp), 7.04 (1H, br t, *J* = 7.3 Hz, H5-Trp), 6.65 (1H, d, *J* = 7.8 Hz, NH-Trp), 4.34 (2H, d, *J* = 7.3 Hz, CH_2-Fmoc), 4.24-4.15 (2H, m, αH-Trp, H9-Fmoc), 3.69 (1H, dd, *J* = 10.3, *J* = 4.88 Hz, CH_2Br-Trp), 3.69 (1H, dd, *J* = 10.3 and 4.88 Hz, CH_2Br-Trp), 3.60 (1H, dd, *J* = 5.86 Hz, βCH_2-Trp), 3.19-3.08 (1H, m, βCH_2-Trp). ^{13}C NMR (150 MHz, acetone-d_6): δ (ppm) 156.0 (1C, C=O urethane), 144.4 (2C, C8a-, C9a-Fmoc), 141.4 (2C, C4a-, C4b-Fmoc), 137.0 (1C, C3a-Trp), 127.9 (1C, C7a-Trp), 127.8 (2C, C3-, C6-Fmoc), 127.2 (2C, C2-, C7-

Fmoc), 125.5 (2C, C1-, C8-Fmoc), 123.7 (1C, C2-Trp), 121.6 (1C, C6-Trp), 120.1 (2C, C4-, C5-Fmoc), 119.0 (1C, C5-Trp), 118.6 (1C, C4-Trp), 111.6 (1C, C7-Trp), 110.9 (1C, C3-Trp), 66.2 (1C, *C*H_2-Fmoc), 53.1 (1C, Cα-Trp), 47.4 (1C, C9-Fmoc), 36.9 (1C, *C*H_2Br), 28.7 (1C, β*C*H_2-Trp). MALDI-TOF MS: *m*/*e* 498.23, 497.3 (M+Na), 476.8, 475.3 (M+H). Anal. Calcd. for $C_{26}H_{23}BrN_2O_2$: C, 65.69; H, 4.88; N, 5.89. Found C, 66.02; H, 5.04; N 5.59.

5.5.1.15 Glycopeptide 22

To a stirred mixture of the bromide **21** (46.4 mg, 98 µmol) and trisaccharide glycosyl thiol **4** (75 mg, 98 µmol) in ethyl acetate (3 mL), saturated aqueous $NaHCO_3$ (3 mL), followed by tetrabutylammonium hydrogen sulfate (TBAHS) (133 mg, 39.2 µmol) was added. The reaction mixture was stirred vigorously at rt for 12 h. It was then diluted with ethyl acetate and successively washed with saturated aqueous $NaHCO_3$ and brine. The organic layer was dried over Na_2SO_4, concentrated, dissolved in CH_2Cl_2, and purified by flash chromatography (Hexanes-EtOAc; 1:1) to afford the glycopeptide **22** (102 mg, 92%) as a white crystalline solid. ^{1}H NMR (500 MHz, CD_2Cl_2): δ (ppm) 8.35 (1H, br s, NH ring-Trp), 7.80 (2H, d, *J* = 7.55 Hz, H4-, H5-Fmoc), 7.68 (1H, d, *J* = 7.78 Hz, H4-Trp), 7.64-7.57 (2H, m, H1-, H8-Fmoc), 7.47-7.38 (3H, m, H3-, H6-Fmoc, H4-Trp), 7.36-7.30 (2H, m, H2-, H7-Fmoc), 7. 23-7.18 (1H, m, H6-Trp), 7.17-7.10 ((1H, m, H5-Trp), 7.07 (1H, br s, H2-Trp), 5.37-5.33 (2H, m, H2-rha, N*H*-Dmab), 5.32-5.28 (2H, m, NH-Trp, H3"-rha), 5.27 (1H, dd, $J_{2",3"}$ = 3.52, $J_{2",1"}$ = 1.82 Hz, H2"-rha), 5.22 (1H, s, H1-rha), 5.12-5.06 (2H, m, H4-, H4"-rha), 5.05-5.03 (2H, m, H3'-, H4'-rha), 4.95 (1H, d, $J_{1',2'}$ = 1.68 Hz, H1'-rha), 4.81 (1H, d, $J_{1",2"}$ = 1.53 Hz,

H1"-rha), 4.45-4.36 (2H, m, CH_2-Fmoc), 4.28-4.14 (3H, m, αH-Trp, H9-Fmoc, H5-rha), 4.07 (1H, dd, $J_{3,4}$ = 9.78 Hz, $J_{3,2}$ = 3.48 Hz, H3-rha), 4.02-3.95 (1H, m, H5"-rha), 3.94-3.91 (1H, m, H2'-rha), 3.90-3.83 (1H, m, H5'-rha), 3.07 (2H, br t, β -CH_2-Trp) 2.85 (2H, br t, CH_2S), 2.22-1.98 (21H, 7 × OAc), 1.34-1.15 (9H, m, 3 × CH_3-rha). ^{13}C NMR (150 MHz, CD_2Cl_2): δ (ppm) 170.5-169.9 (7C, 7 × C=O-OAc), 155.9 (1C, C=O-urethane), 144.3 (2C, C8a-, C9a-Fmoc), 141.5 (2C, C4a-, C4b-Fmoc), 136.5 (1C, C3a-Trp), 127.8 (1C, C7a-Trp), 127.8 (3C, C3-, C6-Fmoc), 127.2 (2C, C2-, C7-Fmoc), 125.3 (2C, C1-, C8-Fmoc), 123.2 (1 C, C2-Trp), 122.3 (1 C, C5-Trp), 120.1 (2 C, C4-, C5-Fmoc), 119.7 (1 C, C6-Trp), 118.9 (1C, C7-Trp), 111.4 (1C, C4-Trp), 111.4 (1C, C3-Trp), 100.3 (1C, C1"-rha), 99.8 (1C, C1'-rha), 83.9 (1C, C1-rha), 77.5 (1C, C2'-rha), 75.1 (1C, C3-rha), 73.1 (1C, C2-rha), 72.9 (1C, C4"-rha), 70.9 (1C, C3'-rha), 70.8 (1C, C4-rha), 70.3 (1C, C4'-rha), 69.9 (1C, C2"-rha), 68.9 (1C, C3"-rha), 67.8 (1C, C5'-rha), 67.6 (1C, C5-rha), 67.4 (1C, C5"-rha), 66.6 (1C, *C*H_2-Fmoc), 51.5 (1C, Cα-Trp), 47.5 (1C, C9-Fmoc), 36.9 (1C, *C*H_2S), 29.6(1C, β*C*H_2-Trp), 21.1-20.6 (7C, 7 × CH_3-OAc), 17.6-17.2 (3C, 3 × *C*6-rha). MALDI-TOF MS: *m/e* 1183.9 (M+Na), 1199.9 (M+K), 1160.1 (M^+). Anal. Calcd. for $C_{58}H_{68}N_2O_{21}S$: C, 59.99; H, 5.90; N, 2.41. Found C, 59.70; H, 6.06; N, 2.37.

5.5.1.16 Fmoc-Asp(ODmab)-OtBu (26)

To a mixture of Fmoc-Asp-OtBu (1.0 g, 2.4 mmol), Dmab-OH (1.6 g, 4.9 mmol), DTBMP (0.5 g, 2.4 mmol), and HOBt (0.6 g, 3.6 mmol) in dry THF (20 ml), DIC (0.37 mL, 2.4 mmol) was added dropwise. The reaction mixture was

stirred for 12 h at rt, concentrated to dryness under vacuum, dissolved in CH_2Cl_2, and purified by flash chromatography (Hexanes-EtOAc; 2:1) to afford the product **26** as a white solid (1.25 g, 71%) after lyophilization in dioxane. ^{1}H NMR (500 MHz, CD_3OD): δ (ppm) 7.75 (2H, d, *J* = 7.5 Hz, H4-, H5-Fmoc), 7.66-7.59 (2H, m, H1-,H8-Fmoc), 7.41 (2H, d, *J* = 8.0 Hz, H-Dmab), 7.35 (3H, t, *J* = 7.5 Hz, H3-, H6-Fmoc), 7.26 (2H, t, *J* = 7.4 Hz, H2-, H7-Fmoc), 7.09 (2H, d, *J* = 8.0 Hz, Ar-Dmab), 4.52 (1H, t, *J* = 6.4 Hz, αH-Asp), 4.33 (1H, dd, *J* = 11.2 and 7.0 Hz, C*H*$_2$-Fmoc), 4.25 (1H, dd, *J* = 11.2, 7.3 Hz, C*H*$_2$-Fmoc), 4.16 (1H, t, *J* = 6.9 Hz, H9-Fmoc), 3.04-2.89 (3H, m, C*H*$_2$CH-Dmab, β-C*H*$_2$-Asp), 2.83 (1H, dd, *J* = 16.1 and 7.3 Hz, β–C*H*$_2$-Asp), 2.45-2.39 (4H, m, 2 × C*H*$_2$ ring-Dmab), 2.01-1.99 (4H, m, 2 × C*H*$_2$ ring-Dmab), 1.82-1.69 (1H, m, CH_2C*H*-Dmab), 1.41 (9H, s, OtBu), 1.04 (6H, s, 2 × C*H*$_3$ ring-Dmab), 0.74-0.67 (6H, m, CH_2CH(C*H*$_3$)$_2$-Dmab). ^{13}C NMR (150 MHz, CD_3OD): δ (ppm) 176.7 (2C, C=O ring-Dmab), 171.7 (1C, C=*C*N Dmab), 170.5 (1C, *C*OODmab), 170.2 (1C, *C*OOtBu), 157. 0 (1C, C=O-urethane), 144.0 (2C, C8a-, C9a-Fmoc), 143.9 (1C, *C*$_{Ar}$-N Dmab), 141.4 (2C, C4a-, C4b-Fmoc), 136.3 (1C, *C*$_{Ar}$-CH_2O Dmab), 129.0 (2C, *C*$_{Ar}$-Dmab), 127.7 (2C, C3-, C6-Fmoc), 127.0 (2C, C2-, C7-Fmoc), 126.5 (2C, *C*$_{Ar}$-Dmab), 125.1 (2C, C1-, C8-Fmoc), 119.9 (2C, C4-, C5-Fmoc), 107.4 (1C, *C*=CN), 82.1 (1C, COO*C*$(CH_3)_3$-OtBu), 66.9 (1C, *C*H_2-Fmoc), 65.5 (1C, C_{Ar}-*C*H_2O-Dmab), 52.4 (2C, 2 × *C*H_2 ring-Dmab), 51.5 (1C, Cα-Asp), 47.1 (1C, C9-Fmoc), 38.2 (1C, *C*H_2C*H*-Dmab), 36.4 (1C, β*C*H_2-Asp), 29.8 (1C, CH_2*C*H-Dmab), 27.1 (2C, 2 × CH_3 ring-Dmab), 27.3 (3C, OtBu), 21.8 (2C, CH_2CH(*C*H_3)$_2$-Dmab). MALDI-TOF MS: *m*/*e* 745.2 (M+Na), 722.7 (M+H).

Anal. Calcd. for $C_{43}H_{50}N_2O_8$: C, 71.45; H, 6.97; N, 3.88. Found C, 71.14; H, 7.24; N, 3.62.

5.5.1.17 Fmoc-Asp(ODmab)-OH (27)

Fmoc-Asp(ODmab)-OtBu (**26**) (1.0 g, 1.4 mmol) was dissolved in a mixture of 1:1 CH_2Cl_2-TFA (10 mL), and the reaction mixture was stirred for 1 h. The volatiles were then removed under vacuum, and the residue was co-evaporated five times with toluene, dissolved in CH_2Cl_2, and purified by flash chromatography (CH_2Cl_2-MeOH; 97:3) to give the product **27** as a pale-yellow solid (0.9g, 97%). ^{1}H NMR (500 MHz, CD_3OD): δ (ppm) 7.77 (2H, d, *J* = 7.5 Hz, H4-, H5-Fmoc), 7.69-7.61 (2H, m, H1-, H8-Fmoc), 7.44 (2H, d, *J* = 8.1 Hz, ArH-Dmab), 7.37 (3H, t, *J* = 7.4 Hz, H3-, H6-Fmoc), 7.28 (2H, t, *J* = 7.4 Hz, H2-, H7-Fmoc), 7.08 (2H, d, *J* = 8.1 Hz, ArH-Dmab), 5.17 (2H, d, *J* = 3.5 Hz, Ar-C*H*$_2$O-Dmab), 4.52 (1H, t, *J* = 6.4 Hz, α–H-Asp), 4.33 (1H, dd, *J* = 11.2, 7.0 Hz, C*H*$_2$-Fmoc), 4.25 (1H, dd, *J* = 11.2, 7.3 Hz, C*H*$_2$-Fmoc), 4.16 (1H, t, *J* = 6.9 Hz, H9-Fmoc), 3.04-2.89 (3H, m, C*H*$_2$CH-Dmab, β–C*H*$_2$-Asp), 2.83 (1H, dd, *J* = 16.1, 7.3 Hz, β–C*H*$_2$-Asp), 2.45-2.39 (4H, m, 2 × C*H*$_2$ ring-Dmab), 2.01-1.99 (4H, m, 2 × CH_2 ring-Dmab), 1.82-1.69 (1H, m, CH_2C*H*-Dmab), 1.41 (9H, s, OtBu), 1.04 (6H, s, 2 × C*H*$_3$ ring-Dmab), 0.74-0.67 (6H, m, CH_2CH(C*H*$_3$)$_2$-Dmab). ^{13}C NMR (150 MHz, CD_3OD): δ (ppm) 176.7 (2C, C=O ring-Dmab), 171.7 (1C, *C*OODmab), 170.5 (1C, C=*C*N-Dmab), 170.2 (1C, *C*OOtBu), 157. 0 (1C, C=O-urethane), 144.0 (2C, C8a-, C9a-Fmoc), 143.9 (1C, *C*$_{Ar}$-N Dmab), 141.4 (2C, C4a-, C4b-Fmoc), 136.3 (1C, *C*$_{Ar}$-CH_2ODmab), 129.0 (2C, *C*$_{Ar}$-Dmab), 127.7 (2C, C3-, C6-

Fmoc), 127.0 (2C, C2-, C7-Fmoc), 126.5 (2C, C_{Ar}-Dmab), 125.1 (2C, C1-, C8-Fmoc), 119.9 (2C, C4-, C5-Fmoc), 107.4 (1C, *C*=CN), 82.1 (1C, COO*C*$(CH_3)_3$-OtBu), 66.9 (1C, *C*H_2-Fmoc), 65.5 (1C, C_{Ar}-*C*H_2O-Dmab), 52.4 (2C, 2 × *C*H_2 ring-Dmab), 51.5 (1C, Cα-Asp), 47.1 (1C, C9-Fmoc), 38.2 (1C, *C*H_2C*H*-Dmab), 36.4 (1C, β−*C*H_2-Asp), 29.8 (1C, CH_2*C*H-Dmab), 27.1 (2C, 2 × *C*H_3 ring-Dmab), 27.3 (3C, OtBu), 21.8 (2C, $CH_2CH(CH_3)_2$-Dmab). MALDI-TOF MS: *m*/*e* 945.2 (M+Na), 722.7 (M+H). Anal. Calcd. for $C_{43}H_{50}N_2O_8$: C, 71.45; H, 6.97; N, 3.88. Found C, 71.14; H, 7.24; N, 3.62.

5.5.1.18 Fmoc-Met-Asp(ODmab)-OH (28)

2-Chlorotrityl resin (0.3 g, loading: 1.69 mmol) was swelled in CH_2Cl_2 (10 ml) for 5 min. The resin was then washed with DMF (10 mL). DIPEA (3 mL) was added, followed by the addition of Fmoc-Asp(ODmab)-OH (**27**) (0.5 g, 0.75 mmol) dissolved in DMF (4 mL). The flask was shaken for 1 h and the resin was washed with DMF (3 × 10 mL) and CH_2Cl_2 (10mL). A mixture of 80:16:4 CH_2Cl_2-MeOH-DIPEA (10 mL) was then introduced, and the flask was shaken for 15 min. The operation was repeated once. The resin was then washed with DMF (3 × 10 mL), and 25% piperidine in DMF (10 mL) was added, and the flask was shaken for 10 min. The operation was repeated for 30 min. The resin was washed with DMF (3 x 10 mL) and Fmoc-Met-OH (0.57 g, 1.5 mmol), HBTU (0.54g, 1.4 mmol), HOBt (0.22 g, 1.4 mmol), and DIPEA (3 mL) dissolved in DMF (7 mL) were added. The flask was then shaken for 1 h. The resin was washed with DMF (3 × 10 mL) and CH_2Cl_2 (3 × 10 mL). TFA (5% in CH_2Cl_2, 10 mL) was

added to the resin and the flask was shaken for 1 h. The solution was collected in a round-bottomed flask and the resin was washed with CH_2Cl_2 (3 × 5 mL) and MeOH (3 × 5 mL). The solvent was then removed under vacuum, and the residue was azeotroped three times with toluene, dissolved in CH_2Cl_2, and purified by flash chromatography (Hexanes-EtOAc; 1:1) to afford the protected dipeptide **28** as a yellow powder (0.4 g, 80%) after lyophilization in dioxane. ^{1}H NMR (500 MHz, CD_3OD): δ (ppm) 7.76 (2H, d, *J* = 7.5 Hz, H4-, H5-Fmoc), 7.67-7.59 (2H, m, H1-, H8-Fmoc), 7.42-7.32 (4H, m, Dmab-ArH, H3-, H6-Fmoc), 7.28 (2H, t, *J* = 7.4 Hz, H2-, H7-Fmoc), 7.11 (2H, d, *J* = 7.9 Hz, Ar-Dmab), 5.09 (2H, s, Ar-C*H*$_2$O-Dmab), 4.40-4.14 (5H, m, C*H*$_2$-Fmoc, αH-Asp, αH-Met, H9-Fmoc), 3.06-2.84 (4H, m, C*H*$_2$CH-Dmab, βC*H*$_2$-Asp), 2.60-2.46 (2H, m, δC*H*$_2$-Met), 2.42 (2H, s, C*H*$_2$ ring-Dmab), 2.06 (2H, s, C*H*$_2$ ring-Dmab), 1.99 (3H, s, SC*H*$_3$-Met), 1.95-1.83 (2H, m, βC*H*$_2$-Met), 1.81-1.71 (1H, m, CH_2C*H*-Dmab), 1.05 (6H, s, 2 × C*H*$_3$ ring-Dmab), 0.71 (6H, d, *J* = 6.6 Hz, CH_2CH(C*H*$_3$)$_2$-Dmab). ^{13}C NMR (150 MHz, CD_3OD): δ (ppm) 176.7 (2C, C=O ring-Dmab), 172.95 (1C, CO-amide), 171.7 (1C, *C*OODmab), 170.5 (1C, C=*C*N Dmab), 157.2 (1C, C=O-urethane), 144.1 (2C, C8a-, C9a-Fmoc), 143.9 (1C, *C*$_{Ar}$-N-Dmab), 141.4 (2C, C4a-, C4b-Fmoc), 136.3 (1C, *C*$_{Ar}$-CH_2O-Dmab), 128.9 (2C, *C*$_{Ar}$-Dmab), 127.6 (2C, C3-, C6-Fmoc), 127.0 (2C, C2-, C7-Fmoc), 126.5 (2C, *C*$_{Ar}$-Dmab), 125.1 (2C, C1-, C8-Fmoc), 119.8 (2C, C4-, C5-Fmoc), 107.4 (1C, *C*=CN), 66.9 (1C, *C*H_2-Fmoc), 65.5 (1C, C_{Ar}-*C*H_2O-Dmab), 54.8 (1C, Cα-Met), 54.3 (1C, Cα-Asp), 52.4 (2C, 2 × *C*H_2 ring-Dmab), 47.2 (1C, C9-Fmoc), 39.0 (1C, *C*H_2CH-Dmab), 36.2 (1C, *C*β-Asp), 31.3 (1C, βC*H*$_2$-Met), 29.9 (1C, Cδ-Met), 29.4 (1C, CH_2*C*H-Dmab), 27.2 (2C, 2 ×

*C*H$_3$ ring-Dmab), 21.7 (2C, CH$_2$CH(*C*H$_3$)$_2$-Dmab), 19.8 (1C, S*C*H$_3$-Met. MALDI-TOF MS: *m*/*e* 706.4 (M+K), 690.1 (M+Na), 667.9 (M+H). Anal. Calcd. for $C_{44}H_{51}N_3O_9S$: C, 66.23; H, 6.44; N, 5.27. Found C, 66.07; H, 6.31; N, 5.36.

5.5.1.19 Fmoc-Met-Asp(ODmab)-Opfp (24)

Fmoc-Met-Asp(ODmab)-OH (**28**) (0.3 g, 0.4 mmol) and pentafluorophenol (0.1 g, 0.56 mmol) were dissolved in dry CH_2Cl_2 (7 mL), DIC (58 µL, 0.4 mmol) was added dropwise, and the reaction mixture was stirred for 3 h at rt. The mixture was then cooled on ice for 1 h and the diisopropylurea was filtered. The filtrate was concentrated, and the crude product was purified by flash chromatography (Hexanes-EtOAc; 3:1→2:1) to afford the activated dipeptide **24** as a white crystalline solid (0.26 g, 73%). This material was only of limited stability at rt and was generally used immediately in the next step. ^{1}H NMR (500 MHz, CD_3OD): δ (ppm) 7.78 (2H, d, *J* = 7.5 Hz, H4-, H5-Fmoc), 7.68-7.61 (2H, m, H1-, H8-Fmoc), 7.42-7.32 (4H, m, ArH-Dmab, H3-, H6-Fmoc), 7.28 (2H, t, *J* = 7.4 Hz, H2-, H7-Fmoc), 7.11 (2H, d, *J* = 7.8 Hz, Ar-Dmab), 5.09 (2H, s, Ar-C*H*$_2$O-Dmab), 4.40-4.14 (5H, m, C*H*$_2$-Fmoc, αH-Asp, αH-Met, H9-Fmoc), 3.06-2.84 (4H, m, C*H*$_2$CH-Dmab, βC*H*$_2$-Asp), 2.60-2.46 (2H, m, δC*H*$_2$-Met), 2.42 (2H, s, C*H*$_2$ ring-Dmab), 2.06 (2H, s, C*H*$_2$ ring-Dmab), 1.99 (3H, s, SC*H*$_3$-Met), 1.95-1.83 (2H, m, βC*H*$_2$-Met), 1.81-1.71 (1H, m, CH$_2$C*H*-Dmab), 1.05 (6H, s, 2 × C*H*$_3$ ring-Dmab), 0.71 (6H, d, *J* = 6.6 Hz, CH$_2$CH(C*H*$_3$)$_2$-Dmab). ^{13}C NMR (150 MHz, CD_3OD): δ (ppm) 176.7 (2C, C=O ring-Dmab), 173.3 (1C, *C*OOPfp), 170.1 (1C, CO-amide), 169.9 (1C, *C*OODmab), 167.1 (1C, C=*C*N-Dmab), 157.2 (1C, C=O-urethane), 144.2 (2C, C8a-, C9a-Fmoc), 143.9 (1C, *C*$_{Ar}$-N-Dmab), 142.1 (1C,

C_{Ar}-OPfp), 141.4-141.3 (3C, C_{Ar}-OPfp, C4a-, C4b-Fmoc), 140.2, 138.9 (1C each, C_{Ar}-OPfp), 136.4 (2C, C_{Ar}-OPfp), 136.1 (1C, *C*$_{Ar}$-CH_2O-Dmab), 129.2 (2C, *C*$_{Ar}$-Dmab) 127.6 (2C, C3-, C6-Fmoc), 127.0 (2C, C2-, C7-Fmoc), 126.6 (2C, *C*$_{Ar}$-Dmab), 125.1 (2C, C1-, C8-Fmoc), 119.8 (2C, C4-, C5-Fmoc), 107.4 (1C, *C*≡CN), 66.8 (1C, *C*H_2-Fmoc), 65.9 (1C, C_{Ar}-*C*H_2O-Dmab), 54.1 (1C, Cα-Met), 52.4 (2C, 2 × *C*H_2 ring-Dmab), 48.8 (1C, Cα-Asp), 47.2 (1C, C9-Fmoc), 39.2 (1C, *C*H_2CH-Dmab), 35.4 (1C, *C*β-Asp), 31.4 (1C, βC*H*$_2$-Met), 29.8 (1C, Cδ-Met), 29.5 (1C, CH_2*C*H-Dmab), 27.2 (2C, 2 × *C*H_3 ring-Dmab), 21.7 (2C, $CH_2CH(CH_3)_2$-Dmab), 14.1 (1C, S*C*H_3-Met). MALDI-TOF MS: *m*/*e* 986.1 (M+Na), 963.6 (M+H).

5.5.1.20 Glycopeptide 25

To a stirred mixture of the glycopeptide **22** (75 mg, 65 μmol) and octanethiol (0.11 mL, 0.65 mmol), DBU (5 μL, 33 μmol) was added, and the reaction mixture was stirred for 1 h. The solvent was evaporated to dryness, and the residue was washed several times with warm ether. The amine product **23** was not purified further but was used directly in the coupling reaction with the protected dipeptide **24**.

To a mixture of the amine **23** (20.6 mg, 22 μmol), and Fmoc-Met-Asp(ODmab)-Opfp (**24**) (21 mg, 22 μmol) and in dry THF, HOBt (5 mg, 33 μmol) was added, and the reaction mixture was stirred at rt for 3 h. The solvent was then removed under vacuum, and the residue was purified by flash chromatography (Hexanes-EtOAc; 2:1) to afford the protected glycopeptide **25** as a white, crystalline solid containing a minor peptide impurity. Further purification by preparative HPLC (C-18 reverse phase, 80:20 to 5:95 H_2O-CH_3CN over 30

min) gave the pure glycopeptide **25** as a colorless solid (28 mg, 72%). ^{1}H NMR (500 MHz, CD_2Cl_2): δ (ppm) 8.45 (1H, br s, NH ring-Trp), 7.82-7.76 (2H, m, H4-, H5-Fmoc), 7.65-7.55 (3H, m, H1-, H8-Fmoc, H7-Trp), 7.45-7.38 (3H, m, ArH-Dmab, H3-, H6-Fmoc), 7.38-7.30 (4H, m, H2-, H7-Fmoc, H4-Trp), 7.29-7.26 (1H, br d, *J* = 8.7 Hz, NH-Asp), 7.19-7.12 (2H, m, H5-Trp, ArH-Dmab), 7.12-7.07 (2H, m, H6-Trp, ArH-Dmab) 7.04 (1H, br s, H2-Trp), 6.77 (1H, br d, *J* = 7.8 Hz, NH-Trp), 5.34 (1H, br s, NH-Dmab), 5.32-5.24 (3H, m, H2-, H2", H3"-rha), 5.23 (1H, s, H1-rha), 5.17-4.97 (6H, m, H3'-, H4-, H4'-, H4"-rha, Ar-CH_2O-Dmab), 4.94 (1H, d, *J* = 1.50 Hz, H1'-rha), 4.79 (1H, br s, H1"-rha), 4.77-4.72 (1H, m, αH-Asp), 4.47 (1H, dd, *J* = 10.7 and 6.4 Hz, CH_2-Fmoc), 4.43-4.32 (2H, m, CH_2-Fmoc, αH-Trp), 4.24 (1H, dd, *J* = 7.32 and 6.4 Hz, H9-Fmoc), 4.18-4.07 (2H, m, H5-rha, αH-Met), 4.04 (1H, dd, *J* = 9.28 and 3.42 Hz, H3-rha), 3.97 (1H, m, H5"-rha), 3.91 (1H, br s, H2'-rha), 3.84 (1H, m, H5'-rha), 3.07-2.89 (4H, m, βCH_2-Trp, CH_2CH-Dmab, βCH_2-Asp), 2.88-2.72 (3H, m, βCH_2-Asp, CH_2S), 2.51-2.49 (2H, m, δCH_2-Met), 2.48 (2H, s, CH_2 ring-Dmab), 2.36 (2H, s, CH_2 ring-Dmab), 2.19-1.98 (26H, m, SCH_3-Met, βCH_2-Met, 7 × CH_3-OAc), 1.87-1.77 (1H, m, CH_2C*H*-Dmab), 1.21-1.13 (9H, m, 3 × H6-rha), 1.07 (6H, s, 2 × CH_3 ring-Dmab), 0.71 (6H, d, *J* = 6.8 Hz, CH_2CH(CH_3)$_2$-Dmab). ^{13}C NMR (150 MHz, CD_2Cl_2): δ (ppm) 176.3 (2C, C=O ring-Dmab), 171.8-169.5 (10C, 11 × C=O), 156.7 (1C, C=O-urethane), 144.0 (2C, C8a-, C9a-Fmoc), 143.9 (1C, C_{Ar}-N-Dmab), 141.5 (2C, C4a-, C4b-Fmoc), 137.3 (1C, C3a-Trp), 136.4 (1C, C_{Ar}-CH_2O- Dmab), 129.1 (2C, C_{Ar}-Dmab), 128.0 (1C, C7a-Trp), 127.9 (3C, C3-, C6-Fmoc), 127.3 (2C, C2-, C7-Fmoc), 126.9 (2C, C_{Ar}-Dmab), 125.2 (2C, C1-, C8-Fmoc), 123.3 (1 C, C2-Trp),

122.2 (1 C, C6-Trp), 120.2 (2 C, C4-, C5-Fmoc), 119.6 (1 C, C5-Trp), 118.9 (1C, C7-Trp), 111.4 (1C, C4-Trp), 111.4 (1C, C3-Trp), 100.2 (1C, C1"-rha), 99.8 (1C, C1'-rha), 83.2 (1C, C1-rha), 77.6 (1C, C2'-rha), 75.2 (1C, C3-rha), 73.1 (1C, C2-rha), 72.9 (1C, C4"-rha), 70.9 (1C, C3'-rha), 70.3 (1C, C4-rha), 70.3 (1C, C4'-rha), 69.9 (1C, C2"-rha), 68.9 (1C, C3"-rha), 67.6 (1C, C5'-rha), 67.4 (1C, C5-rha), 67.3 (1C, C5"-rha),), 67.2 (1C, *C*H_2-Fmoc), 66.0 (1C, C_{Ar}-*C*H_2O-Dmab), 54.9 (1C, Cα-Met), 53.9 (1C, *C*H_2 ring-Dmab), 52.4 (1C, *C*H_2 ring-Dmab), 50.4 (1C, Cα-Trp), 49.8 (1C, Cα-Asp), 47.4 (1C, C9-Fmoc), 38.2 (1C, *C*H_2CH-Dmab), 35.7 (1C, *C*β-Asp), 31.7 (1C, βC*H*$_2$-Met), 29.9 (1C, Cδ-Met), 29.6 (1C, -CH_2*C*H-Dmab), 29.3 (1C, βCH_2-Trp), 28.1 (2C, 2 × *C*H_3 ring-Dmab), 22.5 (2C, $CH_2CH(CH_3)_2$-Dmab), 21.1-20.7 (7C, 7 × *C*H_3-OAc), 17.5-17.1 (3C, 3 × *C*H_3-rha), 15.3 (1C, S*C*H_3-Met), MALDI-TOF MS: *m*/*e* 1741.7 (M+Na), 1757.1 (M+K), 1718.6 (M+H). Anal. Calcd. for $C_{87}H_{107}N_5O_{27}S_2$: C, 60.79; H, 6.27; N, 4.07. Found C, 60.66; H, 6.45; N, 3.71.

5.5.1.21 Aspartimide side product

To a stirred mixture of **25** (13 mg, 7.6 µmol) and octanethiol (13 µL, 76 µmol), DBU (0.6 µL, 33 µmol) was added, and the reaction mixture was stirred for 1 h. The solvent was evaporated to dryness, and the residue was washed several times with warm ether. The amine product **29** was then dissolved in MeOH (3 mL) and MeONa-MeOH (5 drops) was added. The reaction mixture was stirred overnight at rt. Rexin H^+ 101 was then added until the pH was neutral. The rexin was removed by filtration, the solvent was concentrated, and

the crude product was purified by flash chromatography (EtOAc-MeOH-H_2O; 10:3:1) to afford a 2:1 α/β mixture of the aspartimide side product (6.4 mg, 88%) as a white solid, after lyophilization in dioxane. ^{1}H NMR (500 MHz, MeOD) of the major isomer: δ 7.60 (1H, d, *J* = 7.8 Hz, H4-Trp), 7.32 (1H, d, *J* = 8.8 Hz, H7-Trp), 7.11-7.05 (2H, m, H2-, H6-Trp), 7.01 (1H, br t, *J* = 7.1 Hz, H5-Trp), 5.17 (2H, br s, H1'-rha), 5.11 (1H, br s, H1-rha), 4.91 (1H, br s, H1"-rha), 4.40-4.31 (1H, m, αH-Trp), 4.26 (1H, dd, *J* = 4.9 Hz, αH-Asp), 4.14 (1H, dd, *J* = 6.4 Hz, αH-Met), 4.02 (1H, br s, H2-rha), 3.97 (2H, br s, H2'-, H2"-rha), 3.93 (1H, m, H5-rha), 3.86 (1H, dd, *J* = 9.5 and 3.2 Hz, H3'-rha), 3.75-3.63 (4H, m, H5'-, H5", H3, H3"-rha), 3.52 (1H, dd, *J* = 9.7, H4-rha), 3.40-3.31 (2H, m, H4'-, H4"-rha), 3.09-2.67 (2H, m, βCH_2-Trp), 2.86-2.72 (3H, m, βCH_2-Asp, CH_2S-Trp), 2.68-2.52 (3H, m, βCH_2-Asp, δCH_2-Met), 2.19-2.10 (2H, m, βCH_2-Met), 2.09 (3H, s, SCH_3-Met), 1.32-1.20 (9H, m, 3 × CH_3-rha). ^{13}C NMR (125 MHz, MeOD) of the major isomer: δ 177.4, 174.2, (3C, 3 × C=O), 136.5, 127.8, 124.7, 123.1, 121.0, 118.6, 118.2, 111.1 (each, 1C, 8 × C_{Ar}-Trp), 102.7 (1C, C1"-rha), 101.3 (1C, C1'-rha), 86.6 (1C C1-rha,), 78.2 (1C, C2'-rha), 73.2, 72.9, 72.5, 72.3 (each 1C, 3 × C4-, C2-rha), 71.1, 70.9, 70.7, 70.6, 70.1, 69.1, 68.9, (10C, C2, 3 × C3-, 3 × C4-rha, 3 × C5-rha), 53.4, 52.3 51.7 (each 1C, Cα-Met, Cα-Asp, Cα-Trp), 50.1 (1C, β*C*H_2-Asp), 35.5 (1C, S*C*H_2-Trp), 30.9 (1C, β*C*H_2-Met), 29.6 (1C, β*C*H_2-Trp), 28.3 (1C, S*C*H_2-Met), 16.9, ((1C, C6-rha), 16.7 (2C, 2 × C6-rha), 13.9 (1C, S*C*H_3-Met). HRMS Calcd for [$C_{38}H_{56}N_4O_{15}S_2$+Na]: 895.3076. Found: 895.3075.

5.5.1.22 Glycopeptide 1

The amine product **29** (11 mg, 7.3 μmol) was dissolved in 2% NH_2NH_2 in THF (5 mL), and the mixture was stirred for 2 h at rt. The solvent was evaporated, and the residue **30** was dissolved in MeOH (5 mL) and MeONa-MeOH (5 drops) was added. The reaction mixture was stirred overnight at rt. Rexin H^+ 101 was then added until the pH was slightly basic, resin filtered and the filtrate was further neutralized with acetic acid. The solvent was evaporated, and the crude product was washed successively with hexanes (10 mL), CH_2Cl_2 (10 mL), and EtOAc (10 mL). The crude material was further purified by HPLC (C-18 reverse phase, 95:5 to 5:95 H_2O-CH_3CN over 15 min) to afford the desired glycopeptide **1** (6.5 mg, 68%) as a white solid. ^1H NMR (see above): HRMS Calcd for $C_{38}H_{58}N_4O_{16}S_2$: 891.3367. Found: 891.3356.

5.5.2 Molecular modeling

The molecular structures of the glycopeptides **1** and **2** were constructed using SYBYL 6.6 (Tripos, Inc.) with the coordinates of the two 1.8 Å resolution crystal structures of the Fab fragment of SYA/J6 complexed with the octapeptide and the pentasaccharide (PDB entry 1PZ5).[22] The structures of **1** and **2** were then optimized by energy minimization within the binding site to achieve a reasonable structure in each case, employing the standard Tripos molecular mechanics force field[49] and Gasteiger–Marsili charges,[50,51] with a 0.001 kcal/mol energy gradient convergence criterion. The atom charges were retained on both **1** and **2** for the docking calculations. The water was removed. Only polar

hydrogens were added to the protein, and Kollman united-atom partial charges[52] were assigned. Compounds **1** and **2** were then docked into the antibody-combining site of the Fab fragment of SYA/J6 using AUTODOCK 3.0.[26] All active torsions of **1** and **2** were selected to be fully flexible during the docking experiments. The grid maps were constructed using $70 \times 70 \times 70$ points, with grid point spacing of 0.375 Å. A Lamarckian Genetic Algorithm (LGA) was used to search each conformation space for low-energy binding orientations. The default setting was adopted, and 500 LGA docking runs were performed.

5.5.3 Immunochemical analysis

5.5.3.1 Lipopolysaccharide, and O-polysaccharide from *S. flexneri* Y, peptide MDWNMHAA, and monoclonal antibody SYA/J6, used in ELISA

The lipopolysaccharide (LPS) and *O*-polysaccharide from *S. flexneri* Y and monoclonal antibody SYA/J6 (IgG3) were provided by Dr. D. R Bundle[21,22, 31,44-48] and were used as antigens/inhibitors. The mimetic-peptide MDWNMHAA,[24] was used as an inhibitor in ELISA.

5.5.3.2 Competitive-inhibition ELISA studies with lipopolysaccharide and *O*-polysaccharide of *S. flexneri* Y, peptide MDWNMHAA, and glycopeptide as inhibitors

Competition-inhibition ELISA was performed in 96-well plates (NUNC-MaxiSorp, Rochester, NY), coated overnight with 100 μL/well of LPS from *S. flexneri* Y (10 μg/mL in carbonate buffer pH 9.6). Wells were blocked by the

addition of 1% BSA for 2 h at room temperature. The plates were washed three times with a washing solution of 0.05% Tween 20 and 0.9% NaCl. Monoclonal antibody SYA/J6 (~1 μg/mL) was pre-incubated in duplicate with twofold serial dilutions of inhibitors in PBS-T, starting at an initial concentration of 400 μg/mL, for 1 h at room temperature. Then, 100 μL of the mixtures were transferred to plates and incubated for 3 h at room temperature. After washing four times as before, 100 μL per well of alkaline phosphatase-labeled goat anti-mouse IgG (Caltag Laboratories, San Francisco, CA) diluted 1:3000 in PBS-T was added. The plates were incubated overnight at room temperature, and were again washed four times. Substrate solution (100 μL) containing *p*-nitrophenyl phosphate (1 mg/mL, Kirkegaard & Perry lab, Gaithersburg, MD) was added to the wells. After 25-30 min at room temperature, the plates were scanned at 405 nm in a SpectraMax 340 microplate reader. The percentage of inhibition was determined by the decrease in A_{405} value in wells with inhibitors as compared with those without inhibitors.

5.6 Acknowledgements

We are grateful to D. R. Bundle for the generous gifts of the SYA/J6 antibody, the LPS, and O-polysaccharide, and to the Natural Sciences and Engineering Research Council of Canada for financial support.

5.7 REFERENCES

1. Grandi, G. *Trends Biotechnol.* **2001**, *19*, 181-188.
2. Jennings, H. J. *Curr. Top. Microbiol. Immunol.* **1990**, *150*, 97-127.
3. Jennings, H. J. *Adv. Exp. Med. Biol.* **1988**, *228*, 495-550.
4. Lee, C. J. *Mol. Immunol.* **1987**, *24*, 1005-1019.
5. Lindberg, A. A. *Vaccine* **1999**, *17*, S28-36.
6. Weintraub, A. *Carbohydr. Res.* **2003**, *338*, 2539-2547.
7. Mc Cool, T. L.; Harding, C. V.; Greenspan, N. S.; Schreiber, J. R. *Infect. Immun.* **1999**, *67*, 4862.
8. Roy, R. *Drug Discovery Today: Technologies* **2004**, *1*, 327-336.
9. Mond, J. J.; Lees. A.; Snapper, C. M. *Annu. Rev. Immunol.* **1995**, *13*, 655-692.
10. Parker, D. C. *Annu. Rev. Immunol.* **1993,** *11*, 331-360.
11. Gonzalez-Fernandez, A.; Faro, J.; Fernandez, C. *Vaccine* **2008**, *26*, 292-300.
12. Barington, T.; Gyhrs, A.; Kristensen, K.; Heilmann, C. *Infect. Immun.* **1994**, *62*, 9-14.
13. Peeters, C.; Tenbergenmeekes, A. M.; Poolman, J. T.; Beurret, M.; Zegers, B. J. M.; Rijkers, G. T. *Infect. Immun.* **1991**, *59*, 3504-3510.
14. Johnson, M. A.; Pinto, B. M. *Topics Curr. Chem.* **2008**, **273**, 55-116.
15. Johnson, M. A.; Pinto, B. M. *Aust. J.Chem.* **2002**, *55*, 13-25.
16. Borrelli, S.; Hossany, R. B.; Pinto, B. M. *Clin. Vaccine Immunol.* **2008,** *15*, 1106-1117.

17. Borrelli, S.; Johnson, M. A.; Hossany, R. B.; Findlay, S. (2007) In *Amer. Chem. Soc. Symp. Ser. 989 on Carbohydrate Vaccines* (Roy, R., ed), American Chemical Society, Washington, p 335.

18. Harris, S. L.; Craig, L.; Mehroke, J. S.; Rashed, M.; Zwick, M. B.; Kenar, K.; Toone, E. J.; Greenspan, N.; Auzanneau, F. I.; MarinoAlbernas, J. R.; Pinto, B. M.; and Scott, J. K. *Proc. Natl. Acad. Sci. U. S. A.* **1997**, *94*, 2454-2459.

19. Borrelli, S.; Hossany, R. B.; Findlay, S.; Pinto, B. M. *Am. J. Immunol.* **2006**, *2*, 73-83.

20. Hale, T. L. (1998) In *Topley and Wilson's Microbiology and Microbial Infections* (Hansler, W. J., Shumman, M., eds), Arnold, London.

21. Vyas, N. K.; Vyas, M. N.; Chervenak, M. C.; Johnson, M. A.; Pinto, B. M.; Bundle, D. R.; Quiocho, F. A. *Biochemistry* **2002**, *41*, 13575-13586.

22. Vyas, N. K.; Vyas, M. N.; Chervenak, M. C.; Bundle, D. R.; Pinto, B. M.; Quiocho, F. A. *Proc. Natl. Acad. Sci. U. S. A.* **2003**, *100*, 15023-15028.

23. Beenhouwer, D. O.; May, R. J.; Valadon, P.; Scharff, M. D. *J. Immunol.* **2002**, *169*, 6992-6999.

24. Hossany, R. B.; Johnson, M. A.; Eniade, A. A.; Pinto, B. M. *Bioorg. Med. Chem.* **2004**, *12*, 3743-3754.

25. Horton, D.; Wander, J. D. (1990) In *Carbohydrate: Chemistry and Biology*, (Pigman, W. W., Horton, D. eds), Academic Press, New York.

26. Morris, G. M.; Goodsell, D. S.; Halliday, R. S.; Huey, R.; Hart, W. E.; Belew, R. K.; Olson, A. J. *J. Comput. Chem.* **1998**, *19*, 1639-1662.

27. Auzanneau, F. I.; Forooghian, F.; Pinto, B. M. *Carbohydr. Res.* **1996**, *291*, 21-41.

28. Hoog, C.; Rotondo, A.; Johnston, B. D.; Pinto, B. M. *Carbohydr. Res.* **2002**, *337*, 2023-2036.

29. Pozgay, V. *Carbohyd. Res.* **1992**, *235*, 295-302.

30. Kartha, K. P. R.; Field, R. A. *Tetrahedron Lett.* **1997**, *38*, 8233-8236.

31. Hecht, S. (1998) In *Recognition of Carbohydrate Antigens by Antibody Binding Sites in Carbohydrates*, Oxford University Press Inc., Oxford.

32. Zhu, X. M.; Schmidt, R. R. *Chem. Eur. J.* **2004**, *10*, 875-887.

33. Mergler, M.; Dick, F. *J. Peptide Sci.* **2005**, *11*, 650-657.

34. Hvidt, T.; Szarek, W. A.; Maclean, D. B. *Can. J. Chem.* **1988**, *66*, 779-782.

35. Sheppeck, J. E.; Kar, H.; Hong, H. *Tetrahedron Lett.* **2000**, *41*, 5329-5333.

36. Cammish, L. E.; Kates, S. A. (2000) In *Fmoc Solid Phase Peptide Synthesis: A Practical Approach* (Chan, W. C.; White, P. D., eds), Oxford University Press Inc., New York.

37. Dourtoglou, V.; Gross, B.; Lambropoulou, V.; Zioudrou, C. *Synthesis* **1984**, *7*, 572-574.

38. Dourtoglou, V.; Ziegler, J. C.; Gross, B. *Tetrahedron Lett.* **1978**, *15*, 1269-1272.

39. Knorr, R.; Trzeciak, A.; Bannwarth, W.; Gillessen, D. *Tetrahedron Lett.* **1989**, *30*, 1927-1930.

40. Chan, W. C.; Bycroft, B. W.; Evans, D. J.; White, P. D. *J. Chem. Soc.-Chem. Commun.* **1995**, *21*, 2209-2210.

41. Barlos, K.; Gatos, D. (2000) In *Fmoc Solid Phase Peptide Synthesis: A Practical Approach* (Chan, W. C., White, P. D., eds), Oxford University Press Inc., New York.

42. Perrin, D. D.; Armarego, W. L. F. (1988) In *Purification of Laboratory Chemicals*, 3rd Ed., Pergamon, London.

43. Kaiser, E.; Colescot.R. ; Bossinge.C.; Cook, P. I. *Anal. Biochem.* **1970**, *34*, 595-598.

44. Altman, E.; Bundle, D. R. *Methods in Enzym.* **1994**, *247*, 243-253.

45. Bundle, D. R.; Gidney, M. A.; Josephson, S.; Wessel, H.-P. (1983) In *ACS Symp. Ser.* (Anderson, H.-P.;Unger, F. M., eds), Vol 231, American Chemical Society, Washington.

46. Bundle, D. R. *Pure Appl. Chem.* **1989**, *61*, 1171-1180.

47. Bundle, D. R.; Altman, E.; Auzanneau, F.I.; Baumann, H.; Eichler, E.; Sigurskjold, B. W. (1994) In *Alfred Benzon Symp. Ser.* (Bock, K., Clausen, H., eds), Vol 36, Munksgaard, Copenhagen.

48. Vyas, M. N.; Vyas, N. K.; Meikle, P. J.; Sinnott, B.; Pinto, B. M.; Bundle, D. R.; Quiocho, F. A. *J. Mol. Biol.* **1993**, *231*, 133-136.

49. Clark, M.; Cramer, R. D.; Vanopdenbosch, N. *J. Comput. Chem.* **1989**, *10*, 982-1012.

50. Gasteiger, J.; Marsili, M. *Tetrahedron* **1980**, *36*, 3219-3228.

51. Gasteiger, J.; Marsili, M. *Org. Magn. Reson.* **1981**, *15*, 353-360.

52. Cornell, W. D., Cieplak, P., Bayly, C. I., Gould, I. R., Merz, K. M., Ferguson, D. M., Spellmeyer, D. C., Fox, T., Caldwell, J. W., and Kollman, P. A. *J. Am. Chem. Soc.* **1995**, *117*, 5179-5197.

CHAPTER 6: PROGRESS TOWARD THE SYNTHESIS OF THE SECOND CHIMERIC GLYCOPEPTIDE CORRESPONDING TO THE *SHIGELLA FLEXNERI* Y O-POLYSACCHARIDE AND ITS PEPTIDE MIMIC MDWNMHAA

This chapter describes the synthetic strategies, and the progress made toward the total synthesis of the second chimeric candidate, the β-glycopeptide, that we had previously designed in an attempt to improve the binding affinity of the octapeptide MDWNMHAA to its cognate antibody. The synthetic work described in this chapter was carried out by the thesis author.

Our strategy involved tethering of three fragments to form the glycopeptide backbone. Each fragment was synthesized using solution and/or solid phase methodology. The key step in the construction of the glycopeptide was the formation of the less thermodynamically favored beta thioether linkage between the peptide and the sugar. The formation of this beta-linkage was successfully achieved in this work. Furthermore, choosing protecting groups on both the peptide portion and the sugar portion that are compatible with all the reaction conditions was one of the challenges in the synthesis of this multifunctional molecule. The three fragments were successfully synthesized and coupled to form the fully

protected glycopeptide. Deprotection of the crude, fully protected glycopeptide afforded the desired β-glycopeptide. However, after purification of the final glycopeptide by reverse-phase HPLC, ^{1}H NMR spectroscopy indicated the presence of a peptide impurity in a 1:1 ratio.

6.1 ABSTRACT

Progress made toward the synthesis of a second glycopeptide, which consists of a trisaccharide and a MDW moiety linked by a β-glycosidic linkage, is described. The key step in the synthesis of the second glycopeptide was to form a thermodynamically less favored β-linkage in one of the three intermediates. A different approach other than the two-phase strategy used in the synthesis of the alpha glycopeptide, was successfully exploited to establish this unfavorable β-linkage. The two other fragments needed to synthesize the glycopeptide were also successfully synthesized. The three fragments were then coupled together to form the fully protected glycopeptide. After purification by reverse-phase HPLC, ^{1}H NMR spectroscopy showed that the desired beta glycopeptide had co-eluted with a peptide impurity.

6.2 INTRODUCTION

Chemical synthesis and testing of target molecules that bind to protein receptors are often followed by modifications of their structures in order to improve their biological activity. The availability of the experimentally determined three-dimensional structures of the protein receptors facilitates such modifications.

The structures of the complexes of the antibody SYA/J6 Fab fragment of both the carbohydrate-mimetic octapeptide MDWNMHAA (Figure 6-1a) and the parent pentasaccharide have been determined by X-ray crystallogryaphy and showed that the NMHAA portion of the mimetic octapeptide, as well as, adopting a well-ordered α-helix, engaged several water molecules in binding to the antibody. Moreover, microcalorimetry experiments revealed that the binding of the octapeptide is only 2-fold higher than the parent pentasaccharide, most probably because of an unfavorable entropy of binding in the octapeptide.[1,2] Recently, we have shown that this mimetic peptide MDWNMHAA is indeed an immunogenic mimic of the *Shigella flexneri* Y cell-surface polysaccharide.[3] With all this information in hand, we propose to further improve the immunogenicity of the mimetic octapeptide by improving its binding affinity.

As described in Chapter 5, in order to improve the binding of the octapeptide, we have targeted the NMHAA portion of the octapeptide which contributes mostly to the unfavorable entropy of binding by engaging several water molecules and adopting a well-ordered α-helix. We have designed, using molecular modeling, two chimeric glycopeptides consisting of a MDW portion

from the octapeptide with a modified W to accommodate the other portion, which is a rhamnose trisaccharide (A-B-C) from the parent pentasaccharide, with a thioglycosidic linkage connecting peptide and carbohydrate moieties. The molecular modeling study showed that the chimeric molecules with either an α- or β- linkage might represent reasonable surrogate ligands for the antibody.

The α-glycopeptide was successfully synthesized but the immunochemical characterization showed no binding to its complementary antibody (Chapter 5).[4] Since the molecular modeling study showed that the β-glycopeptide superpimposed better on the parent ligands than the α-glycopeptide and that the interaction of the W moiety with the hydrophobic pocket within the antibody combining site was more pronounced in the beta than in the alpha glycopeptide,[4] we were prompted to synthesize the second candidate in order to characterize it immunochemically.

This chapter describes the strategy used and the progress made toward the synthesis of this β-glycopeptide.

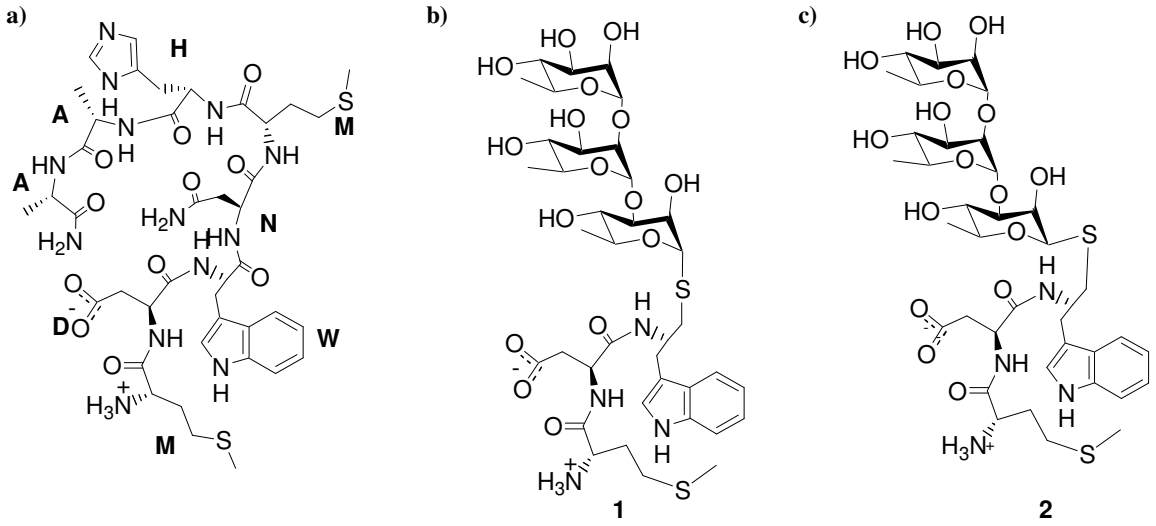

Figure 6-1: Structures of the (a) the *Shigella flexneri* Y mimetic peptide, (b) the chimeric α-glycopeptide **1**, (c) the chimeric β-glycopeptide **2**.

6.3 RESULTS AND DISCUSSION

6.3.1 Molecular modeling

Section 5.4.2 in Chapter 5 described in detail the molecular modeling studies carried out on the two designed chimeric glycopeptides. The results obtained showed that both glycopeptides could fit well into the binding groove without steric clashes. Superpimposition of the two glycopeptides on the parent octapeptide and the parent pentasaccharide showed that the β-glycopeptide superpimposes better on the parent ligands than the alpha glycopeptide (Figure 6.2).[4] It was also observed that the W moiety interacts better with the hydrophobic pocket within the combining site than the α-glycopeptide.[4]

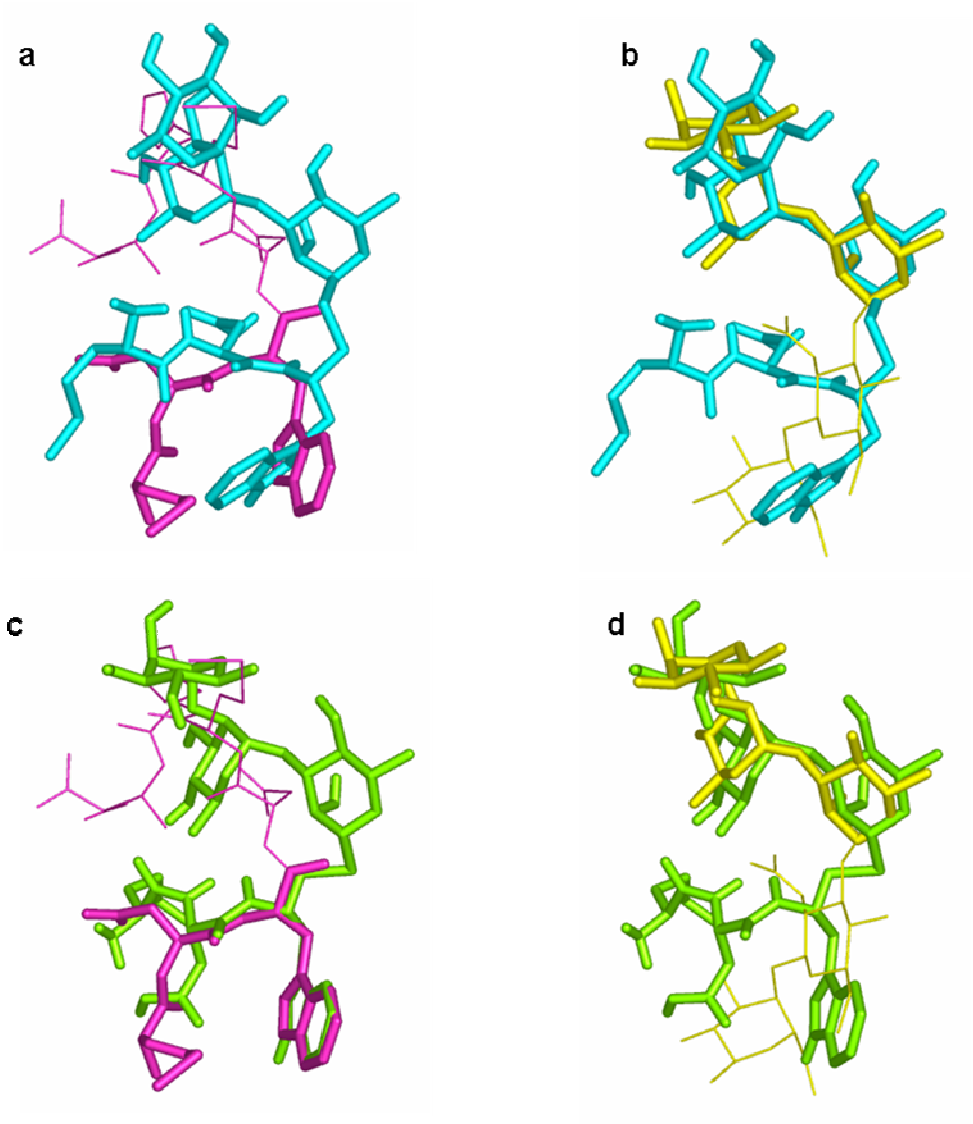

Figure 6-2: Superpimposition of the (a) α-glycopeptide **1** (cyan) on the parent octapeptide (pink), (b) α-glycopeptide **1** (cyan) on the parent pentasaccharide (yellow), (c) β-glycopeptide **2** (green) on the parent octapeptide (pink), (d) β-glycopeptide **2** (green) on the parent pentasaccharide (yellow).

6.3.2 Synthesis

6.3.2.1 Synthesis of the β-glycopeptide

The β-glycopeptide **2** could be prepared by deprotection of the glycopeptide **3**, which, in turn, could be obtained by coupling the dipeptide **4** with the amine **5**. The amine **5** could be prepared by removal of the Fmoc protecting group from the intermediate **6** (Scheme 6-1).

Scheme 6-1: Retrosynthetic analysis of the β-glycopeptide **2**

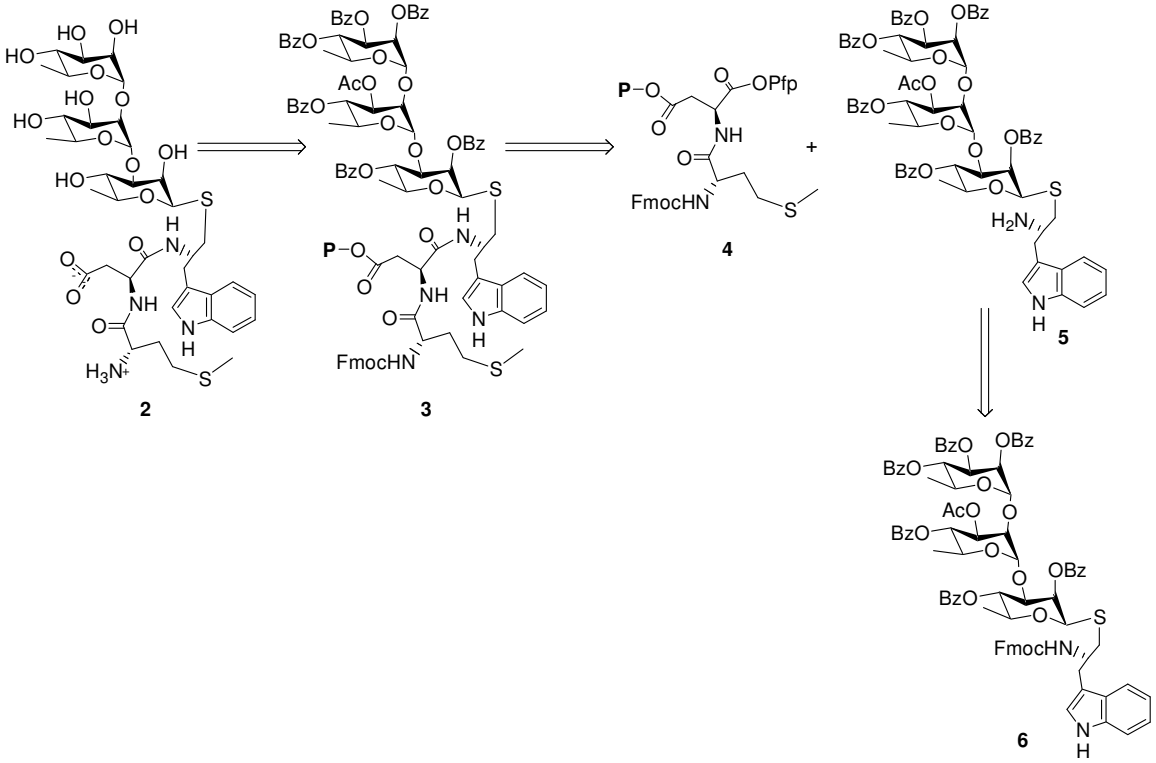

Since formation of a β-rhamnoside in glycosylation reactions is disfavored, a different strategy other than the phase-transfer procedure[5] used to make the α-analogue, was required for the synthesis of fragment **6**. We turned, therefore, to the glycosylation reaction with an ulosyl bromide, known to give β-anomers[6], although to the best of our knowledge, glycosylation of ulosyl bromides with thioether acceptors to form S-β-L-ulosides is unprecedented. Retrosynthetic analysis of compound **6** revealed that it could be synthesized from the trisaccharide ulosyl bromide **7** and the thiol **8** (Scheme 6-2). The ulosyl bromide **7** could be obtained from the rhamnal **9**, which in turn, could be synthesized from L-rhamnose (Scheme 6-2).

Scheme 6-2: Retrosynthetic analysis of intermediate **6**

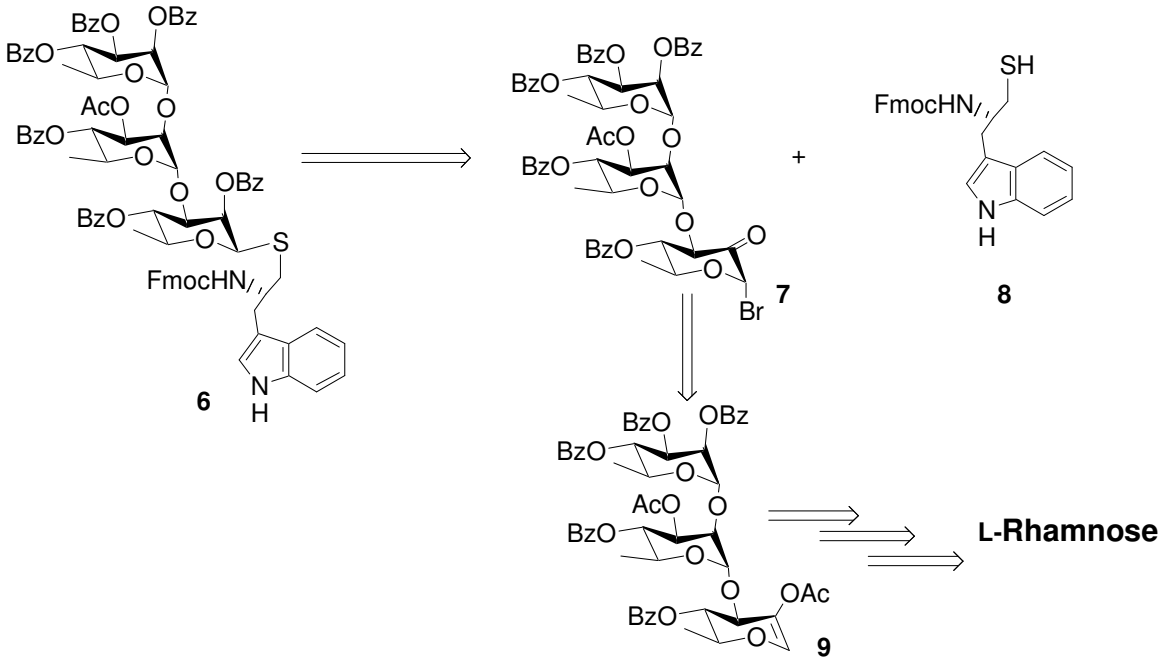

The rhamnal **9** was successfully synthesized in 8 steps as shown in scheme 6-3. L-rhamnose was first benzoylated to give **10**, followed by selective anomeric debenzoylation using NH_2NH_2.OAc in DMF to afford compound **11**. Reaction of the free anomeric hydroxyl group with trichloroacetonitrile gave the trichloroacetimidate **12**, which was then coupled with the rhamnose derivative **13** to give the disaccharide **14** in good yield. The thioglycoside **14** was then converted to its tricholoroacetimide **15** using standard conditions. The glycosylation reaction between the trichloroacetimidate **15** and acceptor **16** proceeded smoothly to give the trisaccharide **17** in good yield. The orthoester **18** was then obtained by first bromination of the thioglycoside trisaccharide **17** using 1 M IBr in CH_2Cl_2, followed by reaction with MeOH/lutidine/tetrabutylammonium bromide. The orthoester **18** was then refluxed in bromobenzene in the presence of a catalytic amount of pyridine to afford successfully the rhamnal **9** in good yield. However, conversion of the rhamnal **9** to the desired ulosyl bromide **7** using NBS/EtOH resulted in the decomposition of the ulosyl bromide **7** (Scheme 6-3).

The two acceptors **13** and **16** used in the synthesis of the rhamnal **9** were successfully synthesized starting from a known diol **19**[7] (Scheme 6-4). The acceptor **13** was derived from the acceptor **16**, which was obtained in two steps starting from the known diol **19**, following standard procedures. The acceptor **16** was then benzoylated to afford the rhamnose derivative **21**, which then underwent a deacetylation reaction to give the acceptor **13** (Scheme 6-4).

Scheme 6-3: Attempted synthesis of the trisaccharide ulosyl bromide **7**

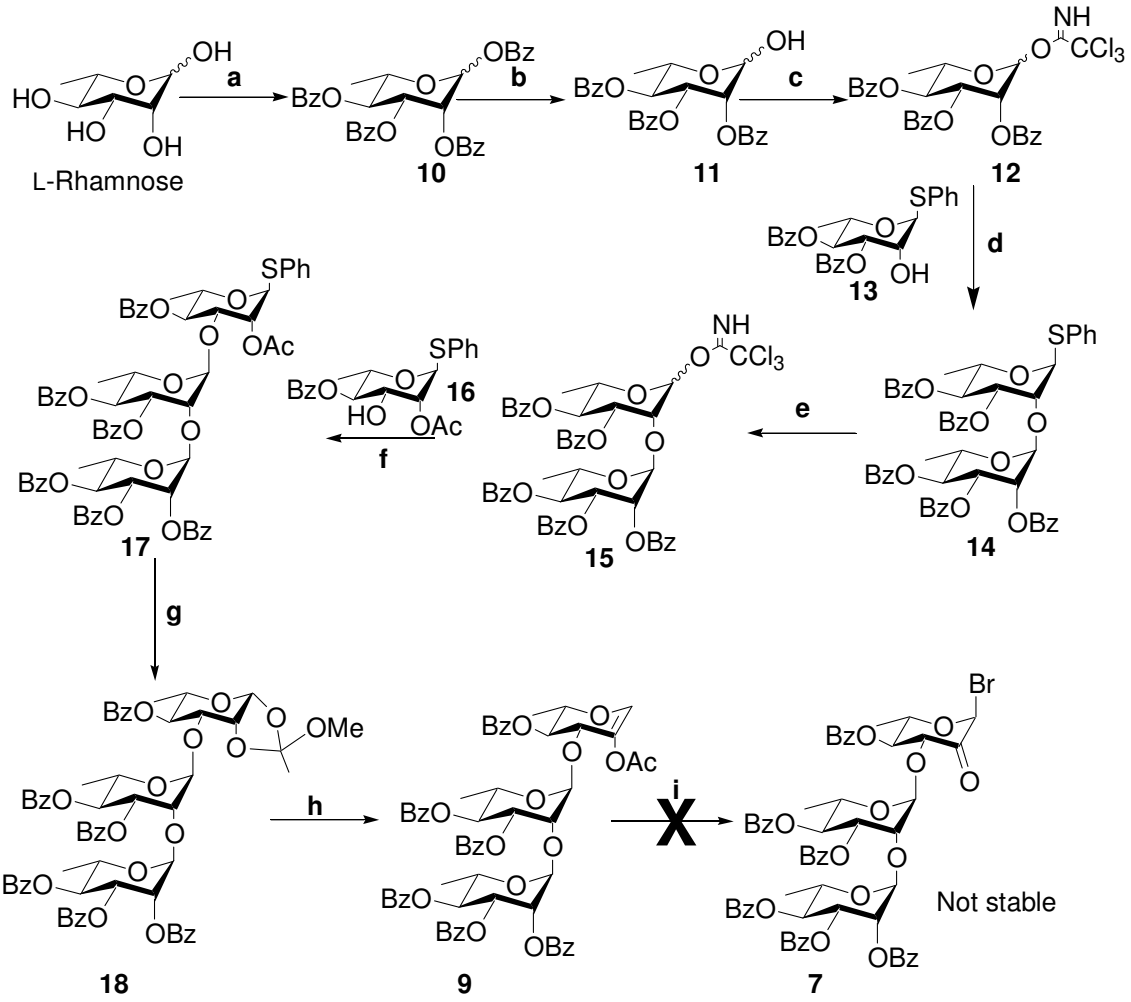

(a) BzCl, py 0 °C→ rt, (b) NH_2NH_2.OAc, DMF, (c) trichlroacetonitrile, DBU, CH_2Cl_2, 0 °C, 78% over 3 steps, (d) TMSOTf, CH_2Cl_2, -30 °C, 92%, (e) i) NBS, acetone:water (9:1), 90%, ii) trichlroacetonitrile, DBU, CH_2Cl_2, 0 °C, 75%, (f) TMSOTf, CH_2Cl_2, -30 °C, 78%, (g) i) 1 M IBr in CH_2Cl_2, 0 °C, ii) 2,4-lutidine, tetrabutylammonium bromide, MeOH, CH_2Cl_2, 50 °C, (h) py, bromobenzene, reflux, 68%, over 2 steps, (i) NBS, dry ethanol, CH_2Cl_2, 0 °C, decomposition.

Scheme 6-4: Synthesis of the two acceptors **13** and **16**

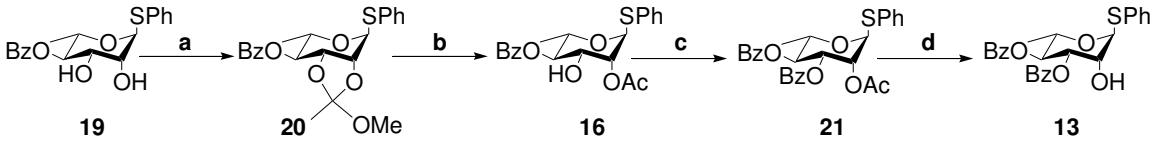

(a) trimethylorthoacetate, PTSA, CH_3CN, (b) 80% AcOH, 88% over 2 steps, (c) BzCl, py 0 ^{o}C→ rt, (d) MeOH, AcCl, 45 ^{o}C, 68% over 2 steps.

Due to the instability of the trisaccharide ulosyl bromide **7**, we were restricted to using mono-rhamnose ulosyl bromide. We reasoned that intermediate **6** could instead be derived from the monosaccharide ulosyl bromide **24**, as shown in Scheme 6-5. From a retrosynthetic analysis, fragment **6** could be prepared, by a glycosylation reaction between the acceptor **22** and the disaccharide trichloroacetimidate donor **15**. Removal of the PMB group from fragment **23** should then afford the acceptor **22**, and a glycosylation reaction between the ulosyl bromide **24** and the thiol **8** should result in the formation of the beta linkage in intermediate **23** (Scheme 6-5).

Scheme 6-5: Retrosynthetic analysis of intermediate **6**

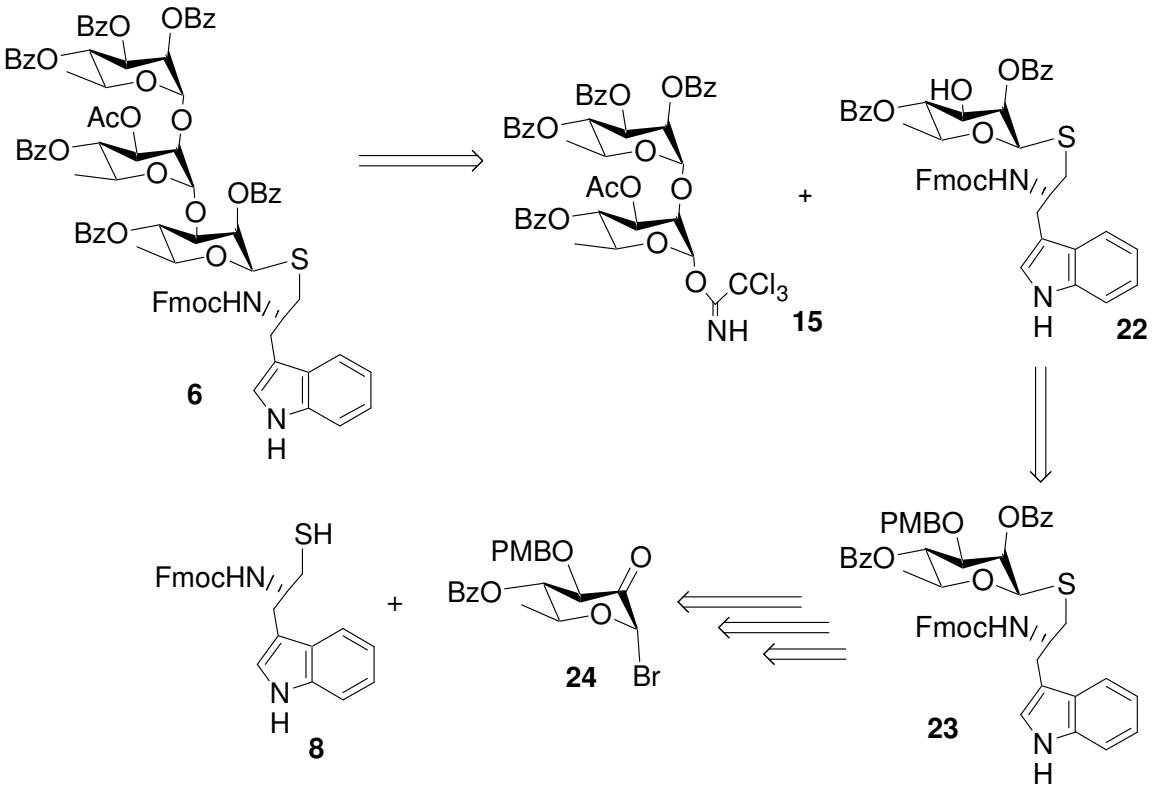

The ulosyl bromide **24** was successfully synthesized in 12 steps starting from the commercially available L-rhamnose (Scheme 6-6). Selective 4-methoxybenzylation at O3, via the 2,3-*O*-stannylidene derivative, followed by acetylation at O2 of the intermediate **19** (47) afforded **25** in 70% overall yield. Treatment of **25** with MeOH/lutidine/tetrabutylammonium bromide, following *S*-bromination using 1 M IBr in CH_2Cl_2, gave the orthoester **26** in moderate yield. When bromine was used instead of IBr, the yield of the orthoester **26** was improved to 90% over the 2 steps. On refluxing the orthoester **26** in bromobenzene for 12 h in the presence of a catalytic amount of pyridine (48), **26**

underwent rearrangement to give the 2-acetoxy-L-rhamnal **27** which, upon treatment with *N*-bromosuccinimide/ethanol in CH_2Cl_2 at 0 °C, yielded successfully the ulosyl bromide **24** in nearly quantitative yield (Scheme 6-6).

Scheme 6-6: Synthesis of the ulosyl bromide **24**

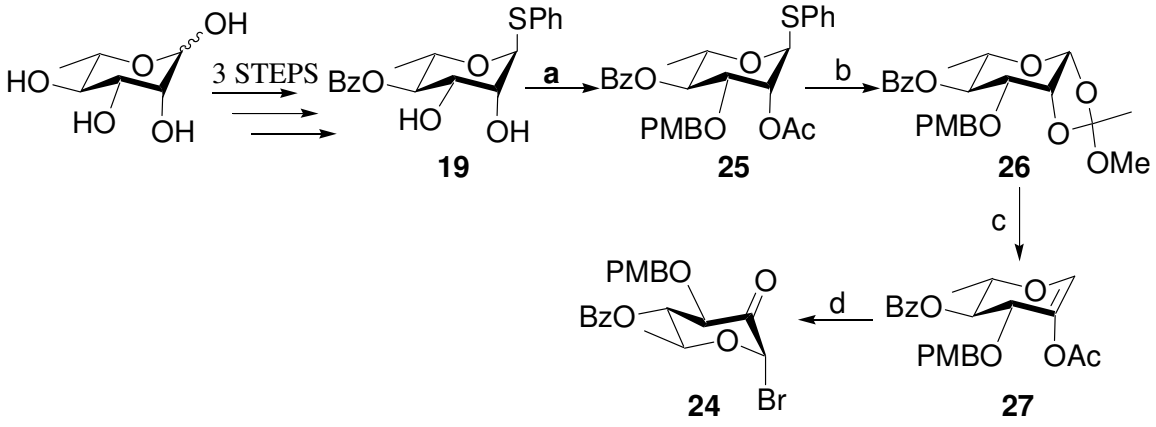

(a) i) Bu_2SnO, reflux under a Dean-Stark trap, ii) Bu_4NI, PMBBr, benzene, iii) Ac_2O/Py, 72% for the 3 steps, (b) i) Br_2, CH_2Cl_2, ii) 2,6-lutidine/Bu_4NBr/MeOH, 90% over 2 steps, (c) PhBr, cat. Py, 70%, (d) NBS/EtOH, 0 °C.

The Fmoc-thiotryptophanol derivative **8**, on the other hand, was prepared in 3 steps (Scheme 6-7) starting from the bromide **28**, which was an intermediate synthesized and used in the synthesis of the α-glycopeptide (Chapter 5). Similar to the conversion of a thiophenol group to a thiol group in the synthesis of the α-glycopeptide, the bromide **28** was successfully converted to the thiol **8** using the same conditions. Thus, the bromide **28** was refluxed with thiourea to afford the

isothiouronium salt **29**, which was then treated with 15% $Na_2S_2O_5$ to produce the desired thiol **8** in good yield (Scheme 6-7).

Scheme 6-7: Synthesis of the Fmoc-thiotryptophanol derivative **8**

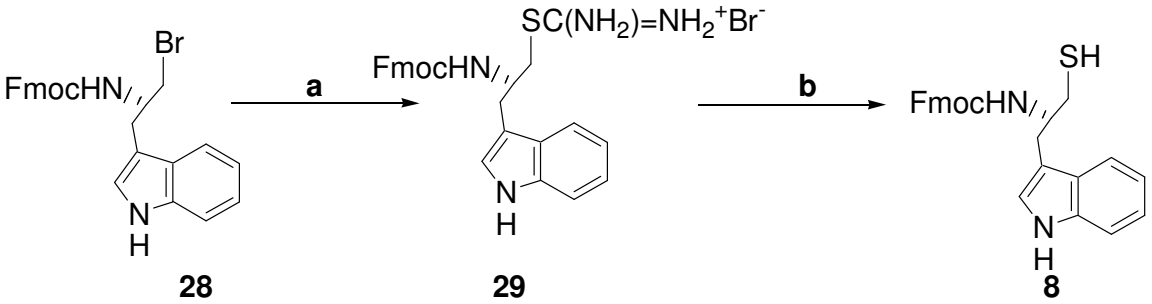

(a) Thiourea, CH_3CN, reflux, b) $Na_2S_2O_5$, CH_2Cl_2/H_2O, reflux, 82% over 2 steps.

With the ulosyl bromide **24** and thiol **8** in hand, the glycosylation reaction was first examined using the standard Koenigs-Knorr conditions (Ag_2CO_3 in dichloromethane at 25 °C). The glycosylation was completed within 30 min, but a mixture of 1:1 α- and β-anomers was obtained. When the glycosylation reaction was repeated in acetone, in which the thiol **8** was more soluble, the ratio was improved to 5:2 in favor of the β-anomer. Moreover, when the reaction was carried out -78 °C in acetone, the glycosylation reaction between **24** and **8** was essentially stereospecific, affording the *S*-β-uloside **30** in 62% yield (Scheme 6-8). The carbonyl group of the *S*-β-uloside **30** was then stereospecifically reduced to its alcohol using sodium borohydride to afford **31**, and in the presence of

benzoyl chloride and pyridine, **31** was converted to the desired fragment **23**. While TFA-mediated cleavage of the PMB ester protecting group at O3 on the glycopeptide **23** was not successful, cleavage using a catalytic amount of the Lewis acid, $SnCl_4$, in the presence of the nucleophile PhSH at -78 ^oC[8], gave the intermediate glycopeptide **22** in excellent yield (Scheme 6-8).

Scheme 6-8: Synthesis of Fragment **22**

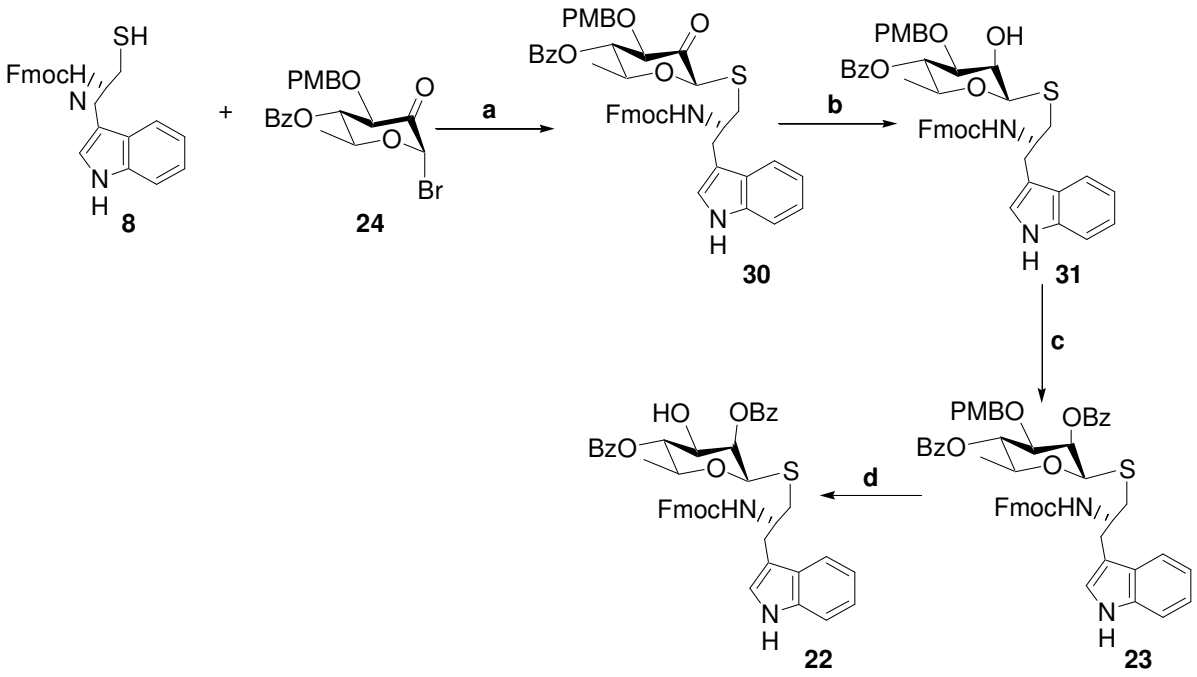

(a) Ag_2CO_3, acetone, -78 ^oC, 62%, (b) $NaBH_4$, CH_2Cl_2:MeOH (1:1), 90%, (c) BzCl, py, 92%, (d) $SnCl_4$/PhSH, -78 ^oC, 96%.

The glycosylation reaction between the two fragments, **22** and the disaccharide trichloroacetimidate donor **15**, was then carried out following standard procedures using TMSOTf as activator. However, the acceptor **22** was found to be quite deactivated and reacted very slowly with the acetamidate **15** to afford the intermediate **6** in very low yield, accompanied by several side products. The glycosylation reaction was then repeated using a more reactive disaccharide sulfoxide donor **32**, instead of the trichloroacetimidate donor **15**. No product was isolated.

The yield of the glycosylation product **6** was improved when the addition of the trichloroacetimidate **15** and TMSOTf was reversed, with **15** added dropwise (Scheme 6-9). After removal of Fmoc from fragment **6** to give the amine **5**, the latter was then coupled with the activated dipeptide **4** to afford the fully protected glycopeptide **3** (Scheme 6-9). Deprotection of the crude glycopeptide **3** was then carried out by first romoving Fmoc using DBU, followed by 2% NH_2NH_2 and NaOAc in meOH to afford the desired glycopeptide **2**. After purification by reverse-phase HPLC, ^{1}H NMR indicated that the final β-glycopepitde **2** had co-eluted with a peptide impurity. The quantity of material obtained was too low to continue with further purification. Unfortunately, owing to time constraints, this synthesis was deferred until a later time.

Scheme 6-9: Synthesis of the fully protected β-glycopeptide **3**

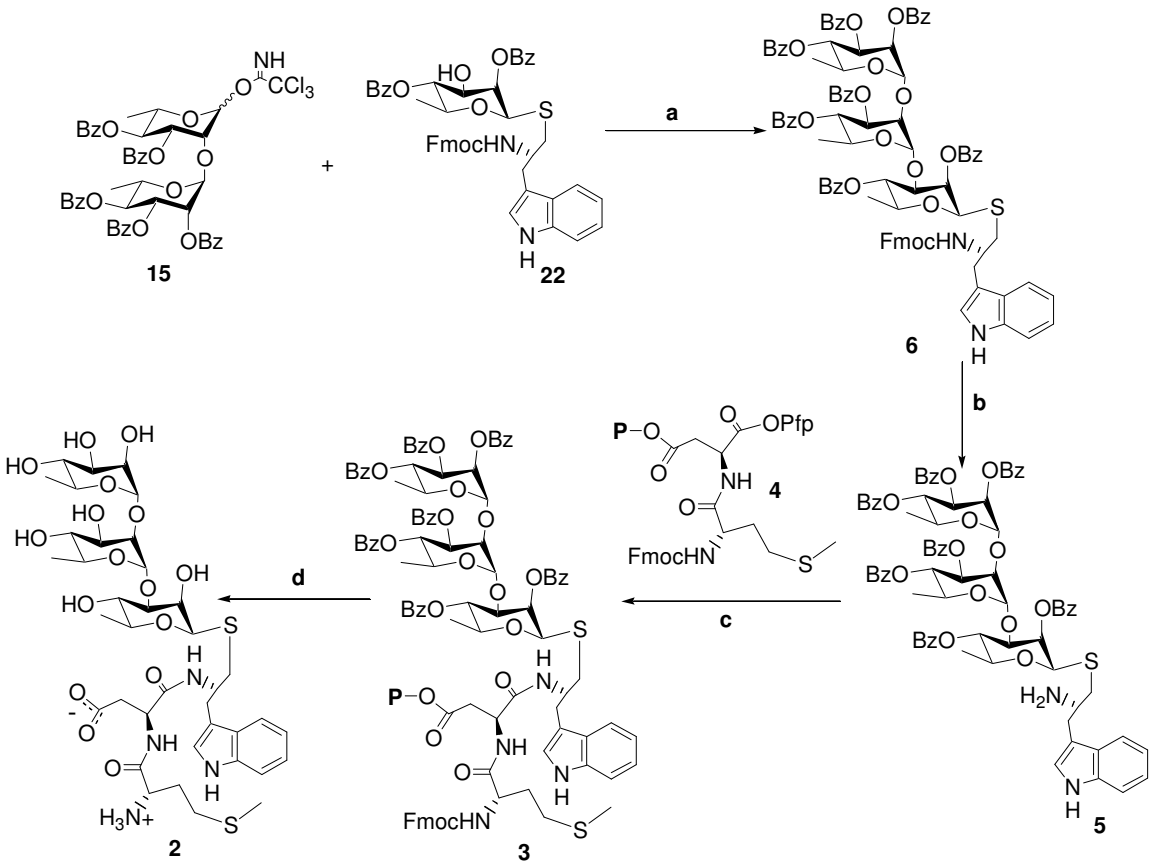

(a) TMSOTf, CH_2Cl_2, -30 °C, 68%, (b) DBU/Octanethiol, THF, (c) **4**, HOBt, DIPEA, THF, (d) i) DBU/octanethiol, THF, ii) 2% NH_2NH_2, THF, iii) NaOMe, MeOH.

6.4 EXPERIMENTAL

6.4.1 Synthesis

6.4.1.1 General methods

The Fmoc amino acids used were purchased from Novabiochem and the other reagents from Aldrich Chemical Co. DMF was freed of amines by

concentrating under high vacuum and was then distilled and stored over molecular sieves whereas the other solvents were distilled according to standard procedures.[9] The dipeptide **3** was synthesized on 2-chlorotrityl resin[10] (Novabiochem) (1.64 mmol/g substitution level), using standard 9-fluorenyl-methoxycarbonyl (Fmoc) chemistry[11] employing the 2-[1-H-Benzotriazole-1-yl]-1.1.13.3-tetramethyluronium hexafluorophosphate/1-hydroxybenzotriazole (HBTU/HOBt) coupling strategy.[12-14] The Kaiser ninhydrin (5% ninhydrin in ethanol, 80% phenol in ethanol and 2% 0.001 M aqueous KCN in pyridine) assay for the amino group[15] was used to monitor both the Fmoc-amino acid coupling and the Fmoc deprotection reactions. 1D and 2D NMR spectra were recorded on 400 and 500 MHz spectrometers. Chemical shifts were referred to internal $CHCl_3$ or external DSS [3-(trimethylsilyl)-1-propanesulfonic acid]; coupling constants were obtained from a first-order analysis of one dimensional spectra, and spectral assignments were based on COSY, HMQC and TOCSY experiments. MALDI-TOF mass spectra were obtained for samples dispersed in a 2,5-dihydroxybenzoic acid matrix on a Perseptive Biosystems Voyager-DE instrument. High resolution mass spectra were LSIMS (FAB), run on a Kratos Concept H double focusing mass spectrometer at 10,000 RP and by the electrospray ionization method, using an Agilent 6210 TOF LC/MS high resolution magnetic sector mass spectrometer.

6.4.1.2 Synthesis of the benzoylated rhamnose 10

To a stirred ice-cold solution of L-rhamnose monohydrate (5g, 25 mmol) in pyridine (60 mL) was added dropwise benzoyl chloride (23 mL, 198 mmol). The

mixture was then stirred at rt for 4 h under N_2. The mixture was cooled to 0 ^oC and ice (6g) was added. The solvent was then removed under high vacuum and the residue dissolved in CH_2Cl_2 (150 mL) was washed successively with water (150 mL), 1 M HCl (150 mL), sat. $NaHCO_3$ (150 mL), and water (150 mL), dried over Na_2SO_4 and filtered. The solvent was evaporated to give **10** as a colorless crystalline solid, which was used directly in the next step without further purification.

6.4.1.3 Synthesis of intermediate 11

To the crude **10** above in DMF (50 mL), hydrazine acetate (4g, 43.9 mmol) was added and the mixture was stirred at rt for 12 h. The mixture was diluted with EtOAc (200 mL) and washed with half sat. NaCl (2 × 100 mL), dried over Na_2SO_4, filtered and the solvent removed. Traces of DMF was removed on high vacuum in a 45 ^oC water bath to afford the crude **11** as a pale yellow oil which was used without further purification in the next step.

6.4.1.4 Synthesis of the trichloroacetimidate 12

To an ice-cold solution of the crude **11** and trichlroacetonitrile (7.5 mL, 75 mmol) in anhydrous CH_2Cl_2 (200 mL), DBU (952 µL, 18.7 mmol) was added and the mixture was stirred at 0 ^oC for 2 h under N_2. The reaction mixture was allowed to warm to rt. It was then concentrated and the crude material was purified by column chromatography (hexanes:EtOAc 3:1 + 1% NEt_3) to afford the trichloroacetimidate **12** (12.1 g, 78% over the 3 steps) as a colorless foam. ^1H NMR (500 MHz, $CDCl_3$): δ (ppm) 8.83 (1H, S, NH-tricloroacetamidate), 8.15-7.24

(15 H, m, ArH-Bz), 6.50 (1H, br s, H1), 5.93-5.86 (2H, m, H2, H3), 5.79 (1H, t, $J_{3,4}$ = $J_{4,5}$ = 10.1 Hz, H4), 4.41 (1H, dq, H5), 1.37 (3H, d, $J_{5,6}$ = 6.1 Hz, H6). ^{13}C NMR (125 MHz, $CDCl_3$): δ (ppm) 165.9-165.5 (3C, 3 × *C*=O-OBz), 160.3 (1C, *C*=NH-trichloroacetimidate), 133.9-128.6 (18C, C_{Ar}-OBz), 95.0 (1C, C1), 91.0 (1C, *C*Cl_3-trichloroacetimidate), 71.2 (1C, C4), 69.9 (2C, C2,C3), 69.4 (2C, C5), 18.0 (1C, C6). HRMS Calcd for [$C_{29}H_{24}NO_8Cl_3$+Na]: 642.0465. Found: 642.0451.

6.4.1.5 Synthesis of the orthoester 20

To the diol **19**[7] (30g, 83.3 mmol) in anhydrous CH_3CN (150 mL), trimethylorthoacetate (35 mL, 274 mmol) and PTSA (0.7 g, 4.1 mmol) were added and the mixture was stirred under vacuum (30 psi) for 1.5 h. Et_3N (2 mL) was added and the solvent was removed to afford the crude **20** which was used without purification in the next step.

6.4.1.6 Synthesis of intermediate 16

The crude **20** above was dissolved in 80% AcOH (500 mL) and the mixture was stirred at rt for 12 h under N_2. The mixture was concentrated under reduced pressure and the crude was purified by column chromatography (hexanes:EtOAc 3:1) to afford the product **16** (29.5 g, 88% over 2 steps) as a colorless crystalline solid. ^{1}H NMR (500 MHz, $CDCl_3$): δ (ppm) 8.13-7.25 (10H, m, ArH), 5.55 (1H, br s, H1), 5.40 (1H, dd, $J_{1,2}$ = 1.1, $J_{2,3}$ = 3.2 Hz, H2), 5.79 (1H, t, $J_{3,4}$ = $J_{4,5}$ = 9.8 Hz, H4), 4.50 (1H, dq, H5), 4.23-4.16 (1H, m, H3), 2.49 (1H, br s, OH), 2.20 (3H, s, C*H*$_3$-OAc), 1.32 (3H, d, $J_{5,6}$ = 6.1 Hz, H6). ^{13}C NMR (125 MHz, $CDCl_3$): δ (ppm) 170.7 (1C, *C*=O-OAc), 167.3 (1C, *C*=O-OBz), 133.8-128.1

(12C, C_{Ar}), 86.0 (1C, C1), 75.7 (1C, C4), 74.5 (1C, C2), 69.6 (1C, C3), 67.7 (1C, C5), 21.3 (3H, *C*H_3-OAc), 17.7 (1C, C6). HRMS Calcd for [$C_{21}H_{22}O_6S$+H]: 403.1215. Found: 403.1202.

6.4.1.7 Synthesis of intermediate 21

To an ice-cold solution of the intermediate **16** (14.1 g, 35 mmol) in pyridine (100 mL), benzoyl chloride (10 mL, 86.1 mmol) was added dropwise. The mixture was stirred at rt for 2 h under N_2. Ice (5 g) was then added and the solvent was concentrated. The crude material was dissolved in CH_2Cl_2 (300 mL), washed successively with water (200 mL), 1 M HCl (200 mL), sat. $NaHCO_3$ (200 mL), and water (200 mL), dried over Na_2SO_4, filtered and the solvent evaporated to afford the crude **21** which was used without further purification in the next step.

6.4.1.8 Synthesis of intermediate 13

To the crude **21** above in MeOH (300 mL), AcCl (15 mL) was added dropwise. The mixture was then stirred at 45 ^oC for 12 h under N_2, cooled to 0 ^oC, and Et_3N was added to neutralize the acid. The solvent was removed and the crude material was partitioned between CH_2Cl_2 (250 mL) and water (200 mL). The organic layer was washed with sat. $NaHCO_3$, dried over Na_2SO_4, filtered and the solvent removed. The crude material was then purified by column chromatography (hexanes:EtOAc 4:1) to afford **13** (11.1 g, 68% over 2 steps). ^1H NMR (500 MHz, $CDCl_3$): δ (ppm) ^1H NMR (500 MHz, $CDCl_3$): δ (ppm) 8.14-7.28 (15H, m, ArH), 5.67 (1H, m, H2), 5.61(1H, br s, H1), 5.35 (1H, t, $J_{3,4} = J_{4,5}$ = 9.8 Hz, H4), 4.59 (1H, dq, H5), 4.35-4.29 (1H, m, H3), 2.56 (1H, d, $J_{2,OH}$ = 7.9 Hz,

O*H*), 1.35 (3H, d, $J_{5,6}$ = 6.4 Hz, H6). ^{13}C NMR (125 MHz, $CDCl_3$): δ (ppm) 167.4 (2C, *C*=O-OBz), 133.8-127.9 (18C, C_{Ar}), 87.8 (1C, C1), 76.0 (1C, C4), 75.1 (1C, C2), 70.0 (1C, C3), 67.8 (1C, C5), 17.7 (1C, C6). HRMS Calcd for [$C_{26}H_{24}O_6S$+H]: 465.1371. Found: 465.1363.

6.4.1.9 Synthesis of the disaccharide 14

The trichloroacetimidate **12** (9.0 g 14.5 mmol) and intermediate **13** (5.9 g, 12.7 mmol) was stirred in CH_2Cl_2 (75 ml) with freshly dessicated molecular sieves (4 g) for 15 min. The mixture was then cooled to -30 °C and TMSOTf (0.1 mL, 0.5 mmol) was added. The mixture was stirred at -30 °C for 30 min under N_2 and then allowed to warm to rt. After stirring for another 30 min at rt, Et_3N (0.5 mL) was added and the mixture was filtered through a pad of Celite. The mixture was diluted with CH_2Cl_2 (100 mL), washed with sat. $NaHCO_3$ (50 ml), and the organic layer was dried over Na_2SO_4, and filtered. The solvent was removed and the crude material was purified by column chromatography (toluene: EtOAc 20:1) to afford the disaccharide **14** (23.2 g, 92%) as a colorless foam. ^{1}H NMR (500 MHz, $CDCl_3$): δ (ppm) 8.26-7.13 (30 H, m, ArH), 5.95 (1H, dd, $J_{2',3'}$ = 3.2, $J_{3',4'}$ = 10.1 Hz, H3'), 5.85-5.63 (5H, m, H1, H2', H3, H4, H4'), 5.16 (1H, br s, H1'), 4.65-4.53 (2H, m, H2, H5), 4.33 (1H, dq, H5'), 1.44 (3H, d, $J_{5,6}$ = 6.4 Hz, H6), 1.28 (3H, d, $J_{5',6'}$ = 6.1 Hz, H6'). ^{13}C NMR (125 MHz, $CDCl_3$): δ (ppm) 166.1-165.3 (5C, 5 × *C*=O-OBz), 133.6-128.4 (30C, Ar), 99.8 (1C, C1'), 87.5 (1 C, C1), 78.6 (1C, C2), 74.1 (1C, C3), 72.2 (1C, C4), 71.9 (1C, C4'), 70.8 (1C, C2'), 69.9 (1C, C3'), 68.7 (1C, C5), 68.0 (1C, C5'), 17.9 (1C, C6), 17.7 (1C, C6'). HRMS Calcd for [$C_{53}H_{46}O_{13}S$+Na]: 945.2556. Found: 945.2560.

6.4.1.10 Synthesis of the trichloroacetimidate 15

To the disaccharide **14** (8.7 g, 9.4 mmol) in acetone:water (9:1, 140 mL) was added NBS (5.4 g, 28.2 mmol) and the mixture was stirred for 2 h. The mixture was then concentrated until turbidity arose. The residue was dissolved in EtOAc (300 mL), washed with sat. $NaHCO_3$ (3 × 100 mL), water (3 × 100 mL), dried over Na_2SO_4, and filtered. The solvent was removed and the crude material was purified by column chromatography (hexanes:EtOAc 5:1) to afford the hemiacetal (7.1 g, 90%) as a colorless foam.

To an ice-cold solution of the hemiacetal (6.0 g, 7.8 mmol) in CH_2Cl_2 (75 mL) were added trichloroacetonitrile (2.2 mL, 21.7 mmol) followed by DBU (93 µL, 3 mmol) and the mixture was stirred for 2 h at 0 °C under N_2. The solvent was then removed and the crude material was purified by colomn chromatography (hexanes:EtOAc 5:1 + 1% Et_3N) to afford the trichloroacetimidate **15** (5.3 g, 75%) as a colorless foam. This material is of limited stability and was used directly in the next step. ^{1}H NMR (500 MHz, $CDCl_3$): δ (ppm) 8.83 (1H, S, NH-tricloroacetimidate), 8.30-7.17 (25H, m, ArH), 6.52 (1H, br d, (1H, dd, $J_{5,6}$ = 1.3 Hz, H1), 5.97 (1H, dd, $J_{2',3'}$ = 3.3, $J_{3',4'}$ = 10.1 Hz, H3'), 5.86-5.66 (4H, m, H2', H3, H4, H4'), 5.23 (1H, br s, H1'), 4.59 (1H, br s, H2), H5), 4.33 (1H, dq, H5'), 1.44 (3H, d, $J_{5,6}$ = 6.4 Hz, H6), 1.28 (3H, d, $J_{5',6'}$ = 6.1 Hz, H6'). ^{13}C NMR (125 MHz, $CDCl_3$): δ (ppm) 166.1-165.0 (5C, 5 × *C*=O-OBz), 160.6 (1C, *C*=NH-trichloroacetimidate), 133.9-128.4 (30C, C_{Ar}), 99.7 (1C, C1'), 96.6 (1C, C1), 94.8 (1C, *C*Cl_3-trichloroacetimidate), 75.4 (1C, C2), 72.7-67.9 (7C, C2', C3, C3', C4, C4', C5, C5'), 18.0 (2C, C6, C6').

6.4.1.11 Synthesis of the trisaccharide 17

The tricholoroacetimidate **15** (2 g, 2.0 mmol) and intermediate **16** (760 mg, 1.9 mmol) was stirred in CH_2Cl_2 (20 ml) with molecular sieves (2 g) for 15 min under N_2. The mixture was then cooled to -40 ^oC, TMSOTf (28 µL, 0.16 mmol) was added, and the mixture was stirred at -30 ^oC for 30 min under N_2 and allowed to warm to rt over a period of 30 min. Et_3N (0.3 mL) was then added and the mixture was filtered through a pad of Celite. The mixture was diluted with CH_2Cl_2 (100 mL), washed with sat. $NaHCO_3$ (50 ml), and the organic layer was dried over Na_2SO_4, and filtered. The solvent was removed and the crude material was purified by column chromatography (hexanes:EtOAc 5:1) to afford the trisaccharide **17** (1.8 g, 78%) as a colorless foam. ^1H NMR (500 MHz, $CDCl_3$): δ (ppm) 8.13-7.13 (35H, m, ArH), 5.82 (1H, dd, $J_{2'',3''}$ = 3.2 , $J_{3'',4''}$ = 10.1 Hz, H3''), 5.68-5.61 (3H, m s, H2, H2'', H3'), 5.58 (3H, t, $J_{3',4'} = J_{4',5'}$ = 9.6 Hz, H4'), 5.50 (1H, s, H1), 5.49-5.45 (2H, m, H4, H4''), 5.22 (1H, br s, H1'), 4.69 (1H, d, H1''), 4.46 (1H, dq, H5), 4.39 (1H, dd, $J_{2,3}$ = 3.2, $J_{3,4}$ = 9.8 Hz, H3), 4.18 (1H, dq, H5''), 4.05 (1H, dq, H5'), 4.03 (1H, br s, H2'), 2.23 (3H, s, CH_3-OAc), 1.39 (3H, d, $J_{5',6'}$ = 6.1 Hz H6'), 1.30 (3H, d, $J_{5,6}$ = 6.3 Hz,H6), 1.00 (3H, d, $J_{5'',6''}$ = 6.1 Hz, H6''). ^{13}C NMR (125 MHz, $CDCl_3$): δ (ppm) 170.5 (1C, *C*H_3-OAc), 166.1-164.9 (6C, 6 × *C*=O-OBz), 133.6-128.1 (35C, C_{Ar}), 99.4 (1C, C1'), 99.2 (1C, C1''), 86.0 (1C, C1), 77.3 (1C, C2'), 74.1 (1C, C3), 73.4-70.4 (6C, C2, C2'', C3', C4, C4', C4''), 69.5 (1C, C3''), 68.4 (1C, C5), 68.1 (1C, C5'), 67.8 (1C, C5''), 21.3 (1C, *C*H_3-OAc), 18.0 (1C, C6'), 17.9 (1C, C6), 17.8 (1C, C6''). HRMS Calcd for [$C_{68}H_{62}O_{19}S$+H]: 1215.3684. Found: 1215.3674.

6.4.1.12 Synthesis of the trisaccharide orthoester 18

To an ice-cold solution of the trisaccharide **17** (500 mg, 0.4 mmol) in CH_2Cl_2 (10 mL), 1 M IBr in CH_2Cl_2 (0.5 mL) was added dropwise. The mixture was stirred for 30 min at 0 ^oC under N_2 and then diluted with cold CH_2Cl_2 (10 mL), washed with cold 5% aq. $Na_2S_2O_3$ (15 mL), and cold sat. $NaHCO_3$ (15 mL). The organic layer was dried over Na_2SO_4, filtered, and the solvent evaporated to give the trisaccharide bromide as a foam.

This foam was then dissolved in CH_2Cl_2 (2 mL) and 2,4-lutidine (109 µL) and tetrabutylammonium bromide (87 mg, 0.3 mmol) were added. The mixture was stirred at rt for 5 min and anhyd. MeOH (2 mL) was added. The mixture was stirred at rt for 2 h under N_2. The solvent was then removed and the residue in CH_2Cl_2 (15 mL) was washed with water (2 × 15 mL), sat. $NaHCO_3$ (15 mL), and water (15 mL). The organic layer was dried over Na_2SO_4, filtered, and the solvent evaporated. The crude orthoester **18** was used without further purification in the next step.

6.4.1.13 Synthesis of the rhamnal 9

The crude **18** and pyridine (65 µL) in bromobenzene (10 mL) was stirred under reflux for 3 h under N_2. The solvent was removed under reduced pressure and the residue was purified by column chromatography (toluene:EtOAc 25:1) to afford the rhamnal **9** (0.3 g, 68% over the 2 steps) as a colorless foam. . ^1H NMR (500 MHz, $CDCl_3$): δ (ppm) 8.08-7.14 (30H, m, ArH), 6.77 (1H, s, H1), 5.95 (1H, dd, $J_{2'',3''}$ = 3.4 , $J_{3'',4''}$ = 10.2 Hz, H3''), 5.84 (2H, br s, H2, H2''), 5.77 (1H, dd, $J_{2',3'}$ = 3.1, $J_{3',4'}$ = 10.1 Hz, H3'), 5.67 (2H, t, $J_{3',4'}$ = $J_{3'',4'''}$ = $J_{4',5'}$ = $J_{4'',5''}$ = 9.9 Hz,

H4', H4''), 5.37 (1H, s, H1'), 5.35 (1H, t, $J_{3,4}$ = $J_{4,5}$ = 4.2 Hz, H4), 5.09 (1H, s, H1''), 4.67 (1H, d, $J_{3,4}$ = 3.5 Hz, H3), 4.67 (1H, dq, H5), 4.36 (1H, dq, H5''), 4.29 (1H, br s, H2'), 4.24 (1H, dq, H5'), 2.23 (3H, s, CH_3-OAc), 1.52 (3H, d, $J_{5,6}$ = 6.9 Hz,H6), 1.38 (3H, d, $J_{5',6'}$ = 6.3 Hz H6'), 1.36 (3H, d, $J_{5'',6''}$ = 6.3 Hz, H6''). ^{13}C NMR (125 MHz, $CDCl_3$): δ (ppm) 169.8 (1C, *C*H_3-OAc), 166.1-165.2 (6C, 6 × *C*=O-OBz), 139.3 (1C, C1), 133.7-128.1 (30C, C_{Ar}), 99.9 (1C, C1''), 97.6 (1C, C1'), 77.3 (1C, C2'), 72.9 (1C, C5), 72.7 (1C, C4), 72.0 (2C, C4', C4''), 71.4 (1C, C3), 70.9 (1C, C3'), 70.7 (1C, C2''), 69.9 (1C, C3''), 67.9 (1C, C5''), 67.7 (1C, C5'), 21.0 (1C, *C*H_3-OAc), 18.0-17.7 (2C, C6', C6''), 16.3 (1C, C6). HRMS Calcd for [$C_{62}H_{56}O_{19}$+H]: 1105.3494. Found: 1105.3488.

6.4.1.14 Attempted synthesis of the trisaccharide ulosyl bromide 7

Rhamnal **9** (100 mg, 80 µmol) and absolute ethanol (6.2 µL, 0.1 mmol) were stirred in dry CH_2Cl_2 (5 mL) with freshly dessicated molecular sieves (1g) for 15 min under N_2. The mixture was then cooled to 0 °C and NBS (20 mg, 0.1 mmol) was added. Stirring was continued for 15 min at 0 °C under N_2 followed by immediate work-up by dilution with cold CH_2Cl_2 (10 mL), filtering through a pad of Celite, and washing with cold $Na_2S_2O_3$ (10%, 2 × 10 mL) and ice water (2 × 10 mL). The organic layer was then dried over Na_2SO_4 and the solvent evaporated to give a colorless foam (98 mg). Maldi TOF mass spectroscopy and TLC showed the disappearance of the product after work-up and appearance of several side products.

6.4.1.15 Synthesis of the intermediate 25

To a solution of the diol **19**[7] (6.3 g, 17.5 mmol) in benzene (125 mL), n-dibutyltin oxide (5.3 g, 21 mmol) was added and the suspension was stirred at reflux under a Dean-Stark trap for 12 h. Evaporation of the solvent gave a gummy solid, which was then dissolved in benzene (50 mL). PMB-Br (5 mL, 34.9 mmol) and tetrabutyl ammonium iodide (6.6 g, 17.5 mmol) were added and the mixture was stirred at 50 ^{o}C for 24 h under N_2. The brown solution was then concentrated and the residue was stirred with EtOAc (150 mL). The solid was removed by filtration though a pad of Celite and the filtrate was concentrated to a syrup that was dissolved in pyridine (40 mL). The mixture was then cooled to 0 ^{o}C and acetic acid (40 mL) was added dropwise. The mixture was stirred at rt for 12 h under N_2 and the solvent evaporated. The crude material was then purified by column chromatography (hexanes:EtOAc 4:1 + 1% Et_3N) to furnish **25** (6.6 g, 72% over 3 steps) as a colorless hard solid. ^{1}H NMR (500 MHz, $CDCl_3$): δ (ppm) 8.07-6.60 (14H, m, ArH), 5.65 (1H, br s, H2), 5.49 (1H, br s, H1), 5.35 (1H, t, $J_{3,4}$ = $J_{4,5}$ = 9.9 Hz, H4), 4.58 (1H, d, $J_{a,b}$ = 12.1 Hz, OCH_{2a}-PMB), 4.41-4.35 (1H, m, H5, OCH_{2b}-PMB), 3.89 (1H, dd, $J_{2,3}$ = 3.1, $J_{3,4}$ = 9.9 Hz, H3), 3.76 (3H, s, OCH_3-PMB), 2.19 (3H, s, CH_3-OAc), 1.27 (3H, d, $J_{5,6}$ = 6.4 Hz, H6). ^{13}C NMR (125 MHz, $CDCl_3$): δ (ppm) 170.6 (1C, *C*=O-OAc), 165.9 (1C, *C*=O-OBz), 159.5 (1C, C_{Ar}OMe-PMB), 133.8-114.0 (17C, C_{Ar}), 86.5 (1C, C1), 74.0 (1C, C3), 73.1 (1C, C4), 70.9 (1C, O*C*H_2-PMB), 70.2 (1C, C2), 69.3 (1C, C5), 55.4 (1C, O*C*H_3-PMB), 21.3 (3H, *C*H_3-OAc), 17.7 (1C, C6). HRMS Calcd for [$C_{29}H_{30}O_7$+Na]: 545.1609. Found: 545.1598.

6.4.1.16 Synthesis of the orthoester 26

Bromine (0.66 mL, 12.6 mmol) was added to a cold solution of **25** (6.4 g, 12.4 mmol) in CH_2Cl_2 (50 mL) and the mixture was stirred at 0 ^oC under N_2 for 30 min. The solvent was removed and the residue was further dried under high vacuum for 30 min to remove traces of bromine. The resulting syrup was then dissolved in dry CH_2Cl_2 (20 mL) and 2,4-lutidine (2.2 mL) and tetrabutyl ammonium bromide (2.2 g, 6.2 mmol) were added. The mixture was stirred at rt for 5 min under N_2 and anhydrous MeOH (15 mL) was added. The mixture was further stirred for 2 h under N_2. The solvent was then removed and the syrup was dissolved in CH_2Cl_2 (400 mL), washed with water (3 $\times$ 300 mL), sat. $NaHCO_3$ (400 mL), and water (300 mL). The organic layer was dried over Na_2SO_4, filtered, and the solvent evaporated. The residue was purified by column chromatography (hexanes:EtOAc 3:1 + 1% Et_3N) to afford the product **26** (4.8 g, 90%) as a colorless crystalline solid. ^1H NMR (500 MHz, $CDCl_3$): δ (ppm) 8.07-7.45 (5H, m, ArH-OBz), 7.17 (2H, d, $J_{o,m}$ = 8.1 Hz, *ortho*ArH-PMB), 6.74 (2H, d, *meta*ArH-PMB), 5.38 (1H, d, $J_{1,2}$ = 2.1 Hz, H1), 5.29 (1H, t, $J_{3,4} = J_{4,5}$ = 9.6 Hz, H4), 4.65 (1H, d, $J_{a,b}$ = 12.2 Hz, OCH_{2a}-PMB), 4.57 (1H, d, OCH_{2b}-PMB), 4.50 (1H, dd, $J_{2,3}$ = 4.4 Hz, H2), 3.79 (1H, dd, H3), 3.77 (3H, s, OCH_3-PMB), 3.53 (1H, dq, H5), 3.29 (3H, s, OCH_3-orthoester), 1.78 (3H, s, CH_3-orthoester), 1.25 (3H, d, $J_{5,6}$ = 6.3 Hz, H6). ^{13}C NMR (125 MHz, $CDCl_3$): δ (ppm) 165.6 (1C, *C*=O-OBz), 159.6 (1C, C_{Ar}OMe-PMB), 133.4-114.0 (11C, C_{Ar}), 97.7 (1C, C1), 77.4 (1C, C2), 75.3 (1C, C3), 72.6 (1C, C4), 71.4 (1C, O*C*H_2-PMB), 69.6 (1C, C5),

55.4 (1C, O*C*H_3-PMB), 50.2 (1C, O*C*H_3-orthoester), 24.5 (1C, *C*H_3-orthoester), 17.8 (1C, C6). HRMS Calcd for [$C_{24}H_{28}O_8$+Na]: 467.1681. Found: 467.1660.

6.4.1.17 Synthesis of the rhamnal 27

The orthoester **26** (4.5 g, 10.2 mmol) and pyridine (1.7 mL) in bromobenzene (95 mL) was stirred under reflux for 6 h. The solvent was removed under reduced pressure and the residue was purified by column chromatography (toluene:EtOAc 20:1) to afford the rhamnal **27** (6.7 g, 70%) as a white powder. ^{1}H NMR (500 MHz, $CDCl_3$): δ (ppm) 8.08-7.43 (5H, m, ArH-OBz), 7.23 (2H, d, $J_{o,m}$ = 8.6 Hz, *ortho*ArH-PMB), 6.81 (2H, d, *meta*ArH-PMB), 6.63 (1H, s, H1), 5.39 (1H, t, $J_{3,4}$ = $J_{4,5}$ = 4.9 Hz, H4), 4.59 (2H, s, OC*H*$_2$-PMB), 4.41-4.34 (2H, m, H3, H5), 3.76 (3H, s, OC*H*$_3$-PMB), 2.07 (3H, s, C*H*$_3$-OAc), 1.43 (3H, d, $J_{5,6}$ = 6.6 Hz, H6). ^{13}C NMR (125 MHz, $CDCl_3$): δ (ppm) 169.9 (1C, *C*=O-OAc), 165.7 (1C, *C*=O-OBz), 159.5 (1C, *C*$_{Ar}$OMe-PMB), 138.2 (1C, C1), 133.6-114.0 (12C, C_{Ar}, C2), 73.1 (1C, C3), 72.3 (1C, C5), 72.2 (1C, C4), 71.2 (1C, O*C*H_2-PMB), 55.4 (1C, O*C*H_3-PMB), 20.9 (1C, *C*H_3-OAc), 16.3 (1C, C6). Anal. Calcd. for $C_{23}H_{24}O_7$: C, 64.53; H, 5.27. Found: C, 64.70; H, 5.25.

6.4.1.18 Synthesis of the thiol 8

The bromide **28**[4] (7.1 g, 14.9 mmol) in acetonitrile (200 mL) was refluxed with thiourea (3.5 g, 46.6 mmol) for 12 h under N_2. The solvent was removed, the crude material **29** was dissolved in EtOAc (250 mL), and the mixture was refluxed with 15% $Na_2S_2O_5$ (150 mL) for 5 h under N_2. The $Na_2S_2O_5$ layer was extracted with EtOAc (3 × 200 mL), the extracts were combined with the original

EtOAc layer, then washed with half saturated NaCl (3 × 300 mL), dried over Na_2SO_4, and concentrated. The residue was purified by column chromatography (CH_2Cl_2:MeOH 100:1) to afford the thiol **8** (5.2 g, 82% over 2 steps) as a white solid. ^{1}H NMR (500 MHz, acetone-d_6): δ 10.07 (1H, br s, NH ring-Trp), 7.87 (2H, d, J = 7.4 Hz, H4-, H5-Fmoc), 7.71-7.64 (3H, m, H1-, H8-Fmoc, H4-Trp), 7.45-7.37(3H, m, H3-, H6-Fmoc, H7-Trp), 7.35 (2H, m, H2-, H7-Fmoc), 7.22 (1H, br s, H2-Trp), 7.11 (1H, br t, $J_{5,6}$ = $J_{6,7}$ = 7.1 Hz, H6-Trp), 7.04 (1H, br t, $J_{4,5}$ = 7.3 Hz, H5-Trp), 6.48 (1H, d, $J_{NH,\alpha}$ = 7.8 Hz, NH-Trp), 4.35 (2H, dd, $J_{9,10}$ = 7.0 Hz, CH_2-Fmoc), 4.20 (1H, t, H9-Fmoc), 4.10-4.01 (1H, m, αH-Trp), 3.15-3.04 (2H, m, CH_2SH-Trp), 2.84 (1H, br s, SH-Trp), 2.76 (1H, dd, $J_{a,b}$ = 13.9, $J_{a,\alpha}$ = 6.0 Hz, βCH_{2a}-Trp), 2.70 (1H, dd, $J_{b,\alpha}$ = 6.9 Hz, βCH_{2b}-Trp), ^{13}C NMR (125 MHz, acetone-d_6): δ (ppm) 156.2 (1C, C=O-urethane), 144.3 (2C, C8a-, C9a-Fmoc), 141.4 (2C, C4a-, C4b-Fmoc), 137.0 (1C, C3a-Trp), 128.2 (1C, C7a-Trp), 127.8 (2C, C3-, C6-Fmoc), 127.2 (2C, C2-, C7-Fmoc), 125.5 (2C, C1-, C8-Fmoc), 123.5 (1C, C2-Trp), 121.5 (1C, C5-Trp), 120.1 (2C, C4-, C5-Fmoc), 118.9 (1C, C4-Trp), 118.7 (1C, C6-Trp), 112.1 (1C, C3-Trp), 111.5 (1C, C7-Trp), 66.0 (1C, CH$_2$-Fmoc), 54.5 (1C, Cα-Trp), 47.5 (1C, C9-Fmoc), 29.0 (1C, CH$_2$SH), 28.3 (1C, βCH$_2$-Trp). MALDI-TOF MS: *m/e* 451.0 (M+Na), 429.0 (M+H). Anal. Calcd. for $C_{26}H_{24}N_2O_2S$: C, 72.87; H, 5.64; N 6.54. Found: C, 72.76; H, 5.60; N 6.24.

6.4.1.19 Synthesis of the ulosyl bromide 24

Rhamnal **27** (198 mg, 0.5 mmol) and absolute ethanol (35 µL, 0.6 mmol) were stirred in dry CH_2Cl_2 (10 mL) with freshly dessicated molecular sieves (1g)

for 15 min under N_2. The mixture was then cooled to 0 °C and NBS (107 mg, 0.6 mmol) was added. Stirring was continued for 15 min at 0 °C under N_2 followed by immediate work-up by dilution with cold CH_2Cl_2 (15 mL), filtration through a pad of Celite, and washing with cold $Na_2S_2O_3$ (10%, 2 × 15 mL) and ice water (2 × 15 mL). The organic layer was then dried over Na_2SO_4 and the solvent evaporated to give **24** as a colorless foam, which was used without further purification in the next step.

6.4.1.20 Synthesis of S-β-Uloside 30

The thiol **8** (0.32 g, 0.75 mmol) was first dissolved in acetone (20 mL) with warming. The crude ulosyl bromide **24** was then added and the mixture was stirred over freshly desiccated molecular sieves for 15 min under N_2. The mixture was then cooled to -78 °C and Ag_2CO_3 (0.23 g, 0.75 mmol) was added. Stirring was continued at -78 °C for 30 min under N_2. The mixture was then filtered cold through a pad of Celite and the mixture concentrated. The residue was then purified by column chromatography (hexanes/EtOAc 3:1) to give the S-β-Uloside **30** (0.37 g, 62%) as a colorless crystalline solid. ^{1}H NMR (500 MHz, $CDCl_3$): δ (ppm) 8.09-6.51 (23H, m, NH ring-Trp, ArH), 5.21 (1H, d, $J_{NH,\alpha}$ = 7.3 Hz, NH-Trp), 5.19 (1H, t, $J_{3,4}$ = $J_{4,5}$ = 9.7 Hz, H4-rha), 5.04 (1H, br s, H1-rha), 4.74 (1H, d, $J_{a,b}$ = 12.3 Hz, OCH_{2a}-PMB), 4.39 (1H, d, OCH_{2b}-PMB), 4.36-4.26 (2H, m, CH_2-Fmoc), 4.24-4.18 (1H, m, αH-Trp), 4.14 (1H, t, $J_{9,a}$ = $J_{9,b}$ = 7.1 Hz, H9-Fmoc), 4.04 (1H, d, H3-rha), 3.72 (1H, dq, H5-rha), 3.63 (3H, s, OCH_3-PMB), 3.11 (1H, dd, $J_{a,b}$ = 14.6, $J_{a,\alpha}$ = 5.3 Hz, β-CH_{2a}-Trp), 2.98 (1H, dd, $J_{b,\alpha}$ = 6.9 Hz,

β-CH_{2b}-Trp), 2.86 (1H, dd, $J_{a,b}$ = 13.9, $J_{a,\alpha}$ = 4.6 Hz, CH_{2a}S), 2.67 (2H, dd, $J_{a,\alpha}$ = 6.9 Hz, CH_{2a}S, O*H*-rha), 1.11 (3H, d, $J_{5,6}$ = 6.2 Hz, H6-rha). ^{13}C NMR (125 MHz, $CDCl_3$): δ (ppm) 170.6 (1C, *C*=O-OAc), 165.9 (1C, *C*=O-OBz), 157.1 (1C, C=O-rha), 155.6 (1C, C=O-urethane), 159.4 (1C, C_{Ar}OMe-PMB), 144.3 (2C, C8a-, C9a-Fmoc), 141.5 (2C, C4a-, C4b-Fmoc), 136.4 (1C, C3a-Trp), 134.0-111.5 (25C, C_{Ar}), 86.7 (1C, C1-rha), 81.6 (1C, C3-rha), 76.6 (1C, C4-rha), 75.5 (1C, C5-rha), 72.7 (1C, O*C*H_2-PMB), 66.9 (1C, *C*H_2-Fmoc), 55.4 (1C, O*C*H_3-PMB), 51.0 (1C, Cα-Trp), 47.3 (1C, C9-Fmoc), 33.9 (1C, *C*H_2S), 29.7 (1C, β*C*H_2-Trp), 17.8 (1C, C6-rha). HRMS Calcd for [$C_{47}H_{44}N_2O_8$+H]: 797.2896. Found: 797.2867.

6.4.1.21 Synthesis of the intermediate 31

The *S*-β-Uloside **30** (300 mg, 0.37 mmol) was dissolved in CH_2Cl_2:MeOH (1:1) (15 mL) and cooled to 0 °C. $NaBH_4$ (120 mg, 3.1 mmol) was then added and the mixture was stirred for 2 h at 0 °C. The mixture was then diluted with CH_2Cl_2 (10 mL) and washed successively with water (15 mL), aqueous 1% citric acid solution (2 × 15 mL), and water (15 mL). The organic layer was dried over Na_2SO_4, and concentrated. The crude **31** was used without further purification in the next step.

6.4.1.22 Synthesis of the intermediate 23

Benzoyl chloride (42 uL, 0.4 mmol) was added dropwise to a cooled solution (0 °C) of the crude fragment **31** in pyridine (20 mL). The mixture was stirred at rt for 2 h under N_2. Sat. $NaHCO_3$ was then added to quench the

reaction. The solvent was evaporated, the residue dissolved in CH_2Cl_2 (50 mL), then washed successively with water (50 mL), saturated $NaHCO_3$ (50 mL), and water (50 mL), dried over Na_2SO_4, filtered, and concentrated. The crude material was then purified by column chromatography (hexanes:EtOAc 2:1) to afford the product **23** (0.31 g, 92% over 2 steps) as a colorless crystalline solid. ^{1}H NMR (500 MHz, $CDCl_3$): δ (ppm) 8.12-6.44 (29H, m, NH ring-Trp, ArH), 5.82 (1H, br s, H2-rha), 5.23 (1H, t, $J_{3,4} = J_{4,5}$ = 9.5 Hz, H4-rha), 5.08 (1H, d, $J_{NH,\alpha}$ = 7.5 Hz, NH-Trp), 4.69 (1H, s, H1-rha), 4.50 (1H, d, $J_{a,b}$ = 12.6 Hz, OCH_{2a}-PMB), 4.39-4.31 (2H, m, CH_{2a}-, H9-Fmoc), 4.29 (1H, d, OCH_{2b}-PMB), 4.21-4.12 (2H, m, αH-Trp, CH_{2b}-Fmoc), 3.64-3.55 (1H, m, H3-rha), 3.61 (3H, s, OCH_3-PMB), 3.38 (1H, dq, H5), 3.09 (1H, dd, $J_{a,b}$ = 14.8, $J_{a,\alpha}$ = 4.0 Hz, βCH_{2a}-Trp), 3.00-2.86 (2H, m, βCH_{2b}-Trp, CH_{2a}S), 2.65 (1H, dd, $J_{a,b}$ = 14.8, $J_{b,\alpha}$ = 6.9 Hz, CH_{2b}S), 1.15 (3H, d, $J_{5,6}$ = 6.0 Hz, H6-rha). ^{13}C NMR (125 MHz, $CDCl_3$): δ (ppm) 166.2 (1C, *C*=O-OBz), 165.7 (1C, *C*=O-OBz), 159.4 (1C, C_{Ar}OMe-PMB), 156.4 (1C, C=O-urethane), 144.2 (2C, C8a-, C9a-Fmoc), 141.6 (2C, C4a-, C4b-Fmoc), 136.5 (1C, C3a-Trp), 133.5-111.4 (31C, C_{Ar}), 82.8 (1C, C1-rha), 76.5 (1C, C3-rha), 72.8 (1C, C4-rha), 70.4 (1C, O*C*H_2-PMB), 70.1 (1C, C2-rha), 67.0 (1C, *C*H_2-Fmoc), 55.3 (1C, C5-rha), 51.1 (1C, Cα-Trp), 47.5 (1C, C9-Fmoc), 35.7 (1C, *C*H_2S), 29.6 (1C, β*C*H_2-Trp), 18.1 (1C, C6-rha). HRMS Calcd for [$C_{54}H_{50}N_2O_9S$+H]: 903.3315. Found: 903.3314.

6.4.1.23 Synthesis of the intermediate 22

Tin (IV) chloride (21 µL, 0.18 mmol) was added to a solution of **23** (150 mg, 0.17 mmol) and thiophenol (21 µL, 0.2 mmol) in anhydrous CH_2Cl_2 (10 mL) at -78 °C. The resulting pink solution was stirred at -78 °C under N_2 for 30 min. Aqueous sat. $NaHCO_3$ (10 mL) was added and the mixture was extracted with CH_2Cl_2 (3 × 15 mL). The combined organic phases was washed with brine (15 mL), dried over Na_2SO_4, filtered, and concentrated. The crude material was purified by column chromatography (hexanes:EtOAc 2:1) to afford the product **22** (125 mg, 96%) as a colorless crystalline solid. 8.12-6.44 (24H, m, NH ring-Trp, ArH), 5.64 (1H, br s, H2-rha), 5.23 (2H, m, H4-rha, NH-Trp), 4.73 (1H, s, H1-rha), 4.37-4.28 (2H, m, C*H*$_2$-Fmoc), 4.21-4.09 (2H, m, αH-Trp, H9-Fmoc), 3.94-3.86 (1H, m, H3-rha), 3.44 (1H, dq, H5), 3.04 (1H, dd, $J_{a,b}$ = 14.6, $J_{a,\alpha}$ = 4.6 Hz, βCH_{2a}-Trp), 2.97-2.84 (2H, m, βCH_{2b}-Trp, CH_{2a}S), 2.74 (lH, br s, OH), 2.61 (1H, dd, $J_{a,b}$ = 13.9, $J_{b,\alpha}$ = 6.4 Hz, CH_{2b}S), 1.18 (3H, d, $J_{5,6}$ = 4.2 Hz, H6-rha). ^{13}C NMR (125 MHz, $CDCl_3$): δ (ppm) 167.1 (1C, *C*=O-OBz), 166.8 (1C, *C*=O-OBz), 156.4 (1C, C=O-urethane), 144.2 (2C, C8a-, C9a-Fmoc), 141.6 (2C, C4a-, C4b-Fmoc), 136.5 (1C, C3a-Trp), 133.8-111.5 (25C, C_{Ar}), 83.1 (1C, C1-rha), 75.3 (1C, C5-rha), 75.1 (1C, C4-rha), 74.1 (1C, C2-rha), 72.9 (1C, C3-rha), 67.0 (1C, *C*H_2-Fmoc), 60.7 (1C, Cα-Trp), 47.5 (1C, C9-Fmoc), 35.7 (1C, *C*H_2S), 29.5 (1C, β*C*H_2-Trp), 18.1 (1C, C6-rha). HRMS Calcd for [$C_{46}H_{42}N_2O_8S$+H]: 783.2740. Found: 783.2730.

6.4.1.24 Synthesis of the intermediate 6 (using the standard procedure)

Fragment **22** (50 mg, 64 µmol) and trichloroacetimidate **15** (60 mg, 64 µmol) in dry CH_2Cl_2 (5 mL) was stirred with freshly dessicated molecular sieves for 10 min under N_2. The mixture was then cooled to -40 ^oC and TMSOTf (10 µL, 16 µmol) was then added. The mixture was stirred at this temperature for 2 h under N_2. Et_3N (100 µL) was added and the mixture was allowed to warm to rt and filtered through a pad of Celite with the aid of more CH_2Cl_2 (15 mL). The filtrate was then washed with sat. $NaHCO_3$ (15 mL), dried over Na_2SO_4, filtered, and concentrated. Maldi TOF MS indicated the presence of the product **6** and TLC showed the presence of the starting materials **15** and **22** along with several side products. The product **6** could not be separated because it had same Rf as the starting acceptor **15**.

6.4.1.25 Synthesis of the intermediate 6 (using sulfoxide 32 as donor)

$NaHCO_3$ (6 mg, 71 µmmol) and mCPBA (375 mg, 77%, 1.12 mmol) were added to a stirred solution of disaccharide **14** (1.0 g, 1.1 mmol) in CH_2Cl_2 (25 mL) at -78 ^oC under N_2. The temperature was slowly raised to -25 ^oC over a period of 30 min and was quenched with the addition of dimethyl sulfide. The mixture was allowed to warm to rt and was diluted with CH_2Cl_2 (25 mL), washed with water (40 mL), sat. $NaHCO_3$ (40 mL), aq. Na_2CO_3 (40 mL) and brine (25 mL), dried over Na_2SO_4, filtered, and concentrated. The residue was further washed with

warm ether (2 × 25 mL) to furnish the crude sulfoxide **32** as a colorless foam, which was used directly in the next step.

The acceptor **22** (35 mg, 45 µmol) and DTBMP (37 mg, 180 µmol) in dry CH_2Cl_2 (5 mL), were stirred with freshly dessicated molecular sieves (500 mg) for 30 min under N_2. The suspension was then cooled to -78 ^oC and a solution of triflic anhydride (35 µL, 180 µmol) in dry CH_2Cl_2 (350 µL), was added. A solution of the sulfoxide (2.2 equiv.) in dry CH_2Cl_2 (3 mL), was added over a period of 15 min. No desired product was observed based on maldi TOF MS and TLC.

6.4.1.26 Improved synthesis of the intermediate 6 using the trichloroacetimidate 15 (reverse addition)

The acceptor **22** (30 mg, 61.3 µmol) in dry CH_2Cl_2 (5 mL) was stirred with freshly dessicated molecular sieves (100 mg) for 10 min under N_2. The mixture was then cooled to -40 ^oC and TMSOTf (3.5 µL, 18.5 µmol) was added. The trichloroacetimidate **15** (40 mg, 61.3 µmol) in dry CH_2Cl_2 (300 µL) was added dropwise over a period of 20 min. A second portion of TMSOTf (3.5 µL, 18.5 µmol) was added followed by dropwise addition of the trichloroacetimidate **15** (40 mg, 61.3 µmol). Maldi TOF MS indicated the disappearance of acceptor **22**. Et_3N was added to the cold reaction mixture which was filtered with the aid of more cold CH_2Cl_2 (10 mL). The filtrate was washed with cold sat. $NaHCO_3$ (10 mL), dried over Na_2SO_4, filtered, and concentrated. The residue was purified by column chromatography (hexanes:EtOAc 2:1) to afford the desired intermediate **6** (41.5 mg, 68%) as a colorless crystalline solid. ^1H NMR (600 MHz, $CDCl_3$): δ (ppm) 8.61 (1H, br s, NH-Trp ring), 8.26-7.02 (48H, m, ArH, NH-Asp), 6.84 (1H,

br d, $J_{\alpha,NH}$ = 8.0 Hz, NH-Trp), 5.95 (1H, br s, NH-Dmab), 5.69-5.45 (4H, m, H2-, H2", H3"-, H1-rha), 5.43-5.17 (6H, m, H3'-, H4-, H4'-, H4"-rha, Ar-CH_2O-Dmab), 4.95 (1H, br s, H1'-rha), 4.89 (1H, br s, H1"-rha), 4.80 (1H, br s, H1-rha), 4.72-4.66 (1H, m, αH-Asp), 4.54 (1H, m, CH_2-Fmoc), 4.41-4.25 (2H, m, CH_2-Fmoc, αH-Trp), 4.24-4.15 (1H, m, H9-Fmoc), 3.85-3.76 (2H, m, H5-rha, αH-Met), 4.04 (1H, m, H3-rha), 3.73-3.61 (2H, m, H5"-, H5'-rha), 3.31-3.00 (5H, m, βCH_2-Trp, CH_2CH-Dmab, βCH_2-Asp, H2'-rha), 2.89-2.63 (3H, m, βCH_2-Asp, CH_2S), 2.51-2.49 (2H, m, δCH_2-Met), 2.48 (2H, s, CH_2 ring-Dmab), 2.36 (2H, s, CH_2 ring-Dmab), 2.19-1.98 (19H, m, SCH_3-Met, βCH_2-Met), 1.87-1.77 (1H, m, CH_2CH-Dmab), 1.21-1.13 (9H, m, 3 × CH_3-rha), 1.07 (6H, s, 2 × CH_3 ring-Dmab), 0.71 (6H, d, J = 6.8 Hz, CH_2CH(CH_3)$_2$-Dmab). ^{13}C NMR (150 MHz, CD_2Cl_2): δ (ppm) 177.6 (2C, C=O ring-Dmab), 173.8-170.5 (10C, 11 × C=O), 157.6 (1C, C=O-urethane), 144.4 (2C, C8a-, C9a-Fmoc), 143.6 (1C, C_{Ar}-N-Dmab), 141.5 (2C, C4a-, C4b-Fmoc), 137.3 (1C, C3a-Trp), 136.4 (1C, C_{Ar}-CH_2O- Dmab), 129.1 (2C, C_{Ar}-Dmab), 128.0 (1C, C7a-Trp), 127.9 (3C, C3-, C6-Fmoc), 127.3 (2C, C2-, C7-Fmoc), 126.9 (2C, C_{Ar}-Dmab), 125.2 (2C, C1-, C8-Fmoc), 123.3 (1 C, C2-Trp), 122.2 (1 C, C6-Trp), 120.2 (2 C, C4-, C5-Fmoc), 119.6 (1 C, C5-Trp), 118.9 (1C, C7-Trp), 112.4 (1C, C4-Trp), 111.4 (1C, C3-Trp), 104.7 (1C, C1-rha), 100.2 (1C, C1"-rha), 99.8 (1C, C1'-rha), 76.6 (1C, C2'-rha), 74.2 (1C, C3-rha), 73.1 (1C, C2-rha), 73.9 (1C, C4"-rha), 70.9 (1C, C3'-rha), 70.3 (1C, C4-rha), 70.3 (1C, C4'-rha), 69.9 (1C, C2"-rha), 68.9 (1C, C3"-rha), 67.6 (1C, C5'-rha), 67.4 (1C, C5-rha), 67.3 (1C, C5"-rha),), 67.2 (1C, CH$_2$-Fmoc), 65.3 (1C, C_{Ar}-CH$_2$O-Dmab), 54.9 (1C, Cα-Met), 54.9 (1C, CH$_2$ ring-Dmab), 52.4 (1C, CH$_2$ ring-Dmab), 50.4

(1C, Cα-Trp), 49.8 (1C, Cα-Asp), 47.4 (1C, C9-Fmoc), 38.2 (1C, *C*H_2CH-Dmab), 35.7 (1C, *C*β-Asp), 32.7 (1C, βC*H*$_2$-Met), 29.9 (1C, Cδ-Met), 29.4 (1C, -CH_2*C*H-Dmab), 29.3 (1C, βCH_2-Trp), 28.1 (2C, 2 × *C*H_3 ring-Dmab), 22.5 (2C, CH_2CH(*C*H_3)$_2$-Dmab), 17.9-17.5 (3C, 3 × C6-rha), 15.8 (1C, S*C*H_3-Met). HRMS Calcd for [$C_{93}H_{82}N_2O_{21}$S+H]: 1595.5209. Found: 1595.5284.

6.4.1.27 Synthesis of the amine 5

To a stirred mixture of the glycopeptide **6** (10.6 mg, 6.7 μmol) and octanethiol (10.6 μL, 38 μmol), DBU (1 drop) was added and the reaction mixture was stirred at rt for 1 h under N_2. The mixture was evaporated to dryness and the residue was washed several times with warm ether. The amine **5** was not purified further but used directly in the coupling reaction with the protected dipeptide **4**.

6.4.1.28 Synthesis of the fully protected glycopeptide 3

To a mixture of Fmoc-Met-Asp(ODmab)-OPfp[4] (**4**) (6.6 mg, 6.7 μmol) and crude amine **5** in dry THF (1 mL), HOBt (13.5 mg, 13.5 μmol) was added and the reaction mixture was stirred at rt for 2 h. The solvent was then removed under vacuum and the residue was used directly in the deprotection step.

6.4.1.29 Attempted synthesis of the final beta-glycopeptide 2

To a stirred mixture of the crude, fully protected glycopeptide **3** and octanethiol (3.5 μL, 22.5 μmol) in THF (1 mL), DBU (3.5 μL, 16.7 μmol) was added and the reaction mixture was stirred for 1 h. The solvent was evaporated

to dryness and the residue was washed several times with warm ether. The amine product was then dissolved in 2% NH_2NH_2 in THF (1 mL) and the mixture was stirred for 1 h at rt. The solvent was evaporated and the residue was dissolved in MeOH (5 mL) and MeONa/MeOH (5 drops) was added. The reaction mixture was stirred fort 2 h at rt. Rexin H^+ 101 was then added until the pH was slightly basic, the resin was removed by filtration, and the filtrate was further neutralized with acetic acid. The solvent was evaporated and the crude product was washed successively with Hexanes (10 mL), CH_2Cl_2 (10 mL), and EtOAc (10 mL). The crude material was further purified by HPLC (C-18 reverse phase, 95:5 to 5:95 H_2O:CH_3CN over 15 min) to give the product **2** (6 mg) as a white powder. ^1H NMR spectroscopy showed that the desired glycopeptide **2** had co-eluted with a peptide impurity (1:1).

6.5 ACKNOWLEDGEMENT

We are grateful to the Natural Sciences and Engineering Research Council of Canada for financial support.

6.6 REFERENCES

1. Vyas, N. K.; Vyas, M. N.; Chervenak, M. C.; Johnson, M. A.; Pinto, B. M.; Bundle, D. R.; Quiocho, F. A. *Biochemistry* **2002**, *41*, 13575-13586.
2. Vyas, N. K.; Vyas, M. N.; Chervenak, M. C.; Bundle, D. R.; Pinto, B. M.; Quiocho, F. A. *Proc. Natl. Acad. Sci. U. S. A.* **2003**, *100*, 15023-15028.
3. Borrelli, S.; Hossany, R. B.; Pinto, B. M. *Clin. Vaccine Immunol.* **2008,** *15*, 1106-1117.
4. Hossany, R. B.; Wen X.; Pinto, B. M. *Carbohydr. Res.* **2009**, *344*, 1412-1427.
5. Zhu, X. M.; Schmidt, R. R. *Chem. Eur. J.* **2004**, *10*, 875-887.
6. Lichtenthaler, F. W., and Metz, T. *Eur. J. Org. Chem.* **2003**, *16*, 3081-3093.
7. Pozgay, V. *Carbohydr. Res.* **1992**, *235*, 295-302.
8. Yu, W. S., Su, M., Gao, X. B., Yang, Z. Q., and Jin, Z. D. *Tetrahedron Lett.* **2000**, *41*, 4015-4017.
9. Perrin, D. D.; Armarego, W. L. F. (1988) In *Purification of Laboratory Chemicals*, 3rd.; Pergamon: London.
10. Barlos, K.; Gatos, D. (2000) In *Fmoc Solid Phase Peptide Synthesis: A Practical Approach* (Chan, W. C., White, P. D., eds), Oxford University Press Inc., New York.
11. Cammish, L. E.; Kates, S. A. (2000) In *Fmoc Solid Phase Peptide Synthesis: A Practical Approach* (Chan, W. C.; White, P. D., eds), Oxford University Press Inc., New York.

12. Dourtoglou, V.; Gross, B.; Lambropoulou, V.; Zioudrou, C. *Synthesis* **1984**, *7*, 572-574.

13. Dourtoglou, V.; Ziegler, J. C.; Gross, B. *Tetrahedron Lett.* **1978**, *15*, 1269-1272.

14. Knorr, R.; Trzeciak, A.; Bannwarth, W.; Gillessen, D. *Tetrahedron Lett.* **1989**, *30*, 1927-1930.

15. Kaiser, E.; Colescot.R. ; Bossinge.C.; Cook, P. I. *Anal. Biochem.* **1970**, *34*, 595-598.

CHAPTER 7: DESIGN, AND PROGRESS TOWARD THE SYNTHESIS OF A GLYCOPEPTIDE MIMIC CORRESPONDING TO THE O-POLYSACCHARIDE ANTIGEN OF THE *STREPTOCOCCUS* GROUP A

Conformational epitopes displayed by a polysaccharide with several repeating units may be prominent factors accounting for immunogenicity of longer fragments of polysaccharide over smaller fragments that lack these conformational topographies. In order to study this phenomenon, we have designed by molecular modeling a glycopeptide, which we hypothesize, could mimic structurally the conformational epitopes that are displayed by the *Streptococcus* Group A polysaccharide consisiting of several repeating units. This chapter describes the design of this mimic and the progress made toward its synthesis. The molecular modeling study of the glycopeptide was performed by Dr. Xin Wen. The synthetic work toward the synthesis of the designed glycopeptide was carried out by the thesis author.

Our aim is to demonstrate if we could use this designed glycopeptide to specifically direct the immune response against a discontinuous conformational epitope adopted by the *Streptococcus* Group A polysaccharide with several repeating units. This would provide insight into the importance of conformational epitopes in immunogenicity.

Molecular modeling showed that a 16-mer of L-4-hydroxyproline with a pendant Glc*N*Ac moiety attached to the hydroxyl units of each proline derivative could be a reasonable surrogate that could mimic structurally the conformational epitope of the *Streptococcus* Group A polysaccharide.

The approach chosen to synthesize this candidate was first to prepare a monomer unit in solution, comprising a hydroxyproline unit glycosylated at the hydroxyl group with a Glc*N*Ac moiety, followed by the construction of the 16-mer on solid support. In the current work, the monomer unit was successfully synthesized. Future work will be to construct the 16-mer on solid support using a solid phase strategy and to study its immunochemical properties.

7.1 Abstract

In search of new classes of compounds as mimics of carbohydrates, we have designed by molecular modeling, a structural mimic of the *Streptococcus* Group A polysaccharide, which could be used as a surrogate ligand in the development of a vaccine against the *Streptococcus* Group A. This mimic, a glycopeptide, is a 16-mer of L-4-hydroxyproline with a Glc*N*Ac moiety attached to the hydroxyl group of each proline. Toward the synthesis of the 16-mer, a monomer unit was successfully prepared in solution employing a glycosylation reaction between a Glc*N*Ac sulfoxide derivative and Fmoc-L-4-hydroxyproline pentafluorophenylester. The glycopeptide could be constructed on solid support using this synthesized monomer unit, and the immunogenicity of the 16-mer could then be studied.

7.2 INTRODUCTION

One of the antigenic biomolecules found on bacterial pathogens is their cell-surface polysaccharide.[1-4] Some of these polysaccharides, when converted to T-cell dependent antigens on conjugation to carrier proteins, have been successful as vaccines against bacterial pathogens especially in children (under two years) and immunodeficient persons.[4] However, many of these polysaccharides, even when attached to carrier proteins, were found to be weakly immunogenic, most probably, because these polysaccharides comprise

sugar units that might mimic antigens on human tissue.[5] Furthermore, immune responses against these polysaccharides-based vaccines can result in autoimmune reactions.[6,7]

An alternative approach to facilitate vaccine design to target carbohydrate antigens is the use of molecular mimicry.[6,8] Currently, this area comprises, (1) the use of anti-idiotypic antibodies that mimic carbohydrate antigens[9,10], (2) the use of phage-displayed libraries to identify peptide mimotopes for carbohydrates[7,11,12], (3) the use of 3-D modeling to design structural mimics of carbohydrates.[13,14] While the use of phage-displayed libraries is an effective method used to identify lead molecules,[10,11] the use of 3-D modeling to design new mimics is gaining much attention due to the advent of computer technology.[13,14]

An epitope on a bacterial polysaccharide to which an anti-carbohydrate antibody is directed to can either be continuous or discontinuous. While a continuous epitope comprises a small linear sequential fragment from the carbohydrate, a discontinuous (also called conformational) epitope is composed of several fragments which are not linear but separated along the carbohydrate sequence which are brought together in spatial proximity when the whole carbohydrate adopts secondary structures such as helices. Although, in general, anti-carbohydrate antibodies recognize continuous epitopes on native carbohydrate antigens, there have been long debates on the question of whether or not a subset of antibodies against a polysaccharide antigen recognizes a discontinuous conformational epitope on the polysaccharide. This is because it

was found that smaller fragments of certain polysaccharides, even though they could effectively bind anti-carbohydrate antibodies, failed to elicit production of antibodies that recognized the whole polysaccharide, while a longer fragment of the same polysaccharide was immunogenic.[9,15-17] This could be explained by the fact that certain longer fragments of polysaccharide could adopt conformations such as helices that are not possible in smaller fragments,[9,15-17] and as immunogens these longer fragments could elicit antibodies that recognized these conformations in the polysaccharide, and thus account for their immunogenicity.[18]

If mimics could be identified that could specifically direct antibodies at these conformational epitopes, thus avoiding recognition of sugar-containing oligosaccharides in linear epitopes found on human tissues, this could be useful in the development of vaccines against pathogens where carbohydrate-based vaccines would pose a problem. Several long peptide sequences that displayed similar conformations to poorly immunogenic polysaccharides have been identified from phage-displayed libraries and the basis of mimicry in these systems is in progress.[5,6,19,20]

In this study, we chose the *Streptococcus* Group A polysaccharide as a model to design, using 3-D modeling, a structural mimic that could target a discontinuous conformational epitope on the polysaccharide. It was previously shown that the cell-wall polysaccharide of the *Streptococcus* Group A, with several repeating units, adopts a helical structure with the rhamnose units forming the barrel of a helix with the immunodominant Glc*N*Ac moieties displayed

on the periphery (Figure 7-1a).[21,22] Poly-L-4-hydroxyproline also adopts a Type II left-handed helix comprising three prolyl residues per turn with trans-peptide bonds.[23] This motif usually occurs in globular proteins, notably in the fibrous protein collagen.[24] We propose to mimic the conformation displayed by the *Streptococcus* Group A polysaccharide by constructing, by molecular modeling, the barrel of the helix with 16 repeating L-4-hydroxyproline residues, with the immunodominant sugar, Glc*N*Ac unit attached to the hydroxyl group of each proline moiety (Figure 7-1b).

Studying the immunogenicity of this newly design glycopeptide would improve our understanding of the importance of conformational epitopes in immunogenicity as well as characterize it as a potential surrogate for the development as vaccines against the *Streptococcus* Group A. Furthermore, due to its larger size as compared to the mimetic peptide DRPVPY, identified from phage-displayed libraries, the newly design glycopeptide could be a potential immunogen on its own without attachment to a carrier protein. The carrier-suppression effect experienced when the DRPVPY-TT was used as immunogen (chapter 3) might then be prevented. This remains to be tested.

We now report progress towards the synthesis of this newly designed structural mimic of the Group A *Streptococcus*.

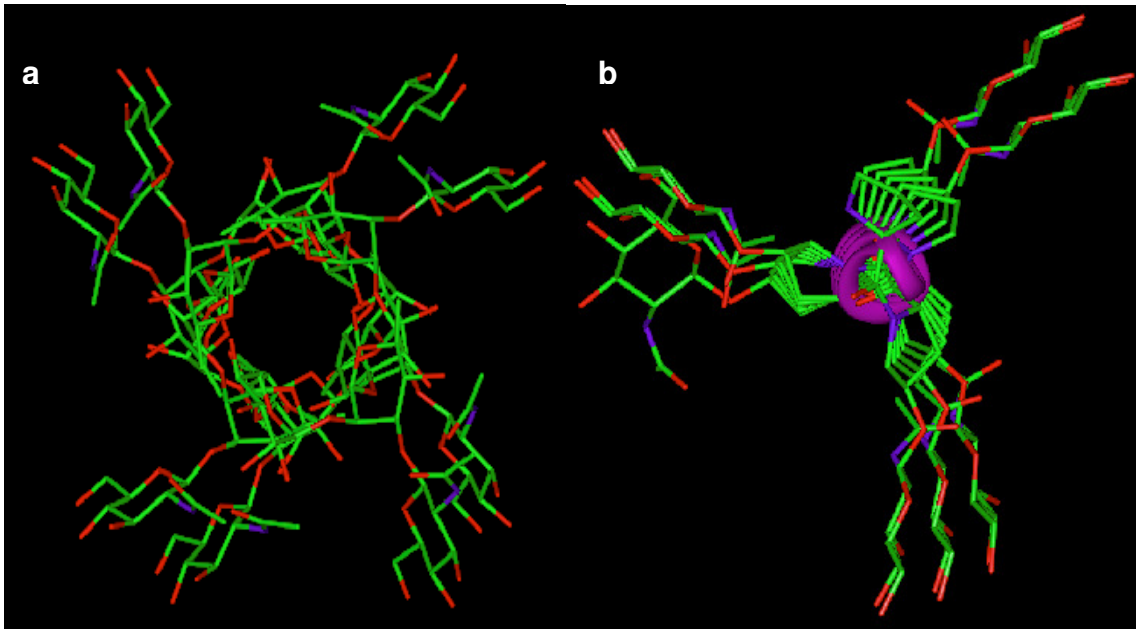

Figure 7-1: Structure of (a) the cell-wall polysaccharide of *Streptococcus* Group A, (b) its mimetic 16-mer glycopeptide.

7.3 RESULTS AND DISCUSSION

7.3.1 Synthesis

From a retrosynthetic analysis, the 16-mer **1** could be obtained by deprotecting the glycopeptide **2**, followed by acetylation of the free amines on the sugar (Scheme 7-1). The glycopeptide **2** could be constructed on solid support using the monomer unit **3**, which in turn, could be synthesized from a glycosylation reaction between the sulfoxide **4** and the Fmoc-4-OH-Pro-Opfp **5** (Scheme 7-1). The pentafluorophenylester (Opfp) group, introduced on the

carboxylic end of **5**, would serve both as a protecting group in the glycosylation step as well as an activating agent in the solid-phase synthesis of **2**.

Scheme 7-1: Retrosynthetic analysis of the 16-mer **1**

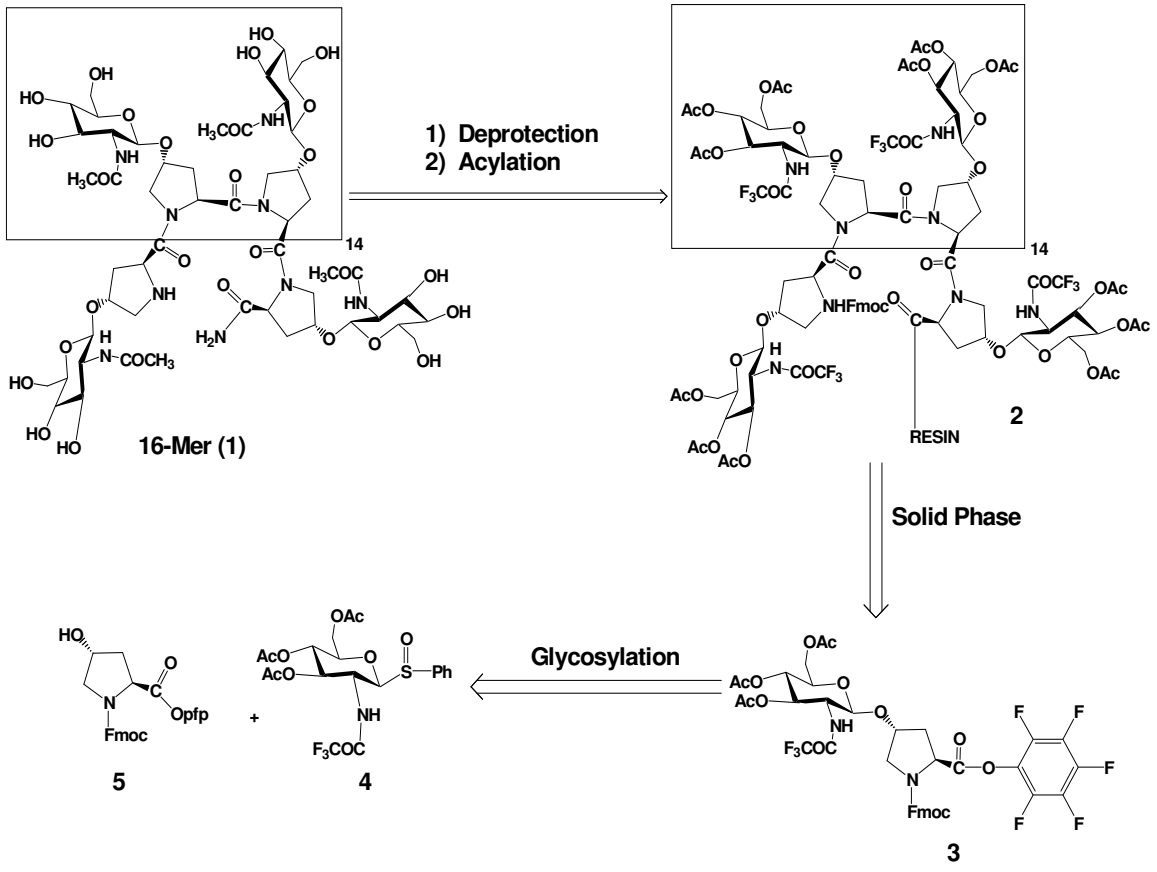

The sulfoxide **4**, was prepared in 6 steps from the commercially available D-(+)-glucosamine hydrochloride, following a similar procedure reported in the literature.[25] The ester **5** on the other hand was obtained from an esterification reaction between the commercially available 4-OH-Pro (Hyp) and

pentafluorophenol (pfpOH), using DIC/HOBt/DIPEA as coupling agent in THF (Scheme 7-2). The glycosylation reaction was then attempted using standard conditions and the desired β-glycoside **3** was obtained exclusively in good yield (Scheme 7-3).

Scheme 7-2: Synthesis of the ester **5**

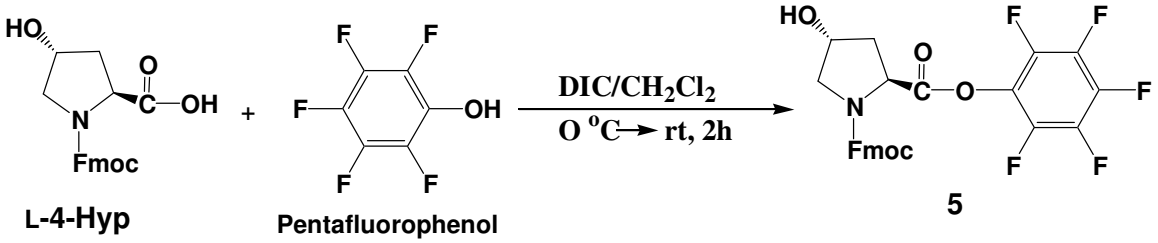

Scheme 7-3: Synthesis of the monomer unit **3**

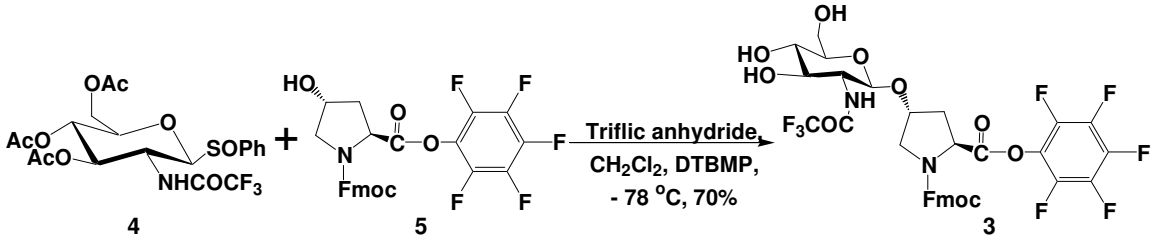

The fully protected glycopeptide **2** will then be constructed from the monomer unit **3** on Rink amide resin using a solid-phase strategy. Before cleavage of the glycopeptide **2** from the resin, the protecting groups on the sugar moieties will be removed under basic conditions and the free amino groups of the

sugars will be acetylated. The final 16-mer will then be obtained as a carboxamide by cleavage of the glycopeptide from the resin.

7.4 EXPERIMENTAL

7.4.1 Synthesis

7.4.1.1 General methods

The Fmoc amino acid used was purchased from Novabiochem and the other reagents from Aldrich Chemical Co. Solvents were distilled according to standard procedures.[26] 1D and 2D NMR spectra were recorded on 400 and 500 MHz spectrometers. Chemical shifts were referred to internal $CHCl_3$ or external DSS [3-(trimethylsilyl)-1-propanesulfonic acid]; coupling constants were obtained from a first-order analysis of one-dimensional spectra, and spectral assignments were based on COSY, HMQC and TOCSY experiments. Processing of the data was performed with MestRec software. Analytical thin-layer chromatography (TLC) was performed on aluminum plates precoated with Silica Gel 60F-254 as the adsorbent. The developed plates were air-dried, exposed to UV light, and/or sprayed with a solution containing 3% ninhydrin in EtOH and heated. Column chromatography was performed with Silica Gel 60 (230-400 mesh). MALDI-TOF mass spectra were obtained for samples dispersed in a 2,5-dihydroxybenzoic acid matrix on a Perseptive Biosystems Voyager-DE instrument.

7.4.1.2 Synthesis of the ester 5

DIC (180 mg, 222 µL, 1.5 µmol) was added to a stirred, ice-cold solution of Fmoc-Hyp-OH (500mg, 1.5 µmol) and pentafluorophenol (261 mg, 1.5 µmol) in THF (7 mL). Stirring was continued at 0 ^{o}C for 1 h and at rt for 1 h. The solid was removed by filtration, and the filtrate was concentrated to give the Fmoc-Hyp-Opfp as a glassy solid, which was used directly in the glycosylation reaction.

7.4.1.3 Synthesis of the monomer unit 3

The crude Fmoc-Hyp-Opfp, sulfoxide **4**[25] (0.7g, 1.4 mmol), and DTBMP (846 mg, 4.2 mmol) in dried CH_2Cl_2 (15 mL) were stirred with molecular sieves (1 g) for 15 mins. The mixture was then cooled to -78 ^{o}C, triflic anhydride (310 mg, 186 µL, 1.1 mmol) was added, and the mixture was stirred at -78 ^{o}C for 2 h. The reaction mixture was quenched with sat. $NaHCO_3$, allowed to warm to rt, and filtered through a pad of Celite. The filtrate was diluted with CH_2Cl_2 (50 mL), and washed successively with sat. $NaHCO_3$ (50 mL), water (50 mL), and brine (50 mL), dried over Na_2SO_4, filtered, and concentrated. The crude material dissolved in CH_2Cl_2 was purified by flash chromatography (hexanes:EtOAc 3:1) to afford the desired product **3** (mixture of rotamers) as a colorless foam (869 mg, 70%). ^{1}H NMR (400 MHz, $CDCl_3$): δ (ppm) 7.75 (2H, d, $J_{3,4} = J_{4,5} = 7.5$ Hz, H4-, H5-Fmoc), 7.57 (2H, d, $J_{1,2} = J_{7,8} = 7.6$ Hz, H1-, H8-Fmoc), 7.41-7.32 (2H, m, H3-, H6-Fmoc), 7.31-7.23 (2H, m, H2-, H7-Fmoc), 6.61 (1H, d, $J_{NH,2} = 6.8$ Hz, N*H*COCF$_3$), 5.35 (1H, t, $J_{2,3} = J_{3,4} = 10.0$ Hz, H3-Glc*N*HCOCF$_3$), 5.08 (1H, t, $J_{4,5} = 10.0$ Hz, H4-Glc*N*HCOCF$_3$), 4.90 (1H, d, $J_{1,2} = 8.3$ Hz, H1-Glc*N*HCOCF$_3$), 4.71 (1H, d, $J_{\alpha,\beta} = 7.1$ Hz, αH-Hyp), 4.56-4.50 (1H, m, γH-Hyp), 4.43-4.34 (2H, m, C*H*$_2$-

Fmoc, H9-Fmoc), 4.29-4.22 (2H, m, H6a-Glc*N*HCOCF_3, CH_2-Fmoc), 4.12 (1H, dd, $J_{a,b}$ = 12.4, $J_{5,6}$ = 2.9 Hz, H6b-Glc*N*HCOCF_3), 3.90-3.80 (2H, m, δH-Hyp, H2-Glc*N*HCOCF_3), 3.80-3.71 (2H, m, δH-Hyp, H5-Glc*N*HCOCF_3), 2.59-2.51 (1H, m, βH-Hyp), 2.50-2.42 (1H, m, βH-Hyp), 2.05 (3H, s, CH_3-OAc), 2.03 (6H, s, 2 × CH_3-OAc). ^{13}C NMR (150 MHz, $CDCl_3$): δ (ppm), 171.1 (1C, *C*OCF_3), 169.5 (1C, *C*OOpfp), 157.8 (1C, C=O-urethane), 144.3 (2C, C8a-, C9a-Fmoc), 141.4-141.3 (6C, C_{Ar}-Opfp, C4a-, C4b-Fmoc), 128.1 (2C, C3-, C6-Fmoc), 129.2 (1C, C_{Ar}-Opfp), 127.4 (2C, C2-, C7-Fmoc), 125.3 (2C, C1-, C8-Fmoc), 120.2 (2C, C4-, C5-Fmoc), 99.6 (1C, C1-Glc*N*HCOCF_3), 77.1 (1C, Cγ-Hyp), 72.5 (1C, C5-Glc*N*HCOCF_3), 71.3 (1C, C3-Glc*N*HCOCF_3), 68.8 (1C, *C*H_2-Fmoc), 68.3 (1C, C4-Glc*N*HCOCF_3), 62.0 (1C, C6-Glc*N*HCOCF_3), 57.5 (1C, Cα-Hyp), 55.6 (1C, C2-Glc*N*HCOCF_3), 53.6 (1C, Cδ-Hyp), 47.2 (1C, C9-Fmoc), 37.3 (1C, Cβ-Hyp), 20.9-20.7 (3C, *C*H_3-OAc). MALDI-TOF MS: *m*/*e* 924.5 (M+Na), 902.8 (M+H). Anal. Calcd. for $C_{40}H_{34}F_8N_2O_{13}$: C, 53.22; H, 3.80; N, 3.10. Found C, 53.35; H, 3.91; N, 3.23.

7.5 ACKNOWLEDGEMENTS

We are grateful to the Natural Sciences and Engineering Research Council of Canada for financial support.

7.6 REFERENCES

1. **Jennings, H. J. *Curr. Top. Microbiol. Immunol.*** 1990, *150*, 97-127.
2. Jennings, H. J. *Adv. Exp. Med. Biol.* **1988**, *228*, 495-550.
3. Lee, C. J. *Mol. Immunol.* **1987**, *24*, 1005-1019.
4. Lindberg, A. A. *Vaccine* **17**, **1999**, S28-36.
5. Pincus, S. H.; Smith, M. J.; Jennings, H. J.; Burritt, J. B.; Glee, P. M. *J. Immunol*. **1998**, *160*, 293-298.
6. Johnson, M. A.; Pinto, B. M. *Topics Curr. Chem.* **2008**, *273*, 55-116.
7. Zwick, M. B.; Shem, J. K.; Scott, J. K.; *Curr. Opin. Biotechnol.* **1998**, 9, 427-436.
8. Johnson, M. A.; Pinto, B. M. *Aust. J. Chem.* **2002**, *55*, 13-25.
9. Harris, S. L.; Craig, L.; Mehroke, J. S.; Rashed, M.; Zwick, M. B.; Kenar, K.; Toone, E. J.; Greenspan, N.; Auzanneau, F. I.; MarinoAlbernas, J. R.; Pinto, B. M.; and Scott, J. K. *Proc. Natl. Acad. Sci. U. S. A.* **1997**, *94*, 2454-2459.
10. Mariuzza, R. A.; Poljak, R. J. *Curr. Opin. Immunol.* **1993**, *5*, 50-55.
11. Davies, D. R.; Cohen, G. H. *Proc. Natl. Acad. Sci. U. S. A.* **1996**, 93, 7-15.
12. Monzavi-Karbassi, B.; Cunto-Amesty, G.; Luo, P.; Kieber-Emmons, T. *Trends Biotechnol.* **2002**, *20*, 207-214.
13. Wang, L. F.; Yu, M. *Curr. Drug Targets* **2004***, 5,* 1-15.
14. Veselovsky, A.V.; Ivanov, A.S. *Curr. Drug Targets Infect. Disord*. **2003**, *3*, 33-40.

15. Reimer, K. B.; Gidney, M. A. J.; Bundle, D. R.; Pinto, B. M. *Carbohydr. Res.* **1992**, 232, 131-142.

16. Auzanneau, F.-I.; Pinto, B. M. *Bioorg. Med. Chem.* **1996**, 4, 2003–2010.

17. Auzanneau, F.-I.; Christensen, M. K.; Harris, S. L.; Meldal, M.; Pinto, B. M. *Can. J. Chem.* **1998**, 76, 1109-1118.

18. Zou, W.; Mackenzie, R.; Therien, L.; Hirama, T.; Yang, Q.; Gidney, M. A.; Jennings, H. J. *J. Immunol.* **1999**, *163*, 820-825.

19. Brisson, J.-R.; Baumann, H.; Imberty, A.; Perez, S.; Jennings, H. J. *Biochemistry* **1992**, *31*, 4996-5004.

20. Evans, S. V.; Sigurskjold, B. W.; Jennings, H. J.; Brisson, J.-R.; To, R.; Tse, W. C.; Altman, E.; Frosch, M.; Weisgerber, C.; Kratzin, H. D.; Klebert, S.; Vaesen M.; Bitter-Suermann, D.; Rose, D. R.; Young, N. M.; Bundle, D. R. *Biochemistry* **1995**, *34*, 6737-6744.

21. Kreis, U. C.; Varma, V.; Pinto, B. M. *Int. J. Biol. Macromol.* **1995**, 17, 117-130.

22. Stuike-Prill, R.; Pinto, B. M. *Carbohydr. Res.* **1995**, 279, 59-73.

23. MacArthur, M. W.; Thorton, J. M. *J. Mol. Biol.* **1991**, *218*, 397-412.

24. Adzhubei, A. A.; Sternberg, M. J.; *J. Mol. Biol.* **1993**, *229*, 472-493.

25. Silva, D. J.; Sofia, M. J. *J. Org. Chem.* **1999**, *64*, 5926-5929.

26. Perrin, D. D.; Armarego, W. L. F. Purification of Laboratory Chemicals, 3rd.; Pergamon: London, 1988.

APPENDIX A: ^{1}H NMR SPECTRA (CHAPTER 5)

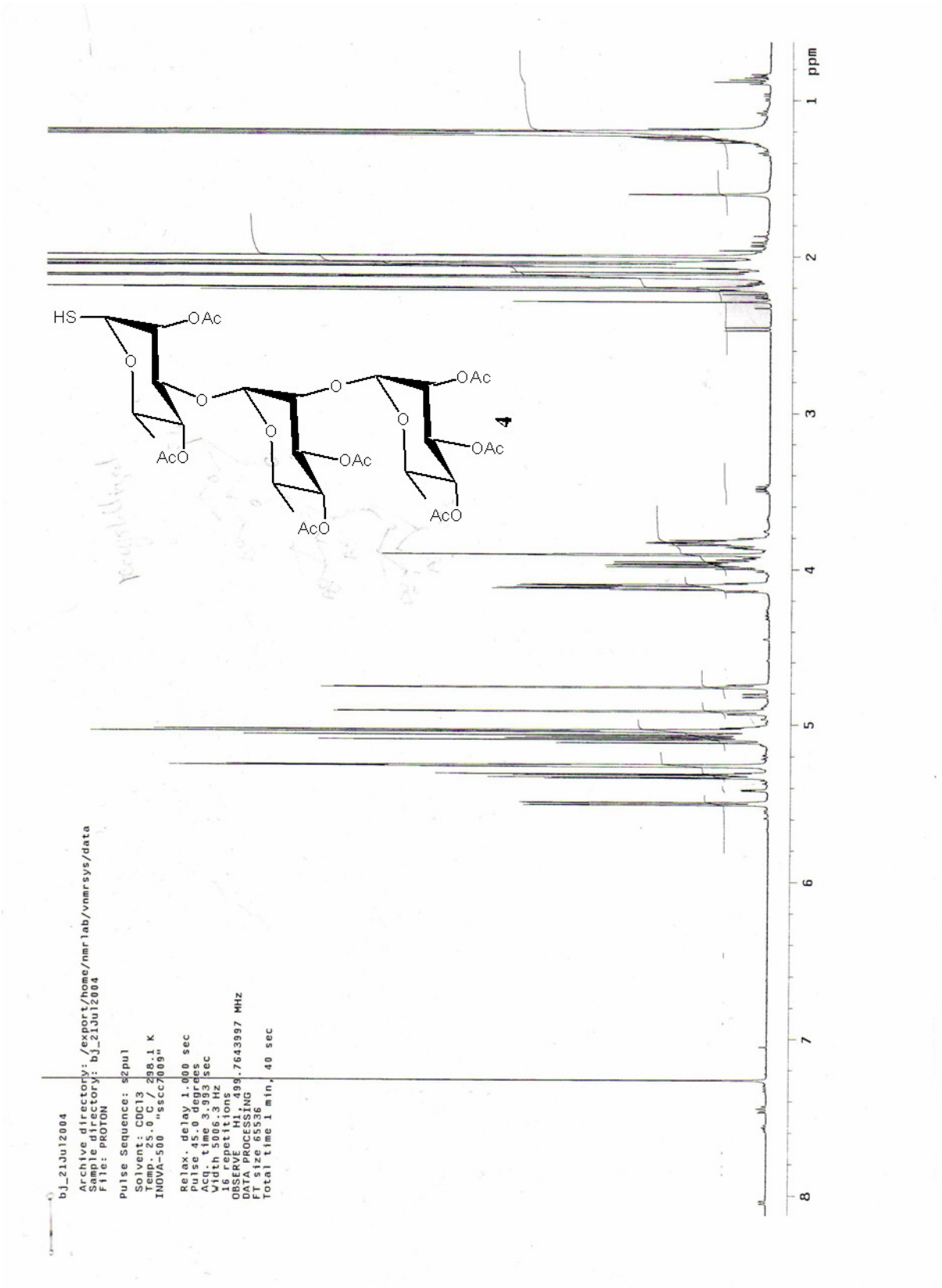
bj_21Jul2004
Archive directory: /export/home/nmrlab/vnmrsys/data
Sample directory: bj_21Jul2004
File: PROTON
Pulse Sequence: s2pul
Solvent: CDCl3
Temp: 25.0 C / 298.1 K
INOVA-500 "sscc7009"
Relax. delay 1.000 sec
Pulse 45.0 degrees
Acq. time 3.993 sec
Width 5006.3 Hz
1 repetitions
OBSERVE H1, 499.7643997 MHz
DATA PROCESSING
FT size 65536
Total time 1 min, 40 sec
HS
OAc
O
AcO
4
ppm
1
2
3
4
5
6
7
8

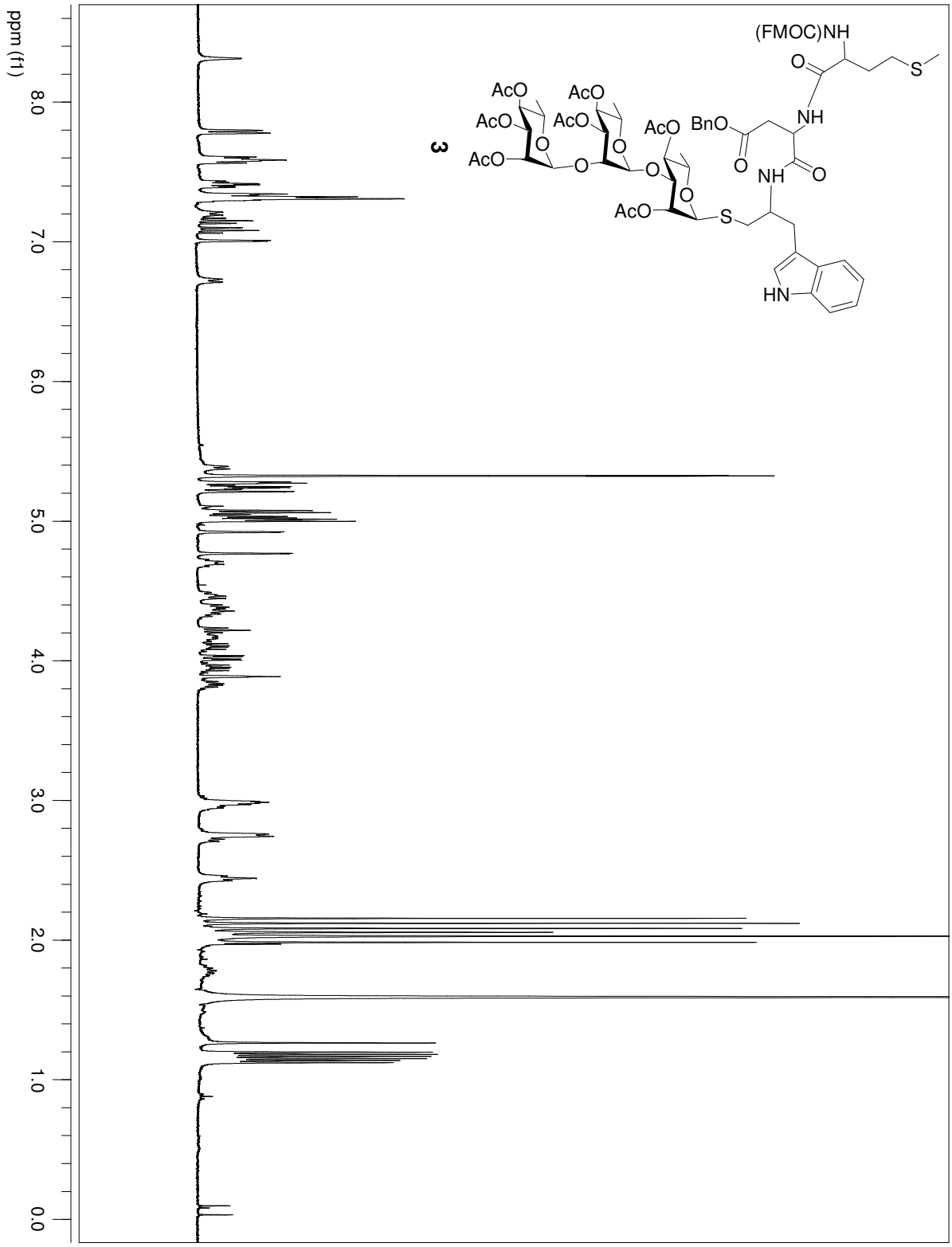
ppm (f1)
8.0
7.0
6.0
5.0
4.0
3.0
2.0
1.0
0.0
3
(FMOC)NH
O
S
AcO
AcO
AcO
O
AcO
AcO
AcO
O
O
AcO
O
BnO
NH
O
NH
O
AcO
O
S
HN

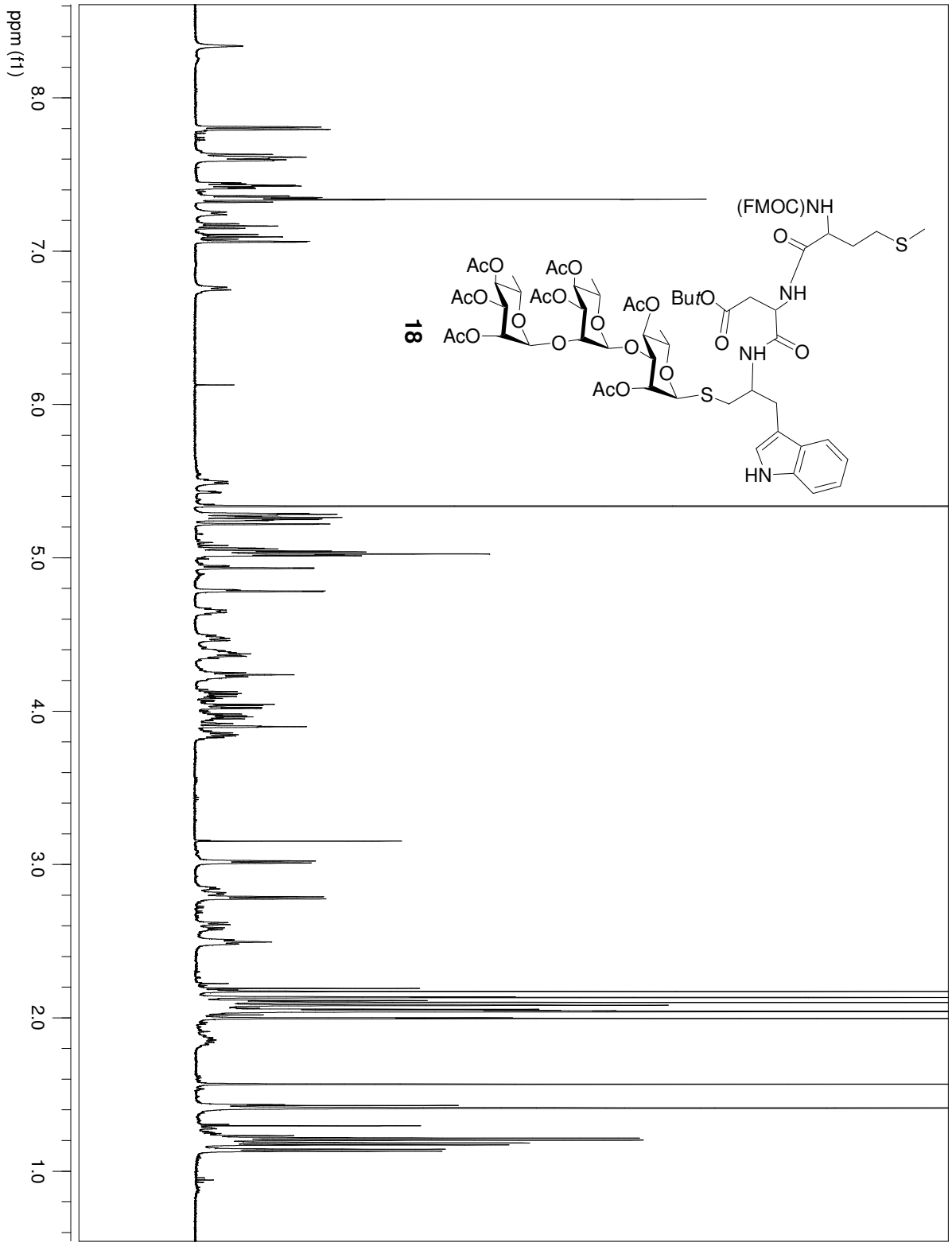
ppm (f1)
8.0
7.0
6.0
5.0
4.0
3.0
2.0
1.0
18
(FMOC)NH
AcO
AcO
AcO
AcO
AcO
AcO
AcO
AcO
But O
NH
NH
S
S
HN
O

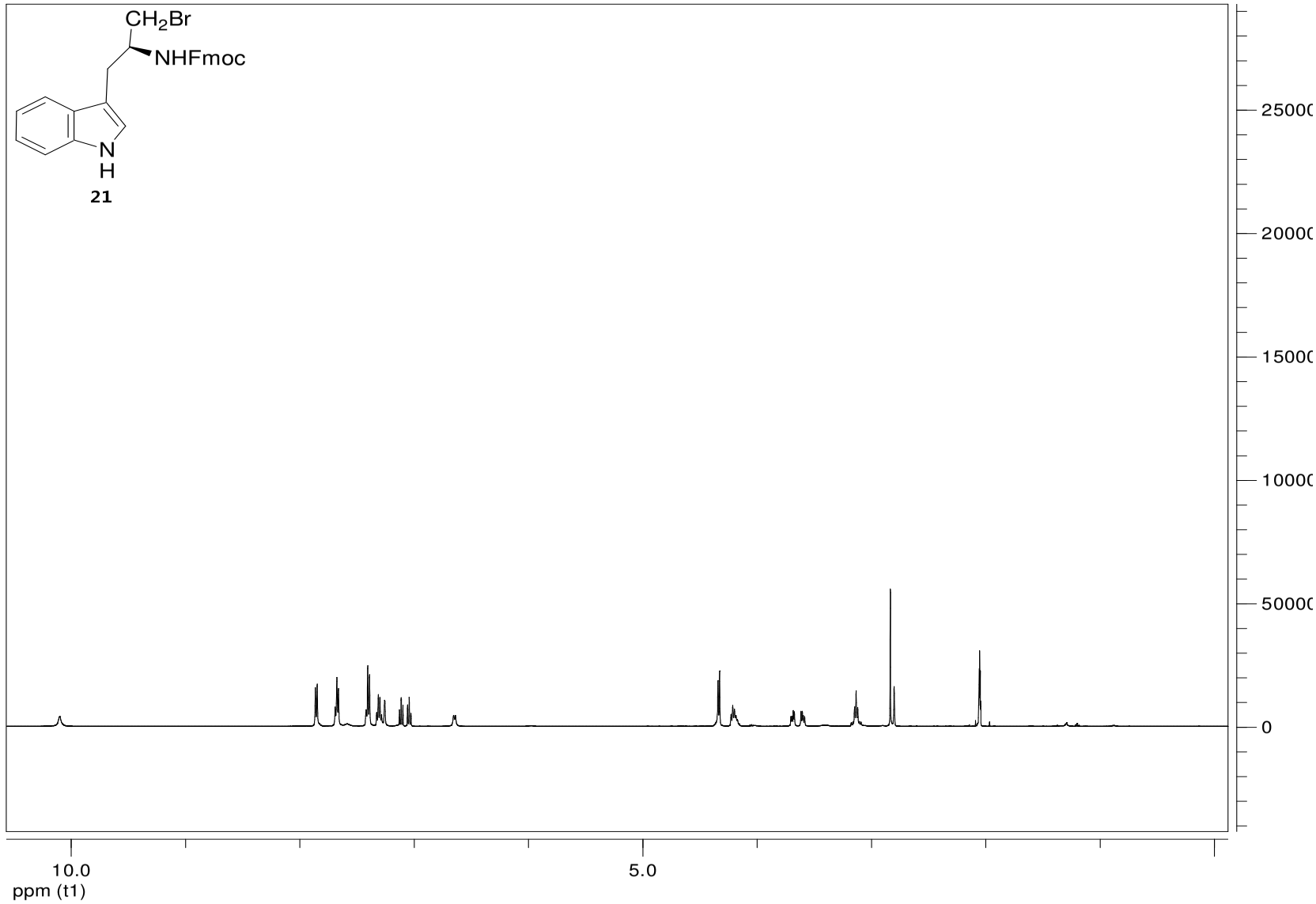
CH2Br
NHFmoc
N
H
21
25000
20000
15000
10000
50000
0
10.0
ppm (t1)
5.0

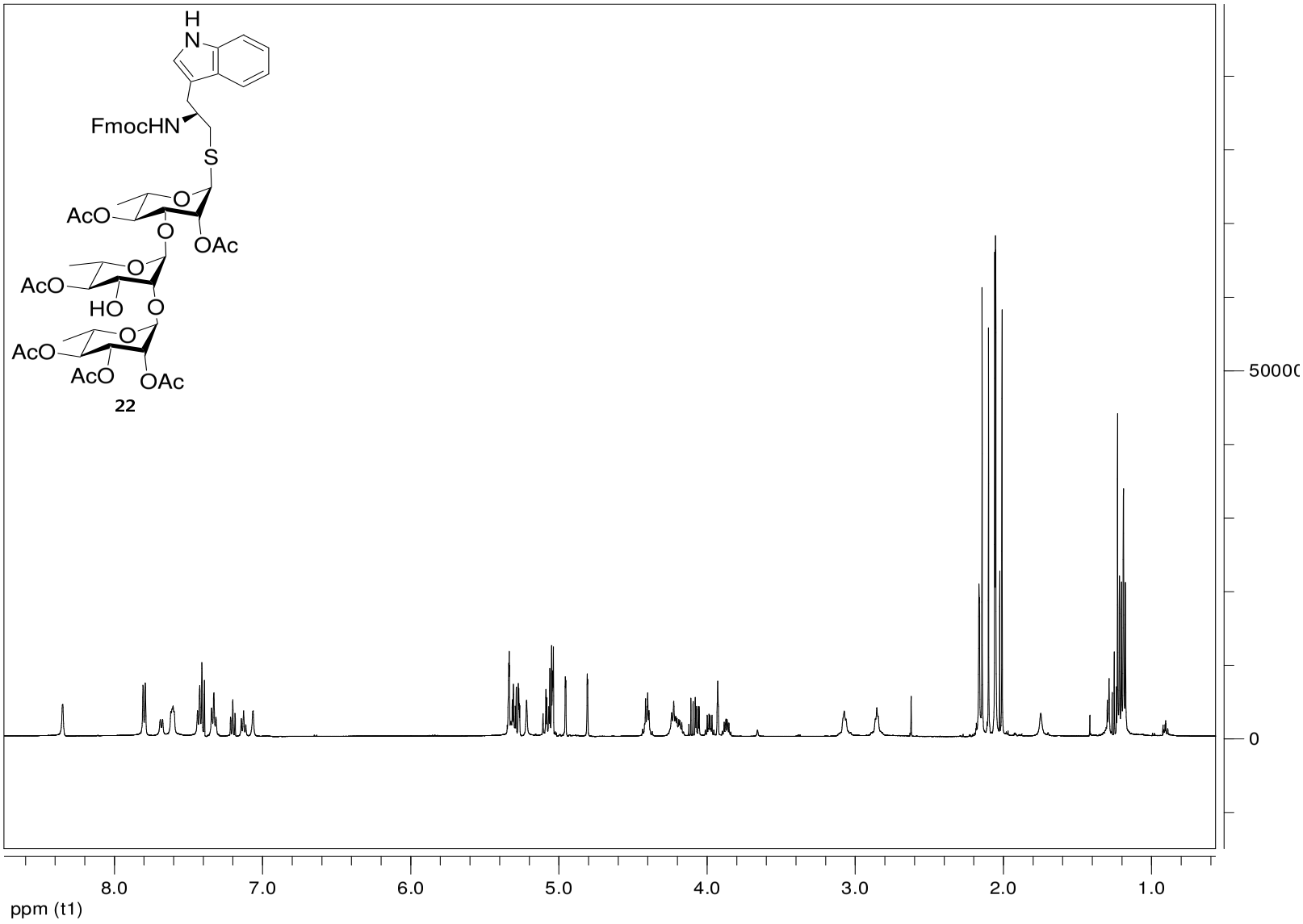
H
N
FmocHN
S
O
AcO
O
OAc
O
AcO
HO
O
O
AcO
AcO
OAc
22
50000
0
8.0
7.0
6.0
5.0
4.0
3.0
2.0
1.0
ppm (t1)

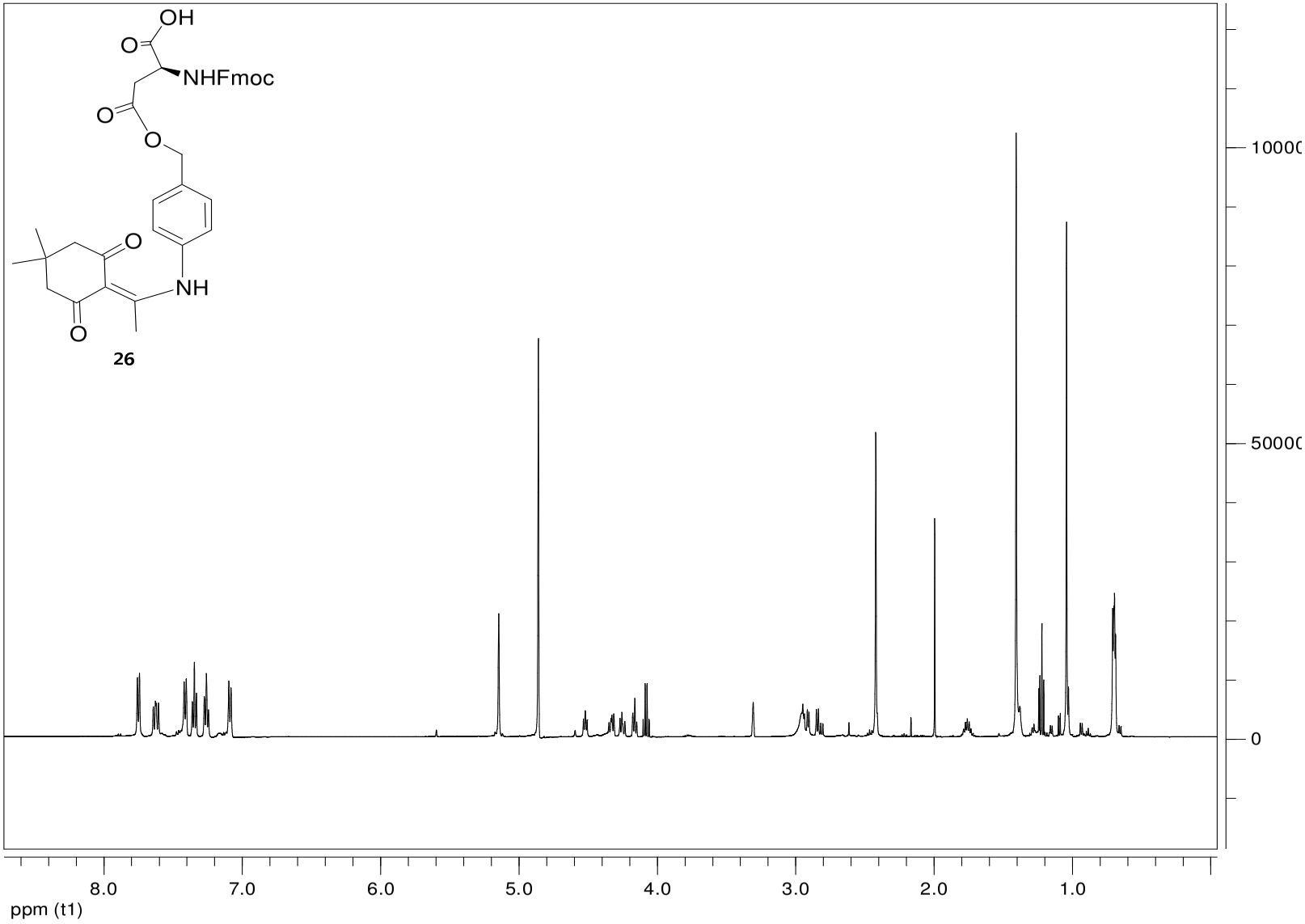
OH
O
NHFmoc
O
O
O
NH
O
26
10000
50000
0
8.0
7.0
6.0
5.0
4.0
3.0
2.0
1.0
ppm (t1)

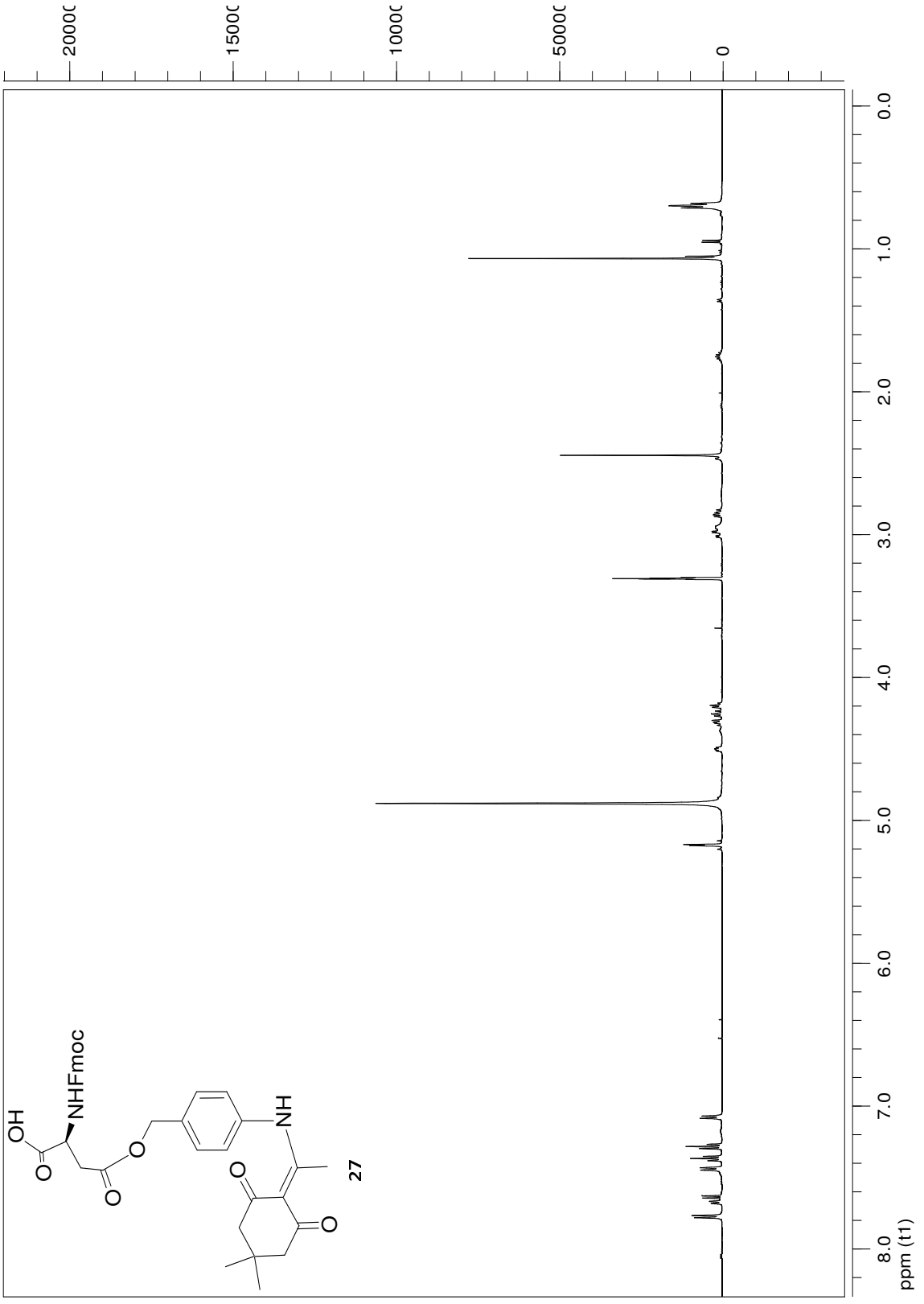
OH
NHFmoc
O
O
O
NH
O
O
27
20000
15000
10000
5000
0
0.0
1.0
2.0
3.0
4.0
5.0
6.0
7.0
8.0
ppm (t1)

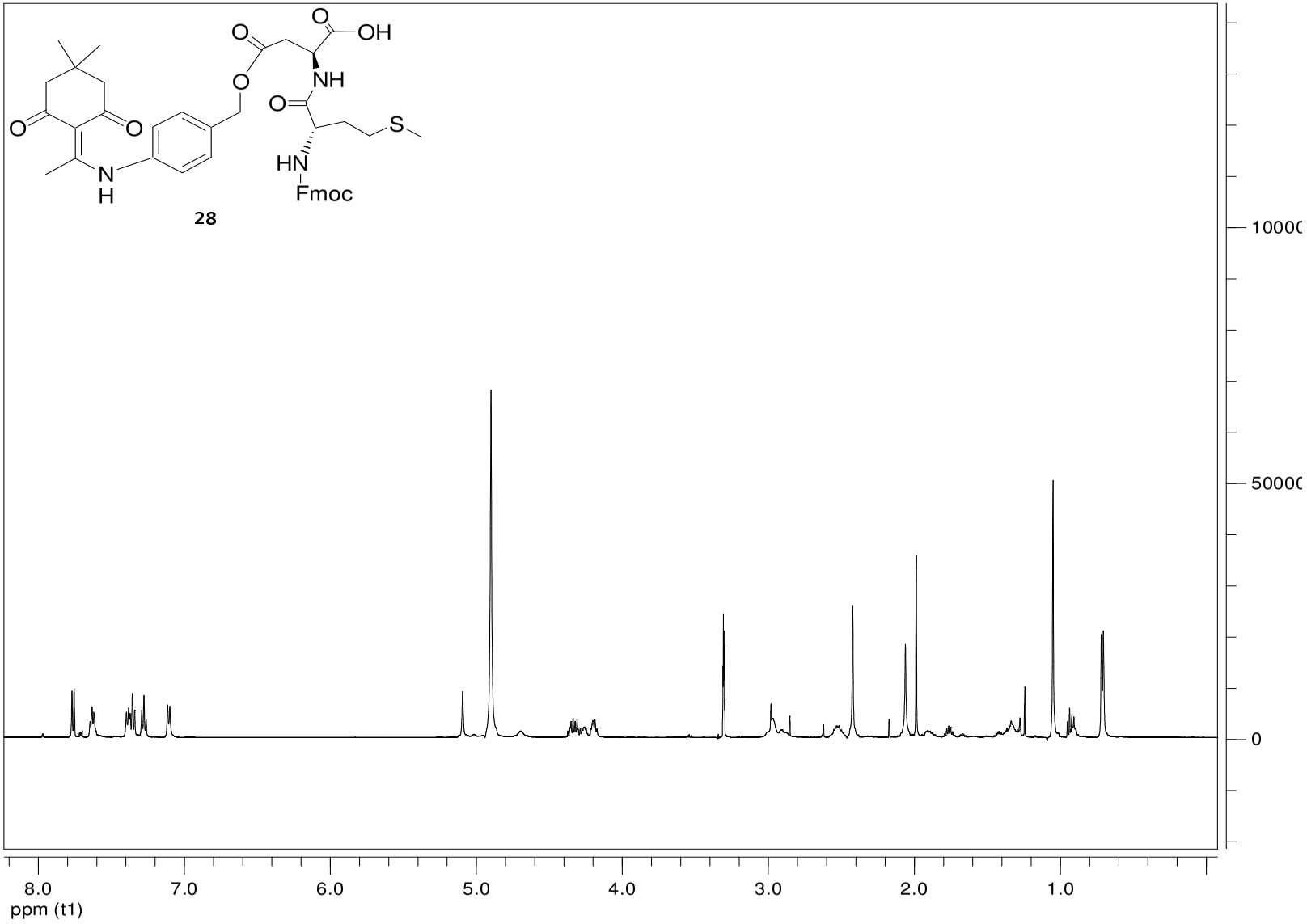
O
OH
O
NH
O
O
O
O
S
N
H
HN
Fmoc
28
10000
50000
0
8.0
7.0
6.0
5.0
4.0
3.0
2.0
1.0
ppm (t1)

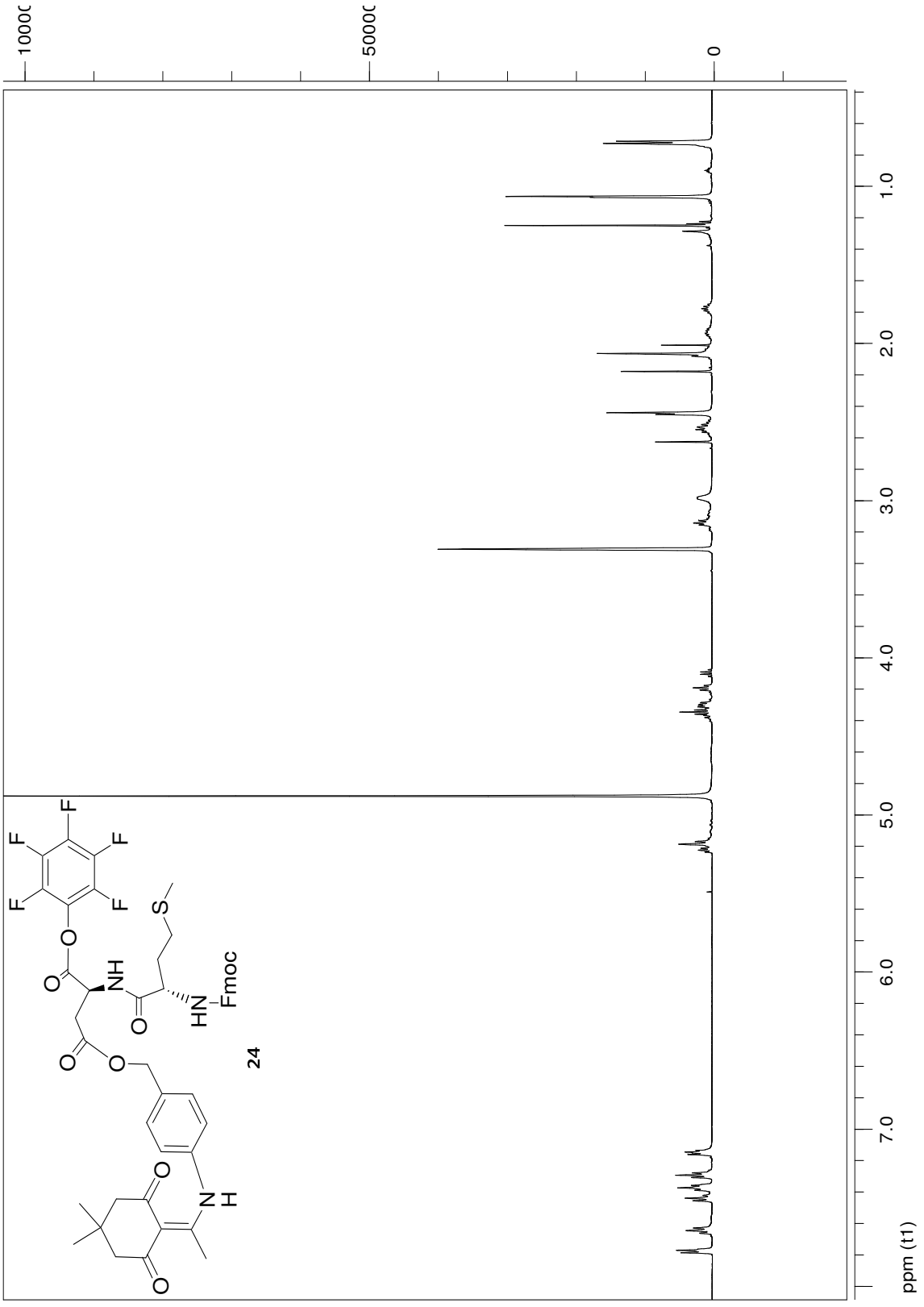
10000
5000
0
1.0
2.0
3.0
4.0
5.0
6.0
7.0
ppm (t1)
F
F
F
F
F
O
O
NH
O
HN
Fmoc
S
O
O
O
N
H
O
O
24

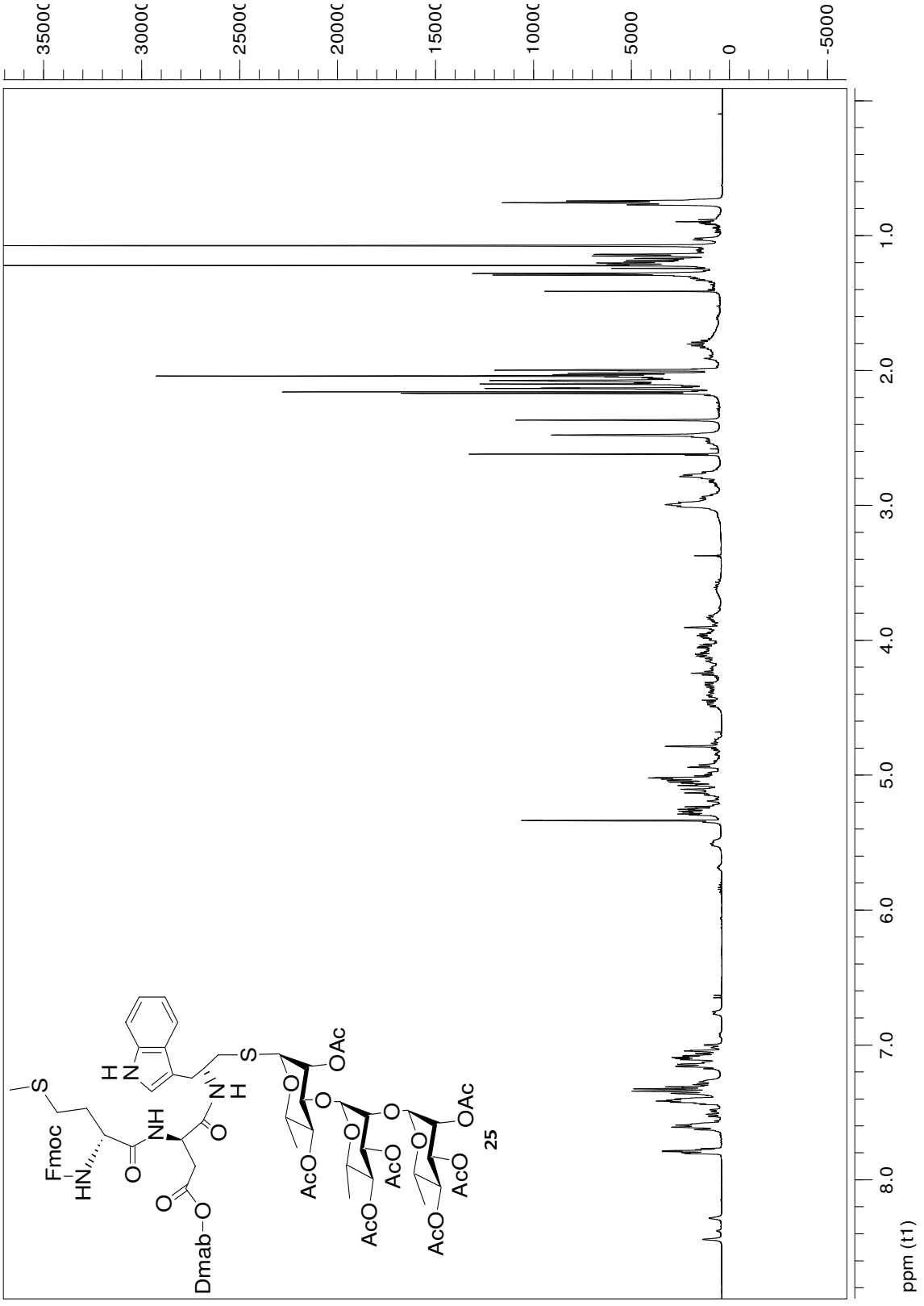
3500
3000
2500
2000
1500
1000
5000
0
-5000
1.0
2.0
3.0
4.0
5.0
6.0
7.0
8.0
ppm (t1)
Fmoc
HN
NH
Dmab–O
AcO
OAc
25

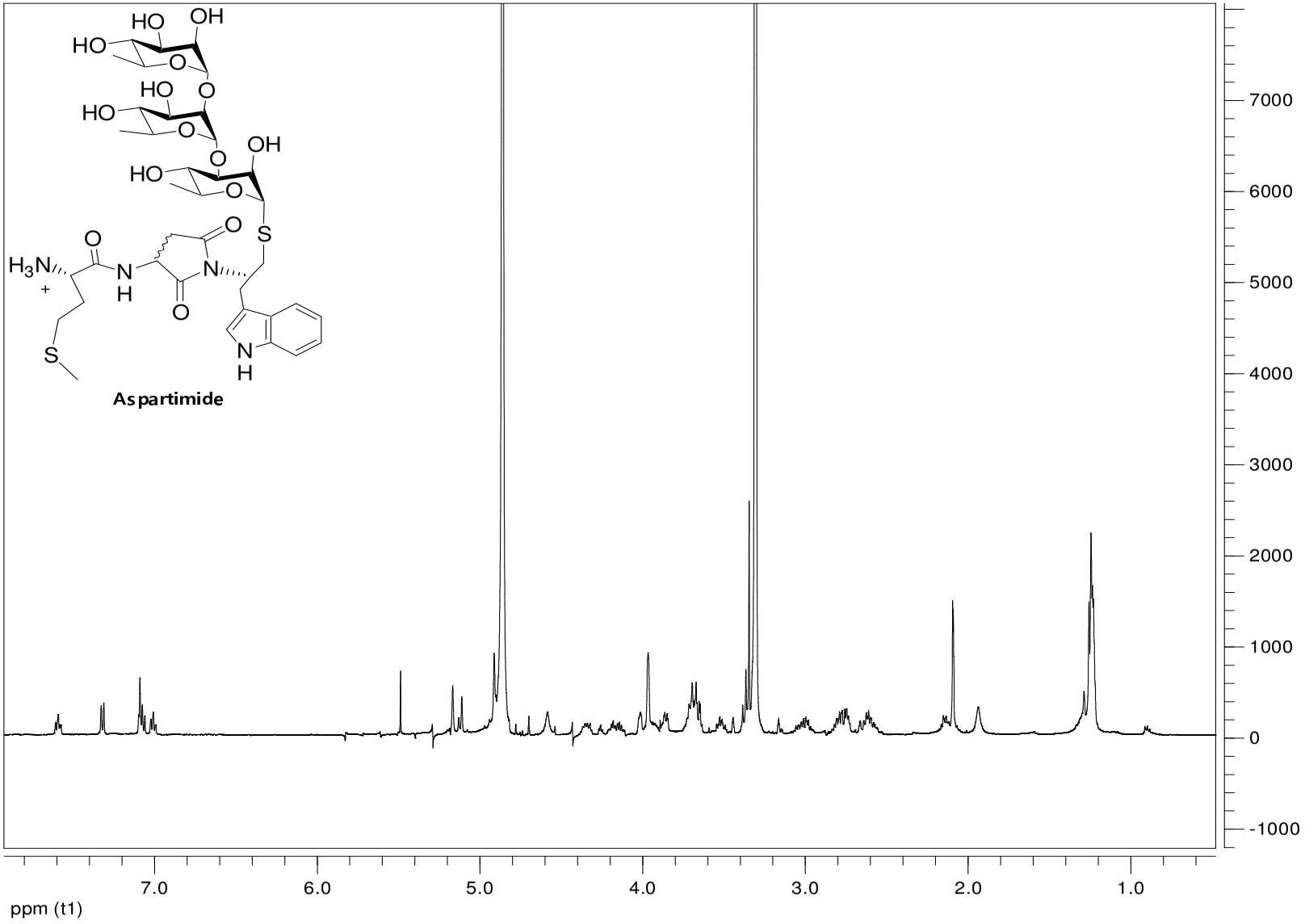
Aspartimide
7000
6000
5000
4000
3000
2000
1000
0
-1000
7.0
6.0
5.0
4.0
3.0
2.0
1.0
ppm (t1)

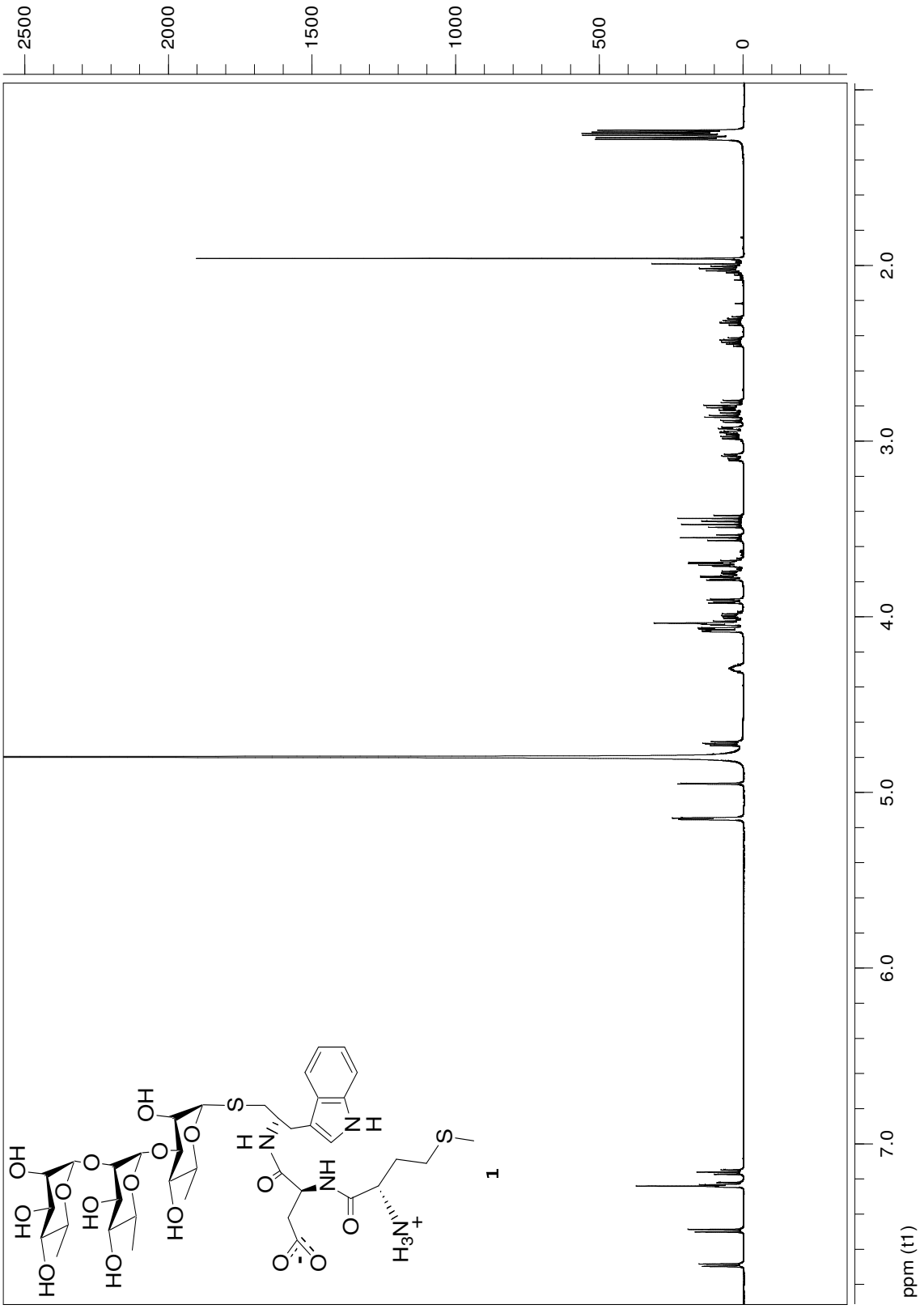
2500
2000
1500
1000
500
0
2.0
3.0
4.0
5.0
6.0
7.0
ppm (t1)
1

APPENDIX B: ^{1}H NMR SPECTRA (CHAPTER 6)

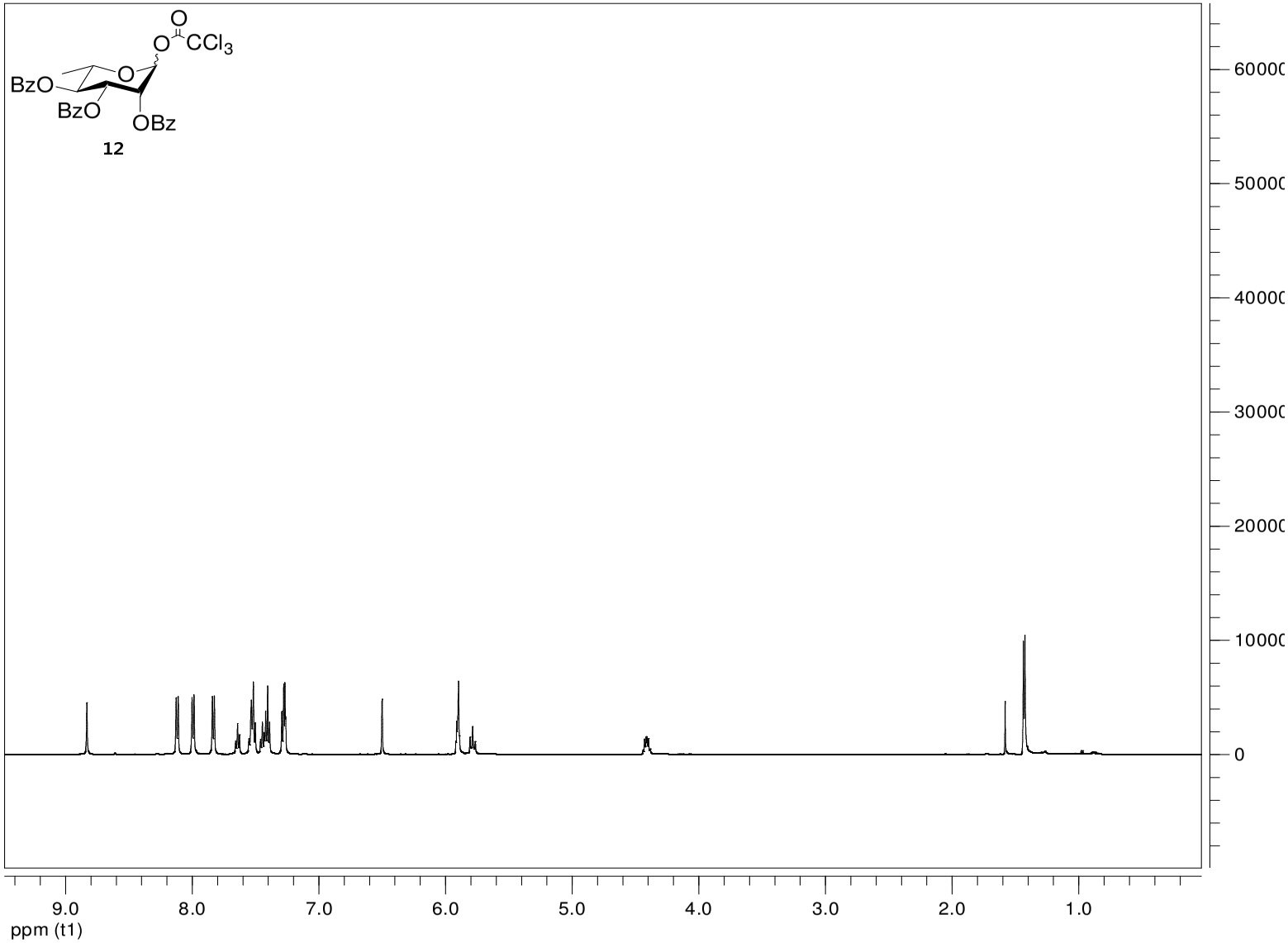
O
O
CCl3
O
BzO
BzO
OBz
12
60000
50000
40000
30000
20000
10000
0
9.0
8.0
7.0
6.0
5.0
4.0
3.0
2.0
1.0
ppm (t1)

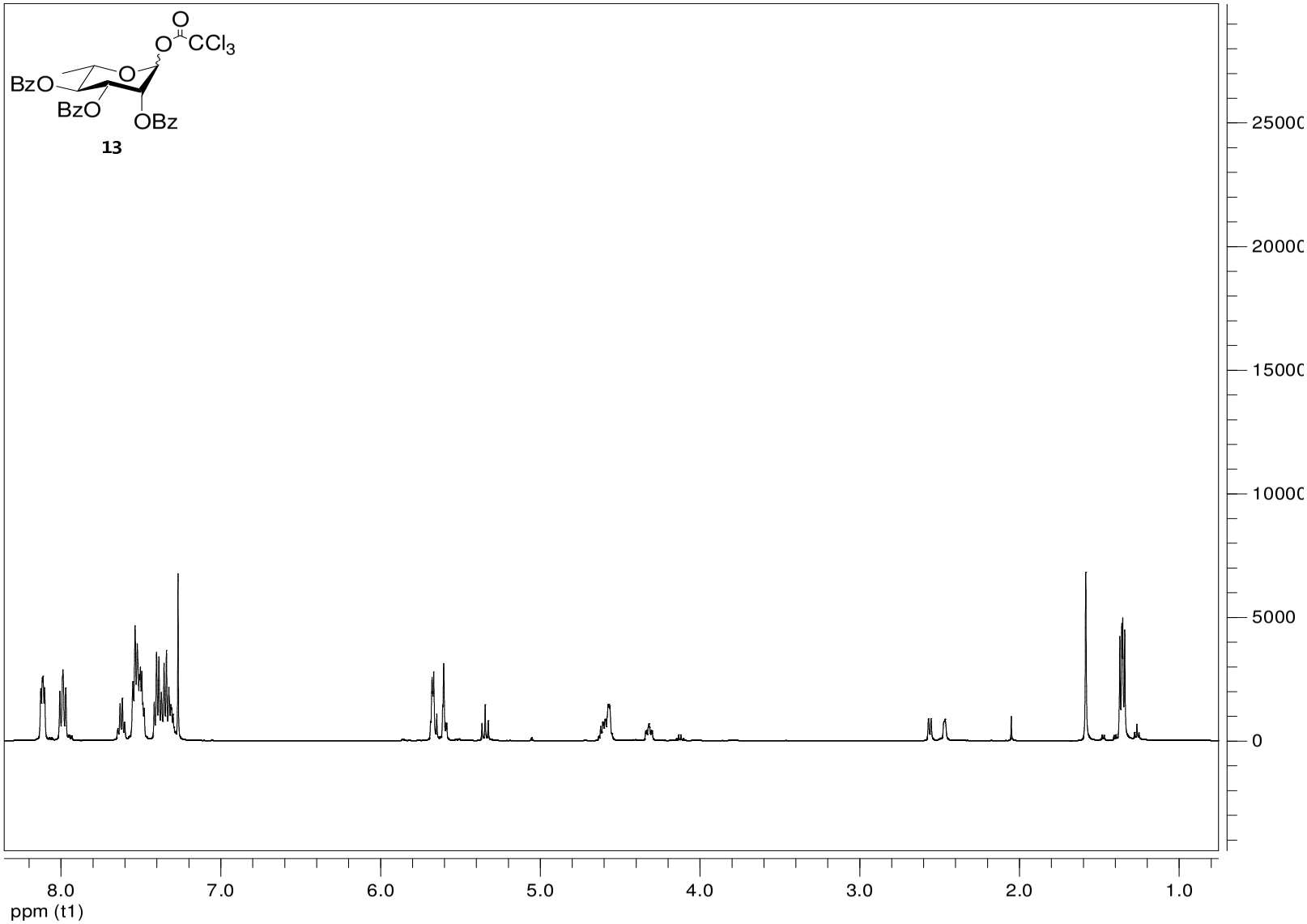
O
O
CCl3
O
BzO
BzO
OBz
13
25000
20000
15000
10000
5000
0
8.0
7.0
6.0
5.0
4.0
3.0
2.0
1.0
ppm (t1)

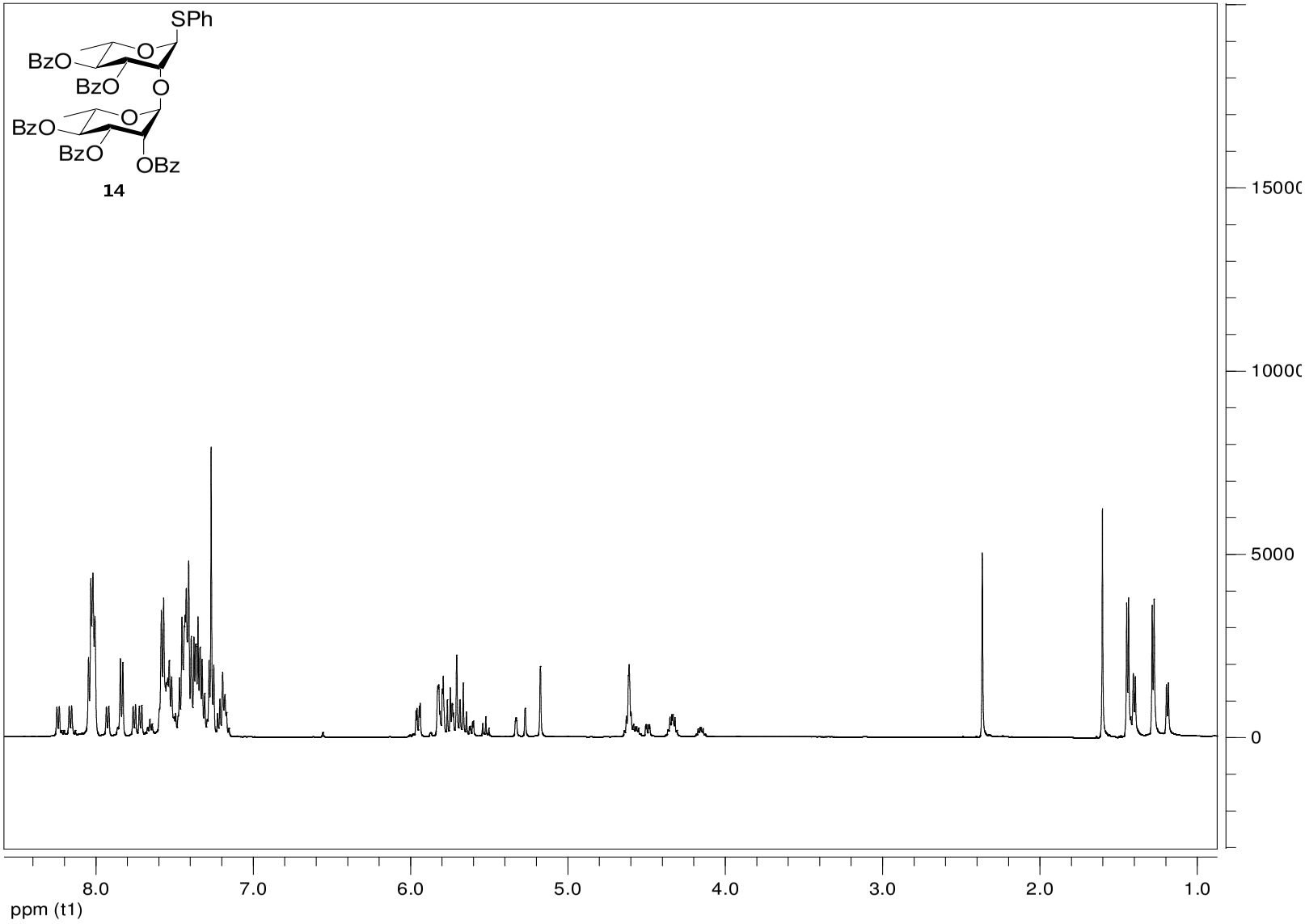
SPh
BzO
BzO
O
O
BzO
BzO
O
OBz
14
15000
10000
5000
0
8.0
7.0
6.0
5.0
4.0
3.0
2.0
1.0
ppm (t1)

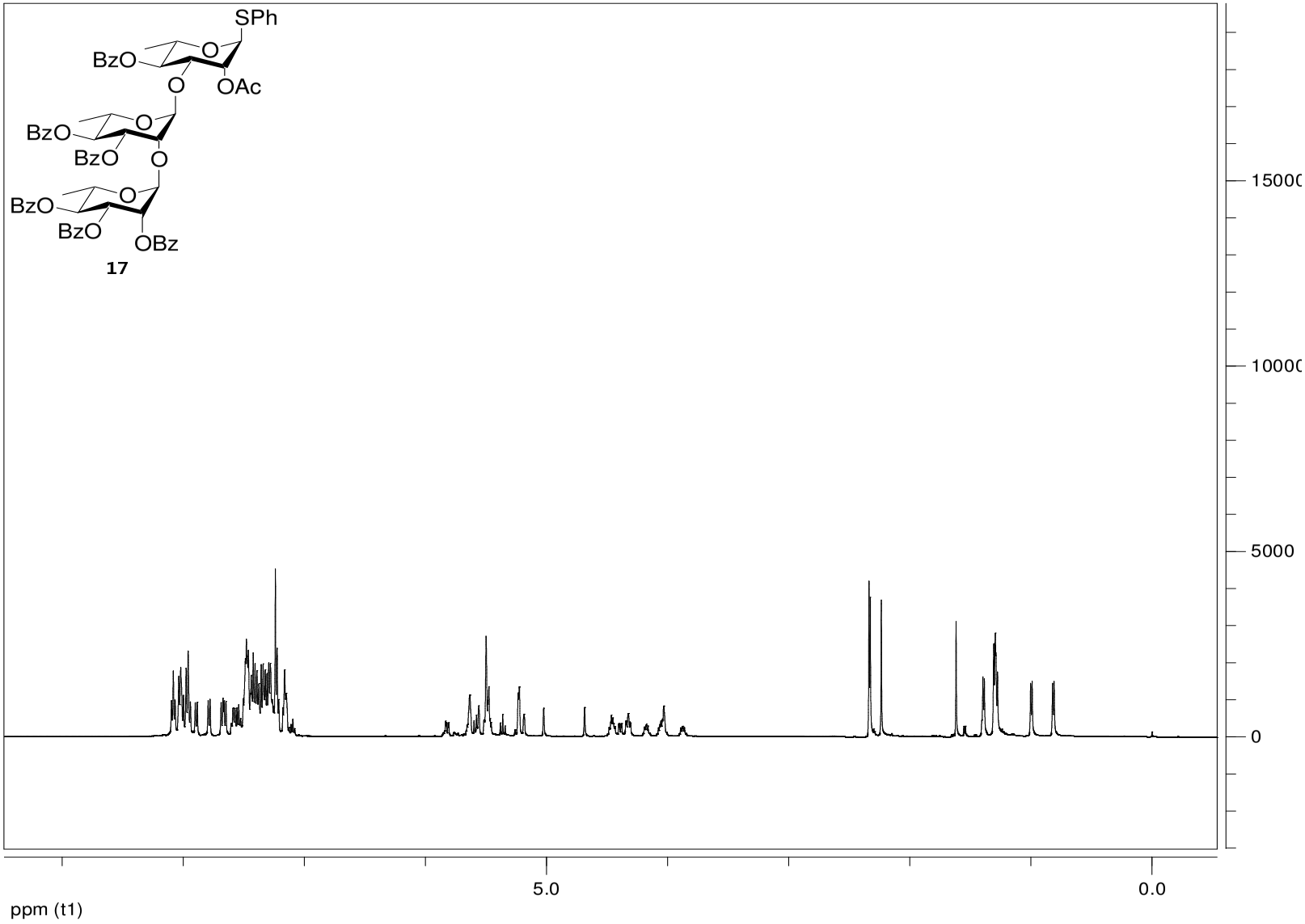
SPh
BzO
O
OAc
BzO
O
BzO
O
BzO
O
BzO
OBz
17
15000
10000
5000
0
5.0
0.0
ppm (t1)

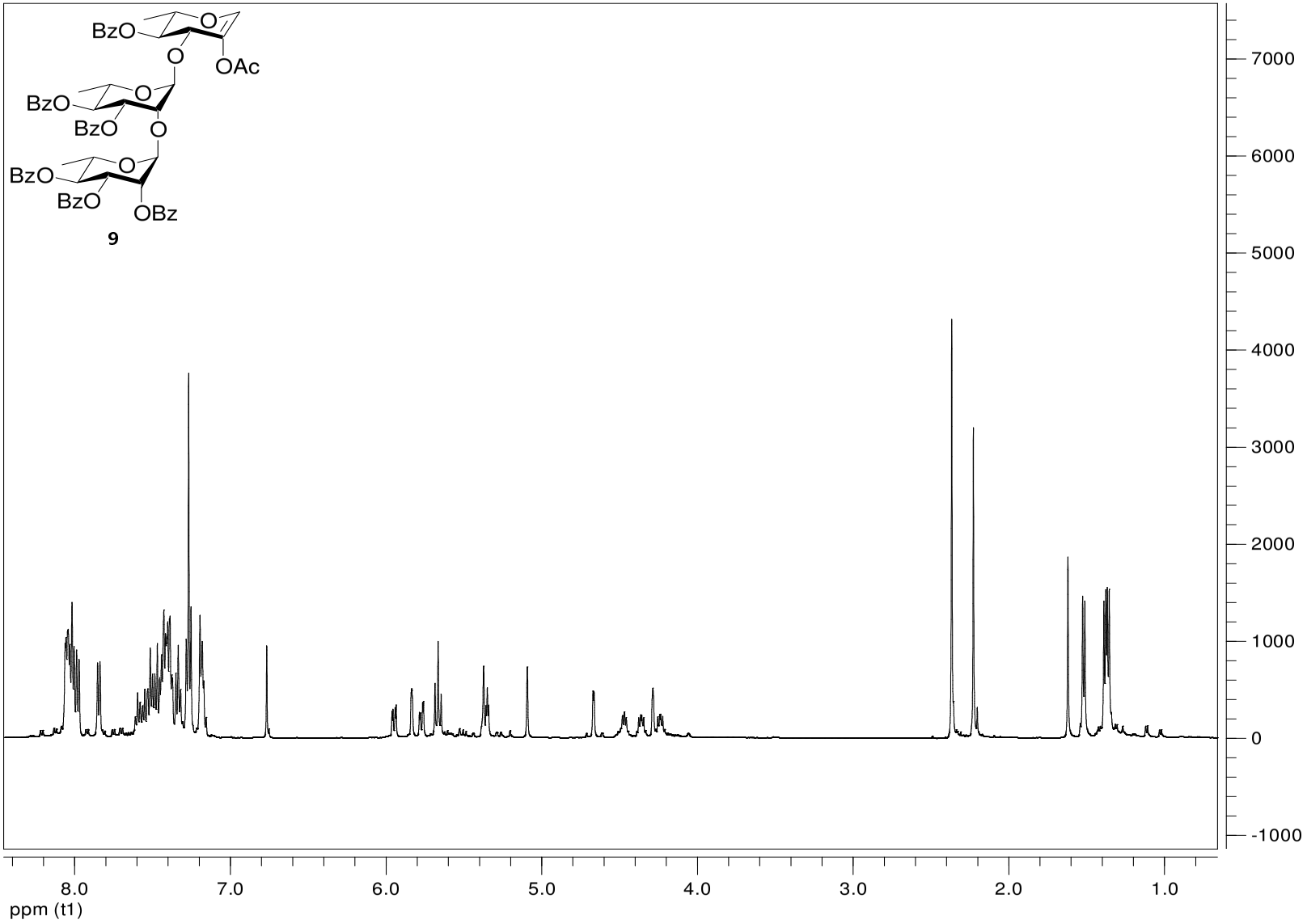
BzO
O
OAc
BzO
O
BzO
BzO
O
BzO
O
BzO
OBz
9
7000
6000
5000
4000
3000
2000
1000
0
-1000
8.0
7.0
6.0
5.0
4.0
3.0
2.0
1.0
ppm (t1)

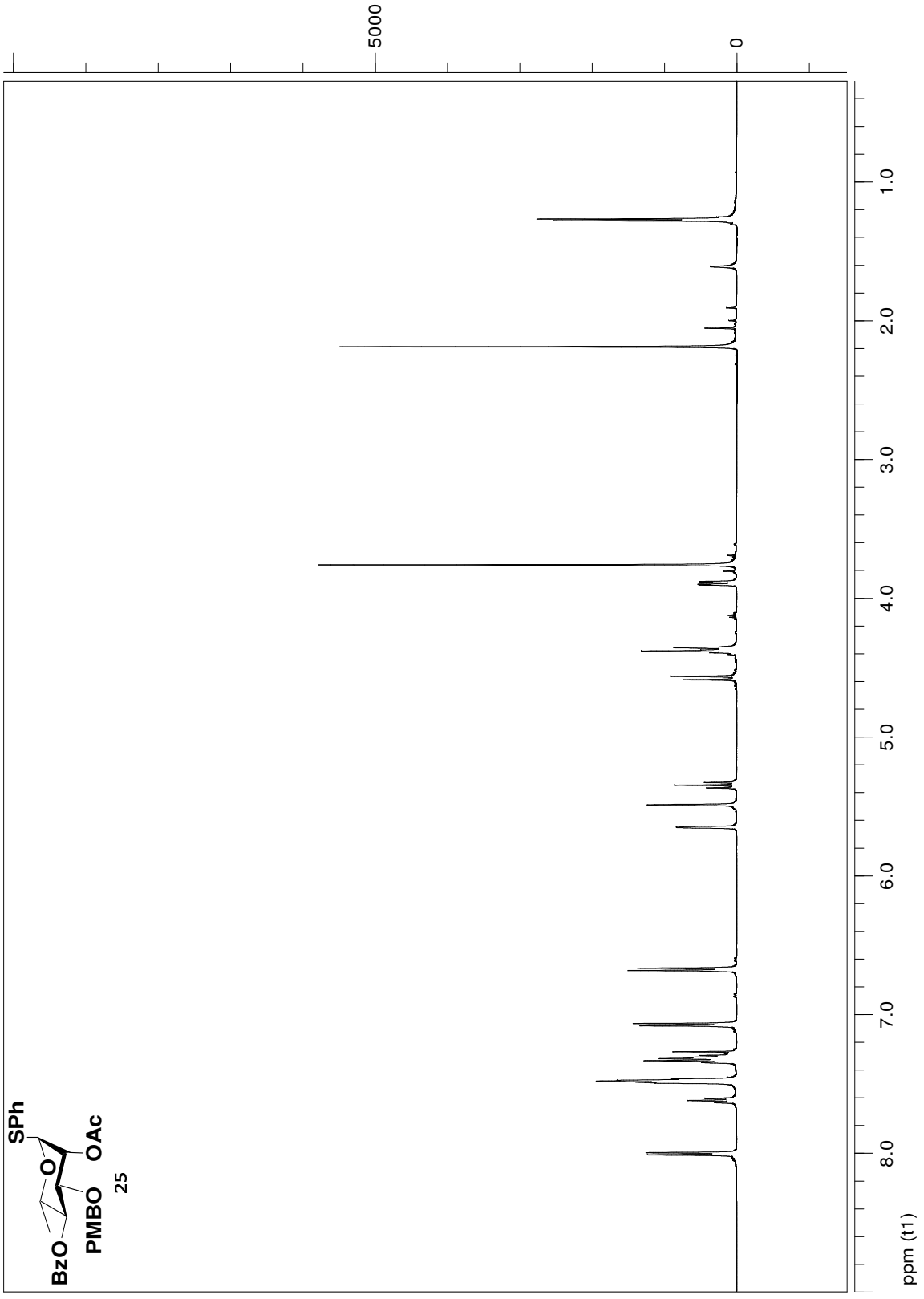
5000
0
SPh
O
OAc
BzO
PMBO
25
1.0
2.0
3.0
4.0
5.0
6.0
7.0
8.0
ppm (t1)

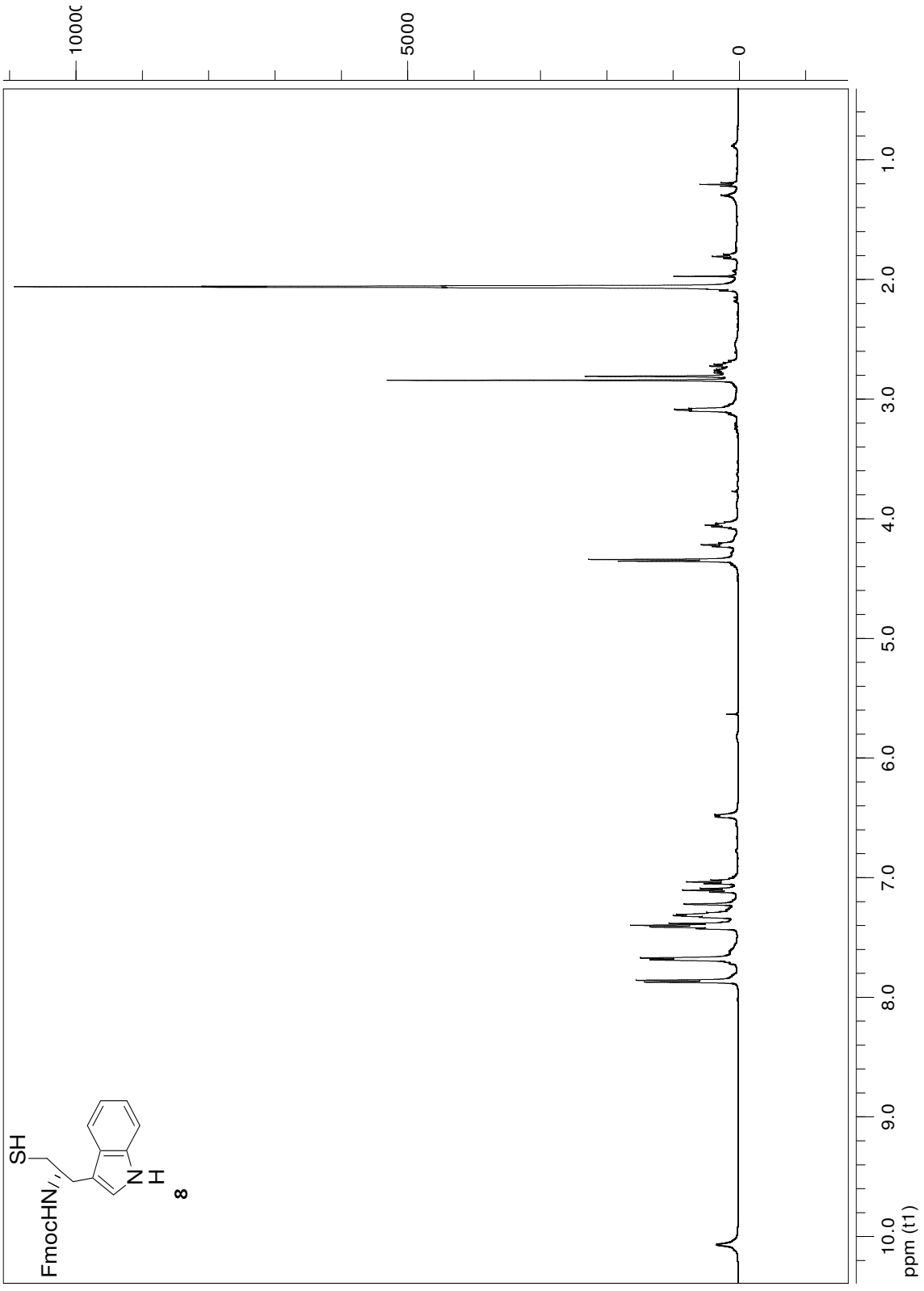
10000
5000
0
SH
FmocHN
H
N
8
1.0
2.0
3.0
4.0
5.0
6.0
7.0
8.0
9.0
10.0
ppm (t1)

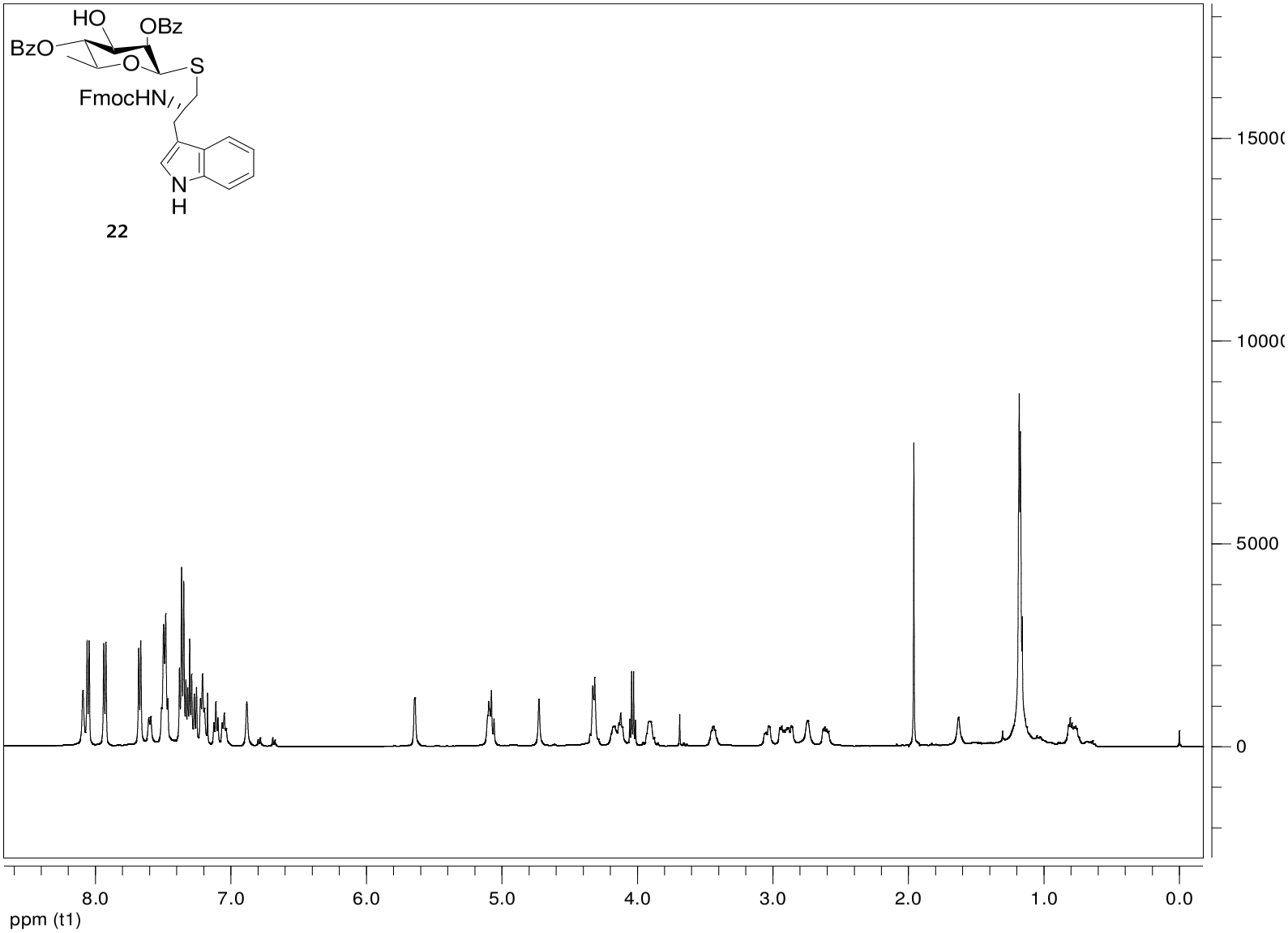
HO
OBz
BzO
O
S
FmocHN
N
H
22
15000
10000
5000
0
8.0
7.0
6.0
5.0
4.0
3.0
2.0
1.0
0.0
ppm (t1)

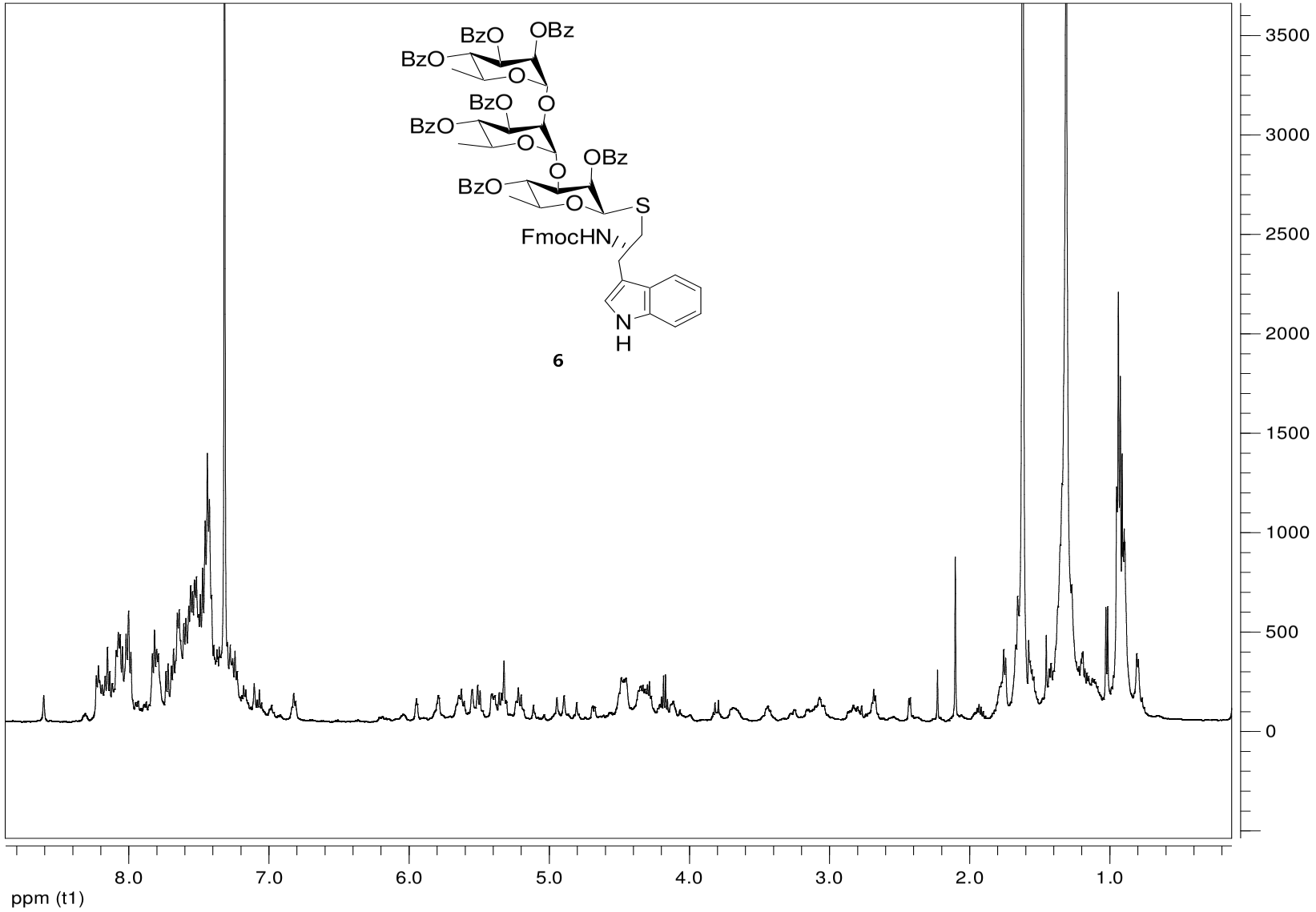
BzO
OBz
BzO
O
BzO
O
BzO
O
BzO
OBz
BzO
O
S
FmocHN
N
H
6
3500
3000
2500
2000
1500
1000
500
0
8.0
7.0
6.0
5.0
4.0
3.0
2.0
1.0
ppm (t1)

APPENDIX C: ^{1}H NMR SPECTRUM (CHAPTER 7)

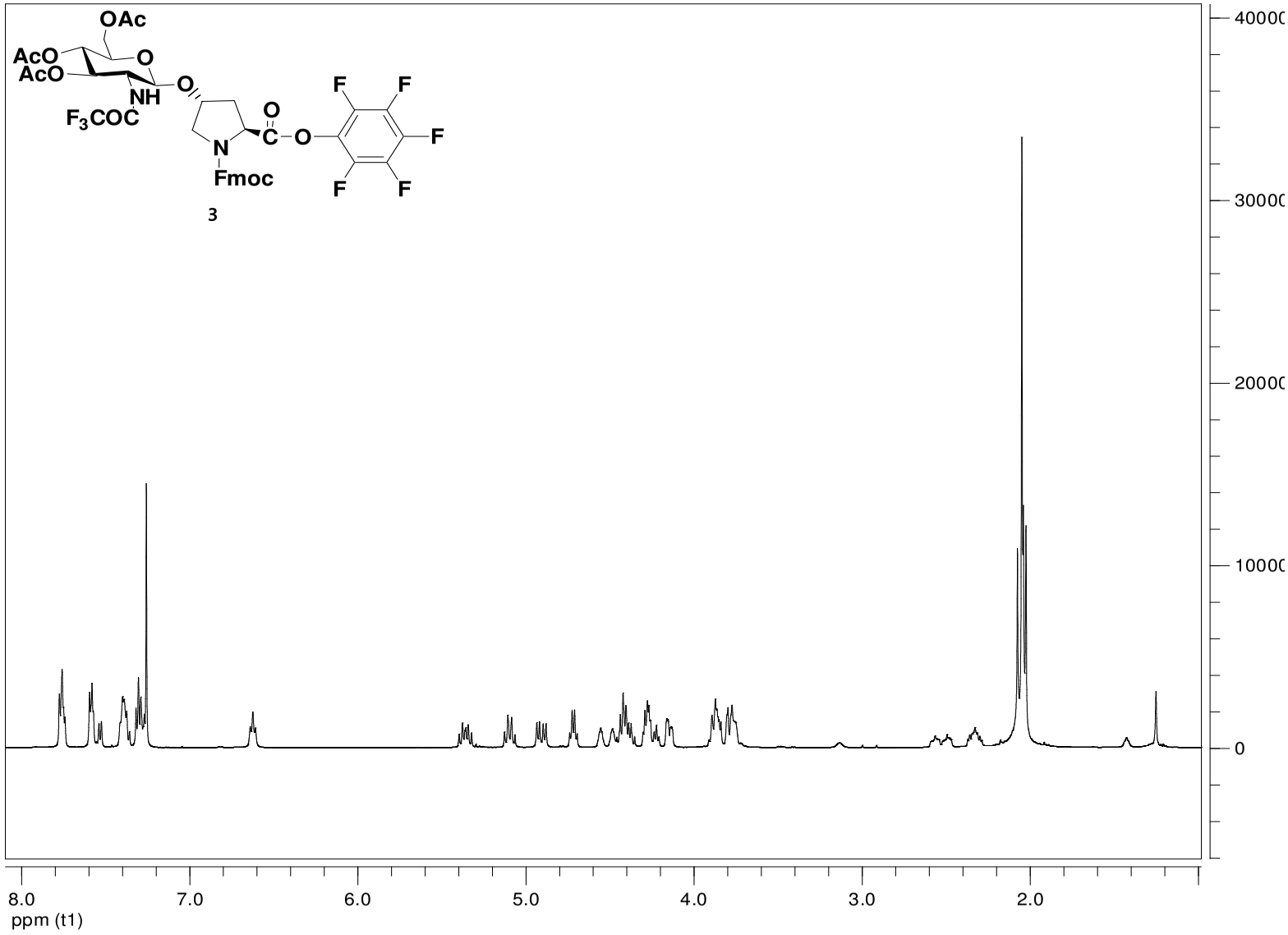
OAc
AcO
AcO
O
NH
F3COC
O
O
N
Fmoc
C
O
F
F
F
F
F
3
40000
30000
20000
10000
0
8.0
7.0
6.0
5.0
4.0
3.0
2.0
ppm (t1)